

Mechanistic Modelling of Radial Polymer Flow in Porous Media



Jørgen Gausdal Jacobsen

Thesis for the degree of Philosophiae Doctor (PhD)
University of Bergen, Norway
2020

UNIVERSITY OF BERGEN



Mechanistic Modelling of Radial Polymer Flow in Porous Media

Jørgen Gausdal Jacobsen



Thesis for the degree of Philosophiae Doctor (PhD)
at the University of Bergen

Date of defense: 29.09.2020

© Copyright Jørgen Gausdal Jacobsen

The material in this publication is covered by the provisions of the Copyright Act.

Year: 2020

Title: Mechanistic Modelling of Radial Polymer Flow in Porous Media

Name: Jørgen Gausdal Jacobsen

Print: Skipnes Kommunikasjon / University of Bergen

Scientific environment

This dissertation was submitted June 22nd 2020 as part of the fulfilment for the degree of Philosophiae Doctor (PhD) at the University of Bergen (UoB), Department of Chemistry. The thesis is based on simulations carried out at the Norwegian Research Centre (NORCE), formerly Uni Research, during the period 2017-2020. The doctoral fellowship position was funded by the Research Council of Norway as part of the PETROMAKS 2 project “Upscaling EOR LAB2FIELD”.



Acknowledgements

First and foremost, I would like to express my sincere gratitude and appreciation to my supervisor, Professor Arne Skauge. Thank you for providing me with the opportunity to be admitted to the PhD programme at the University of Bergen. Your astonishing professional knowledge, motivational abilities and guidance have been key success factors during my PhD.

I would also like to thank my co-supervisor, Øystein Pettersen, for his many contributions in terms of discussions and general inputs to the research methodology applied in this thesis.

Special thanks goes to Ken Sorbie and Tormod Skauge who have contributed greatly to my PhD in terms of good ideas and fruitful discussions.

Gratitude is also extended towards Hege Ommedal for her administrative guidance as PhD-coordinator at the Department of Chemistry.

Furthermore, I am very grateful for the financial support of the Research Council of Norway and Energi Simulation.

My colleagues at Norce have been invaluable to me during my PhD. Especially Abdul Majid Murad, Iselin Salmo, Morten Aarra, Jonas Solbakken and Mohammed Alzaabi. Thank you for being such good colleagues and creating an excellent work environment.

Finally, I would like to thank my dear family for their unconditional support throughout this process. In particular, my fantastic mother and father (Hildegunn and Åge), and also my brothers (Petter and Kristoffer) who have been very motivating, and for that I will always be grateful. Lastly, I would like to thank my amazing girlfriend (Stina) for her love and support during this hectic period of my life.

Abstract

Polymer flooding is one of the most successful chemically enhanced oil recovery (EOR) methods, and has primarily been implemented to accelerate oil production by sweep improvement. However, research from the last couple of decades have identified several additional benefits associated with polymer flooding. Firstly, improved polymer properties have extended their use in reservoirs with high temperature and high salinity. Secondly, improved understanding of the viscoelastic flow behavior of flexible polymers have revealed that they may in some cases mobilize capillary trapped oil as well. Despite of the recent progress, extensive research remains to quantify the appropriate flow mechanisms and accurately describe polymer flow in porous media.

Simulations and history match operations performed in this thesis are aimed at improving the modelling of radial polymer flow in porous media. This has been achieved by (1) evaluating the accuracy and robustness of two different history match methods which are used to estimate the in-situ rheology of non-Newtonian fluids in radial flow, (2) investigating potential rate and memory effects (at the Darcy scale) of viscoelastic polymer solutions in radial flow, and (3) quantifying polymer in-situ rheology and polymer injectivity.

The accuracy and robustness of both history match methods which are used to estimate the in-situ rheology of non-Newtonian fluids in radial flow was clearly demonstrated in radial flow experiments where effective (or cumulative) error was below 5 % of the maximum preset transducer pressure range. Thereby, the observed shear-thinning behavior of partially hydrolyzed polyacrylamide (HPAM) at low flux in porous media could not be attributed to insufficiently accurate pressure transducers during in-house flow experiments, as suggested by some researchers.

The estimation of polymer in-situ rheology showed invariance between excluding and including the polymer pressure data outside the near-wellbore region. Thus, it was proposed that the polymer in-situ rheology is mainly defined by the pressure data originating from the near-wellbore region during radial polymer flow. Results showed that not only could the polymer in-situ rheology be (quantitatively) estimated from

measurements of stabilized pressure, but could also be (qualitatively) identified from the pressure build-up during radial flow experiments. Consequently, the anchoring data from the pressure build-up during radial polymer flow was proposed as an additional tool for history matching field injectivity tests.

Rate and memory effects (at the Darcy scale) of several HPAM polymers were investigated in flow through Bentheimer sandstone discs. Results showed that no rate effects occurred for mechanically undegraded polymer (Flopaam 3330S). However, rate effects were observed for mechanically degraded polymers (Flopaam 3630S and Flopaam 5115SH) where the onset of shear-thickening increased with volumetric injection rate. While memory effects (at the Darcy scale) were absent for the mechanically undegraded and relatively low molecular weight polymer, Flopaam 3330S, the mechanically degraded and relatively higher molecular weight (18 MDa) polymer, Flopaam 3630S, exhibited memory effects in which apparent viscosity decreased with radial distance. As mechanical degradation is suggested to be confined to the near-wellbore region in radial polymer flow, the memory effect was proposed to originate from the elastic properties of the polymer.

In accordance with recent literature, the in-situ rheology of HPAM was shown to depend on flow geometry. During single and two-phase polymer flow, the shear-thinning behavior of HPAM was much more pronounced, and the extent of shear-thickening significantly reduced in radial compared to linear flow. Furthermore, the onset of shear-thickening during single-phase flow occurred at significantly higher velocities in radial relative to linear flow. However, this behavior was not consistent during two-phase flow as the onset of shear-thickening during linear and radial polymer flow coincided. Moreover, comparative studies of polymer flow in radial versus linear flow geometries during single and two-phase flow revealed that the impact of oil was to reduce apparent in-situ viscosity of HPAM. The low-flux in-situ rheology behavior was addressed and showed Newtonian behavior in linear flow while significant shear-thinning was observed during radial flow. Thus, both flow geometry and presence of oil were suggested to be key factors for estimating polymer in-situ rheology.

List of publications

Paper 1:

Skauge, A., Zamani, N., Jacobsen, J. G., Shiran, B. S., Al-Shakry, B. & Skauge, T. (2018): *Polymer Flow in Porous Media: Relevance to Enhanced Oil Recovery*, Colloids and Interfaces, Vol. 2: 1-27.

Paper 2:

Jacobsen, J. G., Alzaabi, M., Skauge, T., Sorbie, K. & Skauge, A. (2019): *Analysis and Simulation of Polymer Injectivity*. Presented at the 20th European Symposium on Improved Oil Recovery, Pau, France, 8-11 April.

Paper 3:

Jacobsen, J. G., Shiran, B. S., Skauge, T., Sorbie, K. S. & Skauge, A. (2020): *Qualification of New Methods for Measuring In Situ Rheology of Non-Newtonian Fluids in Porous Media*, Polymers, Vol 11: 1-13.

Paper 4:

Alzaabi, M., Jacobsen, J. G., Sumaiti, A. A., Masalmeh, S., Pettersen, Ø. & Skauge, A. (2020): *Polymer Injectivity Test Design Using Numerical Simulation*, Polymers, Vol. 12: 1-23.

All papers were either open access or overdue copyright. Reprints were made with permission from the Multidisciplinary Digital Publishing Institute (MDPI) and the European Association of Geoscientists & Engineers (EAGE).

Contents

Scientific environment.....	III
Acknowledgements.....	V
Abstract.....	VII
List of publications.....	IX
List of figures	XV
Nomenclature.....	XVII
1. Introduction.....	1
1.1 Motivation of study.....	2
1.2 Main objectives.....	3
1.3 Paper contents.....	3
1.4 Organization of thesis.....	4
2. Oil recovery.....	5
2.1 Conventional recovery mechanisms.....	5
2.2 Recovery efficiency.....	6
2.3 Enhanced oil recovery (EOR).....	6
3. Polymer flooding technology.....	9
3.1 Introduction.....	9
3.2 Polymers.....	10
3.3 Polymer retention.....	12
3.4 Polymer degradation.....	13
3.5 Resistance factors.....	15
3.6 Field experience.....	16
4. Polymer rheology.....	17
4.1 Bulk rheology.....	17

4.1.1 Upper Newtonian plateau (1).....	19
4.1.2 Shear-thinning region (2).....	19
4.1.3 Lower Newtonian plateau (3).....	19
4.2 Viscoelastic fluids.....	20
4.3 In-situ rheology.....	22
4.4 Viscoelastic flow in porous media.....	24
4.4.1 Upper Newtonian plateau (1).....	25
4.4.2 Shear-thinning region (2).....	26
4.4.3 Lower Newtonian plateau (3).....	28
4.4.4 Shear-thickening region (4).....	28
4.4.5 Mechanical degradation (5).....	31
4.5 Reduction of residual oil by viscoelastic polymers.....	32
5. Polymer injectivity.....	33
5.1 Factors influencing polymer injectivity.....	33
5.1.1 Debris in the polymer (1).....	33
5.1.2 In-situ polymer rheology (2).....	34
5.1.3 Polymer mechanical degradation (3).....	35
5.2 Injectivity models.....	35
6. Estimation of polymer in-situ rheology.....	37
6.1 Polymer in-situ rheology from linear flow experiments.....	37
6.2 Polymer in-situ rheology from radial flow experiments.....	38
6.3 History match methods for radial flow experiments.....	40
6.3.1 Single port match method (SPMM).....	40
6.3.2 Disc match method (DMM).....	41
6.4 Simulation and history match tools.....	42
6.4.1 Simulation tool.....	42
6.4.2 Automatic history match tool.....	42
6.5 Radial simulation model and sensitivity analysis.....	43

7. Results and discussion	47
7.1 Introduction.....	47
7.2 Qualification of history match methods for radial flow.....	48
7.2.1 <i>Pressure measurement noise analysis</i>	48
7.2.2 <i>Pressure measurement error analysis</i>	51
7.2.3 <i>Evaluation of radial history match methods</i>	53
7.2.4 <i>Analysis of pressure build-up during radial polymer flow</i>	55
7.3 Rate and memory effects of HPAM in radial flow.....	57
7.3.1 <i>Rate effects</i>	58
7.3.2 <i>Memory effects</i>	62
7.4 Quantification of polymer in-situ rheology and injectivity.....	64
7.4.1 <i>Impact of flow geometry</i>	64
7.4.2 <i>Impact of oil</i>	68
7.4.3 <i>Behavior of HPAM at low flux in porous media</i>	72
7.5 Summary of observations.....	74
7.5.1 <i>Qualification of history match methods for radial flow</i>	74
7.5.2 <i>Rate and memory effects of HPAM in radial flow</i>	75
7.5.3 <i>Quantification of polymer in-situ rheology and injectivity</i>	76
8. Conclusions and suggestions for future studies	79
8.1 Conclusions.....	79
8.1.1 <i>Qualification of history match methods for radial flow</i>	79
8.1.2 <i>Rate and memory effects of HPAM in radial flow</i>	80
8.1.3 <i>Quantification of polymer in-situ rheology and injectivity</i>	80
8.2 Suggestions for future studies.....	81
References	83
Appendix: Papers (1-4)	95

List of Figures

Figure 1.1: Primary energy consumption by fuel and resulting CO ₂ emissions in four different scenarios.....	1
Figure 2.1: Oil recovery classifications.....	7
Figure 3.1: The primary chain structure of HPAM.....	10
Figure 4.1: Schematic illustration of a dynamic fluid volume in simple shear flow...	17
Figure 4.2: Typical shear viscosity curve for polymer solutions in simple shear flow.....	19
Figure 4.3: Relaxation times for Flopaam 3630S in low salinity (left) and high salinity (right) brine solutions.....	21
Figure 4.4: Schematic illustration of viscoelastic polymer flow in porous media.....	22
Figure 4.5: Schematic illustration of a typical in-situ rheology curve for viscoelastic fluids (e.g. HPAM).....	25
Figure 6.1: Schematic illustration of linear flow experiment.....	37
Figure 6.2: Disc used for radial flow experiments.....	39
Figure 6.3: Simulation model used in conjunction with simulations in STARS.....	44
Figure 6.4: Sensitivity analysis of grid block size.....	45
Figure 7.1: Comparison of reference and estimated in-situ rheology curves after ± 10 % pressure measurement noise, using the DMM.....	49
Figure 7.2: Comparison of reference and arithmetic average of estimated in-situ rheology curves (0.5 – 3.0 mL/min) after ± 10 % pressure measurement noise, using the DMM.....	50
Figure 7.3: Comparison of reference and estimated in-situ rheology curves after ± 10 % pressure measurement noise, using the DMM with (a) 9 pressure ports (entire disc) and (b) 5 pressure ports (first 4 cm of the radial distance).....	51
Figure 7.4: Comparison of reference and estimated in-situ rheology curves after typical (± 1 %) pressure measurement error, using the DMM.....	52
Figure 7.5: Comparison of reference and estimated in-situ rheology curves after typical (± 1 %) pressure measurement error, using the SPMM.....	53

Figure 7.6: In-situ rheology curves obtained from history matching a radial polymer flow experiment, using the DMM and SPMM.....	54
Figure 7.7: Injection BHP versus time during initial (prior to polymer flow) and final brine flood (after polymer tapering).....	56
Figure 7.8: Injection BHP versus time during polymer flow.....	57
Figure 7.9: In-situ rheology curves obtained from history matching mechanically undegraded HPAM (Flopaam 3330S), using the DMM.....	58
Figure 7.10: In-situ rheology curves obtained from history matching mechanically degraded HPAM (Flopaam 5115SH), using the DMM.....	59
Figure 7.11: In-situ rheology curves obtained from history matching mechanically degraded HPAM (Flopaam 3630S), using the DMM.....	60
Figure 7.12: Onset of shear-thickening (velocity) as a function of volumetric injection rate for mechanically degraded HPAM (Flopaam 3630S).....	61
Figure 7.13: In-situ rheology curves obtained from history matching mechanically undegraded HPAM (Flopaam 3330S), using the SPMM.....	62
Figure 7.14: In-situ rheology curves obtained from history matching mechanically degraded HPAM (Flopaam 3630S), using the SPMM.....	63
Figure 7.15: Impact of flow geometry on polymer in-situ rheology in 1-phase flow.....	65
Figure 7.16: Effects of polymer concentration on in-situ rheology during linear single-phase flow.....	67
Figure 7.17: Impact of flow geometry on polymer in-situ rheology in 2-phase flow.....	67
Figure 7.18: Impact of oil on polymer in-situ rheology in linear flow.....	69
Figure 7.19: Impact of oil on polymer in-situ rheology in radial flow.....	70
Figure 7.20: (a) Linear and (b) polynomial fit to pressure data during brine flow.....	71
Figure 7.21: Resistance factor calculations using linear and polynomial fit to the brine flow pressure data obtained after polymer flow.....	72
Figure 7.22: Impact of flow geometry on polymer in-situ rheology in (a) linear, and (b) radial flow.....	73

Nomenclature

Abbreviations:

A	area, cross sectional area
BHP	bottom-hole pressure
BP	British Petroleum
CMG	Computer Modelling Group Ltd.
ΔP	generated pressure drop
dP	differential pressure
D	Darcy, diameter
Da	Dalton
DMM	disc match method
EAGE	European Association of Geoscientists & Engineers
E_D	microscopic displacement efficiency
E_R	recovery efficiency
E_V	macroscopic (or volumetric) sweep efficiency
EOR	enhanced oil recovery
F	force
FHF	field history file
G	Young's modulus
G'	storage modulus
G''	loss modulus
GDP	gross domestic product
h	disc thickness
HPAM	partially hydrolyzed polyacrylamide
I	injectivity
IOR	improved oil recovery
IPV	inaccessible pore volume
k	permeability
k_r	relative permeability
K	flow consistency index
L	length
M	mobility ratio
MCMC	Markov Chain Monte Carlo
MDPI	Multidisciplinary Digital Publishing Institute
n	power law flow behavior index
N_{De}	Deborah number
N_{Re}	Reynolds number
NORCE	Norwegian Research Centre

PhD	philosophiae doctor
PSO	Particle Swarm Optimization
Q	volumetric injection rate
r	radius, radial distance
R_F	resistance factor
R_K	permeability reduction factor
R_{RF}	residual resistance factor
SPMM	single port match method
S_{or}	residual oil saturation
t	time
u	Darcy velocity
UoB	University of Bergen
v	velocity
WAG	water-alternating-gas

Greek Letters

α	correction factor
λ	mobility, polymer relaxation time
μ	viscosity
ω	frequency
ϕ	porosity
ρ	density
τ	shear stress
θ	time
γ	strain
$\dot{\gamma}$	shear rate

Subscripts

0	zero-shear
∞	infinite-shear
a	after
app	apparent
b	before, brine
c	critical
e	production rim
f	polymer relaxation
m	amplitude
p	polymer, polymer process

1. Introduction

In all scenarios which were evaluated in the 2019 edition of the BP Energy Outlook, gross domestic product (GDP) more than doubles globally by 2040 (BP Annual Energy Outlook, 2019). The consequent increase in energy demand is illustrated as primary energy consumption by fuel and resulting CO₂ emissions in figure 1.1. In all four scenarios, vast amounts of oil are required, which relative to coal is a preferred source of energy. Thus, maintaining oil production is a prerequisite to meet future energy demands while reducing emissions.

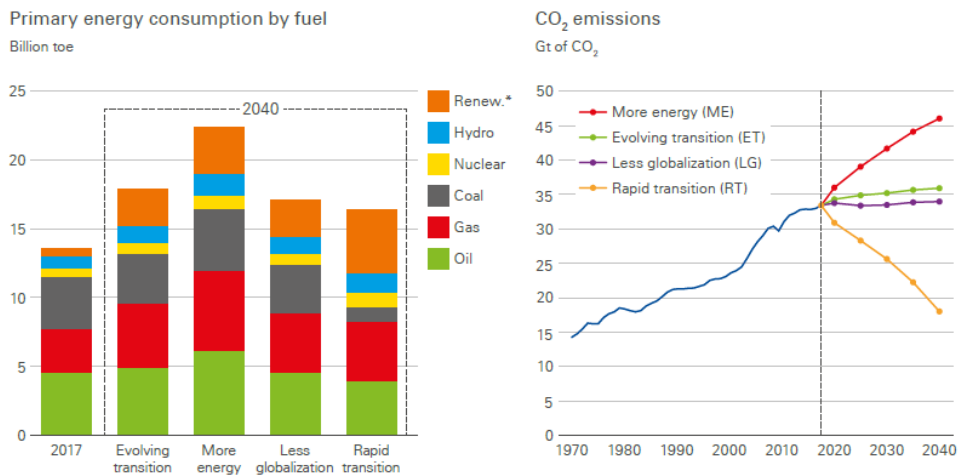


Figure 1.1: Primary energy consumption by fuel and resulting CO₂ emissions in four different scenarios (BP Annual Energy Outlook, 2019).

As petroleum fields worldwide are maturing, recovery efficiencies must increase in order to maintain a sufficient level of oil supply. Using conventional recovery mechanisms such as pressure depletion (primary) and water/gas injection (secondary), global recovery factors are averaging merely 35 % (Thomas, 2019). Especially for heterogeneous and heavy oil reservoirs, recovery factors associated with conventional recovery mechanisms may be far below the global average. This is due to limited cross flow between adjacent layers in heterogeneous reservoirs and the development of frontal instabilities (viscous fingering) in the process of displacing viscous crudes with

lower viscosity fluids. Consequently, large volumes of oil are bypassed and tremendous potential remains for unconventional, or enhanced oil recovery (EOR) methods.

Polymer flooding is the most frequently implemented chemical EOR process, and has received increased attention after several successful polymer flood projects have been reported in the literature (Standnes & Skjevrak, 2014; Sheng et al., 2015). It has primarily been used to accelerate oil production by sweep improvement. However, promising results have emerged in recent years, suggesting it may be able to mobilize capillary trapped oil as well (Azad & Trivedi, 2019). During polymer flooding, the injection brine is viscosified by adding water-soluble polymers, thereby stabilizing the displacement process by means of improved crossflow and reduction of the viscosity contrast between the injected solution and displaced fluids.

In subsequent chapters, background material concerning the inadequacies of conventional recovery mechanisms, potential for polymer flooding, and flow mechanisms of polymer solutions, is presented. These theoretical sections should be adequate to comprehend the results presented in this thesis.

1.1 Motivation of study

Polymer flooding is a mature subject of study, which dates back to the early 1960s (Pye, 1964; Sandiford, 1964). With the advent of extensive research, the perception of polymer flooding has shifted from a simple augmented water flood towards being identified as an extremely complex EOR process. This is mainly due to the non-Newtonian nature of polymers as they flow through porous media. Despite nearly sixty years of research, significant controversy and uncertainties are still associated with several topics within polymer flooding technology.

One of these controversial topics constitute polymer in-situ rheology. In contrast to the prevailing paradigm, results from recent years indicate that polymer in-situ rheology and, by extension, polymer injectivity, is significantly different in linear compared to radial flow (Skauge et al., 2016). Since radial flow geometry best mimics the polymer flow out from the injector in oil reservoirs, polymer in-situ rheology should be

estimated from radial rather than linear flow experiments. Furthermore, it has been implicitly assumed that polymer in-situ rheology is unaffected by the presence of oil, as the majority of polymer in-situ rheology studies have been based on single-phase experiments. If oil has a significant effect on polymer in-situ rheology, it should be quantified and included in the modelling of polymer flow in porous media.

1.2 Main objectives

Based on the aforementioned issues related to the modelling of polymer in-situ rheology, the following main objectives of this thesis are stated as follows:

- **Evaluate** the accuracy and robustness of the history match methods used to estimate polymer in-situ rheology and injectivity from radial flow experiments.
- **Investigate** potential rate and memory effects of viscoelastic polymers (at the Darcy scale) during radial flow experiments.
- **Quantify** polymer in-situ rheology and polymer injectivity in porous media.

1.3 Paper contents

Paper 1 (Skauge et al., 2018) provides a comprehensive review of recent developments within the research of polymer flow in porous media, with emphasis on polymer in-situ rheology and injectivity. Furthermore, the impact of oil on polymer in-situ rheology is quantified in Bentheimer sandstone. Results from both linear and radial flow experiments are included in the paper.

Paper 2 (Jacobsen et al., 2019) investigate the influence of pressure measurement noise on the estimated polymer in-situ rheology, using a recently developed history match method which is applicable for radial flow experiments with internal pressure ports. Moreover, the sensitivity of polymer in-situ rheology to the disc size used for radial flow experiments, is assessed.

Paper 3 (Jacobsen et al., 2020) evaluate the robustness and accuracy of two different history match methods which are used to estimate polymer in-situ rheology from radial flow experiments. In addition, an analysis of potential rate and memory effects of an undegraded partially hydrolyzed polyacrylamide (HPAM) polymer in flow through a radial Bentheimer sandstone disc was performed.

Paper 4 (Alzaabi et al., 2020) focus on maximizing the anchoring data from field injectivity tests, which are used to estimate polymer in-situ rheology. Consequently, pressure build-up and stabilized injection bottom-hole pressure (BHP) during radial polymer flow was analysed at both the laboratory and field scale.

1.4 Organization of thesis

In chapter 1, the overarching motivation and main objectives of this thesis is briefly stated. Chapter 2 introduces conventional petroleum production and associated challenges. Chapter 3 gives an overview of polymer flooding technology, where relevant topics for this particular thesis are included. In chapter 4 and 5, the main topics of this thesis are presented, i.e. polymer (in-situ) rheology and injectivity, respectively. Estimation of polymer in-situ rheology from flow experiments, simulation tools, history match methods and sensitivity analyses are provided in chapter 6. Chapter 7 summarize and discuss the principal results and observations obtained during the course of this thesis. Finally, general conclusions and suggestions for future studies are reviewed in chapter 8.

2. Oil recovery

In this chapter, how petroleum hydrocarbons are produced is discussed in terms of recovery mechanisms and corresponding efficiencies at both the microscopic and macroscopic scale. Inadequacies of conventional recovery mechanisms are emphasized and the rationale for implementation of enhanced recovery methods is highlighted.

2.1 Conventional recovery mechanisms

The production of petroleum hydrocarbons from subsurface reservoirs may be divided into three different production phases: primary, secondary and tertiary recovery. The initial production phase is generally characterized by primary recovery and refers to the volume of hydrocarbons produced as a result of the natural energy prevailing in the reservoir (Thomas, 2019). Mechanisms of primary recovery may be exemplified by depletion drive, gravity drainage, gas cap drive, rock and/or liquid expansion and aquifer drive. As reservoir pressure decrease during primary recovery, it may at some point drop below the bubble point and dissolved gas will start to bubble out from the oil solution. Since gas is much more mobile relative to oil, some oil will be left behind in the reservoir and production impairment occurs. To counteract this occurrence, secondary recovery by water flooding is conventionally implemented. Here, the injection of water aims to maintain pressure above the bubble point and displace hydrocarbons towards the producers. Water injection is by far the most frequently applied secondary recovery mechanism, mainly due to its availability (especially offshore) and low cost. In some cases, secondary recovery may constitute gas injection if economic incentives are prevailing. Water and gas may also be injected into the same reservoir by the process of water-alternating-gas (WAG) injection.

Primary and secondary recovery mechanisms may be efficient for producing light oils, but can be severely inefficient in producing heavier crudes and in heterogeneous reservoirs. This is mainly due to the viscosity contrast between the injected water solution and the viscous oil, which may induce front instabilities. The mobility ratio is a helpful parameter in assessing the stability of the displacement front, and is defined

as the ratio of the mobility of the displacing fluid, λ_1 , to the mobility of the displaced fluid, λ_2 , (Lake et al., 2014):

$$M = \frac{\lambda_1}{\lambda_2} = \frac{k_{r,1} \mu_2}{k_{r,2} \mu_1} \quad \text{Eq. 2.1}$$

where k_r is relative permeability to the particular fluid and μ is fluid viscosity. As the mobility ratio increase, the displacement front between the two immiscible fluids becomes increasingly unstable.

2.2 Recovery efficiency

The recovery efficiency, E_R , during petroleum production from a subsurface reservoir is the ratio of produced fluid volume to the fluid volume originally in place. It may also be defined as the product of the microscopic displacement efficiency, E_D , and the macroscopic (or volumetric) sweep efficiency, E_V (Fanchi & Christiansen, 2017):

$$E_R = E_D \times E_V \quad \text{Eq. 2.2}$$

The microscopic displacement efficiency is a measure of how much capillary trapped oil is mobilized (or displaced) at the pore scale, and thus depends predominantly on interfacial tensions and wettability states. In contrast, the macroscopic sweep efficiency refers to the volume of oil contacted by the injected fluid and is thereby influenced principally by viscous rather than capillary forces. Thus, bypassed oil is defined as the macroscopically uncontacted oil, while residual oil saturation constitutes the capillary trapped oil in conjunction with the microscopic displacement efficiency. Since recovery efficiencies in heterogeneous reservoirs containing viscous crudes are typically much lower than the global average of 35 %, tremendous potential remains for EOR methods.

2.3 Enhanced oil recovery (EOR)

EOR can be defined as incremental oil recovery by the injection of materials not normally present in the reservoir (Lake et al., 2014). This may be achieved by either

increasing the viscous forces of the injected material or by reducing the capillary forces between the materials involved in the displacement process. The principal classes of EOR methods include thermal, solvent, chemical and others (figure 2.1).

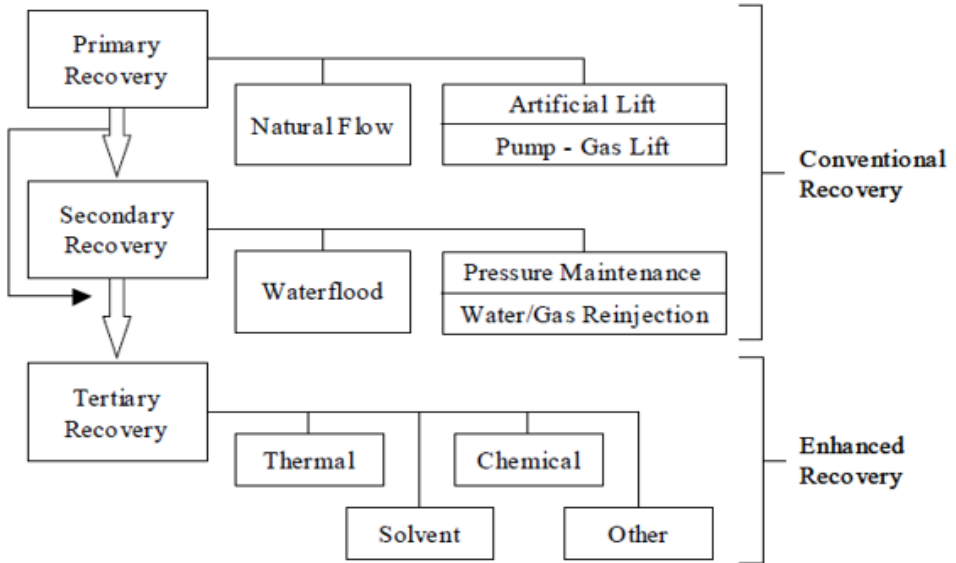


Figure 2.1: Oil recovery classifications (Lake et al., 2014).

EOR is often associated with tertiary recovery due to its frequent implementation in the tertiary production phase. However, this need not be the case as EOR methods may be implemented at both the primary and secondary recovery stage. A well-known example concerns the production of sufficiently viscous crudes, when uneconomic flow during primary and secondary recovery mechanisms precludes their implementation. In these situations, thermal EOR may be the only means of recovering significant amounts of oil. Thus, the EOR method applied in this case would chronologically be considered primary recovery (Green & Willhite, 1998).

During recent decades, improved oil recovery (IOR) has sometimes been used interchangeably with EOR. Although the distinction between them is ambiguous, IOR typically refers to any process that improves oil recovery. Thereby, IOR encompass EOR processes, but also other practices such as waterflooding, pressure maintenance, infill drilling and horizontal wells (Lake et al., 2014).

3. Polymer flooding technology

3.1 Introduction

Polymer flooding consists of adding polymers (powder or emulsion) to the injection brine during a waterflood, thereby viscosifying the water and reducing its mobility (Thomas, 2019). It has primarily been implemented to mitigate the propensity for viscous instabilities, thus accelerating oil production by sweep improvement.

The concept of using viscosified water to increase the efficiency of a water flood dates back to the early 1940s, when Detling (Shell Development Company) obtained a patent covering the use of several additives for viscous water flooding (Sandiford, 1964). However, the viscosifying agents patented at that time were deemed economically infeasible due to the quantities required to bring about a substantial mobility reduction. It was not until the mid 1960s, after the pioneering work of several researchers (Pye, 1964; Sandiford, 1964; Mungan et al., 1966; Gogarty, 1967), that the synthetic polymer HPAM was identified as a potential economic viscosifying agent. Their experimental results showed that addition of HPAM in low quantities to the injected solution could significantly increase oil recovery from rock cores. The significant viscosity increase by adding small amounts of HPAM in solution was attributed to its high intrinsic viscosity, which is a measure of its polymer molecular weight (Sorbie, 1991). HPAM was originally proposed as a mobility control agent due to its large commercial availability and low production costs.

Polymers may be injected into oil reservoirs for purposes other than polymer flooding. During conformance, or water shut-off treatments, concentrated polymer gels are injected to mitigate excessive water production by plugging high permeability thief zones. Consequently, the injection water is diverted to less permeable, unswept zones of the reservoir, thus improving volumetric sweep efficiency (Seright, 1995; Seright et al., 2012). In contrast, polymer floods are intended to directly displace oil from less permeable zones, and thereby substitute rather than compliment pure water injection.

3.2 Polymers

Polymers are macromolecular compounds made up of repeating units, named after the monomer(s) used in the polymerization process (Carraher, 2003). Their molecular weight may range from a few thousand to several million Daltons (Da), potentially yielding extremely viscous materials. However, due to the complex process of polymer synthesis, polymers are usually polydisperse, i.e. they have a wide molecular weight distribution. Consequently, polymer samples are generally comprised of macromolecules of the same chemical structure, but with varying chain lengths.

Both the biopolymer Xanthan and the synthetic polymer HPAM have been used in conjunction with polymer flooding projects (Standnes & Skjevra, 2014; Sheng et al., 2015). Since HPAM is by far the most frequently applied polymer, it will be of sole focus in this thesis. HPAM is an anionic copolymer of acrylamide and acrylic acid, where a certain fraction of the backbone acrylamide units has been hydrolyzed (Carraher, 2003), as shown in figure 3.1.

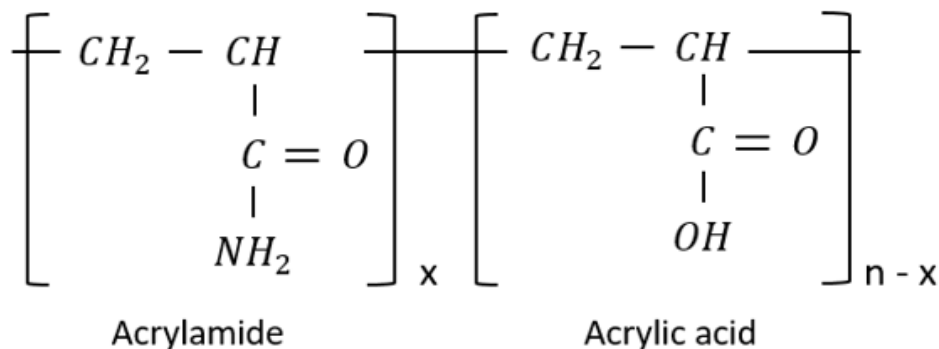


Figure 3.1: The primary chain structure of HPAM (Modified from Sorbie, 1991).

During the hydrolysis process, some of the amide groups are converted into carboxyl groups. The degree of hydrolysis is selected to optimize properties such as water solubility, retention (chapter 3.3), and to increase the viscosifying ability of the polymer (Lake et al., 2014). Since the degree of hydrolysis significantly influence several flow properties of HPAM (Martin, 1975), an optimum value exist for any given system, and is generally between 15-33 % (Green & Willhite, 1998).

Polyelectrolytes such as HPAM are generally distinguished from non-ionic polymers by the significant impact that ionic species (e.g. salt) and pH have on their viscosity (Sorbie, 1991). The anionic polymer molecules in aqueous solution will be surrounded by a cloud of oppositely charged counterions, thus forming an electrical double layer. When these clouds of counterions approach each other, they will be repelled coulombically. Due to the flexible chain structure of the HPAM molecule, this repulsion will increase the hydrodynamic size of the molecule, thereby increasing solution viscosity. However, in solutions containing positively charged ionic species, the thickness of the electrical double layer decrease, and consequently, polymer viscosity is reduced. The reduction in viscosity becomes more severe with ionic valence, i.e. divalent ions (e.g. Ca^{2+}) reduce viscosity more than monovalent ions (e.g. Na^+) (Mungan, 1972; Ward & Martin, 1981; Guetni et al., 2019).

In accordance with the aforementioned ionic species, the effect of lowering the pH of a polymer solution is to neutralize the ionic carboxylate groups, thereby promoting a reduction in electrostatic effects (Sorbie, 1991). Consequently, the hydrodynamic size and viscosity of the polymer decrease (Mungan, 1969). This effect is more pronounced in low-salinity solutions where the propensity for hydrodynamic size reduction is more severe. However, pH has very limited effect on polymer viscosity in the pH range normally encountered in oil reservoirs (Szabo, 1979).

The average molecular weight of HPAMs used in EOR operations is in the range of 2-35 MDa (Thomas, 2019), depending on reservoir properties such as permeability and connate water salinity. Since higher molecular weights enable lower concentrations of added polymer to achieve a certain solution viscosity, project economics will always favor maximizing polymer molecular weight. However, to avoid plugging of the formation, and to ensure technical success of the project, lower molecular weights than the economic optimum are generally chosen (Guo, 2017).

Polymer floods are typically applying concentrations in the semi-dilute regime mainly due to the viscosifying abilities of polymers above the critical overlap concentration, coupled with their favorable flow properties in porous media (Skauge et al., 2016).

3.3 Polymer retention

In flow through porous media, polymer molecules may be retained by mechanisms such as adsorption, mechanical entrapment and hydrodynamic retention/entrapment (Sorbie, 1991). The former mechanism may occur both statically and dynamically, while the two latter are exclusively dynamic mechanisms, i.e. they only occur in flow through porous media. Collectively, these phenomena will retard the flow of polymer solutions and may decrease permeability of the porous medium.

Adsorption refers to either physisorption, in which electrostatic forces act between porous media and polymer solutions, or chemisorption where chemical bonds between porous media walls and polymer molecules are formed. Polymer adsorption of HPAM on rock surfaces is dominated by physisorption, and is considered instantaneous and irreversible (Zhang & Seright, 2014). In the semi-dilute concentration regime, the amount of polymer adsorption increase with molecular weight (Hirasaki & Pope, 1974; Wever et al. 2018), concentration (Szabo, 1975; Dominguez & Willhite, 1977; Zhang & Seright, 2014), salinity (Smith, 1970; Szabo, 1975; Broseta, 1995), in carbonates compared to silica (Smith, 1970), and in absence compared to presence of residual oil (Szabo, 1975; Broseta et al., 1995; Wever et al., 2018).

Due to the relatively large hydrodynamic size of polymer molecules, retention may also occur in terms of mechanical entrapment. Here, polymer molecules are trapped (or lodged) between narrow pore throats in the porous medium (Dominguez & Willhite, 1977). The mechanism of mechanical entrapment is very similar to the well-known phenomenon of deep bed filtration (Herzig et al., 1970; Tien & Payatakes, 1979). According to the physical picture of mechanical entrapment in porous media, the distribution of mechanically entrapped polymer is expected to be largest at the inlet and decrease exponentially along the core. Not surprisingly, mechanical entrapment increase with the ratio of polymer hydrodynamic size to pore throat size, i.e. with increasing molecular weight and decreasing porous medium permeability (Mungan et al., 1966; Gogarty, 1967; Szabo, 1975; Dominguez & Willhite, 1977).

The last, and perhaps least understood retention mechanism constitute hydrodynamic retention/entrapment. Here, polymer molecules are temporarily trapped in stagnant flow regions by hydrodynamic drag forces (Sorbie, 1991). During hydrodynamic retention, the total level of retention increase with flow rate (Maerker, 1973; Dominguez & Willhite, 1977; Chauveteau, 1981). Observations show that hydrodynamic retention in porous media increase with polymer molecular weight and decrease with core permeability (Chen et al., 2016). However, hydrodynamic retention is considered reversible (Maerker, 1973; Chauveteau, 1981; Zhang & Seright, 2015; Chen et al., 2016) and is suggested to have limited effect on polymer in-situ rheology (Zhang & Seright, 2015).

3.4 Polymer degradation

Polymers may be degraded during propagation through porous media by three principal mechanisms, namely: chemical, biological and mechanical degradation.

Chemical degradation refers to the breakdown of polymer molecules by short-term reactions with contaminants (e.g. oxygen) or through attack of the backbone acrylamide units by processes such as hydrolysis (Sorbie, 1991). At elevated temperatures, chemical degradation may sometimes be referred to as thermal degradation. However, even though reaction rates are thermally accelerated, the degradation process is normally classified as chemical rather than thermal (Sorbie, 1991; Lake et al., 2014; Sheng, 2015). Polymer flow experiments that were history matched in this thesis were of low duration (weeks to months) and were conducted at room temperature. Consequently, process kinetics were limited, and chemical degradation was of minor significance for the HPAM polymers investigated.

Biological degradation refers to the microbial breakdown of polymer molecules by reaction with bacteria. Addition of a biocide is generally used to prevent occurrences of biological degradation. The synthetic HPAM polymers investigated in this thesis were not exposed to any significant extent of biological degradation during flow experiments due to their synthetic rather than biological nature.

The flexible coil structure of HPAM renders it highly susceptible to mechanical degradation during flow through porous media. Mechanical degradation refers to the breakdown (i.e. rupture) of polymer molecules as they are exposed to high mechanical stresses in flow through the porous medium (Sorbie, 1991). The effect of mechanical degradation is to significantly reduce the average molecular weight of the injected solution, thereby decreasing the hydrodynamic size of the polymer molecules. This can strongly reduce the polymer solution effectiveness in improving the mobility ratio inside the reservoir. The level of mechanical degradation experienced by semi-dilute polymer solutions in flow through porous media generally increase with polymer molecular weight (Morris & Jackson, 1978; Noïk et al., 1995; Stavland et al., 2010), solvent salinity (Smith, 1970; Maerker, 1975; Noïk et al., 1995), with decreasing porous medium permeability (Smith, 1970; Maerker, 1975; Morris & Jackson, 1978), and is independent of polymer concentration (Maerker, 1975; Noïk et al., 1995).

Several attempts have been made to predict the degree of HPAM mechanical degradation in porous media by using correlating groups, depending on factors such as stretch rate, dimensionless length, and maximum polymer flux at the sandface (Maerker, 1975; Morris & Jackson, 1978; Seright, 1983). Moreover, Seright (1983) showed that linear regression of internal pressure readings during polymer flow may be used to estimate the entrance pressure drop, and thus the degree of mechanical degradation experienced by the polymer in flow through linear core plugs. However, the flow out from the injectors in oil reservoirs are best mimicked by radial flow geometry, and mechanical degradation is thereby confined to the near-wellbore region where the injected solution attain its maximum velocities (Åsen et al., 2019). In contrast, the flow velocity remains constant in linear flow such that mechanical degradation of the polymer persists far beyond the injection point (Al-Shakry et al., 2018b). Consequently, the degree of polymer mechanical degradation occurring under realistic reservoir flow conditions may be overestimated based on linear core floods.

Mechanical degradation is typically measured by either screen factor measurements, or injected versus effluent viscosity measurements (Sorbie, 1991). During screen factor measurements, polymer solutions and corresponding solvents are typically flown

through a pack of five 100-mesh screens of known mesh density (Jennings et al., 1971). The screen factor is defined as the ratio of the flow time for the polymer solution to the flow time for the corresponding solvent. During injected versus effluent measurements, polymer viscosity is measured before injection and compared to viscosity measured after flow in porous media. In both measurement methods, the loss of screen factor and viscosity, respectively, are correlated to the irreversible viscosity loss associated with the occurrence of mechanical degradation in flow through porous media.

3.5 Resistance factors

Since polymers not only viscosify injected solutions, but also reduce the permeability of the porous medium by means of retention mechanisms, the polymer pressure response will be coupled by these two contributors during porous media flow. To separate the flow resistance caused by the viscosity enhancement from that caused by permeability reduction, three different factors have been introduced.

The resistance factor, R_F , is a measure of how much a single-phase polymer solution is able to reduce fluid mobility, relative to that of brine. Consequently, the resistance factor encompass both the polymer viscosity enhancement and permeability reduction caused by the polymer, and is defined as (Lake et al., 2014),

$$R_F = \frac{\lambda_b}{\lambda_p} = R_k \frac{\mu_p}{\mu_b} \quad \text{Eq. 3.1}$$

where R_k is the permeability reduction factor, defined as the ratio of permeability to brine and permeability to the polymer. The permeability reduction factor thus encompass both the reversible and irreversible permeability reduction caused by the polymer. Lastly, the residual resistance factor (R_{RF}) is a sole measure of the irreversible permeability reduction due to polymer retention, and is defined as the ratio of brine mobility before ($\lambda_{b,b}$) and after ($\lambda_{b,a}$) polymer flow:

$$R_{RF} = \frac{\lambda_{b,b}}{\lambda_{b,a}} \quad \text{Eq. 3.2}$$

3.6 Field experience

Polymer flooding is the most frequently implemented chemical EOR technique, and extensive field experience have been reported in the literature (Standnes & Skjevraak, 2014; Sheng et al., 2015). A comprehensive literature review encompassing 72 implemented and well-documented polymer field projects were reported by Standnes and Skjevraak (2014). Technical assessment of these projects revealed that 40 of them were classified as successes and only 6 were deemed discouraging. The remaining projects were either classified as promising (11), too early to tell (8), inconclusive (2), not evaluated (2), or did not report the technical assessment (3). In 92 % of the projects, HPAM was used as the polymer, while the remaining projects were implemented using biopolymers.

Various causes were reported as being responsible for the 6 technically discouraging cases. Mechanical degradation was reported in two of these projects, resulting in an irreversible viscosity loss which induced a lower target in-situ viscosity than expected. In another project, the salinity effect on polymer solution viscosity from mixing low salinity injection brine with high salinity formation water, was underestimated. Injectivity decline was reported in four cases and was suggested to be caused by plugging (mechanical entrapment) in low permeable media, and due to unexpectedly high levels of polymer adsorption.

During the last decade, polymer flooding has been evaluated for implementation in an increasing number of fields, both offshore and onshore. However, the discouraging cases demonstrate the need for improved polymer flow models for porous media. Accurate estimation of in-situ rheology and injectivity are crucial for evaluating both the technical and economic feasibility of any polymer flood project. Improving the modelling of polymer flow in porous media may not only facilitate an increase in implementation by de-risking projects, but may also help to avoid technical failures in circumstances where polymer flooding is not the best suited enhanced oil recovery mechanism. For these reasons, the main focus of this thesis is on the modelling of rheology and injectivity during polymer flow in porous media.

4. Polymer rheology

4.1 Bulk rheology

Rheology is the study of the flow behavior of fluids as they undergo deformation, and is a vast area of research (Sorbie, 1991). For polymer flooding applications, viscosity is of special interest, and is a measure of the internal resistance of fluids to deformation at a specified rate. For purely viscous fluids, the viscosity may be defined as its resistance to shear. The shearing stress, τ , between two thin fluid layers is given by,

$$\tau = \frac{F}{A} \quad \text{Eq. 4.1}$$

where F is the force vector parallel to the contact area, A , between the two fluid layers. As fluids are subjected to external shear stress, velocities of internal layers will be accelerated by means of viscous friction. To envisage the influence of shear stress on the velocities of internal fluid layers, we may consider a dynamic fluid volume confined between two plates, as shown in figure 4.1.

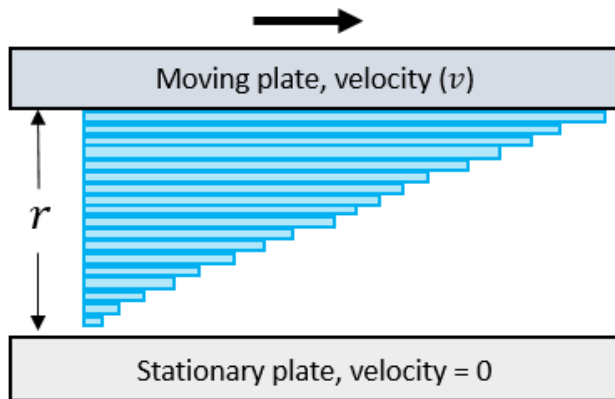


Figure 4.1: Schematic illustration of a dynamic fluid volume in simple shear flow.

While the upper plate is moving at a particular velocity, v , the bottom plate is stationary ($v = 0$). Thus, the fluid volume is subjected to an external shear stress originating from the upper plate. This results in a deformation of the fluid as fluid layers are accelerated in the flow direction. However, the resulting velocity of each fluid layer will decrease

with distance, r , from the moving plate, and the fluid layer immediately adjacent to the stationary plate will attain zero velocity. Thus, as a fluid is subjected to an external shear stress, a velocity gradient will develop within the fluid. This velocity gradient is known as shear rate, $\dot{\gamma}$, and is defined as,

$$\dot{\gamma} = \frac{dv}{dr} \quad \text{Eq. 4.2}$$

The relatively simple case where only shear stress is acting on the fluid volume and normal stress components are absent, is referred to as simple shear flow. Most low molecular weight substances exhibit Newtonian flow characteristics, i.e. in simple shear flow at constant pressure and temperature, the velocity gradient (shear rate) is linear. Consequently, shear stress will be proportional to the rate of shear, and the constant of proportionality is the dynamic fluid viscosity, μ (Deshpande et al., 2010),

$$\tau = \mu\dot{\gamma} \quad \text{Eq. 4.3}$$

Thus, for Newtonian fluids, their viscosity value is independent of shear rate. However, for a large class of high molecular weight substances, such as polymers, flow characteristics deviate significantly from Newtonian behavior, and are collectively classified as non-Newtonian fluids. For these fluids, the apparent viscosity, μ_{app} , is a viscosity function that depends on the shear rate,

$$\tau = \mu_{app}(\dot{\gamma})\dot{\gamma} \quad \text{Eq. 4.4}$$

and is typically measured as a function of shear rate using a rheometer. During the measurement process, polymer solutions in simple shear flow are subjected to various shear rates in a stepwise manner. It is not until steady state conditions are achieved that viscosity measurements are performed, and at this state is referred to as bulk viscosity. In simple shear flow, polymer solutions (e.g. HPAM) in the semi-dilute concentration regime typically exhibit a shear viscosity curve as shown in figure 4.2.

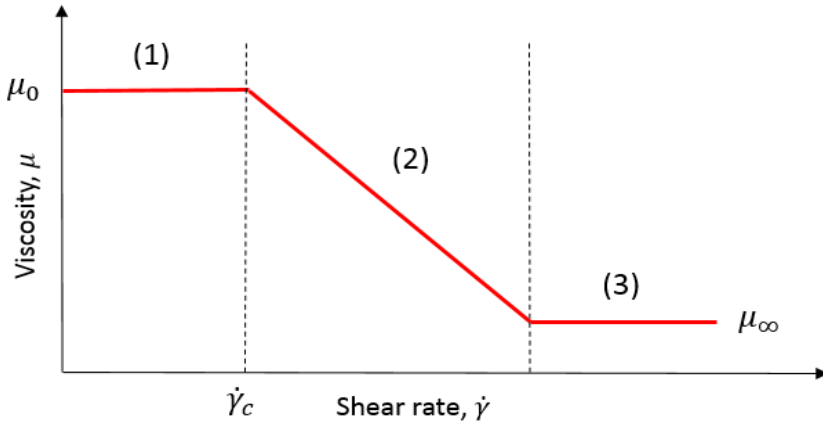


Figure 4.2: Typical shear viscosity curve for polymer solutions in simple shear flow.

4.1.1 Upper Newtonian plateau (1)

The hydrodynamic size of polymer coils and their concentration determines the polymer solution viscosity at low shear rates. In this shear rate regime, the interactions between polymer coils remains unchanged, and Newtonian behavior prevails. This region is typically referred to as the upper Newtonian plateau where the polymer attains its zero-shear viscosity value (μ_0).

4.1.2 Shear-thinning region (2)

As shear rates are increased beyond the upper Newtonian plateau, polymer coils are effectively forced apart and aligned in the flow direction. Consequently, interactions between polymer coils decrease and less friction forces arise as the polymer solution is flowing. Thus, the viscosity decreases with shear in this regime, and is referred to as shear-thinning (or pseudoplastic) behavior. The onset of shear-thinning is generally referred to as the critical shear rate, $\dot{\gamma}_c$.

4.1.3 Lower Newtonian plateau (3)

At shear rates exceeding those in the shear-thinning regime, interactions between polymer coils cease to exist and the polymer attain a minima viscosity value. This region is typically referred to as the lower Newtonian plateau where the polymer attains its infinite-shear viscosity value (μ_∞).

In the literature, several models have been suggested to describe polymer viscosity as a function of shear rate in simple shear flow. The most commonly encountered analytical model is the power law model, which consider only the shear-thinning region of the viscosity – shear rate relationship (Bird et al., 1960),

$$\mu(\dot{\gamma}) = K\dot{\gamma}^{n-1} \quad \text{Eq. 4.5}$$

where K is the flow consistency index and n is the flow behavior index (Deshpande et al., 2010). Thus, for a Newtonian fluid, n approach unity and K is merely the constant viscosity.

Another widely used model, which describes the three possible polymer behaviors in simple shear flow (figure 4.2) is given by the Carreau equation (Carreau, 1972),

$$\mu(\dot{\gamma}) = \mu_{\infty} + (\mu_0 - \mu_{\infty})[1 + (\lambda\dot{\gamma})^2]^{(n-1)/2} \quad \text{Eq. 4.6}$$

where μ_0 is the zero-shear viscosity, μ_{∞} is the infinite-shear viscosity, λ is the polymer relaxation time (chapter 4.2), and n is the power law flow behavior index.

4.2 Viscoelastic fluids

For an ideal elastic solid, shear stress is directly proportional to strain, γ , and the constant of proportionality is the Young's modulus, G , (Deshpande et al., 2010) i.e.,

$$\tau = G\gamma \quad \text{Eq. 4.7}$$

At the other extreme, Newtonian behavior was previously mentioned where shear stress was proportional to the rate of shear. In contrast to purely viscous fluids or perfectly elastic (Hookean) solids, viscoelastic fluids (e.g. HPAM) might demonstrate viscous and elastic responses simultaneously as they undergo deformation.

Viscoelastic fluids are commonly characterized by oscillatory shear flow measurements, which may be performed by rheometers. This characterization is performed by evaluating the response of viscoelastic fluids to strain that varies sinusoidally with time, t (Sorbie, 1991),

$$\gamma = \gamma_m \sin(\omega t) \quad \text{Eq. 4.8}$$

where γ_m is the amplitude and ω is the frequency of applied strain. Since shear stress for Hookean solids are linearly proportional to strain, while for Newtonian fluids, shear stress is linearly proportional to the rate of strain (i.e. shear rate), the viscous and elastic response will be out of phase by $\pi/2$. Thus, the component which is out of phase is associated with the viscous response of the fluid and the in-phase component is associated with the elastic response. Here, the latter is characterized by an elastic (or storage) modulus, G' , and provides information about the degree of elasticity of the fluid, while the former is characterized by the viscous (or loss) modulus, G'' , and provides information about the viscous properties of the solution.

Due to their elasticity, viscoelastic fluids will have a certain degree of memory of their flow history. Thus, as a viscoelastic fluid is subjected to deformation, it will attempt to return to its equilibrium state (or steady state condition). The required time for an elastic material to reach steady state conditions after deformation is referred to as the relaxation time. Not surprisingly, the relaxation time increases with the degree of viscoelasticity, or with the memory of the fluid. Thus, the relaxation time for Hookean solids are infinite, while Newtonian fluids have zero relaxation time. Polymer relaxation time may be estimated by plotting the storage (G') and loss (G'') moduli of the fluid as a function of angular velocity (Heemskerk et al., 1984; Volpert et al., 1998; Delshad et al., 2008; Erincik et al., 2018), as shown in figure 4.3.

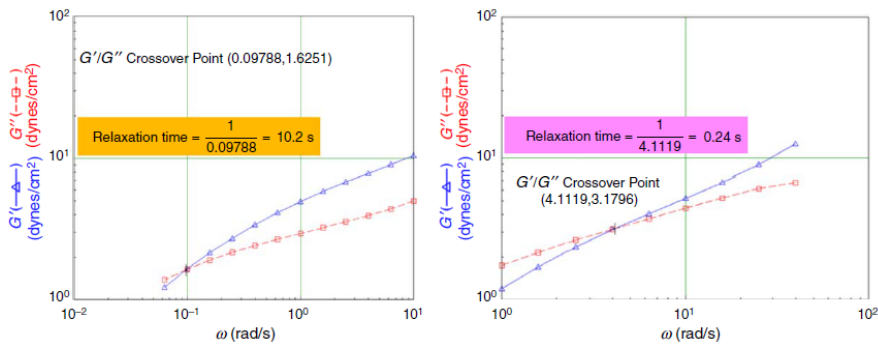


Figure 4.3: Relaxation times for Flopaam 3630S in low salinity (left) and high salinity (right) brine solutions (Erincik et al., 2018).

4.3 In-situ rheology

Polymer molecules are subjected to significantly different flow conditions in porous media compared to simple shear flow. Porous media exhibit an inherently complex geometry, including variations in pore sizes and geometries, where successive contraction-expansion channels (i.e. pore throats and pore bodies) have significant influence on the flow properties of viscoelastic polymers, as shown in figure 4.4 (Urbissinova et al., 2010).

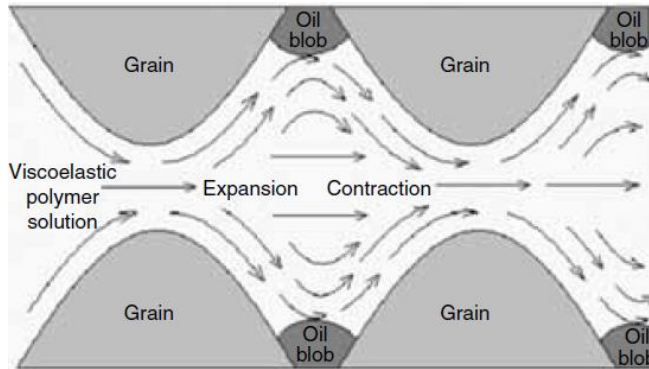


Figure 4.4: Schematic illustration of viscoelastic polymer flow in porous media (Urbissinova et al., 2010).

In contrast to simple shear flow, polymer solutions are exposed to a wide range of local shear rates at a particular volumetric flow rate in the porous medium. Furthermore, flow phenomena such as polymer retention and mechanical degradation adds on to the complexity of the polymer flow. To account for the contrasting flow conditions in simple shear compared to porous media flow, the macroscopic parameter apparent in-situ viscosity, μ_{app} , has been suggested to describe the fluid flow behavior of polymer solutions in porous media (Sorbie, 1991). This parameter is derived from Darcy's law for single-phase, non-Newtonian fluids,

$$\mu_{app} = \frac{kA \Delta P}{Q L} \quad \text{Eq. 4.9}$$

where k is porous medium (or absolute) permeability, A is cross sectional area of flow, Q is volumetric flow rate, and ΔP is pressure drop across a core of length, L .

Since polymer in-situ viscosity cannot be measured directly, it is typically estimated based on pressure measurements during flow experiments in rock cores, where brine and polymer solutions are injected alternatingly. While the pressure drop during brine flow is used to calculate porous medium permeability, pressure drop during polymer flow is used to estimate polymer in-situ viscosity as a function of flow rate (or Darcy velocity). However, since the polymer is retained as it flows through porous media, permeability to brine after polymer flooding may deviate significantly from the value obtained prior to polymer flow, i.e. the residual resistance factor (R_{RF}) is above unity.

There is an ongoing debate in the scientific community regarding which of these permeability values is the most representative to obtain the correct (or ‘true’) in-situ viscosity for the polymer (Skauge et al., 2015).

Advocates of using permeability to brine before polymer flow stresses the fact that some polymer typically remains in the porous medium, even after significant amount of post flush. Consequently, as the porous medium is flooded with brine after polymer flow, rate effects (e.g. hydrodynamic retention) may significantly affect pressure measurements, and in turn the permeability obtained. The polymer in-situ viscosity is therefore represented by the resistance factor (R_F) in circumstances where permeability to brine before polymer flow is used, and thereby incorporate both the viscosity enhancement and permeability reducing capability of polymer relative to brine.

Researchers favouring the use of permeability to brine after polymer flow asserts that since most of the polymer can be removed from the porous media after tapering (stepwise reduction of polymer concentration during injection) and significant post flush, polymer phenomena should be minimized during the subsequent brine flow. Furthermore, they claim that the flow of polymer may significantly alter the flow path of the subsequent brine through the porous medium. Therefore, the permeability obtained before polymer flow may not be representative of the actual flow path of the polymer and thus is an incorrect measure of the permeability to polymer. In cases where

permeability after polymer flow is used, the polymer in-situ viscosity is represented by the ratio of resistance factor to residual resistance factor (R_F/R_{RF}), and thus decouples the viscosity enhancement ability from the permeability reducing capability of the polymer relative to that of brine.

Due to the time-consuming and costly nature of polymer in-situ rheology measurements by core flood experiments, several attempts have been made to relate bulk and in-situ rheology based on polymer solution and porous media properties (Christopher & Middleman, 1965; Savins, 1969; Teeuw & Hesselink, 1980; Cannella et al., 1988; Sorbie et al., 1989; Fletcher et al., 1991; Pearson & Tardy, 2002; Lopez et al., 2003; Sochi, 2010). The various methods for describing the flow of non-Newtonian fluids in porous media consists of continuum models, capillary bundle models, numerical models, and pore-scale network models (Sochi, 2010).

To effectively relate the bulk and in-situ rheology of non-Newtonian fluids, flow velocities must be converted into ‘apparent’ shear rates within the porous medium (Sorbie, 1991). A widely used expression for relating the Darcy velocity, u , of flowing polymer solutions in porous media to the apparent (or effective) shear rate, $\dot{\gamma}$, was developed empirically by Chauveteau & Zaitoun (1981),

$$\dot{\gamma} = \alpha \frac{4u}{\sqrt{8k/\phi}} \quad \text{Eq. 4.10}$$

where α is a correction factor which is characteristic of the geometry and tortuosity of the porous medium, k is porous medium permeability and ϕ is porosity. However, since no universally accepted model for relating bulk and in-situ rheology exists, in-situ polymer rheology is modelled by performing flow experiment in rock cores.

4.4 Viscoelastic flow in porous media

The different rheological behaviors of viscoelastic fluids (e.g. HPAM) in flow through porous media, as estimated by flow experiments in rock cores, are shown in figure 4.5.

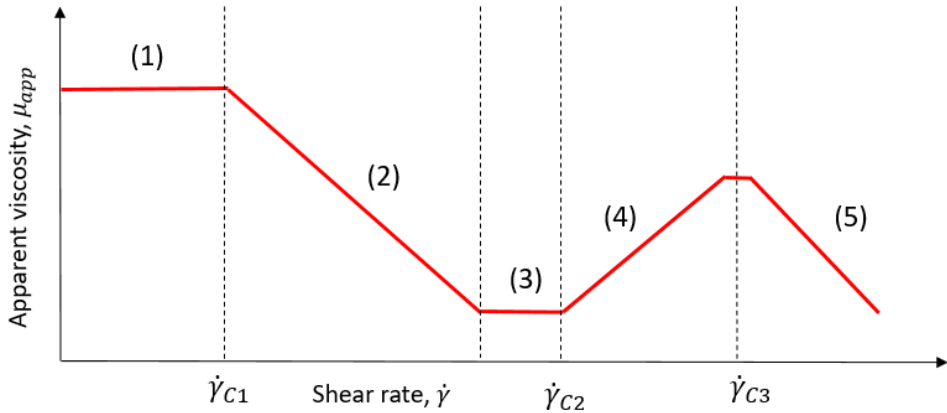


Figure 4.5: Schematic illustration of a typical in-situ rheology curve for viscoelastic fluids (e.g. HPAM).

4.4.1 Upper Newtonian plateau (1)

In accordance with its behavior in bulk flow, polymers may attain the zero-shear viscosity value at the upper Newtonian plateau. However, the zero-shear in-situ viscosity of polymers may be below the bulk fluid viscosity (Sorbie, 1991; Chauveteau et al., 1984; Zaitoun & Kohler, 1987). In these cases, the reduced in-situ viscosity could indicate that the polymer had a lower apparent concentration within the porous medium or that a slip effect was in operation where the layer adjacent to porous media walls was depleted of polymer. Within the semi-dilute concentration regime, the in-situ viscosity of HPAM is below its value in bulk for both adsorbing and non-adsorbing porous media (Chauveteau et al., 1984). Due to the relative increase of polymer concentration in the faster streamlines in the centre of pores, the effect of surface exclusion from pore walls is to accelerate the polymer solution through porous media. Another effect which accelerates polymer solutions relative to brine in flow through porous media is the inaccessible pore volume (IPV) phenomenon (Dawson & Lantz, 1972; Lötsch et al., 1985). In such circumstances, the polymer macromolecules are too large to enter a certain fraction of pore throats and are thereby not able to propagate through the entire pore space. Consequently, polymer molecules move in a subset of (larger) pores and tend to move ahead of tracer species which are transported through all pores.

Although they both accelerate the flow of polymer solutions in porous media, the mechanisms of the IPV and depleted layer phenomena, are significantly different. While the IPV phenomenon is due to steric hindrance of polymer molecules through small pores and only occurs in low permeability porous media, the depleted layer effect is due to the mechanism of steric repulsion between polymer molecules and pore walls, and occurs in all permeability ranges. In contrast, aforementioned polymer flow phenomena such as irreversible adsorption, mechanical entrapment and hydrodynamic retention will delay rather than promote earlier breakthrough of the polymer front.

4.4.2 Shear-thinning region (2)

As viscoelastic fluids propagate through porous media, the flow is generally characterized by both shear and extensional flow components. In the shear-thinning (or pseudoplastic) regime, viscous flow dominates and extension (or stretching) of the polymer molecules is negligible (Jones & Walters, 1989). Thus, the mechanism responsible for the shear-thinning behavior is very similar to that in bulk flow where separation of polymer coils and alignment in the flow direction reduce resistance to flow.

While the occurrence of shear-thinning in simple shear flow is well established, the behavior of semi-dilute polymer solutions at low flux through linear core plugs has been ambiguously reported in the literature. Based on flow experiments in linear core plugs, there has been reported Newtonian or near-Newtonian (Pye, 1964; Smith, 1970; Jennings et al., 1971; Seright et al., 2009; Seright et al., 2011; Rodriguez et al., 2014; Skauge et al., 2015; Zhang & Seright, 2015; Al-Shakry et al., 2018b), mild shear-thinning (Heemskerk et al., 1984; Masuda et al., 1992) and significant shear-thinning behavior of HPAM (Gogarty, 1967; Dupas et al., 2013; Manichand et al., 2013; Delamaide et al., 2014).

Seright et al. (2011) attempted to clarify the observed behavior of HPAM at low flux in flow through porous media by suggesting a set of limiting conditions for which occurrence of shear-thinning behavior was likely to occur. They suggested that occurrences of significant shear-thinning for undegraded HPAM in low permeability

porous media was caused by ultrahigh molecular weight polymers, or microgels. Due to their high propensity for being mechanically entrapped by the porous medium, these high molecular weight species are likely to reduce permeability and significantly increase the resistance factor at low flux. However, they suspected that these high molecular weight species would not propagate very far into the reservoir formation and that they might be retained by filtration or mechanically degraded at realistic reservoir conditions. They did recognize that in low salinity conditions (below 0.3% TDS), where the probability of mechanical degradation is limited (Maerker, 1975), and in very permeable porous media (above 1 Darcy permeability) where ultrahigh molecular weight species are able to effectively propagate far into the formation without forming external or internal filter cakes, shear-thinning behavior was likely to occur. In circumstances beyond their limitations, they suggested that the observed shear-thinning of HPAM could be an experimental artifact due to the use of insufficiently accurate pressure transducers during flow experiments. Indeed, in all aforementioned investigations where significant shear-thinning was reported, either the salinity of the make-up brine was below 0.3% TDS (Gogarty, 1967), or the porous medium permeability was significantly higher than 1 Darcy (Dupas et al., 2013; Manichand et al., 2013; Delamaide et al., 2014).

In contrast to the explanation provided by Seright et al. (2011), where microgels were considered responsible for the shear-thinning behavior of HPAM, Al-Shakry et al. (2019a) showed that concentrated solutions which had been either prefiltered or presheared, i.e. microgel-free, still exhibited shear-thinning behavior in porous media. Furthermore, Skauge et al. (2016) showed that linear and radial polymer flow were significantly different for a viscoelastic HPAM polymer in flow through Bentheimer sandstone. While Newtonian behavior was observed at low flux in linear flow, significant shear-thinning was observed during radial flow experiments.

Thus, it may appear that the mechanism(s) responsible for the existence of shear-thinning behavior of viscoelastic polymer solutions in porous media are still not quantified and that the flow geometry should be taken into account when modelling polymer flow in porous media.

Whether an EOR polymer shows Newtonian or shear-thinning behavior at low flux may have tremendous influence on the polymer solution's ability to provide improved mobility ratio conditions deep in the reservoir. Since shear-thinning solutions generally provide much higher viscosities at low flux (i.e. deep reservoir velocities) compared to Newtonian solutions, expected recovery will be significantly affected by the choice of polymer behavior. Consequently, modelling the polymer flow in an oil reservoir using Newtonian behavior if the fluid actually exhibits shear-thinning behavior would underestimate the economic and technical feasibility of the polymer flood project.

4.4.3 Lower Newtonian plateau (3)

While the lower Newtonian plateau is associated with the decreasing and ultimate cease of interactions between polymer coils in bulk flow, the situation is significantly different for viscoelastic fluids in flow through porous media. In porous medium flow, the lower Newtonian plateau represents the flux interval where neither the viscous nor elastic components of viscoelastic fluids dominate. Consequently, the flow behavior is apparently Newtonian. For fluids which shows no shear-thinning behavior in porous media, this region will merge with the upper Newtonian plateau.

4.4.4 Shear-thickening region (4)

Above some critical flow rate ($\dot{\gamma}_{c2}$), but still in the laminar flow regime, the elastic nature of HPAM will dominate its viscous counterpart. Consequently, the polymer molecules are subjected to significant amounts of stretching as the flow becomes extensional dominated. The significant increase in flow resistance during extensional flow is referred to as shear-thickening behavior and was first reported for viscoelastic polymer flow through porous glass beads (Dauben & Menzie, 1967).

Shear-thickening behavior has been used interchangeably in the polymer literature with extensional viscosity (Zamani et al. 2015), elongational viscosity (Vik et al. 2018), strain-thickening behavior (Glasbergen et al., 2015) dilatant behavior (Skauge et al. 2016) and viscoelastic behavior (Seright et al. 2011). However, these terminologies may not necessarily be identical since the origin of the increased flow resistance might be deviating. While concepts such as elongational viscosity and viscoelastic behavior

explicitly state that the increased flow resistance is (at least partly) due to the elastic properties of the polymer, concepts such as shear-thickening and dilatant behavior are more general and does not specify the origin of the increased flow resistance. In this thesis, shear-thickening behavior is used to describe the increased flow resistance with flux, and may originate from inelastic (viscous) and elastic polymer behavior.

Even though the shear-thickening behavior of HPAM in porous media is well-documented (Pye, 1964; Smith, 1970; Heemskerk et al., 1984; Masuda et al., 1992; Seright et al., 2011; Skauge et al., 2016; Al-Shakry, 2019a), and wide consensus exist concerning its occurrence, there is an ongoing debate in the scientific community regarding its origin (Rodriguez et al., 1993). Two main theories are adhered to by researchers, namely the coil stretch theory (De Gennes, 1974) and the transient network theory (Odell et al., 1988).

According to the coil stretch theory, the elongation (or stretching) of polymer molecules is accompanied by an accumulation of polymer molecules at the fluid surface rather than in the bulk of the fluid volume. Consequently, interactions between polymer molecules and porous media walls increase, which promotes higher resistance to flow. In contrast, the transient network theory asserts that the increased flow resistance as polymer molecules are stretched is due to the formation of transient networks internally in the fluid rather than increased friction forces at the fluid surface.

The flow of Newtonian fluids is often characterized by the dimensionless Reynolds number, N_{Re} , where the transition between different flow regimes such as laminar and turbulent flow may be quantified. The Reynolds number expresses the ratio of inertial to viscous forces, and for flow through a conduit may be defined as (Fanchi and Christiansen, 2017),

$$N_{Re} = \frac{\rho v D}{\mu} \quad \text{Eq. 4.11}$$

where ρ is fluid density, v is velocity through the conduit, D is diameter of the conduit, and μ is the bulk fluid viscosity. The Reynolds number is often of interest since the shift from laminar to turbulent flow for Newtonian fluids typically accompanies a

significant increase in flow resistance. However, for viscoelastic fluid flow in porous media, the sharp increase in flow resistance associated with shear-thickening behavior occurs in the laminar flow regime. Thus, the Reynolds number is not an appropriate parameter to differentiate between the different flow regimes of interest within polymer flooding applications. Thus, for viscoelastic polymeric fluids, the onset of shear-thickening ($\dot{\gamma}_{c2}$) associated with the transition from viscous to elastic dominated flow has been determined by using the Deborah number rather than the Reynolds number. The Deborah number, N_{De} , may be interpreted as the ratio of elastic to viscous forces and is generally defined as the ratio of the characteristic time of the polymeric fluid, θ_f , to the duration of the process, θ_p (Sorbie, 1991):

$$N_{De} = \frac{\theta_f}{\theta_p} \quad \text{Eq. 4.12}$$

For flow of viscoelastic polymer solutions through a porous medium, the characteristic time corresponds to the polymer relaxation time and the process time is equivalent to the travel time between successive pore throats. Consequently, the Deborah number is zero for Newtonian fluids (zero relaxation time) and infinite for Hookean solids (infinite relaxation time). The Deborah number has been used extensively in the literature to describe the polymer's viscoelastic effects (Marshall & Metzner, 1967; Savins, 1969; Bird et al. 1987; Vorwerk & Brunn, 1991; Kozicki, 2002) and particularly during polymer flooding studies (Heemskerk et al., 1984; Azad & Trivedi, 2017; Qi et al., 2017; Erincik et al., 2018).

Large discrepancies exist in the magnitude of the reported Deborah number in the literature, which is suggested to be the consequence of the inconsistency in using different relaxation and residential times (Azad & Trivedi, 2019). Furthermore, the Deborah number does not take into account the microscopic features of the porous medium, which have significant impact on the onset of extensional flow (Zamani et al., 2015). Thus, the Deborah number on its own is not considered to be adequate to predict the onset of extensional flow for viscoelastic polymer solutions in porous media.

The onset of shear-thickening for EOR polymers is of great concern for polymer flooding applications. As polymer solutions becomes increasingly shear-thickening, injection pressure increase and thus the injectivity (how easily the polymer may be injected) decreases. Consequently, as the onset of shear-thickening shifts towards lower velocities, the injectability at a particular volumetric injection rate is reduced. Thereby, the onset of shear-thickening has been given high attention in the literature.

Based on flow experiments using HPAM solutions in the semi-dilute concentration regime, the onset of shear-thickening shifts towards lower velocities with increasing polymer molecular weight (Heemskerk et al., 1984; Seright et al., 2009; Dupas et al., 2013; Skauge et al., 2015), aspect ratio of the porous medium (Chauveteau, 1981), in linear compared to radial flow (Skauge et al., 2016), with decreasing permeability (Heemskerk et al., 1984; Seright et al., 2011; Al-Shakry et al., 2019b), temperature (Heemskerk et al., 1984), and solvent salinity (Heemskerk et al., 1984; Chauveteau, 1981), and is independent of concentration (Seright et al., 2011; Skauge et al., 2015; Clarke et al., 2016).

4.4.5 Mechanical degradation (5)

As the flow resistance increases during extensional flow, the stress will at some point become so large that the bonds between the polymer molecules in solution are effectively pulled apart, and is referred to as mechanical degradation of the polymer (as described in chapter 3.4). This is an irreversible process where the solution viscosity abruptly decreases. As shear rates are increased further, the degree of mechanical degradation increases until the viscosity ultimately approach that of the solvent at infinitely high shear rates.

4.5 Reduction of residual oil by viscoelastic polymers

Although polymer flooding has primarily been implemented to accelerate oil production by sweep improvement, results from recent decades indicate that injection of viscoelastic polymer solutions may increase the microscopic displacement efficiency as well (Azad & Trivedi, 2019). The elastic properties of polymer solutions in flow through porous media are considered responsible for the reduction in residual oil saturation (S_{or}), where the majority of pore scale studies explain the S_{or} -reduction through the development of normal stress components during extensional flow (Wang et al., 2000; Xia et al., 2004; Yin et al., 2006; Jiang et al., 2008; Urbissinova et al., 2010; Afsharpoor & Balhoff, 2013; Vermolen et al., 2014; Qi et al., 2017). Furthermore, adsorption (Zaitoun & Kohler, 1987), elastic turbulence (Clarke et al. 2016), and wettability alteration (Seright, 2017) have been suggested as additional mechanisms that reduce S_{or} during polymer flooding.

5. Polymer injectivity

The injectability of polymer solutions into an oil reservoir is crucial to the economic feasibility of any polymer flood project (Wang et al., 2007; Sheng et al., 2015). Indeed, based on a simple cost analysis performed by Seright (2010), poor injectivity was suggested to have a more pronounced effect on the economics of heavy oil projects than the cost of the polymer itself. Injectivity, I , may be defined as the ratio of volumetric injection rate, Q , to the generated injection pressure, ΔP , (Seright, 1983):

$$I = \frac{Q}{\Delta P} \quad \text{Eq. 5.1}$$

5.1 Factors influencing polymer injectivity

While the viscosifying ability of water soluble polymers, which is imperative for mobility control, is the most obvious reason for an anticipated injectivity decline, several other mechanisms may have an impact as well. The three principal properties of EOR polymers which affect injectivity are (1) debris in the polymer, (2) in-situ polymer rheology, and (3) polymer mechanical degradation (Seright et al., 2009; Dupas et al., 2013; De Simoni et al., 2018).

5.1.1 Debris in the polymer (1)

During injection into oil reservoirs, debris in the polymer solution may accumulate at the sandface and lead to near-wellbore plugging (Burnett, 1975). As an external filter cake develops at the sandface, the generated injection pressure will increase and injectivity is reduced. Typically, filter tests using membrane or sand filters are used to assess plugging (Sorbie, 1991). However, since throughputs during lab filter tests are much lower than field throughputs, significant uncertainties in measurements may ensue (Seright et al. 2009). Formation plugging by polymers may be mitigated by pre-filtering or pre-shearing the polymer solution before injection (Glasbergen et al., 2015). While pre-filtering a polymer solution constitutes removing the insoluble particles which may accumulate at the sandface during injection, pre-shearing the polymer solution effectively removes the high molecular weight part of the molecular weight

distribution by mechanically shearing the polymer prior to injection. In conjunction with results reported by Dupas et al. (2013), Al-Shakry et al. (2019a) showed that pre-shearing HPAM solutions could improve injectivity while maintaining the low-flux in-situ viscosities. Thereby, injectivity could be improved while maintaining the mobility control properties of the injected solution which provides enhanced mobility ratio conditions for the displacement process. However, as polymer solutions were pre-sheared, the viscoelastic properties, which are considered responsible for the reduction of residual oil saturation, were less pronounced. Thus, the increasing injectivity may be at the cost of incremental oil recovery. In contrast, pre-filtering may improve the filterability of the polymer solution without affecting its viscoelastic properties and may be the preferred mitigation measure in some cases.

5.1.2 In-situ polymer rheology (2)

The non-Newtonian rheology of polymers as they flow through porous media is suggested to be the most crucial factor that affects polymer injectivity (Yerramilli et al., 2013; Li & Delshad, 2014). Since the flow out from the injectors in oil reservoirs is radial, the principal pressure drop occurs in the near-wellbore region where the injected fluid attains its maximum flow velocities. In this flow regime, viscoelastic polymer solutions such as HPAM typically exhibit shear-thickening flow behavior. Since the degree (or slope) of shear-thickening increase with molecular weight (Heemskerk et al., 1984; Dupas et al., 2013; Al-Shakry et al., 2019a), pre-shearing may be a viable option to reduce the viscoelastic properties and the associated shear-thickening ability of the polymer solution. However, since the viscoelastic properties of the polymer solution are considered responsible for its ability to improve microscopic displacement efficiency during flooding, it might again become a trade-off between injectivity and incremental oil recovery. Reduction in polymer concentration, which reduces polymer solution viscosity, can be another obvious mitigation for injectivity decline in cases where polymer in-situ rheology is the principal cause. However, this may reduce the polymer solution effectiveness in improving the mobility ratio deep inside the reservoir.

5.1.3 *Polymer mechanical degradation (3)*

As flow velocities are increased beyond some critical value, mechanical degradation of the polymer and an associated entrance pressure drop is recorded (Seright, 1983; Seright et al., 2011). Consequently, an irreversible viscosity reduction is imparted on the injected polymer solution as the high molecular weight polymer species are degraded into smaller ones. Due to the radial flow out from the injector in oil reservoirs, mechanical degradation occurs in the near-wellbore region where the polymer solution attain its highest velocities. Thus, mechanical degradation is considered to be a near-well effect with only minor degradation occurring deeper in the formation (Åsen et al., 2019). In conjunction with the mitigation measure for the shear-thickening behavior of HPAM solutions, preshearing may be performed to reduce mechanical degradation of the polymer in the near-wellbore region.

Polymer injection above the formation-parting pressure, and associated fracture growth, are often crucial to achieve acceptable injectivities (Seright, 2017). Indeed, under the proper circumstances, fractures can increase fluid injectivity, oil productivity, and sweep efficiency (Wang et al., 2008). In addition, fractures reduces the risk of mechanical degradation for polyacrylamide solutions. The key is to predict how the fractures would extend in the formation to determine whether the fracture growth will be adverse or favorable for the reservoir sweep efficiency. In cases where fracture growth is detrimental to the reservoir sweep and needs to be avoided, injection rates must be lowered and thus injectivity decline ensues. Additional details concerning the effects of fracture growth on injectivity can be found elsewhere (Saripalli et al., 1999; Gadde & Sharma, 2001; Wang et al., 2008; Lee et al., 2011; Zechner et al., 2015).

5.2 Injectivity models

Several researchers have proposed different models to estimate the injectivity of viscoelastic polymers. Seright (1983) developed a simple model for predicting polymer injectivity for viscoelastic fluids. His model separates the generated injection pressure into individual contributions for Newtonian flow, two-phase flow, entrance pressure (mechanical degradation) and shear-thickening. However, the model appears to

significantly overestimate the injection pressure drop during radial flow, especially at high flux, which is most critical for injectivity.

Yerramilli et al. (2013) proposed a numerical model for predicting polymer injectivity during single-phase flow of polymer solutions in porous media. However, since this model is only valid in the shear-thinning regime, it may not be able to provide accurate estimates for viscoelastic polymer solutions which additionally exhibit shear-thickening behavior in the porous medium.

Li & Delshad (2014) developed and implemented an analytical polymer injectivity model in simulation software. The model improved calculations, especially for coarse well block sizes, and was able to incorporate both the shear-thinning and shear-thickening behavior of polymers. Polymer injectivity was successfully captured by simulation of a pilot field-scale polymer flood without the need to introduce empirical parameters.

Lotfollahi et al. (2016) proposed an injectivity model which they successfully used to history match field injection pressures at different rate steps. Furthermore, they attributed the pressure increase in polymer injectors to (1) the formation of an oil bank, (2) shear-thickening behavior near the wellbore, and (3) external cake build-up by polymer plugging.

Despite of extensive research and improved injectivity models, the prediction of polymer injectivity remains elusive. Indeed, polymer injectivity is subject to a high degree of controversy and discussions in the literature. In particular, it has been implicitly assumed that the in-situ rheology of polymers may be estimated from linear flow experiments. However, significant deviation was observed between linear and radial polymer flow by Skauge et al. (2016) which suggest that the radial flow geometry of polymer solutions as they are injected into oil reservoirs should be taken into account. Thus, before accurate and reliable polymer injectivity models can be developed, polymer in-situ rheology must be quantified in radial flow since it best mimicks the flow out from the injector in oil reservoirs. Consequently, the focus of this thesis is on the mechanistic modelling of radial polymer flow in porous media.

6. Estimation of polymer in-situ rheology

As polymer molecules are subjected to significantly different flow conditions in porous media compared to simple shear flow, polymer in-situ rheology cannot be measured in rheometers, and is therefore estimated based on pressure measurements during flow in rock cores. The purpose of this chapter is thereby to provide adequate background material concerning the methodology for estimating polymer in-situ rheology from flow experiments.

6.1 Polymer in-situ rheology from linear flow experiments

Generally, polymer in-situ rheology has been estimated by conducting flow experiments in linear core plugs, as shown in figure 6.1. During linear flow experiments, brine and polymer solutions are alternatingly injected into the porous rock and the steady state (or stabilized) pressure drop across the core plug is measured at specified injection rates.

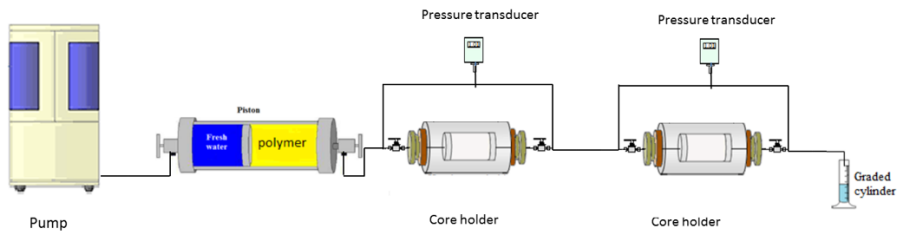


Figure 6.1: Schematic illustration of linear flow experiment (Skauge et al., 2015).

The polymer in-situ rheology is then estimated by calculating resistance factors at each volumetric injection rate, defined as,

$$R_F = \frac{\Delta P_p}{\Delta P_b} \quad \text{Eq. 6.1}$$

where ΔP_p and ΔP_b is the pressure drop across the core during polymer and brine flow, respectively. Consequently, a single (discrete) value of resistance factor is obtained for each volumetric injection rate.

As mentioned in chapter 4.3, there is an ongoing debate in the scientific community on whether to use the measured pressure drop during the brine flow before or after the injection of polymer. In circumstances where the pressure drop before polymer injection is used, apparent in-situ viscosity of the polymer is represented by the resistance factor (R_F) and thus incorporate the viscofying ability and the permeability reducing capability of the polymer. Conversely, when the pressure drop after polymer flow is used, apparent in-situ viscosity is represented by the ratio of resistance factor to residual resistance factor (R_F/R_{RF}), and thereby decouples the apparent in-situ viscosity from the irreversible permeability reduction.

In circumstances where the polymer is mechanically degraded during linear flow, the functional form of the in-situ rheology curve may become distorted as the calculated in-situ viscosity is coupled with mechanical degradation above some critical flow rate. As mentioned in chapter 3.4, Seright (1983) showed that linear regression of internal pressure readings during polymer flow may be used to estimate the entrance pressure drop, and thus the degree of mechanical degradation experienced by the polymer in flow through linear core plugs. However, as velocity remains constant in linear flow, mechanical degradation of the polymer may persist far beyond the injection point (Al-Shakry et al., 2018b; Åsen et al., 2019). Consequently, the entrance pressure drop correlations may underestimate the degree of mechanical degradation unless the degradation can be considered a near-well (or entrance) effect.

6.2 Polymer in-situ rheology from radial flow experiments

Polymer in-situ rheology may also be estimated by conducting flow experiments in radial discs with internal pressure ports distributed between the injector and producer, as shown in figure 6.2. In conjunction with the linear flow experiment, brine and polymer solutions are injected alternatingly. The fluids are injected at the centre of the disc and propagates radially towards the producer at the circumferential rim. The stabilized pressure drop is then measured between each pressure port and the producer, at specified injection rates. The pressure drop, ΔP , between a particular pressure port

at radius r_i and the production rim at r_e , may be described by Darcy's law for radial flow,

$$\Delta P = \frac{\mu_{app} Q}{2\pi h k_b} \ln \frac{r_e}{r_i} \quad \text{Eq. 6.2}$$

where μ_{app} is apparent (in-situ) viscosity, Q is volumetric injection rate, h is disc thickness, and k_b is permeability to brine.

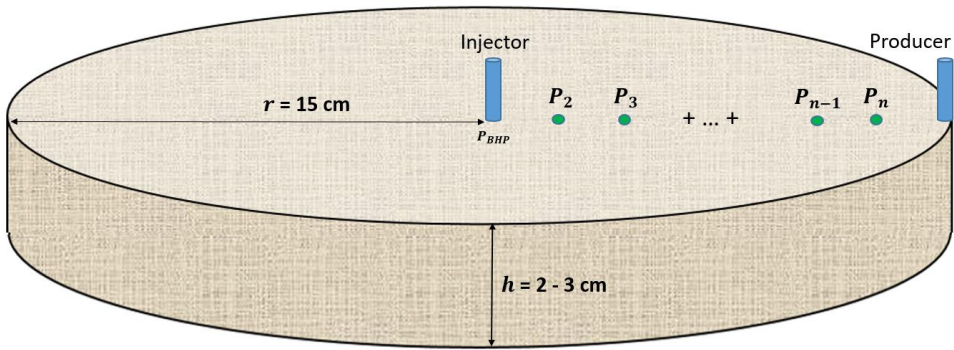


Figure 6.2: Disc used for radial flow experiments.

In contrast to the linear flow regime, velocity decreases as $1/r$ in radial flow. Thus, the polymer is exposed to an interval of flow velocities at each volumetric injection rate, ranging from the maximum velocity at the injection point to the minimum velocity at the production rim.

Unlike linear flow experiments where a single (discrete) value of in-situ viscosity is obtained at each injection rate, continuous in-situ rheology curves are obtained from each injection rate in radial flow experiments. Thus, to estimate permeability and polymer in-situ viscosity from brine and polymer floods during radial flow experiments, respectively, history matching of the pressure data may be performed. History matching is a type of inverse problem where an observed behavior is used to estimate model variables that caused the behavior (Oliver & Chen, 2011). In radial flow experiments, the observed behavior (pressure drop) is used to estimate model variables that caused the behavior such as permeability and polymer in-situ rheology.

In the process of history matching radial flow experiments, the permeability obtained during brine flow (either before or after polymer flow) is used as a constant input parameter when the polymer flow pressure data is being history matched. Thus, history matching radial flow experiments to obtain the polymer in-situ rheology relies on the assumption that permeability to brine and polymer are equal. In cases where the flow path of the polymer deviates significantly from that of brine, indicated by high values of the R_{RF} , the assumption of equal permeabilities could induce uncertainties to the interpretation of results. However, in polymer flow experiments with low values of the R_{RF} , the assumption of equal permeability to brine and polymer may be justified.

6.3 History match methods for radial flow experiments

For radial flow experiments with internal pressure ports distributed between the injector and producer, differential pressure may be history matched as a function of either volumetric injection rate, $dP(Q)$, or radial distance $dP(r)$.

6.3.1 *Single port match method (SPMM)*

Using the single port match method (SPMM), differential pressure during polymer flow is history matched as a function of volumetric injection rate, $dP(Q)$, yielding continuous in-situ rheology curves based on the pressure drop between each pressure port and the producer. While the in-situ rheology curve obtained from history matching the pressure drop between injection bottom-hole pressure (BHP) and the producer spans the entire velocity interval of the polymer, differential pressure between internal pressure ports and the producer span decreasing intervals of the complete in-situ rheology curve as we move towards the producer.

In flow through porous media, polymer solutions will contract and expand in pore throats and pore bodies, respectively. Through a series of pore scale experiments, Chauveteau (1981) showed that the in-situ rheology of HPAM depends on the number of prior contraction events experienced by the fluid, i.e. on the polymer history. Since the number of contraction events increase with radial distance, the polymer will have a different pre-history at different locations in the radial disc. Thus, to investigate

potential memory effects (at the Darcy scale) of elastic polymers, differential pressure between each pressure port and the producer is history matched using the SPMM.

In conjunction with the in-situ rheology obtained from linear flow experiments, rate dependent phenomena such as mechanical degradation may distort the functional relationship of the in-situ rheology curve obtained by the SPMM. Even though mechanical degradation in radial flow is considered to be an entrance (or near-well) effect, the pressure gradient is non-linear in radial flow such that the linear regression method suggested by Seright (1983) cannot be used to estimate the entrance pressure drop, which is correlated with mechanical degradation.

6.3.2 *Disc match method (DMM)*

In radial flow experiments with internal pressure ports, differential pressure may also be history matched as a function of radial distance, $dp(r)$. Thus, an individual in-situ rheology curve is obtained for each volumetric injection rate. However, since the velocity interval varies with volumetric injection rate, obtained in-situ rheology curves will span different velocity intervals. In contrast to the SPMM, each in-situ rheology curve is obtained at a particular injection rate such that rate effects (e.g. mechanical degradation) may be assessed.

In-situ rheology curves obtained using the DMM may be distorted by memory effects because the measured pressure drops originate from a polymer solution with different pre-history at the various locations in the porous media. However, these memory effects could be evaluated using the SPMM. Thus, by combining the SPMM and the DMM, both rate and memory effects can be evaluated separately, and the obtained in-situ rheology curves should optimally be investigated using history match results from both methods.

In two-phase flow experiments, where residual oil is distributed non-uniformly throughout the radial disc, the effective permeability changes as the polymer propagates between the injector and producer. The effect of non-uniform residual oil saturation on the permeability may be accounted for by allowing use of local permeability variation (Skauge et al., 2016). Conversely, individual permeabilities

between each pressure port and the producer (during brine flow) may be estimated using the SPMM. Consequently, the polymer pressure response could be normalized to the same permeability such that deviating flow conditions due to the permeability variation are effectively decoupled from the polymer pressure response. While local permeability variation was used to account for the non-uniform residual oil saturation in Paper 1, correction factors were calculated and the polymer pressure data was normalized in Papers 2-4.

6.4 Simulation and history match tools

6.4.1 *Simulation tool*

The reservoir simulation tool used to history match radial flow experiments in this thesis is the STARS (black oil) simulator by Computer Modelling Group (CMG). STARS was chosen due to its applicability for advanced modelling of polymer flooding processes, and due to its ability to incorporate the full spectrum of possible rheology behaviors exhibited by HPAM in flow through porous media, i.e. shear-thinning, Newtonian and shear-thickening fluid behavior.

In addition to general petrophysical and fluid properties, the script files used to run simulations in STARS contained polymer specific properties and corresponding keywords such as velocity dependent viscosity (SHEARTAB), adsorption (ADSTABLE), inaccessible pore volume (PORFT) and residual resistance factor (RRFT). For additional details regarding keywords and governing mass conservation equations used by the simulator tool, the reader is referred to the STARS user manual (Computer Modelling Group, 2016).

6.4.2 *Automatic history match tool*

The investigation of noise and cumulative pressure measurement error on in-situ rheology from radial flow experiments (Paper 2 and 3) was performed by using the automatic history match tool CMOST by CMG. History match operations were conducted automatically rather than manually to exclude any pre-biasness from affecting the ultimate outcome of the investigations.

Several different history match engines are available to perform automatic history match operations in CMOST. In this thesis, the Particle Swarm Optimization (PSO) engine was mainly used, and proved to be time-efficient and converged to acceptable global history match minima in most cases. However, as mentioned in Paper 2 and Paper 3, the PSO engine experienced difficulties converging towards acceptable global minimum values in a few cases. For these cases, the more robust, albeit more time consuming engine, Bayesian Markow Chain Monte Carlo (MCMC), was used.

To perform automatic history match operations, a field history file (FHF) containing the generic pressure data from an arbitrarily chosen in-situ rheology curve was loaded into the CMOST application. CMOST would then attempt to history match the provided pressure data by determining six various parameters in an implemented fluid equation. The fluid equation which was used in CMOST is an extended version of the Carreau equation (Delshad et al., 2008), which include the shear-thinning, Newtonian and shear-thickening behavior of viscoelastic fluids in flow through porous media:

$$\mu_{app} = \mu_{\infty} + \frac{\mu_0 - \mu_{\infty}}{(1 + (\lambda_1 u)^2)^{\frac{1-n_1}{2}}} + \mu_{max}[1 - \exp(-(\lambda_2 u)^{n_2-1})] \quad \text{Eq. 6.3}$$

where μ_{app} is apparent in-situ viscosity, μ_{∞} and μ_0 are limiting Newtonian viscosities at high and low shear limits, respectively, λ and n are empirical constants, u is superficial velocity of the polymer and μ_{max} is the shear-thickening plateau viscosity.

6.5 Radial simulation model and sensitivity analysis

The simulation model used in conjunction with the STARS simulation tool is illustrated in figure 6.3, which shows the decreasing velocity with distance from the injector in radial flow. In accordance with the discs used for the radial flow experiments which were history matched in this thesis, the simulation model consisted of a radial disc with radius of 15 cm and thickness between 2-3 cm. The radial grid was made up of 150 concentric rings with uniform length, $\Delta r=0.1$ cm.

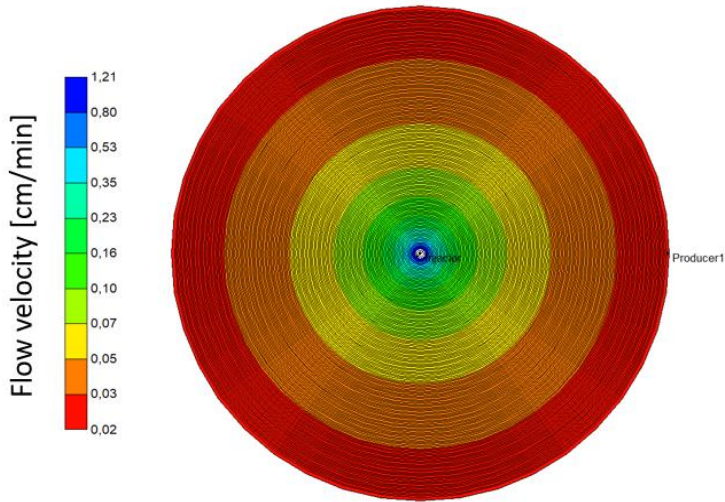


Figure 6.3: Simulation model used in conjunction with simulations in STARS.

Prior to history matching the radial flow experiments, a comprehensive sensitivity analysis on the simulation model was performed, where the following parameters (with associated keywords) were investigated: grid block size, maximum timestep (DTMAX), molecular weight (CMM), polymer adsorption (ADSTABLE), inaccessible pore volume (PORFT), and residual resistance factor (RRFT).

The grid block size of the concentric rings making up the simulation model had significant impact on the stabilized pressure drop. Indeed, the rapid pressure drop with distance from the injector during radial flow increase the sensitivity of the calculations to grid block size. As grid block size approached 0.1 cm, negligible accuracy improvements were obtained, as shown in figure 6.4. Consequently, the simulation model was ran with 150 grid blocks for all simulations conducted in this thesis.

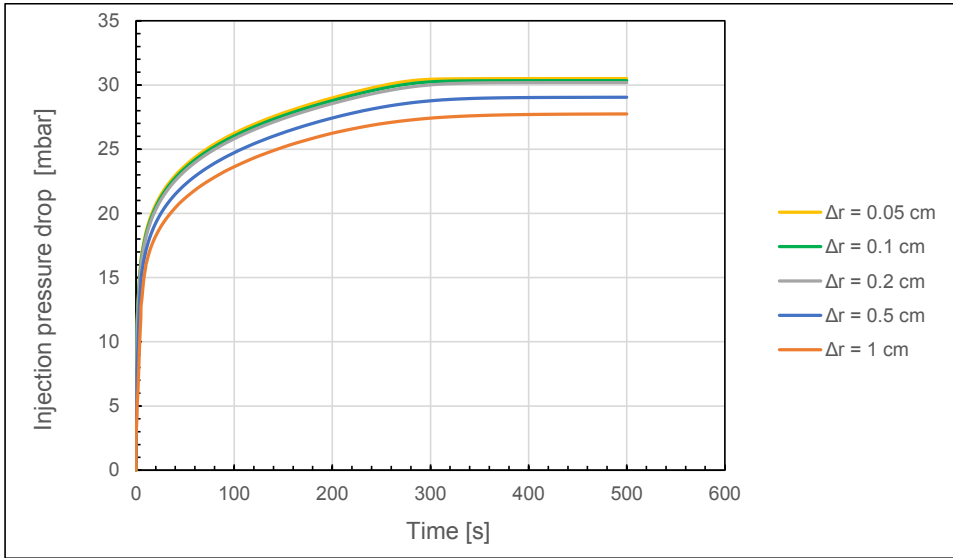


Figure 6.4: Sensitivity analysis of grid block size.

The number of successive iterations performed by STARS is determined by the timestep sizes specified in the simulation file. Results showed that maximum timestep (DTMAX) had negligible influence on the stabilized pressure drop during simulations.

As mentioned in chapter 3, polymer and porous media properties such as polymer molecular weight (CMM), polymer adsorption (ADSTABLE), and inaccessible pore volume (PORFT), have significant influence on the flow of polymer solution in porous media. However, since permeability (PERMI) and the velocity dependent in-situ polymer viscosity (SHEARTAB) were explicitly specified in the simulation file, negligible influence on the stabilized pressure was observed from changing CMM, ADSTABLE or PORFT. The effect of choosing residual resistance factor (RRFT) above unity had the same effect on stabilized pressure as lowering the permeability. However, the RRFT was kept constant ($RRFT = 1$) for all simulations performed.

In conclusion, the only two parameters which were altered and which significantly influenced the stabilized pressure drop were the two tuning parameters during brine and polymer flow, namely permeability (PERMI) and the velocity dependent in-situ viscosity (SHEARTAB). Thus, an explicit analysis of polymer in-situ rheology could be performed using the constructed simulation model in STARS.

7. Results and discussion

7.1 Introduction

The current chapter contains three different sections that summarize and discuss the principal results and observations obtained during the course of this thesis. The chapter is concluded with a final section (7.5) which summarizes the results presented.

Section 7.2 presents the qualification of history match methods which are used to estimate polymer in-situ rheology from radial flow experiments. Herein, the principal results from **Paper 2** and **Paper 3** are presented, where the effects of pressure measurement noise and cumulative measurement error during radial flow experiments on the obtained in-situ rheology curves, are assessed. Lastly, results from **Paper 4** are shown where the pressure build-up during radial polymer flow is analysed to increase anchoring data for in-situ rheology estimation from field injectivity tests.

Section 7.3 summarizes the results on rate and memory effects of the HPAM polymers investigated in **Paper 2** and **Paper 3**. In addition, unpublished results on the rate and memory effects of a higher molecular weight HPAM polymer, is presented.

Section 7.4 quantifies polymer in-situ rheology and polymer injectivity. Here, the main results from **Paper 1** are presented, where the impact of oil on polymer in-situ rheology was investigated. Furthermore, additional analysis is presented on the impact of flow geometry on in-situ rheology in both absence and presence of oil. Lastly, the behavior of HPAM at low flux is addressed and new insights are given.

7.2 Qualification of history match methods for radial flow

Conventionally, pressure drop versus volumetric injection rate data from linear core floods have been used to measure the in-situ rheology of non-Newtonian fluids in porous media. However, linear flow is characterized by steady-state conditions, in contrast to radial flow where both pressure and shear-forces have non-linear gradients. Indeed, Skauge et al. (2016) demonstrated that linear and radial polymer flow in porous media is significantly different, and suggested that the observed deviation was a consequence of the time-dependent nature of the polymer. In their work, the recently developed history match method for radial flow (the disc match method) was employed where differential pressure was history matched as a function of radial distance, $dP(r)$.

7.2.1 Pressure measurement noise analysis

Although the disc match method (DMM) has been applied in several papers recently (Skauge et al., 2016; Skauge et al., 2018), effects of measurement noise from pressure transducers on the estimated in-situ rheology curves, has not been quantified. Moreover, it has been suggested that the observed shear-thinning behavior of HPAM at low flux in porous media may in some cases be an experimental artifact due to the use of insufficiently accurate pressure transducers (Seright et al., 2009).

To quantify the effect of pressure measurement noise on the estimated polymer in-situ rheology using the DMM, a reference (base case) in-situ rheology curve was constructed by specifying the six parameters required in the extended Carreau equation (Eq. 6.3), as shown in Paper 2. This completely generic reference curve was then used as input during simulation runs in STARS in order to create a dataset which was perfect, i.e. without any influence of measurement noise on the pressure data. Furthermore, this dataset was randomly ‘contaminated’ with different degrees of pressure measurement noise (5, 10, and 20 %) to identify the upper noise limit below which reliable estimates of the reference in-situ rheology could be made. Thus, how much pressure measurement noise is tolerable during radial flow experiments (using the DMM) before the estimated in-situ rheology significantly deviate from the reference behavior, and the polymer in-situ rheology signal is lost in noise?

Results from the pressure measurement noise analysis showed that the upper noise limit below which accurate estimates of polymer in-situ rheology could be made (using the DMM) was $\pm 10\%$ pressure measurement noise, as shown in figure 7.1.

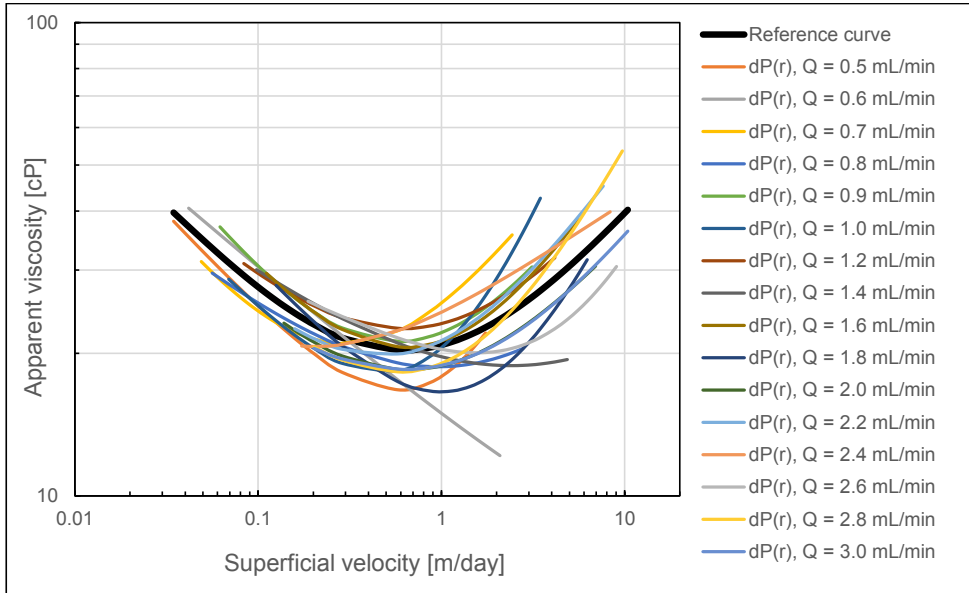


Figure 7.1: Comparison of reference and estimated in-situ rheology curves after $\pm 10\%$ pressure measurement noise, using the DMM.

At low to intermediate flux, all estimated in-situ rheology curves was in agreement with the reference behavior, i.e. significant shear-thinning behavior was observed. At intermediate to high flux, a significant deviation from the reference rheology was observed ($Q = 0.6$ mL/min), in which the estimated in-situ rheology curve displayed shear-thinning rather than the shear-thickening reference behavior. However, the overall behavior of the estimated in-situ rheology curves was compelling, which was evident from their arithmetic average (figure 7.2). Here, the only occurrence of non-negligible deviation from the reference behavior was located at the upper velocity boundary where the number of rates spanning the velocity interval is at its minimum. Thus, reliable estimates of polymer in-situ rheology from history matching radial flow experiments could be made at pressure measurement noise below 10 %, using the DMM.

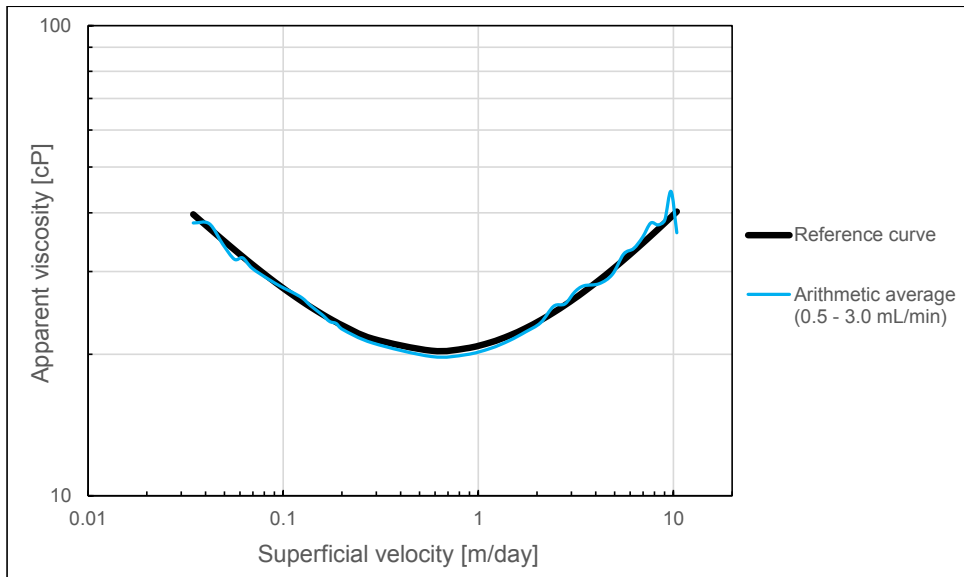


Figure 7.2: Comparison of reference and arithmetic average of estimated in-situ rheology curves (0.5 – 3.0 mL/min) after $\pm 10\%$ pressure measurement noise, using the DMM.

Fuji FCX series pressure transducers are typically used in conjunction with in-house radial flow experiments, and the manufacturer state a maximum uncertainty of $\pm 0.04\%$ of the full-scale (or maximum preset) pressure range. Thus, the assertion made by Seright et al. (2009) that insufficiently accurate pressure transducers is responsible for the observed shear-thinning behavior of HPAM at low flux in porous media is considered very unlikely for in-house flow experiments.

The flow distance between the injector and the production rim, i.e. the radius of the Bentheimer discs used in conjunction with the radial flow experiments which were history matched in this thesis, was 15 cm. To assess the sensitivity of the estimated in-situ rheology to disc radius, the reference dataset containing $\pm 10\%$ pressure measurement noise was history matched a second time using the DMM. However, during the second history match operation, only the pressure data originating from pressure ports distributed between the injector and radial distance of 4 cm was used. Thus, the number of pressure ports used to estimate in-situ rheology by history matching was reduced from 9 to 5.

Results demonstrated that the estimated in-situ rheology curves were nearly invariant between using pressure data from 5 compared to 9 pressure ports, i.e. history matching only the first 4 cm of the radial distance compared to the entire radii of the radial disc (figure 7.3). It was thereby suggested in Paper 2 that the polymer in-situ rheology is mainly defined by the pressure data originating from the near-wellbore region in radial flow.

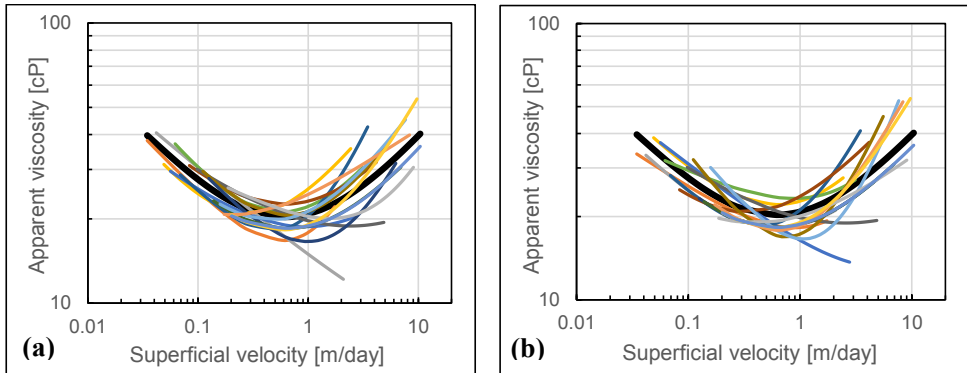


Figure 7.3: Comparison of reference and estimated in-situ rheology curves after ± 10 % pressure measurement noise, using the DMM with (a) 9 pressure ports (entire disc) and (b) 5 pressure ports (first 4 cm of the radial distance).

7.2.2 Pressure measurement error analysis

During radial flow experiments, not only pressure measurement noise, but also additional sources of uncertainties are present such as the manual placement of internal pressure ports and dynamic offset values. During the noise analysis, all pressure ports were assigned the same relative percentage error. However, the uncertainty of pressure transducers are typically stated as a percentage of the full-scale (or maximum preset) pressure range. Thus, if all pressure ports are adjusted to the same maximum pressure range during injection at a particular injection rate, the relative measurement error will increase with radial distance. In addition, static offset values which might deviate from the dynamic ones during polymer flow, are measured for individual pressure ports and may in some cases constitute a significant fraction of the measured pressure values at low injection rates. The pressure measurement noise analysis in Paper 2 was thereby

expanded in Paper 3 to quantify the influence of effective (or realistic) pressure measurement error during radial flow experiments.

In accordance with the noise analysis in paper 2, a reference (base case) in-situ rheology curve was constructed using the extended Carreau equation (Eq. 6.3) to obtain a reference dataset, free of pressure measurement error. While the generic (or reference) dataset in Paper 2 was ‘contaminated’ with a constant relative percentage noise for all pressure ports, the relative error increased with radial distance in the pressure measurement error analysis in Paper 3. Pressure measurement error during in-house radial flow experiments was suggested to be below $\pm 1\%$ of the maximum preset pressure, and was therefore added to the reference dataset and automatically history matched in CMOST using both history match methods, the DMM (figure 7.4) and the SPMM (figure 7.5), as thoroughly explained in Paper 3.

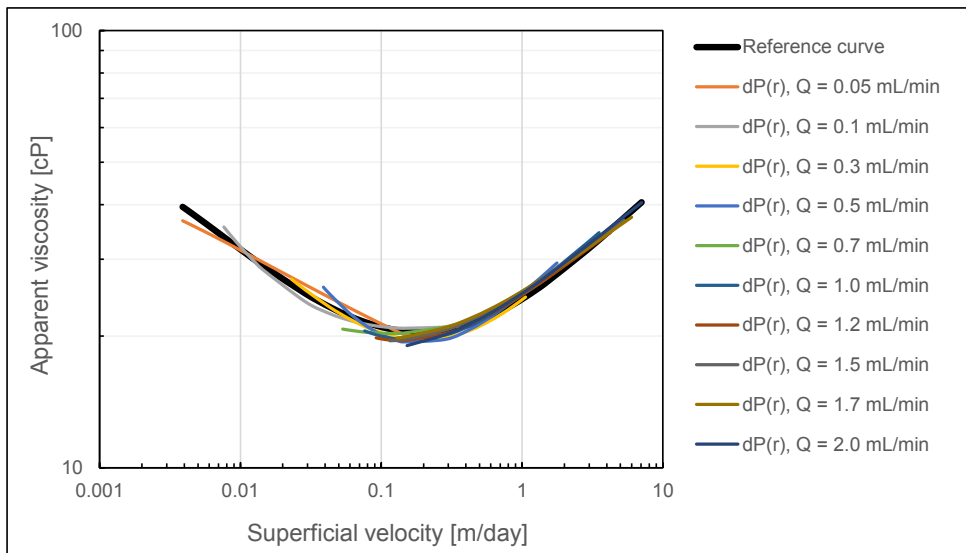


Figure 7.4: Comparison of reference and estimated in-situ rheology curves after typical ($\pm 1\%$) pressure measurement error, using the DMM.

Excellent agreement between the reference and history matched in-situ rheology curves are observed using both the DMM and the SPMM. These results clearly demonstrate the robustness of each method under experimentally realistic error conditions. As expected, the deviation from the reference in-situ rheology increase with radial distance

in accordance with the relative error, as shown in figure 7.5 where the maximum deviation is observed for the in-situ rheology curve obtained from the pressure drop between port 9 (10 cm) and the producer. To identify the threshold error level below which reliable estimates of polymer in-situ rheology could be made, the error was increased in a stepwise manner until significant deviation from the reference in-situ rheology was observed. This error level was determined at $\pm 5\%$ of the maximum (or full-scale) pressure range.

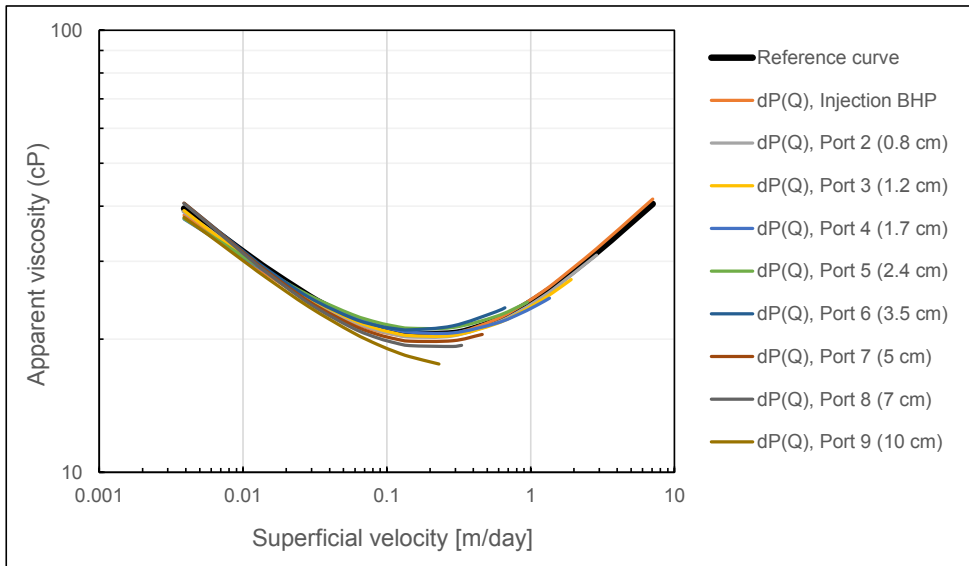


Figure 7.5: Comparison of reference and estimated in-situ rheology curves after typical ($\pm 1\%$) pressure measurement error, using the SPMM.

7.2.3 Evaluation of radial history match methods

To assess the results from the pressure measurement error analysis, a radial polymer flow experiment with internal pressure ports was history matched using the DMM and the SPMM. A relatively low molecular weight HPAM polymer (Flopaam 3330S, 8 MDa, 1000 ppm) was injected into a radial Bentheimer disc, saturated with residual oil. Injected versus effluent bulk viscosity measurements showed negligible occurrence of mechanical degradation. Thus, in the absence of memory and rate effects, pressure measurement error should be solely responsible for discrepancies between the in-situ rheology obtained from the DMM and the SPMM. However, the residual oil saturation was not distributed uniformly between the injector and producer. As explained in Paper

3, non-uniform residual oil saturation and pseudo-skin effects during radial flow experiments may distort the true functional relationship of the history matched polymer in-situ rheology if not accounted for explicitly. Since these effects are also present during brine flow, and since X-ray imaging showed no additional displacement of oil by polymer, they could be incorporated into the permeability and effectively be decoupled from the polymer in-situ rheology.

The SPMM was used to history match the permeability to brine between each pressure port and the producer and confirmed the local permeability variation with radial distance. To account for the local permeability variation, a correction factor was calculated, defined as the ratio of the permeability across the entire disc (global) to the local permeabilities between individual pressure ports and the producer. Internal polymer pressure data was then adjusted by the individual correction factors such that the global permeability would apply for the entire radial distance between the injector and the production rim. Since permeability to brine after polymer flow was used, the history matched in-situ rheology curves using the DMM and the SPMM is shown as (R_F/R_{RF}) in figure 7.6.

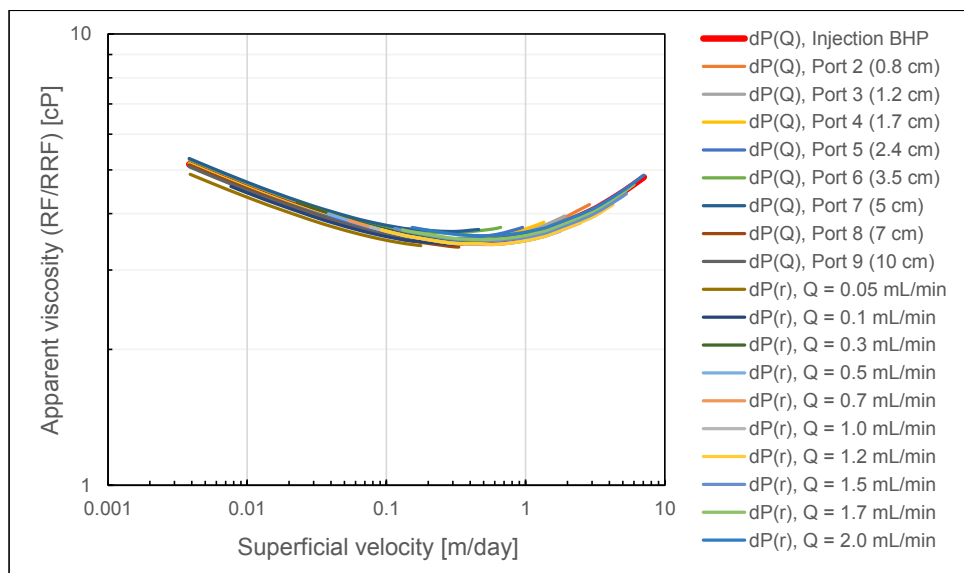


Figure 7.6: In-situ rheology curves obtained from history matching a radial polymer flow experiment, using the DMM and SPMM.

The estimated in-situ rheology curves using the DMM and the SPMM confirms the conclusions drawn from the pressure measurement error analysis in Paper 3. In the absence of memory and rate effects, both history match methods clearly demonstrate overlapping polymer in-situ rheology curves. Based on the strong consistency and accuracy observed, it was concluded that both history match methods are very strong tools for determining polymer in-situ rheology in radial flow systems.

7.2.4 Analysis of pressure build-up during radial polymer flow

While the controlled environment associated with laboratory experiments of radial polymer flow in porous media enable robust and accurate estimation of polymer in-situ rheology, pressure data from field tests are typically exposed to significantly higher uncertainties. In addition, the number of rate steps conducted during field tests are typically sparse such that the pressure data obtained is relatively limited.

History match methods used to estimate in-situ rheology from radial flow experiments (DMM and SPMM) showed robustness up to ± 5 % of the maximum preset pressure range. However, the robustness at these error conditions was in part due to the high number of injection rates, which provided accurate average in-situ rheology curves, as exemplified in figure 7.2. In field tests where the number of injection rates are low, the accuracy and robustness will diminish as the maximum tolerable error is reduced. Furthermore, in contrast to the laboratory radial flow experiment, internal pressure ports are not available during field tests. Thus, the only option available is to history match injection BHP as a function of volumetric injection rate, i.e. using the SPMM, which only provides a single in-situ rheology curve. Thereby, the functional relationship of the polymer in-situ rheology is defined by a limited number of rate steps such that the degree of non-uniqueness of the history match will be high. At least compared to the uniqueness of the in-situ rheology obtained from history matching radial flow experiments using the combination of the DMM and SPMM. For this reason, additional anchoring in the pressure data is desirable to obtain a more accurate and unique polymer in-situ rheology description from field tests.

To increase the anchoring data from the pressure measurements obtained during polymer flow, pressure build-up data from the two-phase radial polymer flow experiment described in chapter 7.2.3, was analysed. Specifically, the stabilization time between rate steps was investigated during both brine (figure 7.7) and polymer flow (figure 7.8). The stabilization time during brine flow was used as a Newtonian reference such that the polymer in-situ rheology behavior could be evaluated based on the relative differences in pressure build-up.

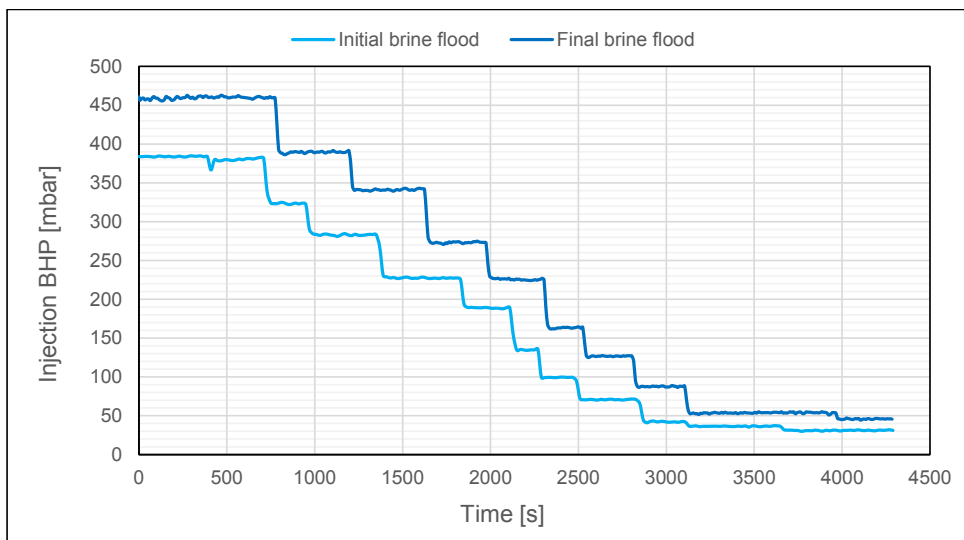


Figure 7.7: Injection BHP versus time during initial (prior to polymer flow) and final brine flood (after polymer tapering).

Injection BHP stabilization time during both brine floods (40 s) was independent of volumetric injection rate. For Newtonian fluids, zero stabilization time is expected in cases where pressure communication in the experimental setup is perfect. The non-zero stabilization time was suggested to be a consequence of partly incomplete pressure communication in the experimental setup due to low values of counter pressure from the production line (2-4 mbar).

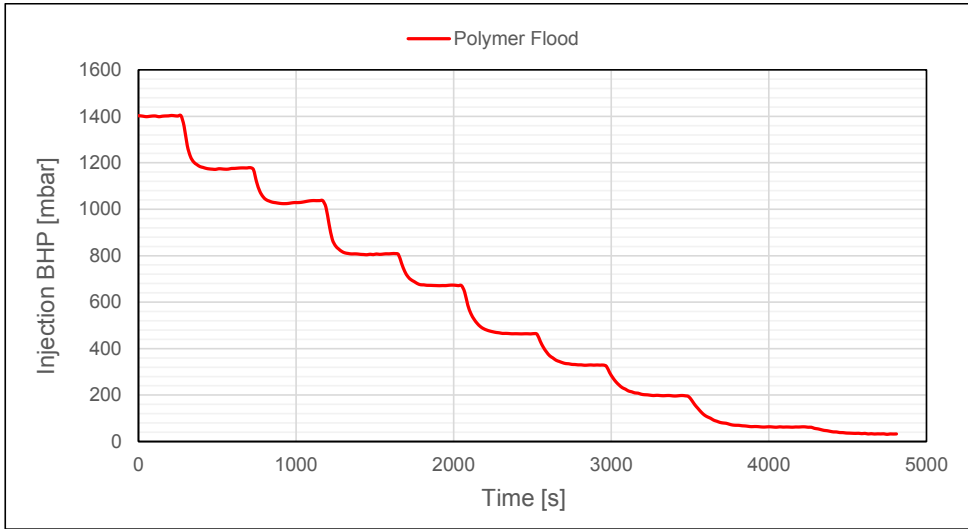


Figure 7.8: Injection BHP versus time during polymer flow.

Pressure stabilization time during polymer flow was significantly higher compared to Newtonian fluid flow (3-9 times). Furthermore, stabilization time decreased monotonically with volumetric injection rate (from 360 s at 0.05 mL/min to 140 s at 2 mL/min). The polymer in-situ rheology was thereby suggested to transition from a distinct behavior in the low-flux regime to a rather different behavior in the high-flux regime. This is in compliance with the history match results obtained from the stabilized pressure, as shown in figure 7.6. Here, the polymer in-situ rheology shows shear-thinning behavior at low flux and transitions into shear-thickening behavior at high flux. These results are also in accordance with the field-scale simulations in Paper 3 and 4 where stabilization time is higher for the shear-thinning fluid behavior compared to significantly lower stabilization times in conjunction with the shear-thickening behavior.

7.3 Rate and memory effects of HPAM in radial flow

In contrast to linear flow experiments where a single (discrete) value of in-situ viscosity is obtained for each volumetric injection rate, continuous in-situ rheology curves are obtained from radial flow experiments with internal pressure ports. Thereby, both rate and memory effects could be quantitatively investigated (Paper 3).

7.3.1 Rate effects

Polymer pressure data from the two-phase radial flow experiment with internal pressure ports described in chapter 7.2.3 was used to assess polymer rate effects. As mentioned, a relatively low molecular weight HPAM polymer (Flopaam 3330S, 8 MDa, 1000 ppm) was injected into a radial Bentheimer disc, saturated with residual oil. Injected versus effluent bulk viscosity measurements showed negligible occurrence of mechanical degradation. Potential rate effects were investigated by history matching the pressure data using the DMM, as shown in figure 7.9. Thus, each obtained in-situ rheology curve originated from pressure data which were measured at a particular volumetric injection rate.

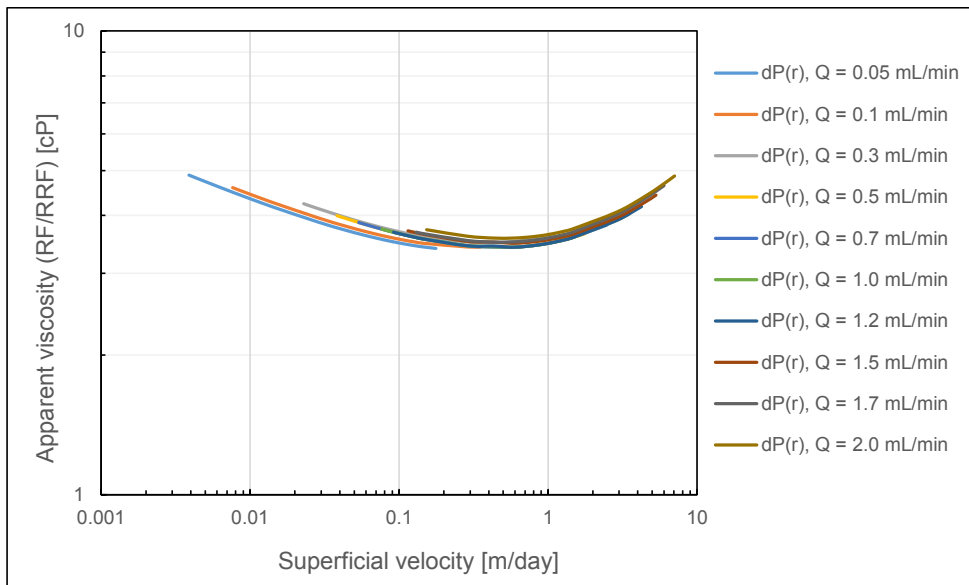


Figure 7.9: In-situ rheology curves obtained from history matching mechanically undegraded HPAM (Flopaam 3330S), using the DMM.

The obtained in-situ rheology curves using the DMM clearly demonstrates the absence of rate effects in circumstances where the polymer is not subjected to mechanical degradation. Consequently, the onset of shear-thickening is independent of volumetric injection rate in radial flow. This conclusion contradicts the assertion made in Paper 2 where it was suggested that the onset of shear-thickening is rate dependent in radial polymer flow (figure 7.10).

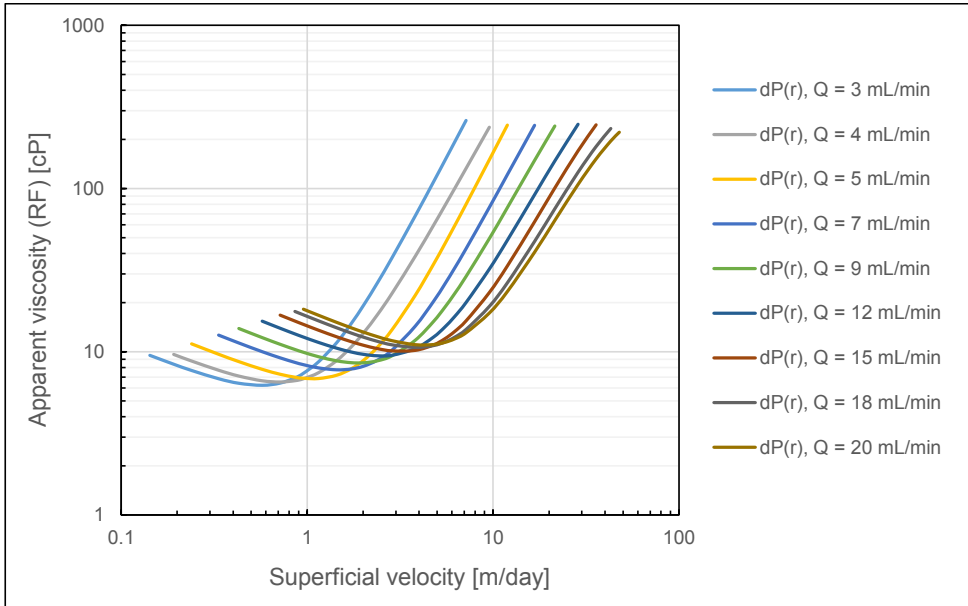


Figure 7.10: In-situ rheology curves obtained from history matching mechanically degraded HPAM (Flopaam 5115SH), using the DMM.

However, the injected HPAM polymer in Paper 2 (Flopaam 5115SH, 15 MDa, 1000 ppm) was exposed to mechanical degradation. Furthermore, since bulk viscosity measurements showed that effluent viscosities decreased with injection rate, mechanical degradation appeared to be rate dependent. As the injection rate, and consequently the degree of mechanical degradation increase, the pressure drop of successively lower molecular weight polymer solutions are measured. Observations from the literature clearly shows that the onset of shear-thickening is shifted towards higher velocities with decreasing molecular weight of the polymer (Heemskerk et al., 1984; Seright et al., 2009; Dupas et al., 2013; Skauge et al., 2015). Thus, the rate dependent onset of shear-thickening in figure 7.10 is suggested to be a mechanical degradation effect rather than a consequence of radial flow.

A curious observation was made in figure 7.10 where apparent viscosity increased with volumetric injection rate as clearly demonstrated by the lower Newtonian plateau viscosities. This could be interpreted as a rate effect associated with some elastic polymer property in flow through Bentheimer sandstone. However, further analysis of

the polymer pressure data revealed injection rate hysteresis. Successive polymer retention during pressure measurements was thereby suggested to be responsible for the increasing apparent viscosity with injection rate. An additional radial flow experiment was therefore history matched to investigate if the observed rate effect was in fact due to polymer retention not being completely satisfied during the measurement process or if the rate dependent behavior could be due to some polymer property which was accentuated with injection rate. A relatively high molecular weight HPAM polymer (Flopaam 3630S, 18 MDa, 2000 ppm) at the upper limit of the semi-dilute concentration regime (Skauge et al., 2015) was injected into a radial Bentheimer disc, saturated with residual oil. Since the elasticity of the polymer increase with molecular weight (Azad & Trivedi, 2019), the higher molecular weight solution should contribute to more pronounced rate effects if they originate from the elastic nature of the polymer. In accordance with the Flopaam 5115SH polymer, the Flopaam 3630S polymer in this experiment was mechanically degraded, as evident by the increasing onset of shear-thickening with volumetric injection rate (figure 7.11).

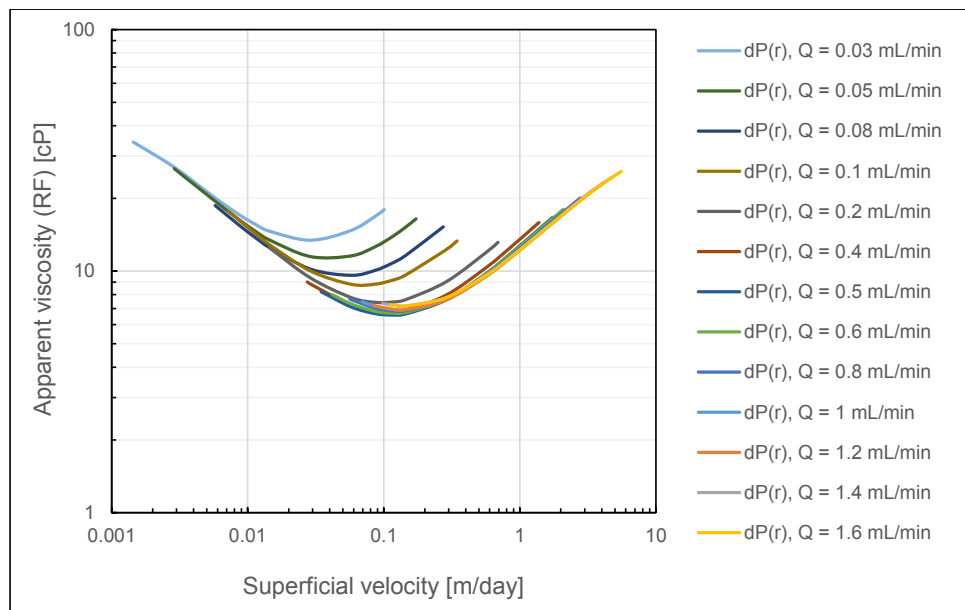


Figure 7.11: In-situ rheology curves obtained from history matching mechanically degraded HPAM (Flopaam 3630S), using the DMM.

In contrast to the mechanically degraded polymer from Paper 2 (Flopaam 5115SH), the higher molecular weight HPAM (Flopaam 3630S) did not exhibit any rate effects in terms of increasing apparent viscosities with injection rate. Thus, in absence of polymer retention during the measurement process, the rate dependent onset of shear-thickening is suggested to be exclusively due to the occurrence of mechanical degradation of the polymer. In accordance with the observations by Al-Shakry et al. (2018a), mechanical degradation thereby affects the elastic properties responsible for the shear-thickening behavior while maintaining its low-flux in-situ viscosities.

As the volumetric injection rate was increased beyond 1 mL/min, it appeared as though the onset of shear-thickening reached a plateau level, as shown in figure 7.12. It is suggested that the lowest volumetric injection rate of 0.03 mL/min exceeds the critical velocity above which mechanical degradation commence. Mechanical degradation is proposed to increase with injection rate until the maximum degradation is attained at 1 mL/min and no further degradation occurs as injection rate is further increased to 1.6 mL/min. Since injected versus effluent viscosity measurements did not include sufficient number of rates within the appropriate rate interval, the suggested hypothesis could not be verified based on bulk viscosity measurements.

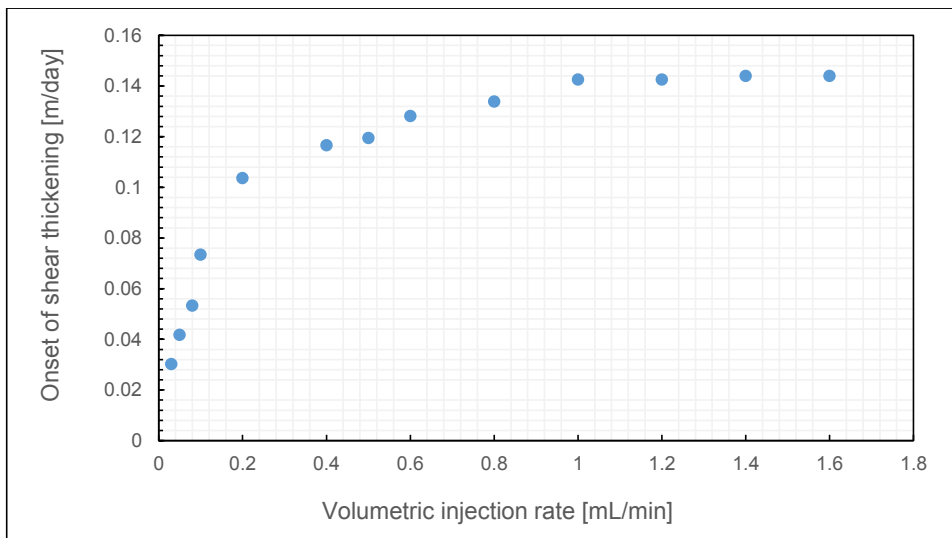


Figure 7.12: Onset of shear-thickening (velocity) as a function of volumetric injection rate for mechanically degraded HPAM (Flopaam 3630S).

7.3.2 Memory effects

The polymer memory effect of HPAM solutions was elegantly demonstrated (at the pore scale) by Chauveteau (1981) in a series of glass model experiments. He observed that the in-situ rheology of HPAM was dependent on the number of prior contraction events experienced by the fluid, i.e. on the polymer history. Memory effects of the undegraded HPAM polymer described in chapter 7.2.3 (Flopaam 3330S, 8 MDa, 1000 ppm) was quantified by history matching the polymer pressure data using the SPMM, as shown in figure 7.13.

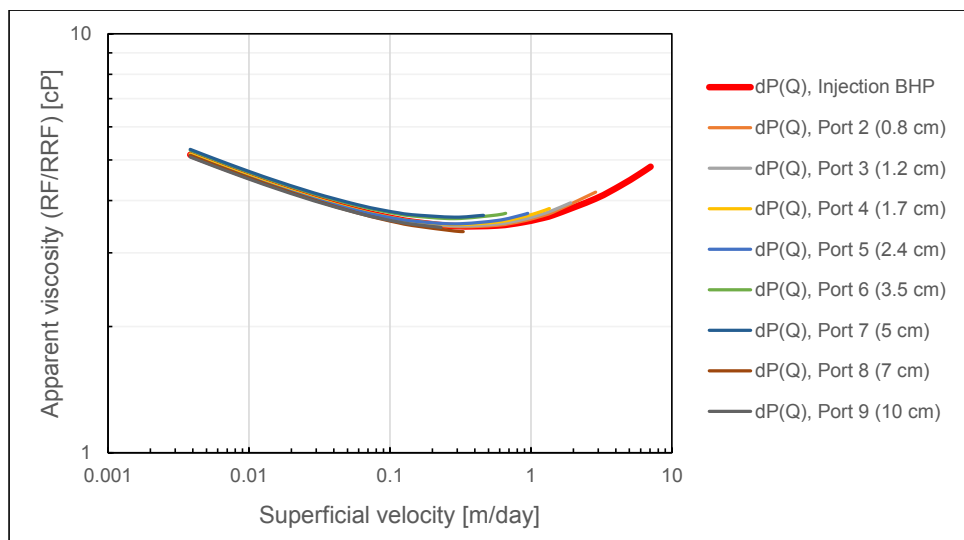


Figure 7.13: In-situ rheology curves obtained from history matching mechanically undegraded HPAM (Flopaam 3330S), using the SPMM.

Each of the obtained in-situ rheology curves originate from polymer pressure data which were measured between a particular pressure port and the producer. Since the number of contraction events experienced by the polymer increase with radial distance, each in-situ rheology curve are history matched from pressure data where the polymer has a different pre-history. If the HPAM polymer exhibit significant memory effects (at the Darcy scale) in flow through the Bentheimer sandstone, it should be observable from deviating in-situ rheology curves obtained by the SPMM. Despite of being history matched based on pressure data where the polymer had a different flow history, the

obtained in-situ rheology curves were overlapping such that no significant memory effects could be observed for the undegraded HPAM polymer.

In paper 3, it was suggested that memory effects in flow through Bentheimer sandstone could be observed for a higher molecular weight polymer. Thus, the mechanically degraded Flopaam 3630S polymer (18 MDa) was also history matched by the use of the SPMM to investigate if any memory effects could be identified (figure 7.14).

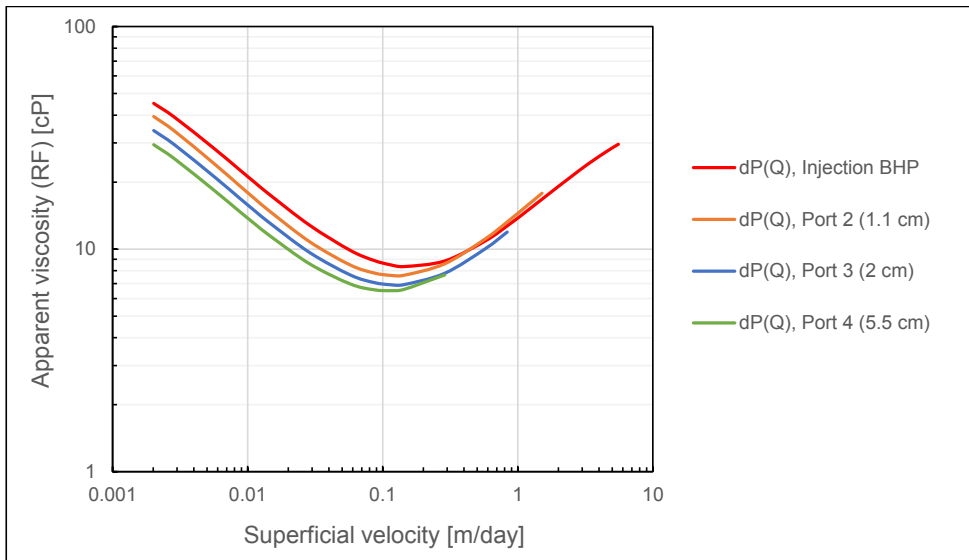


Figure 7.14: In-situ rheology curves obtained from history matching mechanically degraded HPAM (Flopaam 3630S), using the SPMM.

Indeed, the in-situ rheology curves obtained by the SPMM are clearly deviating such that the memory effect could be in operation. Evidently, apparent in-situ viscosity of the polymer is decreasing with radial distance.

The discrepancy between the obtained in-situ viscosity curves might also be suggested to originate from mechanical degradation. However, recent research show that, in contrast to linear flow, mechanical degradation is confined to the near-wellbore region in radial flow (Åsen et al., 2019). The memory effect observed is therefore suggested to originate from the elastic properties of the polymer in flow through Bentheimer sandstone rock.

7.4 Quantification of polymer in-situ rheology and injectivity

The success of polymer flooding depends on the ability of injected solutions to provide enhanced mobility ratio conditions for the displacement process. A prerequisite for accurate evaluation of polymer performance is the control of polymer in-situ rheology and, by extension, polymer injectivity. Despite of nearly sixty years of research, significant controversy and uncertainties is still associated with several topics within polymer in-situ rheology. In this section, the impact of flow geometry and presence of oil on in-situ rheology and polymer injectivity, has been studied. Furthermore, new insights are given on the flow behavior of HPAM at low flux in porous media.

7.4.1 *Impact of flow geometry*

Pressure drop versus volumetric injection rate data from linear core floods have conventionally been used to measure polymer in-situ rheology. However, Skauge et al. (2016) observed significant differences in the flow behavior of HPAM through Bentheimer sandstone in linear cores compared to radial discs. They observed that the degree of shear-thickening was more pronounced in linear flow while the extent of shear-thinning was more pronounced in radial flow. Furthermore, onset of shear-thickening was shifted towards higher velocities in radial flow. Consequently, polymer injectivity and its apparent in-situ viscosity at low flux was expected to be underestimated by the modelling of polymer flow in linear cores as opposed to radial discs.

Results presented by Skauge et al. (2016) were based on polymer flow experiments conducted in the absence of oil. In this thesis, both single and two-phase polymer flow experiments were history matched in an attempt to generalize the effects of flow geometry on polymer in-situ rheology. Comparative studies were conducted in accordance with the study performed by Skauge et al. (2016) where all properties (rock type, polymer type, make-up brine) were equal for the linear and radial flow experiments such that the only influential and deviating factor was the flow geometry. In conjunction with their flow experiments, the relatively high molecular weight HPAM polymer (Flopaam 3630S, 18 MDa) was injected into Bentheimer core plugs

and radial discs. Permeability to brine before polymer flow were used to history match the polymer pressure data from the radial flow experiments. Accordingly, pressure drop during brine flow prior to polymer injection was used to calculate resistance factors from the linear flow experiments. Figure 7.15 shows the impact of flow geometry on the in-situ rheology during single-phase flow. Since the injected polymer solutions were 1500 and 2000-ppm in the linear and radial flow experiment, respectively, apparent in-situ viscosities were normalized to the same lower Newtonian plateau.

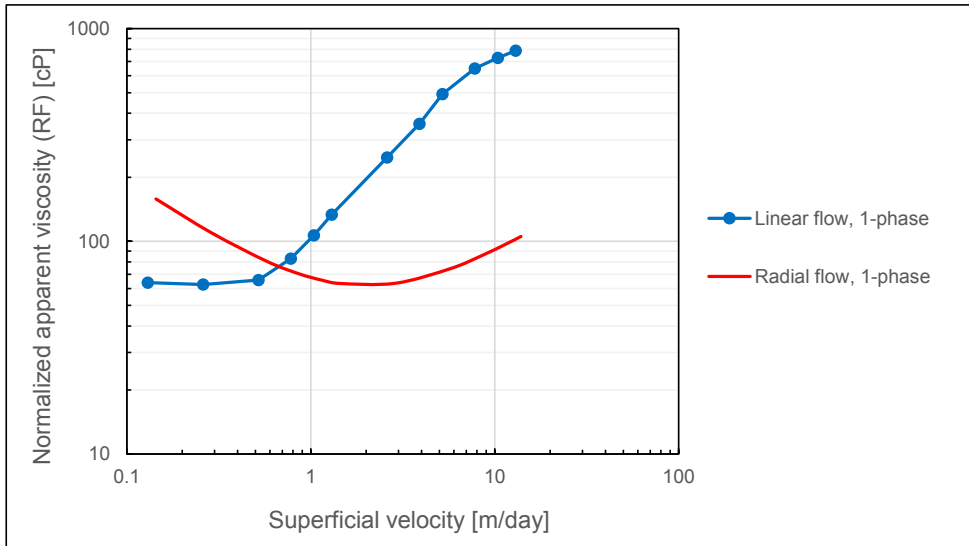


Figure 7.15: Impact of flow geometry on polymer in-situ rheology in 1-phase flow.

In conjunction with the results reported by Skauge et al. (2016), onset of shear-thickening increase in radial compared to linear flow. Furthermore, while the extent of shear-thinning was more pronounced in radial flow, the degree of shear-thickening was reduced. The observed differences between the in-situ rheology obtained in linear relative to radial flow were suggested to be the consequence of the time-dependent elastic nature of the polymer.

According to the Maxwell-model for a viscoelastic fluid (Sorbie, 1991), the fluid behavior is comprised of viscous and elastic response to stress. While the viscous response is related to the inelastic and time-independent behavior of the fluid, the elastic response may be comprised of non-equilibrium phenomena such as kinetic and

memory effects. Kinetic effects is suggested to occur at extreme flow velocities (near-wellbore) in porous media as the polymer molecules propagate through successive contractions (pore throats). Above some critical velocity, the fluid will not be able to relax between contractions such that a kinetic effect is in operation where the pressure builds up with the number of successive contractions. The memory effect (or memory function) incorporates the idea that the stress at the current time is a function of the recent history. This (time-dependent) effect will largely be influenced by the most recent fluid history and is expected to decrease exponentially with time (Sorbie, 1991).

During both linear and radial flow experiments, stabilized pressure drops are used to calculate resistance factors (linear flow experiments) and to obtain in-situ rheology curves by history matching (radial flow experiments). However, as velocity remains constant during linear flow at a particular injection rate, the velocity decreases with distance during radial flow. Thereby, steady state conditions prevail during linear flow while unsteady state conditions is governing radial flow. Since the (time-dependent) memory effect by definition is an unsteady state phenomena, it cannot captured by steady state pressures during linear flow experiments. Consequently, the differences in the obtained in-situ rheology in linear versus radial flow is suggested to originate, at least partly, from the elastic memory effects of the fluid, which can only be quantified by history matching radial flow experiments.

The normalization of apparent viscosities performed in figure 7.15 was expected to be justified since both polymer solutions were within the semi-dilute concentration regime such that the onset of shear-thickening should be independent of concentration (Seright et al., 2011; Skauge et al., 2015; Clarke et al., 2016). To assess this justification, the effects of concentration on polymer in-situ rheology was explicitly investigated in Paper 1, where resistance factors were calculated for two polymer concentrations in the semi-dilute regime (500 and 1500 ppm) during single-phase flow. As clearly demonstrated in figure 7.16, although apparent viscosity increases with polymer concentration, the functional form of the in-situ rheology curves were not affected and the normalization was thereby justified.

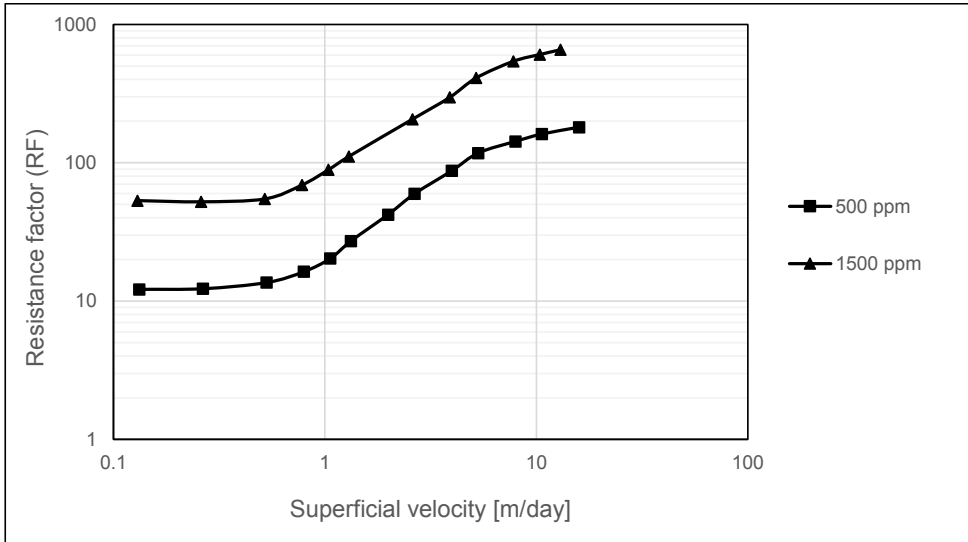


Figure 7.16: Effects of polymer concentration on in-situ rheology during linear single-phase flow.

The impact of flow geometry on polymer in-situ rheology was also quantified in presence of oil (figure 7.17). While a 500-ppm HPAM solution (Flopaam 3630S) was injected during the linear two-phase experiment, a 2000-ppm solution was injected during radial flow.

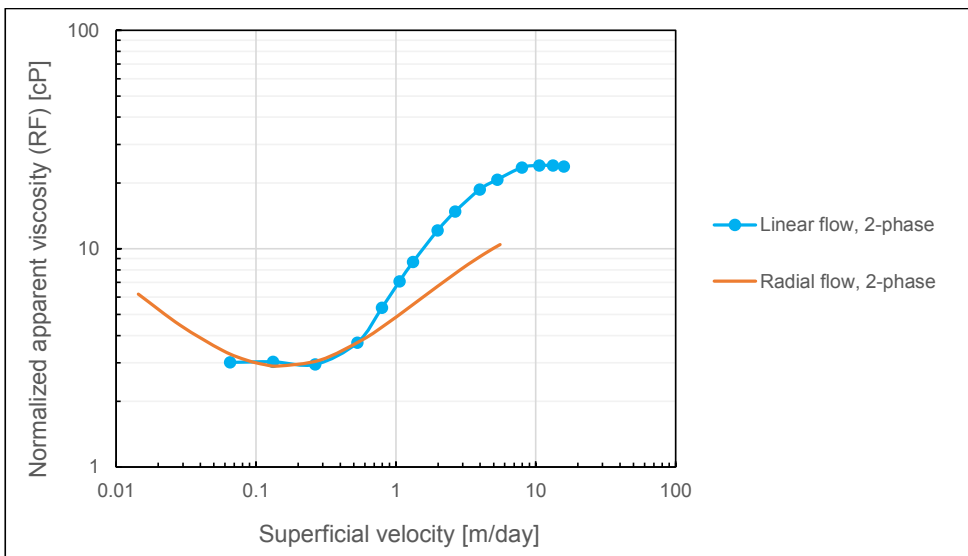


Figure 7.17: Impact of flow geometry on polymer in-situ rheology in 2-phase flow.

Since the injected polymer solutions were both within the semi-dilute concentration regime (Skauge et al., 2015), they were also normalized to the same lower Newtonian plateau. Although the extent of shear-thinning and shear-thickening are consistent with the results obtained during single-phase flow, the onset of shear-thickening commence at the same flow velocity in linear and radial geometry during two-phase polymer flow. Thus, the presence of oil eliminate the shift observed during single-phase flow. This is suggested to be a consequence of the differing velocity distributions in linear compared to radial flow, which are much more pronounced in single-phase compared to two-phase flow. During single-phase flow, the rough surface of the porous media walls and the polymer solutions will generate significant hydrodynamic drag forces. Since steady state conditions are achieved in linear flow while radial flow is governed by unsteady state conditions, the velocity distributions and thus the onset of shear-thickening may be significantly different. However, in two-phase flow, the pore walls are coated with oil films such that the hydrodynamic drag forces are significantly reduced. Thus, as the drag forces are below some critical value, the velocity distributions remains relatively similar such that the onset of shear thickening coincide during two-phase polymer flow in linear cores compared to radial discs.

7.4.2 Impact of oil

In-situ rheology studies of HPAM has mainly been investigated in the absence of oil during single-phase flow experiments in rock cores (Pye, 1964; Smith, 1970; Jennings et al. 1971; Chauveteau, 1981b; Heemskerk et al., 1984; Seright et al., 2009; Seright et al., 2011; Dupas et al., 2013; Manichand et al., 2013; Rodriguez et al., 2014; Zhang & Seright, 2015; Skauge et al., 2015; Skauge et al., 2016). Even though a few in-situ rheology studies of HPAM has been performed in presence of oil (Gogarty, 1967; Masuda et al., 1992; Delamaide et al., 2014), the impact of oil on in-situ rheology has not been quantitatively investigated.

To quantify the impact of oil on polymer in-situ rheology, pressure data from linear and radial flow experiments were used to obtain the in-situ rheology by calculation (linear flow) and history matching (radial flow), as shown in figure 7.18. Flopaam 3630S at 500 ppm and 1500 ppm was injected into the linear cores and radial discs,

respectively. These polymer concentrations were chosen to investigate the impact of oil at the upper and lower concentrations limits of the semi-dilute concentration regime, which would be economically viable for polymer flooding in an oil field.

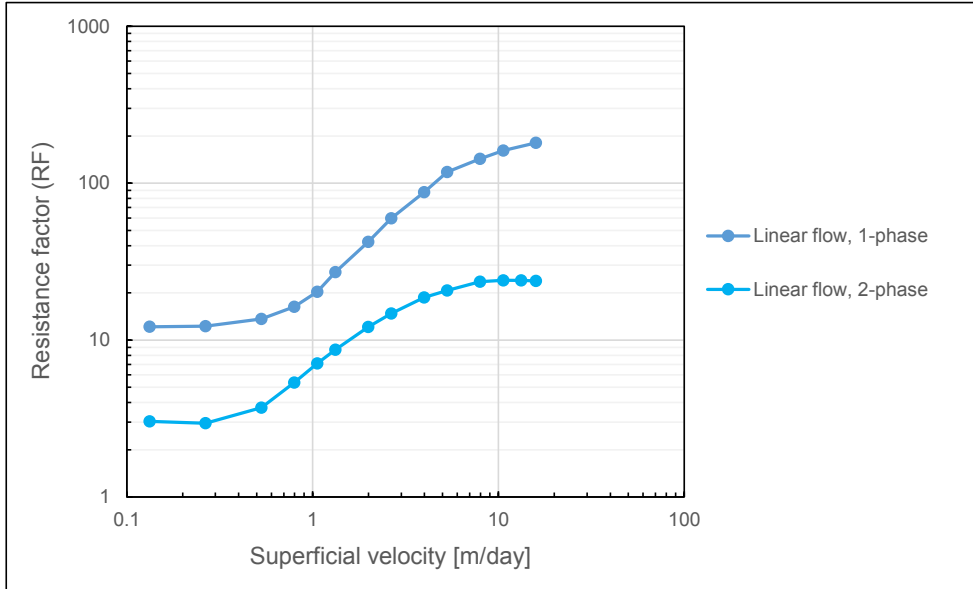


Figure 7.18: Impact of oil on polymer in-situ rheology in linear flow.

The calculated resistance factors clearly demonstrate that the impact of oil is to reduce apparent viscosity in linear flow. The lower resistance factors in the presence of oil is suggested to result from lower adsorption/retention of polymer molecules on the rock surface, in accordance with observations reported by Broseta et al. (1995). Furthermore, the oil layer coating the oil-wet pores is proposed to reduce the hydrodynamic drag forces between the injected polymer solution and the porous media which reduces resistance to flow and thus the calculated resistance factors.

While the onset of shear-thickening is not affected by the presence of residual oil, the slope (degree) of apparent shear-thickening shows strong dependence on the oil presence. Indeed, even though injected versus effluent viscosities revealed that significant degradation ($\sim 20\%$) occurred during single-phase polymer flow, the extent of shear-thickening remained more pronounced in absence compared to presence of oil. This result could be explained by the mechanism of oil redistribution in the porous

medium, as described by Heaviside et al. (1987). While the oil segments at oil wet sites tend to adopt a minimum surface area configuration and thus block the pore throats to brine at low injection rates, the oil segments are forced through the pore throats above some critical pressure gradient. Since the oil now coats the pore bodies rather than the pore throats, permeability to brine was suggested to increase. This effect is expected to be accentuated with the injection of polymer such that the presence of oil is observed to reduce the degree of apparent shear-thickening during polymer flow.

In accordance with the linear flow results, apparent (in-situ) viscosities during radial polymer flow was significantly reduced in two-phase compared to single-phase flow (figure 7.19). As discussed in the previous section (7.4.1), while the onset of shear-thickening occurs at higher flow velocities in radial relative to linear geometry during single-phase flow, this was not the case during two-phase flow, as clearly demonstrated in figure 7.19.

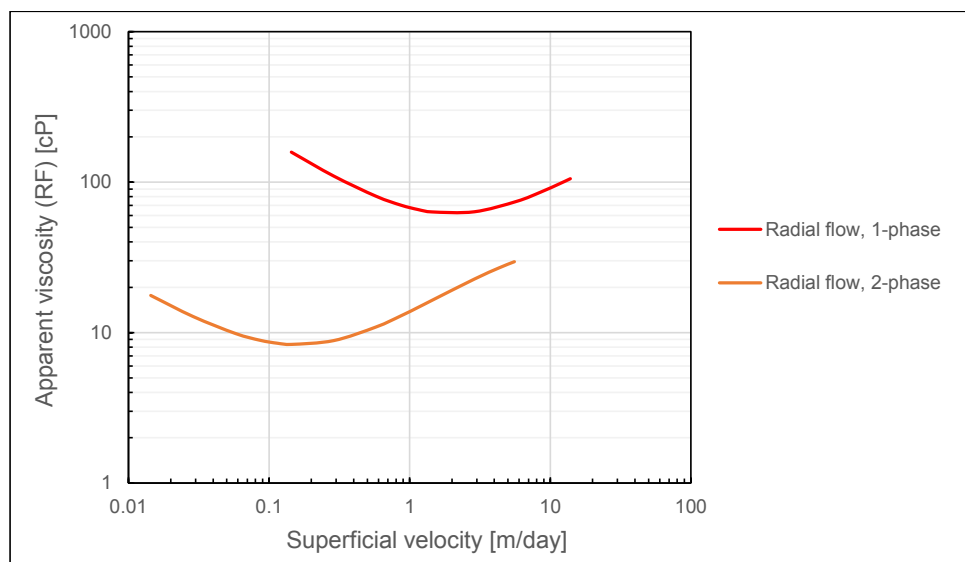


Figure 7.19: Impact of oil on polymer in-situ rheology in radial flow.

The functional relationship of the in-situ rheology curves obtained by history matching the 2000-ppm Flopaam 3630S solution deviates significantly from those presented in paper 1. This is because local permeability variation (Skauge et al., 2016) was used to account for the non-uniform residual oil saturation in Paper 1, while correction factors

were calculated and the polymer pressure was directly adjusted when in-situ rheology curves presented in figure 7.19 was obtained by history matching.

As mentioned in chapter 4.3, discussions are ongoing in the scientific community regarding which brine flood, prior or post polymer flow, is the most appropriate to use as the Newtonian reference to obtain the correct (or ‘true’) apparent viscosity of polymers in porous media. Since some polymer typically remains in the porous medium, even after significant amount of post flush, permeability might be rate dependent. Thus, if permeability is assumed to be constant in these conditions, the true functional relationship of the polymer might be distorted such that rate effects due to porous media permeability is mistaken for polymer rheological behavior. Furthermore, this non-linearity was observed to be accentuated during two-phase flow and was suggested to originate from minor redistributions of oil within the porous media as the flow rate was increased during brine flow, even in circumstances where no oil production was observed (Heaviside et al. 1987).

To investigate the effects of rate dependent permeability on the obtained polymer in-situ rheology, the relationship between pressure drop and volumetric injection rate during brine flow was treated linearly (rate independent) and as a polynomial function (rate dependent), as shown in figure 7.20.

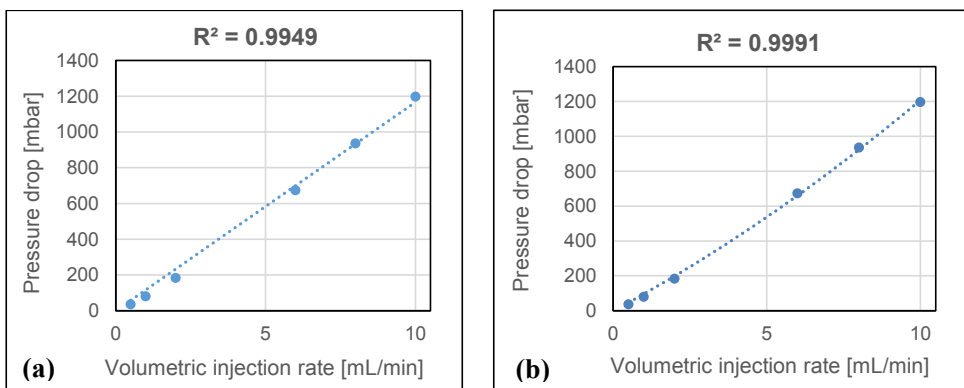


Figure 7.20: (a) Linear and (b) polynomial fit to pressure data during brine flow.

The brine flow data clearly shows a non-linear relationship between pressure drop and volumetric injection rate during brine flow after polymer injection. Interpolation using

the trendlines shown in figure 7.20 was then used to calculate resistance factors for the highest molecular weight HPAM polymer (Flopaam 3630S, 18 MDa, 2000 ppm) in two-phase flow through a radial Bentheimer sandstone disc.

Results (figure 7.21) show that while a minor vertical shift is observed between the two obtained in-situ rheology curves, their functional relationship remains approximately equal. Thus, the non-linearity in the current polymer flow experiment was not sufficient to distort the true functional relationship of the in-situ rheology. Furthermore, since polymer retention and pseudo skin-effects associated with polymer injection is incorporated into the pressure data, the in-situ rheology signal is effectively isolated when using the brine data after polymer injection, as explained in Paper 3. Conversely, if brine data before polymer flow is used, the obtained polymer in-situ rheology will be coupled by these skin and retention effects such that the true in-situ rheology of the polymer might be difficult to obtain.

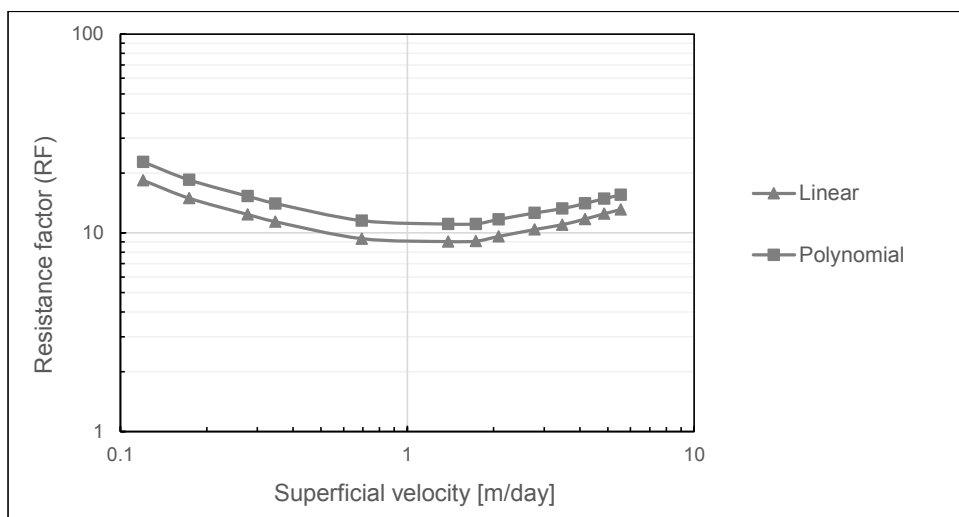


Figure 7.21: Resistance factor calculations using linear and polynomial fit to the brine flow pressure data obtained after polymer flow.

7.4.3 Behavior of HPAM at low flux in porous media

The behavior of HPAM at low flux through linear core plugs has been ambiguously reported in the literature. Based on flow experiments in linear core plugs, there has been reported Newtonian or near-Newtonian (Pye, 1964; Smith, 1970; Jennings et al.,

1971; Seright et al., 2009; Seright et al., 2011; Rodriguez et al., 2014; Skauge et al., 2015; Zhang & Seright, 2015; Al-Shakry et al., 2018b; Al-Shakry et al., 2019a), mild shear-thinning (Heemskerk et al., 1984; Masuda et al., 1992) and significant shear-thinning behavior of HPAM (Gogarty, 1967; Dupas et al., 2013; Manichand et al., 2013; Delamaide et al., 2014).

Seright et al. (2011) attempted to clarify the low-flux behavior of HPAM in porous media and suggested that the observed shear-thinning behavior was either a permeability effect due to plugging of ultrahigh molecular weight species or that these species were able to penetrate deep into the very high permeable formations such that shear-thinning behavior in fact occurred. They concluded that under practical conditions where HPAM is used in conjunction with EOR processes (permeability below 1 D and salinity above 0.3 TDS), the degree of shear-thinning would be slight or non-existent. However, this clarification was based on polymer rheology estimation from linear core flow experiments. Results obtained during the course of this thesis clearly demonstrate the importance of flow geometry on the polymer rheology, as shown in figure 7.22.

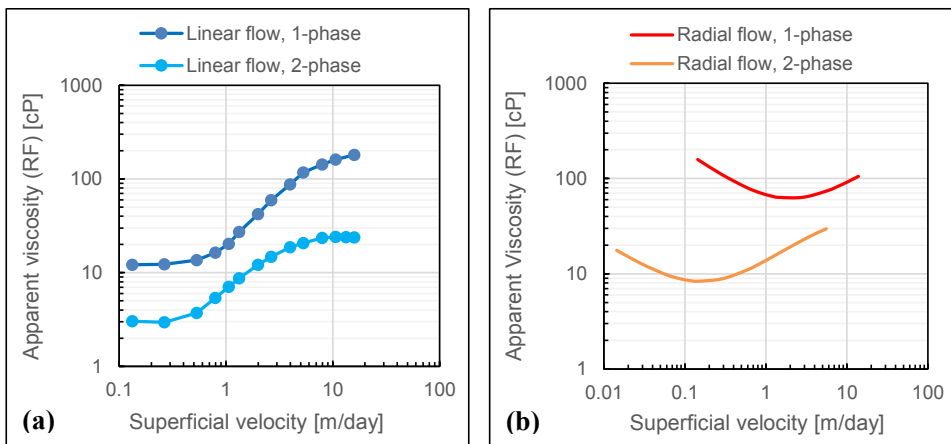


Figure 7.22: Impact of flow geometry on polymer in-situ rheology in (a) linear, and (b) radial flow.

Clearly, while Newtonian behavior at low flux during linear flow in Bentheimer sandstone is in agreement with the clarification by Seright et al. (2011) and the

aforementioned literature, significant shear-thinning behavior is observed during radial polymer flow. It should be emphasized once again that all properties (rock type, polymer type, make-up brine) were the same for the linear and radial flow experiments and the only deviating factor being the flow regime. Thus, the flow geometry is suggested to be a key factor for modelling the low-flux behavior of HPAM in porous media and needs to be taken into account.

7.5 Summary of observations

7.5.1 Qualification of history match methods for radial flow

A comprehensive measurement noise analysis was performed using the recently developed disc match method (DMM) for polymer in-situ rheology estimation from radial flow experiments. An upper acceptable noise level of ~10 % on the pressure measurements was identified below which accurate estimates of polymer in-situ rheology could be made. The polymer in-situ rheology estimation showed invariance between excluding and including the pressure response outside the near-wellbore region at the upper acceptable noise level. It was thereby proposed that the polymer in-situ rheology was mainly defined by the pressure data originating from the near-wellbore region in the radial flow experiment.

A comprehensive analysis was also made on the effective (or cumulative) pressure measurement error during radial flow experiments, using the DMM and the SPMM for in-situ rheology estimation. Here, an upper error level of 5 % of the maximum preset pressure was identified below which accurate estimates of polymer in-situ rheology could be made. History matching pressure data from a radial flow experiment, where a mechanically undegraded polymer (Flopaam 3330S) was injected, clearly demonstrated the robustness and accuracy of the DMM and SPMM in accordance with the generic pressure measurement error analysis.

Analysis of the pressure build-up during radial polymer flow revealed that the in-situ rheological behavior of HPAM could be qualitatively identified based on pressure stabilization time between rate steps. While injection BHP stabilization time during

brine floods was independent of volumetric injection rate, the corresponding stabilization time during polymer flow was significantly increased compared to brine flow, and decreased monotonically with increasing injection rate. The polymer in-situ rheology qualitatively estimated by the pressure build-up was in agreement with the quantitative estimation from stabilized pressure, using the DMM and SPMM.

7.5.2 Rate and memory effects of HPAM in radial flow

Potential rate effects of HPAM in radial flow was investigated by history matching the pressure data from radial flow experiments where mechanically undegraded (Flopaam 3330S) and degraded (Flopaam 5115SH and Flopaam 3630S) HPAM was injected into Bentheimer sandstone rock. Rate effects could be investigated using the DMM since the obtained in-situ rheology curves originate from history matching pressure data at different volumetric injection rates. While no rate effects were observed for the undegraded polymer, significant rate effects were observed for the two degraded polymers, where the onset of shear-thickening occurred at higher flow velocities as mechanical degradation increased. The Flopaam 5115SH polymer displayed rate effects in which apparent in-situ viscosity increased with injection rate. However, this was suggested to be a retention effect where pressure measurements were initiated before polymer retention was satisfied, as revealed by injection rate hysteresis. Indeed, the obtained in-situ rheology from the higher molecular weight polymer, which too was mechanically degraded, confirmed that the rate effects observed in terms of increasing apparent viscosity in fact was due to a retention effect rather than due to the elastic properties of the polymer. Thus, in accordance with observations made by Al-Shakry et al. (2018a), mechanical degradation affected the elastic properties responsible for the shear-thickening behavior while maintaining the low-flux in-situ viscosities of the polymer.

Potential memory effects of HPAM in radial flow was investigated by history matching the pressure data from radial flow experiments where the mechanically undegraded (Flopaam 3330S) and degraded (Flopaam 3630S) HPAM was injected into Bentheimer sandstone rock. Memory effects could be investigated using the SPMM since the polymer has a different flow history at each individual pressure port. Since each

obtained in-situ rheology curve originate from the differential pressure between a specific pressure port and the producer, the obtained rheologies will originate from different memory states of the polymer. While no memory effects was observed for the undegraded and relatively low molecular weight polymer (Flopaam 3330S), the mechanically degraded and high molecular weight polymer (Flopaam 3630S) showed signs of an apparent memory effect in that the obtained rheology curves showed significant discrepancies. As the polymer propagated out from the injector, apparent viscosity decreased with radial distance. The proposed explanations to this observation was either a polymer memory effect or successive mechanical degradation of the polymer between the injector and producer. Since mechanical degradation is assumed to be a near-wellbore phenomenon during radial polymer flow, the memory effect was suggested to originate from the elastic properties of the polymer.

7.5.3 Quantification of polymer in-situ rheology and injectivity

Single and two-phase radial flow experiments were performed to assess the impact of flow geometry and oil on polymer in-situ rheology. Furthermore, the low-flux in-situ rheology behavior of HPAM was addressed and clarified.

The impact of flow geometry on polymer in-situ rheology was investigated by history matching comparative experiments where all properties such as rock type, make-up brine and polymer type were equal for the linear and radial flow experiments. Thus, the only influential and deviating factor was the flow geometry. In accordance with the results reported by Skauge et al. (2016) for single-phase polymer flow, the extent of shear-thinning was more pronounced, the onset of shear-thickening occurred at higher flow velocities, and the degree of shear-thickening was reduced in radial compared to linear flow. However, during two-phase polymer flow, the onset of shear-thickening occurred at the same flow velocity in linear and radial flow. This was suggested to result from the magnitude of the hydrodynamic drag forces in single-phase compared to two-phase flow. The hydrodynamic drag forces between the polymer and the porous medium are assumed to be above some threshold (or critical) value during single-phase flow such that the velocity distribution, and thus the onset of shear-thickening, deviate significantly in radial relative to linear flow. Conversely, during two-phase flow, the

residual oil reduce polymer retention and provides a lubricating effect such that the hydrodynamic drag forces are believed to be below the threshold value and the velocity distribution remains relatively similar for linear and radial flow. Consequently, the onset of shear-thickening coincide in linear and radial flow geometries during two-phase flow.

Results showed that the presence of oil reduce apparent in-situ viscosity in both linear and radial flow. Furthermore, it was observed that while the onset of shear-thickening was not affected by the presence of oil, the degree of shear-thickening showed a strong dependence. Indeed, the extent of shear-thickening remained more pronounced in single-phase compared to two-phase flow despite of significant mechanical degradation (~20 %) occurring during the single-phase flow experiment. This was explained by the mechanism of oil redistribution in the porous medium, as described by Heaviside et al. (1987).

To investigate the effects of using rate-dependent pressure drop during brine flow after polymer injection, a sensitivity analysis was performed where resistance factors were calculated based on linear and non-linear pressure drops with injection rate during brine flow. Results showed that the non-linearity seen during brine flow after polymer injection from in-house experiments is not sufficient to distort the true functional relationship of the obtained polymer in-situ rheology. Indeed, since polymer retention and pseudo skin-effects associated with polymer injection is incorporated into the pressure data, the in-situ rheology signal is effectively isolated when using the brine data after polymer injection.

Lastly, the low-flux behavior of HPAM in porous media was addressed and the clarification made by Seright et al. (2011) was assessed. Even though the linear flow experiments, which showed Newtonian rheology behavior, was in agreement with their clarification, radial flow experiments consistently showed shear-thinning behavior for HPAM at low flux in porous media. Thus, flow geometry was proposed to be a key factor for modelling the low-flux behavior of HPAM in porous media.

8. Conclusions and suggestions for future studies

8.1 Conclusions

In this thesis, mechanistic modelling of radial polymer flow in porous media has been performed by simulation, and through history matching of polymer flow experiments. The objective was to improve the modelling of polymer rheology and injectivity in porous media. This has been conducted by (1) evaluating the accuracy and robustness of the history match methods used to estimate polymer in-situ rheology and injectivity from radial flow experiments, (2) investigating potential rate and memory effects of viscoelastic polymers at the Darcy scale during radial flow experiments, and (3) quantifying polymer rheology and polymer injectivity in porous media.

8.1.1 Qualification of history match methods for radial flow

Based on the robustness and accuracy demonstrated by the history match methods to pressure measurement noise, the assertion that the level of accuracy of pressure transducers may be responsible for the observed shear-thinning behavior in radial flow experiments, is concluded to be very improbable. Furthermore, radial polymer flow experiments should be performed in an experimental setup where effective (or cumulative) measurement error is well below 5 % of the maximum preset pressure to obtain reliable estimates of polymer in-situ rheology.

The in-situ rheology of polymers are mainly defined by the pressure data in the near-wellbore region. Thereby, accurate estimates of polymer in-situ rheology is expected from radial flow experiments performed on discs with radii below one third of the current size (15 cm) for all flow rates applied.

Polymer in-situ rheology may be identified based on the stabilized pressure (quantitatively) and pressure build-up (qualitatively) during radial polymer flow. The additional anchoring data from the analysis of pressure build-up should increase the confidence in estimated in-situ rheologies from field test.

8.1.2 Rate and memory effects of HPAM in radial flow

In presence of mechanical degradation and successive retention before rheology pressure measurements, the HPAM polymers investigated showed no signs of rate effects that could be attributed to their elastic properties. Thus, onset of shear-thickening should be independent of rate for mechanically undegraded polymers in radial flow. Since mechanical degradation was observed to be rate dependent, its occurrence could be identified by radial flow experiments where the onset of shear-thickening increase with injection rate.

Memory effects may have a significant impact on polymer in-situ rheology during radial flow. The apparent memory effect observed in this thesis where apparent viscosity decreased with radial distance is suggested to originate from the elastic properties of the polymer.

8.1.3 Quantification of polymer in-situ rheology and injectivity

Flow geometry and oil has a significant impact on the in-situ rheology of polymer as they flow through porous media. In both single and two-phase flow, extent of shear-thinning is more pronounced and the degree of shear-thickening is significantly reduced in radial relative to linear flow. Thus, modelling the performance of a polymer flood application using linear flow geometry will significantly underestimate both the mobility ratio inside the reservoir and the polymer injectivity.

The onset of shear-thickening occurs at significantly higher flow velocities in radial compared to linear flow during single-phase polymer flow. This is believed to be the consequence of the hydrodynamic drag forces being above some critical value such that the velocity distributions are altered in linear vs radial flow. However, during two-phase flow, the presence of oil reduce the hydrodynamic drag forces between the polymer and the porous media such that the velocity distribution remains relatively unchanged in linear as opposed to radial flow. Thus, the onset of shear-thickening coincide for linear and radial flow geometries during two-phase flow. Consequently, the wettability of the reservoir should be taken into account when modelling polymer in-situ rheology and injectivity.

The impact of oil is to reduce apparent in-situ viscosity, independent of flow geometry. The reduced apparent viscosity in presence of oil is suggested to result from lower adsorption/retention of polymer molecules on the rock surface (Broseta et al., 1995) and the reduction in hydrodynamic drag forces. Additionally, it is proposed that the presence of oil reduce the degree of shear-thickening more than mechanical degradation. This was explained by the rate dependent oil redistribution during fluid flow in porous media, as described by Heaviside et al. (1987).

The low-flux behavior of HPAM agrees with the conclusions made by Seright et al. (2011) during linear flow experiments. However, radial flow experiments showed significant shear-thinning behavior and demonstrated the importance of modelling polymer in-situ rheology in the appropriate flow geometry. As the flow out from the injectors in oil reservoirs typically is governed by a radial flow regime, the low flux in-situ rheology obtained from linear flow experiments would significant underestimate the viscosity enhancement ability of the polymer at low flux in porous media.

8.2 Suggestions for future studies

Despite nearly sixty years of research, significant controversy and uncertainties are still associated with several topics within polymer flooding technology. In particular, polymer in-situ rheology and injectivity are heavily debated subjects in the scientific community. Indeed, as the flow properties of the polymer still is far from completely understood, much work remains to quantify the appropriate mechanisms during porous media flow.

Since the radial flow experiment enable investigation of the unsteady (time-dependent) properties of the polymer, it should be used to further investigate the mechanisms responsible for the differences between linear and radial polymer flow. This entails quantifying the rate and memory effects of polymer solutions as they flow through porous media.

More specifically, the rate dependent mechanical degradation observed in this thesis could be quantitatively investigated by performing radial polymer flow experiments

where a high number of injection rates are performed. By measuring both the porous medium pressure drops and the injected versus effluent viscosities at these rates, the rate dependency can be more thoroughly assessed and compared from the behavior in bulk versus in the porous medium.

The mechanism responsible for the memory effects of the high molecular weight polymer (Flopaam 3630S) was suggested to originate from elastic polymer properties, but could not be completely quantified due to the possible influence of mechanical degradation if not constrained to the near-wellbore region. Thus, it would be interesting to see whether an undegraded and relatively high molecular weight polymer still exhibit apparent memory effects in the absence of mechanical degradation.

References

- Afsharpoor, A. & Balhoff, M. (2013): *Static and Dynamic CFD Modeling of Viscoelastic Polymer: Trapped Oil Displacement and Deformation at the Pore-Level*. Presented at the SPE Annual Technical Conference and Exhibition, New Orleans, Louisiana, USA, 30 September - 2 October 2013. <https://doi.org/10.2118/166114-MS>.
- Al-Shakry, B., Shiran, B. S., Skauge, T. & Skauge, A. (2018a): *Enhanced Oil Recovery by Polymer Flooding: Optimizing Polymer Injectivity*. Presented at the SPE Kingdom of Saudi Arabia Annual Technical Symposium and Exhibition, Dammam, Saudi Arabia, 23-26 April 2018. <https://doi.org/10.2118/192437-MS>.
- Al-Shakry, B., Skauge, T., Shiran, B. S. & Skauge, A. (2018b): *Impact of Mechanical Degradation on Polymer Injectivity in Porous Media*, *Polymers*, Vol. 10: 1-23. <https://doi.org/10.3390/polym10070742>.
- Al-Shakry, B., Skauge, T., Shiran, B. S. & Skauge, A. (2019a): *Polymer Injectivity: Investigation of Mechanical Degradation of Enhanced Oil Recovery Polymers Using In-Situ Rheology*, *Energies*, Vol. 12: 1-25. <https://doi.org/10.3390/en12010049>.
- Al-Shakry, B., Shiran, B. S., Skauge, T. & Skauge, A. (2019b): *Polymer Injectivity: Influence of Permeability in the Flow of EOR Polymers in Porous Media*. Presented at the SPE Europec featured at the 81st EAGE Conference and Exhibition, London, England, 3-6 June 2019. <https://doi.org/10.2118/195495-MS>.
- Alzaabi, M. A., Jacobsen, J. G., Masalmeh, S., Sumaiti, A. A., Pettersen, Ø. & Skauge, A. (2020): *Polymer Injectivity Test Design Using Numerical Simulation*, *Polymers*, Vol. 12: 1-23. <https://doi.org/10.3390/polym12040801>.
- Azad, M. S. & Trivedi, J. J. (2017): *Injectivity Behavior of Copolymer and Associative Polymer Decoded Using Extensional Viscosity Characterization: Effect of Hydrophobic Association*. Presented at the SPE Western Regional Meeting, Bakersfield, California, 21-23 April 2017. <https://doi.org/10.2118/185668-MS>.
- Azad, M. S. & Trivedi, J. J. (2019): *Quantification of the Viscoelastic Effects During Polymer Flooding: A Critical Review*, *Society of Petroleum Engineers Journal*, Vol. 24: 1-27. <https://doi.org/10.2118/195687-PA>.
- Bird, R. B., Stewart, W. E. & Lightfoot, E. N. (1960): *Transport Phenomena*, New York, USA, Wiley.

-
- Bird, R. B., Armstrong, R. C. & Hassager, O. (1987): *Dynamics of Polymeric Liquids*, New York, USA, John Wiley & Sons Inc.
- BP. (2019): *Annual Energy Outlook 2019*. Available from: <http://www.bp.com/content/dam/bp/business-sites/en/global/corporate/pdfs/energy-economics/energy-outlook/bp-energy-outlook-2019.pdf>.
- Broseta, D., Medjahed, F., Lecourtier, J. & Robin, M. (1995): *Polymer Adsorption/Retention in Porous Media: Effects of Core Wettability and Residual Oil*, Society of Petroleum Engineers Advanced Technology Series, Vol. 3: 103-112. <https://doi.org/10.2118/24149-PA>.
- Burnett, D. B. (1975): *Laboratory Studies of Biopolymer Injectivity Behavior Effectiveness of Enzyme Clarification*. Presented at the 45th Annual California Regional Meeting of the Society of Petroleum Engineers of AIME, Ventura, California, USA, 2-4 April 1975. <https://doi.org/10.2118/5372-MS>.
- Cannella, W. J., Huh, C. & Seright, R. S. (1988): *Prediction of Xanthan Rheology in Porous Media*. Presented at the SPE Annual Technical Conference and Exhibition, Houston, Texas, USA, 2-5 October 1988. <https://doi.org/10.2118/18089-MS>.
- Carraher, C. E., Jr. (2003): *Polymer Chemistry*, New York, USA: Marcel Dekker Inc.
- Carreau, P. J. (1972): *Rheological Equations from Molecular Network Theories*, Transactions of the Society of Rheology, Vol. 16: 99-127. <https://doi.org/10.1122/1.549276>.
- Chauveteau, G. (1981): *Molecular Interpretation of Several Different Properties of Flow of Coiled Polymer Solutions Through Porous Media in Oil Recovery Conditions*. Presented at the SPE Annual Technical Conference and Exhibition, San Antonio, Texas, USA, 4-7 October 1981. <https://doi.org/10.2118/10060-MS>.
- Chauveteau, G. & Zaitoun, A. (1981): *Basic rheological behavior of xanthan polysaccharide solutions in porous media: effects of pore size and polymer concentration*. Presented at the First European Symposium on EOR, Bournemouth, England, September 1981.
- Chauveteau, G., Tirrell, M. & Omari, A. (1984): *Concentration Dependence of the Effective Viscosity of Polymer Solutions in Small Pores with Repulsive or Attractive Walls*, Journal of Colloid and Interface Science, Vol. 100: 41-54. [https://doi.org/10.1016/0021-9797\(84\)90410-7](https://doi.org/10.1016/0021-9797(84)90410-7).

-
- Chen, Z., Du, C., Kurnia, I., Lou, J., Zhang, G., Yu, J. & Lee, R. L. (2016): *A Study of Factors Influencing Polymer Hydrodynamic Retention in Porous Media*. Presented at the SPE Improved Oil Recovery Conference, Tulsa, Oklahoma, USA, 11-13 April 2016. <https://doi.org/10.2118/179607-MS>.
- Christopher, R. H. & Middleman, S. (1965): *Power-Law Flow through a Packed Tube*, Industrial & Engineering Chemistry Fundamentals, Vol. 4: 422-426. <https://doi.org/10.1021/i160016a011>.
- Clarke, A., Howe, A. M., Mitchell, J., Staniland, J. & Hawkes, L. A. (2016): *How Viscoelastic-Polymer Flooding Enhances Displacement Efficiency*, Society of Petroleum Engineers Journal, Vol. 21: 675-687. <https://doi.org/10.2118/174654-PA>.
- Computer Modelling Group (2016): *STARS User Guide Advanced Processes & Thermal Reservoir Simulator*, Calgary, Alberta, Canada.
- Dauben, D. L. & Menzie, D. E. (1967): *Flow of Polymer Solutions Through Porous Media*, Journal of Petroleum Technology, Vol. 19: 1065-1073. <https://doi.org/10.2118/1688-PA>.
- Dawson, R. & Lantz, R. B. (1972): *Inaccessible Pore Volume in Polymer Flooding*, Society of Petroleum Engineers Journal, Vol. 12: 448-452. <https://doi.org/10.2118/3522-PA>.
- De Gennes, P. G. (1974): *Coil-stretch transition of dilute flexible polymers under ultrahigh velocity gradients*, Journal of Chemical Physics, Vol. 60: 5030-5042. <https://doi.org/10.1063/1.1681018>.
- De Simoni, M., Boccuni, F., Sambiasi, M., Spagnuolo, M., Albertini, M., Tiani, A. & Masserano, F. (2018): *Polymer Injectivity Analysis and Subsurface Polymer Behavior Evaluation*. Presented at the SPE EOR Conference at Oil and Gas West Asia, Muscat, Oman, 26-28 March 2018. <https://doi.org/10.2118/190383-MS>.
- Delamaide, E., Tabary, R., Renard, G. & Dwyer, P. (2014): *Field Scale Polymer Flooding of Heavy Oil: the Pelikan Lake Story*. Presented at the 21st World Petroleum Congress, Moscow, Russia, 15-19 June 2014.
- Delshad, M., Kim, D. H., Magbagbeola, O. A., Huh, C., Pope, G. A. & Tarahhom, F. (2008): *Mechanistic Interpretation and Utilization of Viscoelastic Behavior of Polymer Solutions for Improved Polymer-Flood Efficiency*. Presented at the SPE Symposium on Improved Oil Recovery, Tulsa, Oklahoma, USA, 20-23 April 2008. <https://doi.org/10.2118/113620-MS>.
- Deshpande, A., Krishnan, J. M. & Kumar, P. B. (2010): *Rheology of Complex Fluids*, New York, USA: Springer.

-
- Dominguez, J. G. & Willhite, G. P. (1977): *Retention and Flow Characteristics of Polymer Solutions in Porous Media*, Society of Petroleum Engineers Journal, Vol. 17: 111-121. <https://doi.org/10.2118/5835-PA>.
- Dupas, A., Henaut, I., Rousseau, D., Poulain, P., Tabary, R., Argillier, J. F. & Aubry, T. (2013): *Impact of Polymer Mechanical Degradation on Shear and Extensional Viscosities: Towards Better Injectivity Forecasts in Polymer Flooding Operations*. Presented at the SPE International Symposium on Oilfield Chemistry, The Woodlands, Texas, USA, 8-10 April 2013. <https://doi.org/10.2118/164083-MS>.
- Erincik, M. Z., Qi, P., Balhoff, M. T. & Pope, G. A. (2018): *New Method to Reduce Residual Oil Saturation by Polymer Flooding*, Society of Petroleum Engineers Journal, Vol. 23: 1944-1956. <https://doi.org/10.2118/187230-PA>.
- Fanchi, J. R. & Christiansen, R. L. (2017): *Introduction to Petroleum Engineering*, New Jersey, USA: John Wiley & Sons Ltd.
- Fletcher, A. J. P., Flew, S. R. G., Lamb, S. P., Lund, T., Bjørnstad, E., Stavland, A. & Gjøvikli, N. B. (1991): *Measurements of Polysaccharide Polymer Properties in Porous Media*. Presented at the SPE International Symposium on Oilfield Chemistry, Anaheim, California, USA, 20-22 February 1991. <https://doi.org/10.2118/21018-MS>.
- Gadde, P. B. & Sharma, M. M. (2001): *Growing Injection Well Fractures and Their Impact on Waterflood Performance*. Presented at the SPE Annual Technical Conference and Exhibition, New Orleans, Louisiana, USA, 30 September – 3 October 2001. <https://doi.org/10.2118/71614-MS>.
- Glasbergen, G., Wever, D., Keijzer, E. & Farajzadeh, R. (2015): *Injectivity Loss in Polymer Floods: Causes, Preventions and Mitigations*. Presented at the SPE Kuwait Oil and Gas Show and Conference, Mishref, Kuwait, 11-14 October 2015. <https://doi.org/10.2118/175383-MS>.
- Gogarty, W. B. (1967): *Mobility Control With Polymer Solutions*, Society of Petroleum Engineers Journal, Vol. 7: 161-173. <https://doi.org/10.2118/1566-B>.
- Green, D. W. & Willhite, G. P. (1998): *Enhanced Oil Recovery*, Texas, USA: Henry L. Doherty Memorial Fund of AIME, Society of Petroleum Engineers.
- Guetni, I., Marliere, C., Rousseau, D., Bihannic, I., Pelletier, M. & Villieras, F. (2019): *Transport of HPAM Solutions in low Permeability Porous Media: Impacts of Salinity and Clay Content*. Presented at the SPE Europec featured at 81st EAGE Conference and Exhibition, London, England, 3-6 June 2019. <https://doi.org/10.2118/195434-MS>.

-
- Guo, H. (2017): *How to Select Polymer Molecular Weight and Concentration to Avoid Blocking in Polymer Flooding*. Presented at the SPE Symposium: Production Enhancement and Cost Optimisation, Kuala Lumpur, Malaysia, 7-8 November 2017. <https://doi.org/10.2118/189255-MS>.
- Heaviside, J., Brown, C. E. & Gamble, I. J. A. (1987): *Relative Permeability for Intermediate Wettability Reservoirs*. Presented at the SPE Annual Technical Conference and Exhibition, Dallas, Texas, USA, 27-30 September 1987. <https://doi.org/10.2118/16968-MS>.
- Heemskerk, J., Rosmalen, R., Janssen-van, R., Holtslag, R. J. & Teeuw, D. (1984): *Quantification of Viscoelastic Effects of Polyacrylamide Solutions*. Presented at the SPE Enhanced Oil Recovery Symposium, Tulsa, Oklahoma, USA, 15-18 April 1984. <https://doi.org/10.2118/12652-MS>.
- Herzig, J. P., Leclerc, D. M. & Le Goff, P. (1970): *Flow of Suspensions through Porous Media – Application to Deep Filtration*, Journal of Industrial & Engineering Chemistry Research, Vol. 62: 8-35. <https://doi.org/10.1021/ie50725a003>.
- Hirasaki, G. J. & Pope, G. A. (1974): *Analysis of Factors Influencing Mobility and Adsorption in the Flow of Polymer Solution Through Porous Media*, Society of Petroleum Engineers Journal, Vol. 14: 337-346. <https://doi.org/10.2118/4026-PA>.
- Jacobsen, J. G., Alzaabi, M., Skauge, T., Sorbie, K. & Skauge, A. (2019): *Analysis and Simulation of Polymer Injectivity*. Presented at the 20th European Symposium on Improved Oil Recovery, Pau, France, 8-11 April 2019. <https://doi.org/10.3997/2214-4609.201900115>.
- Jacobsen, J. G., Shiran, B. S., Skauge, T., Sorbie, K. S. & Skauge, A. (2020): *Qualification of New Methods for Measuring In Situ Rheology of Non-Newtonian Fluids in Porous Media*, Polymers, Vol. 12: 1-13. <https://doi.org/10.3390/polym12020452>.
- Jennings, R. R., Rogers, J. H. & West, T. J. (1971): *Factors Influencing Mobility Control by Polymer Solutions*, Journal of Petroleum Technology, Vol. 23: 391-401. <https://doi.org/10.2118/2867-PA>.
- Jiang, H., Wu, W., Wang, D., Zeng, Y., Zhao, S. & Nie, J. (2008): *The Effect of Elasticity on Displacement Efficiency in the Lab and Results of High Concentration Polymer Flooding in the Field*. Presented at the 2008 SPE Annual Technical Conference and Exhibition, Denver, Colorado, USA, 21-24 September 2008. <https://doi.org/10.2118/115315-MS>.
- Jones, D. M. & Walters, K. (1989): *The behavior of polymer solutions in extension-dominated flows, with applications to Enhanced Oil Recovery*, Rheologica Acta, Vol. 28: 482-498. <https://doi.org/10.1007/BF01332919>.

-
- Kozicki, W. (2002): *Flow of a FENE Fluid in Packed Beds or Porous Media*, Canadian Journal of Chemical Engineering, Vol. 80: 818-829. <https://doi.org/10.1002/cjce.5450800505>.
- Lake, L. W., Johns, R., Rossen, B. & Pope, G. (2014): *Fundamentals of Enhanced Oil Recovery*, New Jersey, USA: Society of Petroleum Engineers.
- Lee, K., Huh, C. & Sharma, M. M. (2011): *Impact of Fracture Growth on Well Injectivity and Reservoir Sweep during Waterflood and Chemical EOR Processes*. Presented at the SPE Annual Technical Conference and Exhibition, Denver, Colorado, USA, 30 October – 2 November 2011. <https://doi.org/10.2118/146778-MS>.
- Li, Z. & Delshad, M. (2014): *Development of an Analytical Injectivity Model for Non-Newtonian Polymer Solutions*, Society of Petroleum Engineers Journal, Vol. 19: 381-389. <https://doi.org/10.2118/163672-PA>.
- Lopez, X., Valvatne, P. H. & Blunt, M. J. (2003): *Predictive network modeling of single-phase non-Newtonian flow in porous media*, Journal of Colloid and Interface Science, Vol. 264: 256-265. [https://doi.org/10.1016/S0021-9797\(03\)00310-2](https://doi.org/10.1016/S0021-9797(03)00310-2).
- Lotfollahi, H., Farajzadeh, R., Delshad, M., Al-Abri, A., Wassing, B. M., Al-Mjeni, R., Awan, K. & Bedrikovetsky, P. (2016): *Mechanistic Simulation of Polymer Injectivity in Field Tests*, Society of Petroleum Engineers Journal, Vol. 21: 1178-1191. <https://doi.org/10.2118/174665-PA>.
- Lötsch, T., Müller, T. & Pusch, G. (1985): *The Effect of Inaccessible Pore Volume on Polymer Coreflood Experiments*. Presented at the International Symposium on Oilfield and Geomthermal Chemistry, Phoenix, Arizona, USA, 9-11 April 1985. <https://doi.org/10.2118/13590-MS>.
- Maerker, J. M. (1973): *Dependence of Polymer Retention on Flow Rate*, Journal of Petroleum Technology, Vol. 25: 1307-1308. <https://doi.org/10.2118/4423-PA>.
- Maerker, J. M. (1975): *Shear Degradation of Partially Hydrolyzed Polyacrylamide Solutions*, Society of Petroleum Engineers Journal, Vol. 15: 311-322. <https://doi.org/10.2118/5101-PA>.
- Manichand, R. N., Let, K. P. M. S., Gil, L., Quillien, B. & Seright, R. S. (2013): *Effective Propagation of HPAM Solutions Through the Tambaredjo Reservoir During a Polymer Flood*, Society of Petroleum Engineers Production & Operations, Vol. 28: 358-368. <https://doi.org/10.2118/164121-PA>.
- Marshall, R. J. & Metzner, A. B. (1967): *Flow of Viscoelastic Fluids Through Porous Media*, Industrial & Engineering Chemistry Fundamentals, Vol. 6: 393-400. <https://doi.org/10.1021/i160023a012>.

-
- Martin, F. D. (1975): *The Effect of Hydrolysis of Polyacrylamide on Solution Viscosity, Polymer Retention and Flow Resistance Properties*. Presented at the Rocky Mountain Regional Meeting of the Society of Petroleum Engineers of AIME, Denver, Colorado, USA, 7-9 April 1975. <https://doi.org/10.2118/5339-MS>.
- Masuda, Y., Tang, K., Miyazawa, M. & Tanaka, S. (1992): *1D Simulation of Polymer Flooding Including the Viscoelastic Effect of Polymer Solution*, Society of Petroleum Engineers Reservoir Engineering, Vol. 7: 247-252. <https://doi.org/10.2118/19499-PA>.
- Morris, C. W. & Jackson, K. M. (1978): *Mechanical Degradation of Polyacrylamide Solutions in Porous Media*. Presented at the SPE Symposium on Improved Methods of Oil Recovery, Tulsa, Oklahoma, USA, 16-17 April 1978. <https://doi.org/10.2118/7064-MS>.
- Mungan, N., Smith, F. W. & Thompson, J. L. (1966): *Some Aspects of Polymer Floods*, Journal of Petroleum Technology, Vol. 18: 1143-1150. <https://doi.org/10.2118/1628-PA>.
- Mungan, N. (1969): *Rheology and Adsorption of Aqueous Polymer Solutions*, Journal of Canadian Petroleum Technology, Vol. 8: 45-50. <https://doi.org/10.2118/69-02-01>.
- Mungan, N. (1972): *Shear Viscosities of Ionic Polyacrylamide Solutions*, Society of Petroleum Engineers Journal, Vol. 12: 469-473. <https://doi.org/10.2118/3521-PA>.
- Noïk, C., Delaplace, P. & Muller, G. (1995): *Physico-Chemical Characteristics of Polyacrylamide Solutions after Mechanical Degradation through a Porous Medium*. Presented at the SPE International Symposium on Oilfield Chemistry, San Antonio, Texas, USA, 14-17 February 1995. <https://doi.org/10.2118/28954-MS>.
- Odell, J. A., Müller, A. J. & Keller, A. (1988): *Non-Newtonian behavior of hydrolysed polyacrylamide in strong elongational flows: a transient network approach*, Polymer, Vol. 29: 1179-1190. [https://doi.org/10.1016/0032-3861\(88\)90042-0](https://doi.org/10.1016/0032-3861(88)90042-0).
- Oliver, D. S. & Chen, Y. (2011): *Recent progress on reservoir history matching: a review*, Computational Geosciences, Vol. 15: 185-221. <https://doi.org/10.1007/s10596-010-9194-2>.
- Pearson, J. R. A. & Tardy, P. M. J. (2002): *Models for flow of non-Newtonian and complex fluids through porous media*, Journal of Non-Newtonian Fluid Mechanics, Vol. 102: 447-473. [https://doi.org/10.1016/S0377-0257\(01\)00191-4](https://doi.org/10.1016/S0377-0257(01)00191-4).

-
- Pye, D. J. (1964): *Improved Secondary Recovery by Control of Water Mobility*, Journal of Petroleum Technology, Vol. 16: 911-916. <https://doi.org/10.2118/845-PA>.
- Qi, P., Ehrenfriend, D. H., Koh, H. & Balhoff, M. T. (2017): *Reduction of Residual Oil Saturation in Sandstone Cores by Use of Viscoelastic Polymers*, Society of Petroleum Engineers Journal, Vol. 22: 447-458. <https://doi.org/10.2118/179689-PA>.
- Rodriguez, F., Rousseau, D., Bekri, S., Djabourov, M. & Bejarano, C. (2014): *Polymer Flooding for Extra-Heavy Oil: New Insights on the Key Polymer Transport Properties in Porous Media*. Presented at the SPE International Heavy Oil Conference and Exhibition, Mangaf, Kuwait, 8-10 December 2014. <https://doi.org/10.2118/172850-MS>.
- Rodriguez, S., Romero, C., Sargenti, M. L., Müller, A. J., Sáez, A. E. & Odell, J. A. (1993): *Flow of polymer solutions through porous media*, Journal of Non-Newtonian Fluid Mechanics, Vol. 49: 63-85. [https://doi.org/10.1016/0377-0257\(93\)85023-4](https://doi.org/10.1016/0377-0257(93)85023-4).
- Sandiford, B. B. (1964): *Laboratory and Field Studies of Water Floods Using Polymer Solutions to Increase Oil Reservoirs*, Journal of Petroleum Technology, Vol. 16: 917-922. <https://doi.org/10.2118/844-PA>.
- Saripalli, K. P., Bryant, S. L. & Sharma, M. M. (1999): *Role of Fracture Face and Formation Plugging in Injection Well Fracturing and Injectivity Decline*. Presented at the SPE/EPA Exploration and Production Environmental Conference, Austin, Texas, USA, 1-3 March 1999. <https://doi.org/10.2118/52731-MS>.
- Savins, J. G. (1969): *Non-Newtonian Flow Through Porous Media*, Industrial & Engineering Chemistry, Vol. 61: 18-47. <https://doi.org/10.1021/ie50718a005>.
- Seright, R. S. (1983): *The Effects of Mechanical Degradation and Viscoelastic Behavior on Injectivity of Polyacrylamide Solutions*, Society of Petroleum Engineers Journal, Vol. 23: 475-485. <https://doi.org/10.2118/9297-PA>.
- Seright, R. S. (1995): *Gel Placement in Fractured Systems*, Society of Petroleum Engineers Production & Facilities, Vol. 10: 241-248. <https://doi.org/10.2118/27740-PA>.
- Seright, R. S., Seheult, J. M. & Talashek, T. (2009): *Injectivity Characteristics of EOR Polymers*, Society of Petroleum Engineers Reservoir Evaluation & Engineering, Vol. 12: 783-792. <https://doi.org/10.2118/115142-PA>.
- Seright, R. S. (2010): *Potential for Polymer Flooding Reservoirs With Viscous Oils*, Society of Petroleum Engineers Reservoir Evaluation & Engineering, Vol. 13: 730-740. <https://doi.org/10.2118/129899-PA>.

-
- Seright, R. S., Fan, T., Wavrik, K. & Balaban, R. d. C. (2011): *New Insights into Polymer Rheology in Porous Media*, Society of Petroleum Engineers Journal, Vol. 16: 35-42. <https://doi.org/10.2118/129200-PA>.
- Seright, R. S., Zhang, G. & Wang, D. (2012): *A Comparison of Polymer Flooding With In-Depth Profile Modification*, Journal of Canadian Petroleum Technology, Vol. 51: 393-402. <https://doi.org/10.2118/146087-PA>.
- Seright, R. S. (2017): *How Much Polymer Should Be Injected During a Polymer Flood? Review of Previous and Current Practices*, Society of Petroleum Engineers Journal, Vol. 22: 1-18. <https://doi.org/10.2118/179543-PA>.
- Sheng, J. J. (2015): *Modern Chemical Enhanced Oil Recovery*, Waltham Massachusetts, USA: Gulf Professional Publishing.
- Sheng, J. J., Leonhardt, B. & Azri, N. (2015): *Status of Polymer-Flooding Technology*, Journal of Canadian Petroleum Technology, Vol. 54: 116-126. <https://doi.org/10.2118/174541-PA>.
- Skauge, T., Kvilhaug, O. A., Skauge, A. (2015): *Influence of Polymer Structural Conformation and Phase Behavior on In-situ Viscosity*. Presented at the 18th European Symposium on Improved Oil Recovery, Dresden, Germany, 14-16 April 2015. <https://doi.org/10.3997/2214-4609.201412154>.
- Skauge, T., Skauge, A., Salmo, I. C., Ormehaug, P. A., Al-Azri, N., Wassing, L. M., Glasbergen, G., van Wunnik, J. N. & Masalmeh, S. K. (2016): *Radial and Linear Polymer Flow – Influence on Injectivity*. Presented at the SPE Improved Oil Recovery Conference, Tulsa, Oklahoma, USA, 11-13 April 2016. <https://doi.org/10.2118/179694-MS>.
- Skauge, A., Zamani, N., Jacobsen, J. G., Shiran, B. S., Al-Shakry, B. & Skauge, T. (2018): *Polymer Flow in Porous Media: Relevance to Enhanced Oil Recovery*, Colloids and Interfaces, Vol. 2: 1-27. <https://doi.org/10.3390/colloids2030027>.
- Smith, F. W. (1970): *The Behavior of Partially Hydrolyzed Polyacrylamide Solutions in Porous Media*, Journal of Petroleum Technology, Vol. 22: 148-156. <https://doi.org/10.2118/2422-PA>.
- Sochi, T. (2010): *Non-Newtonian flow in porous media*, Polymer, Vol. 51: 5007-5023. <https://doi.org/10.1016/j.polymer.2010.07.047>.
- Sorbie, K. S., Clifford, P. J. & Jones, E. R. W. (1989): *The rheology of pseudoplastic fluids in porous media using network modeling*, Journal of Colloid and Interface Science, Vol. 130: 508-534. [https://doi.org/10.1016/0021-9797\(89\)90128-8](https://doi.org/10.1016/0021-9797(89)90128-8).
- Sorbie, K. S. (1991): *Polymer-Improved Oil Recovery*, Glasgow: Blackie & Son Ltd.

-
- Standnes, D. C. & Skjevrak, I. (2014): *Literature review of implemented polymer field projects*, Journal of Petroleum Science and Engineering, Vol. 122: 761-775. <https://doi.org/10.1016/j.petrol.2014.08.024>.
- Stavland, A., Jonsbråten, H. C. & Lohne, A. (2010): *Polymer Flooding – Flow Properties in Porous Media Versus Rheological Parameters*. Presented at the SPE EUROPEC/EAGE Annual Conference and Exhibition, Barcelona, Spain, 14-17 June 2010. <https://doi.org/10.2118/131103-MS>.
- Szabo, M. T. (1975): *Some Aspects of Polymer Retention in Porous Media Using a C¹⁴-Tagged Hydrolyzed Polyacrylamide*, Society of Petroleum Engineers Journal, Vol. 15: 323-337. <https://doi.org/10.2118/4668-PA>.
- Szabo, M. T. (1979): *An Evaluation of Water-Soluble Polymers for Secondary Oil Recovery – Parts 1 and 2*, Journal of Petroleum Technology, Vol. 31: 553-570. <https://doi.org/10.2118/6601-PA>.
- Thomas, A. (2019): *Essentials of Polymer Flooding Technique*, New Jersey, USA: John Wiley & Sons Ltd.
- Teeuw, D. & Hesselink, F. T. (1980): *Power-Law Flow And Hydrodynamic Behavior Of Biopolymer Solutions In Porous Media*. Presented at the SPE Oilfield and Geothermal Chemistry Symposium, Stanford, California, USA, 28-30 May 1980. <https://doi.org/10.2118/8982-MS>.
- Tien, C. & Payatakes, A. C. (1979): *Advances in Deep Bed Filtration*, American Institute of Chemical Engineering Journal, Vol. 25: 737-759. <https://doi.org/10.1002/aic.690250502>.
- Urbissinova, T. S., Trivedi, J. & Kuru, E. (2010): *Effect of Elasticity During Viscoelastic Polymer Flooding: A Possible Mechanism of Increasing the Sweep Efficiency*, Journal of Canadian Petroleum Technology, Vol. 49: 49-56. <https://doi.org/10.2118/133471-PA>.
- Vermolen, E. C. M., Haasterecht, M. J. T. & Masalmeh, S. K. (2014): *A Systematic Study of the Polymer Visco-Elastic Effect on Residual Oil Saturation by Core Flooding*. Presented at the SPE EOR Conference at Oil and Gas West Asia, Muscat, Oman, 31 March – 2 April 2014. <https://doi.org/10.2118/169681-MS>.
- Vik, B., Kedir, A., Kippe, V., Sandengen, K., Skauge, T., Solbakken, J. & Zhu, D. (2018): *Viscous Oil Recovery by Polymer Injection; Impact of In-Situ Polymer Rheology on Water Front Stabilization*. Presented at the SPE Europec featured at the 80th EAGE Conference and Exhibition, Copenhagen, Denmark, 11-14 June 2018. <https://doi.org/10.2118/190866-MS>.
- Volpert, E., Selb, J. & Candau, F. (1998): *Associating behavior of polyacrylamides hydrophobically modified with dihexylacrylamide*, Polymer, Vol. 39: 1025-1033. [https://doi.org/10.1016/S0032-3861\(97\)00393-5](https://doi.org/10.1016/S0032-3861(97)00393-5).

-
- Vorwerk, J. & Brunn, P. O. (1991): *Porous medium flow of the fluid A1: effects of shear and elongation*, Journal of Non-Newtonian Fluid Mechanics, Vol. 41: 119-131. [https://doi.org/10.1016/0377-0257\(91\)87038-Y](https://doi.org/10.1016/0377-0257(91)87038-Y).
- Wang, D., Cheng, J., Yang, Q., Gong, W., Li, Q. & Chen, F. (2000): *Viscous-Elastic Polymer Can Increase Microscale Displacement Efficiency in Cores*. Presented at the 2000 SPE Annual Technical Conference and Exhibition, Dallas, Texas, 1-4 October 2000. <https://doi.org/10.2118/63227-MS>.
- Wang, D., Seright, R. S., Shao, Z. & Wang, J. (2007): *Key Aspects of Project Design for Polymer Flooding at the Daqing Oil Field*, Society of Petroleum Engineers Reservoir Evaluation & Engineering, Vol. 11: 1117-1124. <https://doi.org/10.2118/109682-PA>.
- Wang, D., Han, P., Shao, Z., Hou, W. & Seright, R. S. (2008): *Sweep-Improvement Options for the Daqing Oil Field*, Society of Petroleum Engineers Reservoir Evaluation & Engineering, Vol. 11: 18-26. <https://doi.org/10.2118/99441-PA>.
- Ward, J. S. & Martin, F. D. (1981): *Prediction of Viscosity for Partially Hydrolyzed Polyacrylamide Solutions in the Presence of Calcium and Magnesium Ions*, Society of Petroleum Engineers Journal, Vol. 21: 623-631. <https://doi.org/10.2118/8978-PA>.
- Wever, D. A. Z., Bartlema, H., ten Berge, A. B. G. M., Al-Mjeni, R. & Glasbergen, G. (2018): *The Effect of the Presence of Oil on Polymer Retention in Porous Media from Clastic Reservoirs in the Sultanate of Oman*. Presented at the SPE EOR Conference at Oil and Gas West Asia, Muscat, Oman, 26-28 March 2018. <https://doi.org/10.2118/190430-MS>.
- Xia, H., Ju, Y., Kong, F. & Wu, J. (2004): *Effect of Elastic Behavior of HPAM Solutions on Displacement Efficiency Under Mixed Wettability Conditions*. Presented at the 2004 SPE International Petroleum Conference, Puebla, Mexico, 8-9 November 2004. <https://doi.org/10.2118/90234-MS>.
- Yerramilli, S. S., Zitha, P. L. J. & Yerramilli, R. C. (2013): *Novel Insight into Polymer Injectivity for Polymer Flooding*. Presented at the SPE European Formation Damage Conference & Exhibition, Noordwijk, The Netherlands, 5-7 June 2013. <https://doi.org/10.2118/165195-MS>.
- Yin, H., Wang, D. & Zhong, H. (2006): *Study on Flow Behaviors of Viscoelastic Polymer Solution in Micropore With Dead End*. Presented at the 2006 SPE Annual Technical Conference and Exhibition, San Antonio, Texas, USA, 24-27 September 2006. <https://doi.org/10.2118/101950-MS>.
- Zaitoun, A. & Kohler, N. (1987): *The Role of Adsorption in Polymer Propagation Through Reservoir Rocks*. Presented at the SPE International Symposium on Oilfield Chemistry, San Antonio, Texas, USA, 4-6 February 1987. <https://doi.org/10.2118/16274-MS>.

- Zamani, N., Bondino, I., Kaufmann, R. & Skauge, A. (2015): *Effect of porous media properties on the onset of polymer extensional viscosity*, Journal of Petroleum Science and Engineering, Vol. 133: 483-495. <https://doi.org/10.1016/j.petrol.2015.06.025>.
- Zechner, M., Clemens, T., Suri, A. & Sharma, M. M. (2015): *Simulation of Polymer Injection Under Fracturing Conditions – An Injectivity Pilot in the Matzen Field, Austria*, Society of Petroleum Engineers Reservoir Evaluation & Engineering, Vol. 18: 236-249. <https://doi.org/10.2118/169043-PA>.
- Zhang, G. & Seright, R. S. (2014): *Effect of Concentration on HPAM Retention in Porous Media*, Society of Petroleum Engineers Journal, Vol. 19: 373-380. <https://doi.org/10.2118/166265-PA>.
- Zhang, G. & Seright, R. S. (2015): *Hydrodynamic Retention and Rheology of EOR Polymers in Porous Media*. Presented at the SPE International Symposium on Oilfield Chemistry, The Woodlands, Texas, USA, 13-15 April 2015. <https://doi.org/10.2118/173728-MS>.
- Åsen, S. M., Stavland, A., Strand, D. & Hiorth, A. (2019): *An Experimental Investigation of Polymer Mechanical Degradation at the Centimeter and Meter Scale*, Society of Petroleum Engineers Journal, Vol. 24: 1700-1713. <https://doi.org/10.2118/190225-PA>.

Appendix: Papers (1-4)

Paper 1:

Polymer Flow in Porous Media: Relevance to Enhanced Oil Recovery

Article

Polymer Flow in Porous Media: Relevance to Enhanced Oil Recovery

Arne Skauge^{1,2,*}, Nematollah Zamani³, Jørgen Gausdal Jacobsen^{1,3}, Behruz Shaker Shiran³, Badar Al-Shakry¹  and Tormod Skauge²

¹ Department of Chemistry, University of Bergen, Allegaten 41, N-5020 Bergen, Norway; joja@norceresearch.no (J.G.J.); Badar.Al-Shakry@uni.no (B.A.-S.)

² Energy Research Norway, N-5020 Bergen, Norway; Tormod.Skauge@energyresearch.no

³ Uni Research, N-5020 Bergen, Norway; Nematollah.zamani@uni.no (N.Z.); Behruz.shaker@uni.no (B.S.S.)

* Correspondence: arne.skauge@kj.uib.no; Tel.: +47-5558-3358

Received: 1 June 2018; Accepted: 3 July 2018; Published: 10 July 2018



Abstract: Polymer flooding is one of the most successful chemical EOR (enhanced oil recovery) methods, and is primarily implemented to accelerate oil production by sweep improvement. However, additional benefits have extended the utility of polymer flooding. During the last decade, it has been evaluated for use in an increasing number of fields, both offshore and onshore. This is a consequence of (1) improved polymer properties, which extend their use to HTHS (high temperature high salinity) conditions and (2) increased understanding of flow mechanisms such as those for heavy oil mobilization. A key requirement for studying polymer performance is the control and prediction of in-situ porous medium rheology. The first part of this paper reviews recent developments in polymer flow in porous medium, with a focus on polymer in-situ rheology and injectivity. The second part of this paper reports polymer flow experiments conducted using the most widely applied polymer for EOR processes, HPAM (partially hydrolyzed polyacrylamide). The experiments addressed highrate, near-wellbore behavior (radial flow), reservoir rate steady-state flow (linear flow) and the differences observed in terms of flow conditions. In addition, the impact of oil on polymer rheology was investigated and compared to single-phase polymer flow in Bentheimer sandstone rock material. Results show that the presence of oil leads to a reduction in apparent viscosity.

Keywords: EOR; polymer flooding; in-situ rheology; non-Newtonian flow in porous medium

1. Introduction

The success of polymer flooding depends on the ability of injected solutions to transport polymer molecules deep into a reservoir, thus providing enhanced mobility ratio conditions for the displacement process. In the following sections, we focus on the principal parameters that are crucial in the decision-making process for designing a satisfactory polymer flood design.

The application of polymer flooding to tertiary oil recovery may induce high injection pressures, resulting in injectivity impairment. Since the volumetric injection rate during polymer flooding is constrained by formation fracture pressure, project economics may be significantly affected. Thus, injectivity is a critical parameter and key risk factor for implementation of polymer flood projects.

A large number of injectivity studies, both theoretical and experimental, have been performed in porous media during recent decades, albeit they were mainly studies of linear cores in the absence of residual oil [1–7]. Recently, Skauge et al. [8] performed radial injectivity experiments showing significant reduction in differential pressure compared to linear core floods. This discrepancy in polymer flow in linear cores compared to that in radial disks is partly explained by the of differing pressure conditions that occur when polymer molecules are exposed to transient and semi-transient

pressure conditions in radial disks, as opposed to the steady state conditions experienced in linear core floods. In addition, they observed that the onset of apparent shear thickening occurs at significantly higher flux in radial floods. Based on these results, injectivity was suggested to be underestimated from experiments performed in linear core plugs. However, these experiments were performed in the absence of residual oil. If residual oil has a significant effect on polymer propagation in porous media, experiments performed in its absence will not be able to accurately predict polymer performance.

Experimental studies investigating the effects of residual oil on polymer propagation through porous media have been sparse, although they have generally shown decreasing levels of polymer retention in the presence of residual oil [9,10].

The polymer adsorbs to the rock surface and may also block pores due to polymer size (straining) and flow rate (hydrodynamic retention). In addition, different trapping mechanisms may take place. The polymer retention phenomena influence the flow of polymer in porous media, however, these effects are beyond the scope of this paper. The subject has been reviewed in several other books and papers, e.g., Sorbie [11] and Lake [12].

History matches performed in this study aim to highlight the injectivity of partially hydrolyzed polyacrylamides (HPAMs) in radial disks saturated with residual oil, as these conditions best mimic actual flow conditions in oil reservoirs. Results show that the presence of residual oil reduces the apparent viscosity of HPAM in flow through porous media, thus improving injectivity. These results may facilitate increased implementation of polymer EOR (enhanced oil recovery) projects, as previous projects deemed infeasible may now be economically viable.

2. Theory

2.1. In-Situ Rheology

Polymer viscosity as a function of shear rate is usually measured using a rheometer. During the measurement process, polymer solutions are exposed to different shear rates in a stepwise manner. For each shear rate, polymer viscosity is measured after steady state conditions are achieved; at this state, it is referred to as bulk viscosity. However, polymer molecules experience significantly different flow conditions in rheometers compared to porous media. In particular:

- (I) unlike rheometers, porous media exhibit an inherently complex geometry;
- (II) phenomena such as mechanical degradation may change rheological properties;
- (III) although they only demonstrate shear thinning behavior in rheometers, polymer solutions may exhibit apparent shear thickening behavior above a certain critical flow rate;
- (IV) due to the tortuosity of porous media and existence of several contraction-expansion channels, polymer solutions are exposed to a wide range of shear rates at each flow rate and where extensional viscosity becomes more dominant, resulting in significantly different rheology behavior compared to bulk flow.

To account for these contrasting flow conditions, in-situ viscosity has been suggested to describe the fluid flow behavior of polymer solutions in porous media. In-situ viscosity is a macroscopic parameter that can be calculated using Darcy's law for single-phase non-Newtonian fluids:

$$\mu_{app} = \frac{KA \Delta P}{Q L} \quad (1)$$

It is generally measured in core flood experiments as a function of Darcy velocity. Comparison of in-situ and bulk rheology (Figure 1) shows vertical and horizontal shifts between viscosity curves. Vertical shifts may be due to phenomena such as mechanical degradation, while horizontal shifts are due to a conversion factor between in-situ shear rate and Darcy velocity, shown as α . The red line in Figure 1 shows an increase in apparent viscosity, which is due to polymer adsorption. The adsorbed layer of polymer reduces the effective pore size and blocks smaller pores, both leading to increased

resistance to flow e.g., as determined by an increase in pressure at a given rate compared to a non-adsorbing situation. In contrast, a reduction in pressure (and therefore, in apparent viscosity) can be observed in the presence of depleted layers (see e.g., Sorbie [11]) which leads to slip effects.

Due to the time-consuming nature of in-situ measurements, there have been several attempts to investigate in-situ rheology, both analytically and numerically. In spite of extensive studies [13–22], limited success has been achieved to reliably relate in-situ to bulk viscosity based on polymer solution and porous media properties. Most of these models were developed based on analytical solutions of non-Newtonian flow through capillary bundles, which simplifies the complex geometry of porous media.

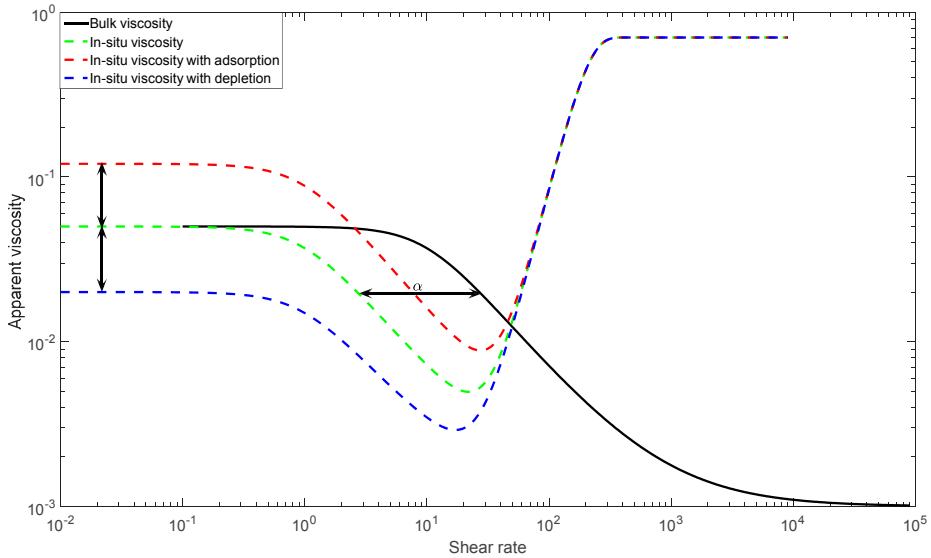


Figure 1. Schematic comparison of in-situ and bulk rheology.

In the following, the calculation procedure of in-situ viscosity is briefly explained:

1. Analytical solutions for a power-law fluid ($\mu = C \dot{\gamma}^{n-1}$) at a given flow rate through a capillary tube with an arbitrary radius (R) can be defined by Equation (2). By comparing Equation (2) with the Poiseuille volumetric flow rate for Newtonian fluids in a tube (Equation (3)), an apparent viscosity and shear rate can be obtained from Equations (4) and (5), respectively.
2. The analytical equation in a single tube (Equation (5)) can be extended to account for real porous media by using the capillary bundle approach [23–25]. An equivalent radius of a capillary bundle model for porous media with known porosity (ϕ), permeability (K) and tortuosity (ψ) can be obtained by Equation (6). By calculating the Darcy velocity and substituting the equivalent radius (Equation (6)) into Equation (5), the apparent shear rate as a function of Darcy velocity can be obtained by Equation (7).

$$Q = \frac{\pi n}{3n+1} \left(\frac{\Delta P}{2CL} \right)^{1/n} R^{\frac{3n+1}{n}} \quad (2)$$

$$Q = \frac{\pi}{8\mu} \frac{\Delta P}{L} R^4 \quad (3)$$

$$\mu_{eff} = C \left(\frac{3n+1}{4n} \right) \left(\frac{R\Delta P}{2CL} \right)^{\frac{n-1}{n}} \quad (4)$$

$$\mu_{app} = C \dot{\gamma}_{app}^{n-1} \Rightarrow \dot{\gamma}_{app} = \left(\frac{3n+1}{4n} \right)^{\frac{1}{n-1}} \left(\frac{R\Delta P}{2CL} \right)^{1/n} \tag{5}$$

$$R_{eq} = \sqrt{\frac{8K\psi}{\phi}} \tag{6}$$

$$\dot{\gamma}_{app} = 4 \left(\frac{3n+1}{4n} \right)^{\frac{n}{n-1}} \frac{U}{\sqrt{8K\phi\psi}} \tag{7}$$

3. The above expressions are considered as an analytical basis for calculating apparent viscosity in porous media. Based on Equation (7), a simplified linear correlation between apparent shear rate and Darcy velocity is generally suggested, i.e., Equation (8), in which the correction factor (α) is the key factor. Some proposed equations for the correction factor are summarized in Table 1. By comparing different coefficients, different values for apparent viscosity may be obtained.

$$\dot{\gamma}_{app} = \alpha \frac{U}{\sqrt{K\phi}} \tag{8}$$

Table 1. Summary of proposed models for correction factor (α).

Model	Equation for Correction Factor (α)	Description
Analytical solution	$4 \left(\frac{3n+1}{4n} \right)^{\frac{n}{n-1}}$	n is the power index in power-law region
Hirasaki and Pope [26]	$\frac{12}{\sqrt{150}} \left(\frac{3n+1}{4n} \right)^{\frac{n}{n-1}}$	n is the power index in power-law region
Cannella et al. [16]	$\frac{\beta}{\sqrt{S_w}} \left(\frac{3n+1}{n} \right)^{\frac{n}{n-1}}$	n is the power index in power-law region, S_w is water saturation, β is a constant equal to 6.

Based on the capillary bundle approach, other models were also proposed by Bird et al. [24], Christopher and Middleman [25], and Teeuw and Hesselink [15], in which the modified Blake-Kozeny model is used for power-law fluids (Equation (9)) and apparent viscosity is obtained using Equation (10).

$$U = \left(\frac{K}{\mu_{app}} \frac{\Delta P}{L} \right)^{1/n} \tag{9}$$

$$\mu_{app} = C \left(\frac{3n+1}{4n} \right)^n \left(\frac{K\phi}{\beta} \right)^{(1-n)/2} \tag{10}$$

Based on the discussion given by Teeuw and Hesselink [15], tortuosity has a dual effect on both shear rate and shear stress calculations. Christopher and Middleman [25] only incorporated tortuosity in shear stress calculations, while Bird et al. [24] incorporated tortuosity into the shear rate term. The various values of β chosen by different authors are summarized in Table 2.

Table 2. β values applied by different authors where $\psi = 25/12$.

Model	β
Bird et al. [24]	$\sqrt{2\psi}$
Christopher and Middleman [25]	$\sqrt{\frac{2}{\psi}}$
Teeuw and Hesselink [15]	$\sqrt{2}$

Hirasaki and Pope [26] conducted several core flood experiments where permeability was in the range 7–23 mD, porosity in the range 18–20% and residual oil between 20% and 32%. Based on these

experiments, they concluded that apparent viscosity could be calculated using the capillary bundle approach and Blake-Kozeny model as follows:

$$\mu_{app} = HU^{n-1} \quad (11)$$

where:

$$H = \frac{C}{12} \left(\frac{9n+3}{n} \right)^n (150K\phi)^{\frac{1-n}{2}} \quad (12)$$

They also included pore size distribution in their calculations:

$$\mu_{app} = \frac{C}{4} \left(\frac{1+3n}{n} \right)^n \frac{\int_0^\infty \sigma(R)R^2 dR}{\left[\int_0^\infty \sigma(R)R^{\frac{1+n}{n}} dR \right]^n} \left(\frac{q}{\phi} \right)^{n-1} \quad (13)$$

Sadowski and Bird [16] used the Ellis model to obtain viscosity from the shear rate. The following equations for apparent viscosity were suggested based on the Blake-Kozeny model and capillary bundle approach:

$$\frac{1}{\mu_{eff}} = \frac{1}{\mu_0} \left(1 + \frac{4}{n+3} \left[\frac{\tau_{RH}}{\tau_{1/2}} \right]^{n-1} \right) \quad (14)$$

$$\tau_{Rh} = \left(\frac{\Delta P}{L} \right) \left[\frac{D_p \phi}{6(1-\phi)} \right] \quad (15)$$

In the above expressions, μ_0 , $\tau_{1/2}$ and n are Ellis model parameters that can be measured in rheometers. By applying these equations, they obtained an acceptable match between experimental and predicted results for low to medium molecular weight polymers.

In summary, none of the proposed models for non-Newtonian fluids in porous media based on the capillary bundle approach are in agreement with all experimental results. Therefore, some known limitations of the capillary bundle approach are noted as follows:

- It neglects complex features of porous media such as tortuosity and pore size distribution.
- It assumes unidirectional flow as it neglects interconnectivity between pores.
- It cannot be representative for flow in an anisotropic medium due to its assumption of unique permeability along propagation direction.
- It assumes a single radius along bundles with no variation in cross-sectional area. The contraction-expansion feature of non-Newtonian flow in porous media is of high importance, especially when studying extensional viscosity, yield stress and elasticity.
- It is generally developed based on rheological models in which analytical solutions for velocity profiles are available (e.g., power-law and Ellis model). Analytical solutions for some models (e.g., Carreau model) are quite difficult and the equation for velocity is implicit (Equation (10) for the Carreau model) and needs to be solved iteratively.

$$\frac{\partial v_z}{\partial r} = -\frac{\Delta p r}{2L} \left\{ \mu_\infty + \frac{\mu_\infty - \mu_0}{\left[1 + \left(\lambda \frac{\partial v_z}{\partial r} \right)^2 \right]^{\frac{n-1}{2}}} \right\} \quad (16)$$

Duda et al. [27] studied polymer solution rheology inside porous media and reported that experimentally measured pressure drops were greater than those predicted by capillary bundle models, especially at lower values of the Carreau power index. Based on their study, a key reason for underestimating correction factors using the capillary bundle approach is the model's failure to capture either the interconnectivity of pores or non-uniform cross-sections of pore bodies and pore throats (i.e., abrupt contractions and expansions, also known as aspect ratio).

According to the aforementioned limitations of the capillary bundle approach and lack of a universally accepted equation for calculating shear rates in porous media, the application of effective medium theory was eventually suggested. This method was able to remediate certain weaknesses in capillary bundle approach, for example, by incorporating pore interconnectivity and variation in cross-sections. Canella et al. [18] extended this method to account for power-law fluids in porous media. Core floods were conducted using xanthan in the concentration range 300–1600 ppm, rock lithology (sandstone and carbonates) in the permeability range 40–800 mD and various oil residuals (0–29%). Their general assumption was that bulk rheological properties of polymer solutions obey the power-law model, and they suggested the following equation for the relation between shear rate and Darcy velocity based on effective medium theory:

$$\dot{\gamma}_{app} = \beta \left(\frac{3n + 1}{4n} \right)^{\frac{n}{n-1}} \frac{q}{\sqrt{K\phi S_w}} \quad (17)$$

Canella et al. achieved a satisfactory match with their experimental results by using a constant value of 6 for β , although this value far exceeds correction factors suggested by other researchers [28–30]. Even though all published results in the literature are not covered by using this correction factor, better agreement between analytical and experimental results was obtained, such as in experiments performed by Teeuw and Hesselink [15] and Gogarty [31].

Canella et al. [18] demonstrated that apparent viscosity depends on both microscopic (connectivity, pore size distribution) and macroscopic properties (permeability, porosity) of porous media. Despite calculation improvements, neither effective medium theory nor the capillary bundle model are able to accurately estimate the correction factor. The great discrepancies in results obtained by the models described above and the wide range of correction factors suggested [17] confirm that a universally accepted model does not yet exist. Insufficiency of these models to predict in-situ viscosity may be attributed to their lack of incorporating time dependence and their use of oversimplified porous media models (e.g., capillary bundle).

To avoid over-simplification of porous media obtained by using the capillary bundle approach, pore network modelling has been suggested. In contrast to the capillary bundle approach, pore network modeling envisages porous media as interconnected bundles with idealized geometries where larger pores (pore bodies) are connected via smaller ones (pore throats). Pore network models have been used by Sorbie et al. [20] to study non-Newtonian fluids that exhibit shear thinning properties; later, several authors studied these phenomena [21,32–35]. Using network modeling, Sorbie et al. [20] showed that in connected (2D) networks of porous media, the average shear rate in the network correlates linearly with the flow rate. This result is not obvious and indeed is rather unexpected. Thus, any formula of the form of Equation (8) which is linear in U , and has a “shift factor”, will do well for shear thinning fluids. The paper also shows that a similar argument holds for extensional flow where the extensional rate in the porous medium correlates linearly with flow rate (U). Lopez et al. [21] applied a pore network model to study non-Newtonian fluids using the same approach as for Newtonian fluids, except that viscosity in each bundle was not assumed to be constant and was considered as a function of pressure drop. Therefore, an iterative approach was suggested to calculate pressure drop and apparent viscosity. Although they obtained satisfactory agreement between analytical and experimental results using this approach, Balhoff and Thompson [34] stated that effects of concentration were neglected, and consequently proposed a new model based on CFD calculations to include effects of concentration in calculating conductivity of pore throats. They used pore network modeling to model shear thinning polymer flow with yield stress within a sand-pack.

Zamani et al. [35] studied the effects of rock microstructures on in-situ rheology using digital rock physics and reported that microscopic properties such as aspect ratio, coordination number and tortuosity may affect deviation of in-situ from bulk rheology.

In some experiments [23,27,31,36], in-situ rheology has been reported to deviate significantly from the behavior in bulk flow, such that in-situ rheology may not be calculated directly from bulk

rheology using the previously mentioned models. To achieve this, one may use these approaches assuming that either in-situ rheological properties are different from bulk rheological properties (e.g., Hejri et al. [36]) or that the relationship between apparent shear rate and Darcy velocity is non-linear (e.g., Gogarty [31]).

Calculation of in-situ rheology is a controversial subject. Until now, there has been no direct method to obtain it and, generally it has been measured by performing core floods. However, Skauge et al. [37] observed significantly different in-situ rheology for HPAM in linear compared to radial geometry. This discrepancy might be due to differing pressure regimes and flux conditions experienced by polymer solutions flowing through these inherently different flow geometries.

The problem with in-situ rheology calculations extends beyond finding the appropriate correction/shift factor. It also encompasses predicting the onset of extensional viscosity, which is treated as a separate subject in the following section.

2.2. Extensional Viscosity

Several experimental results show that, although polymer solutions (e.g., HPAM) only demonstrate shear thinning behavior in a rheometer, they may exhibit apparent shear thickening behavior above a critical shear rate in porous media (Figure 2) [23,27,31,36]. Generally, polymer flow in porous media may be divided into two distinct flow regimes: shear dominant and extensional dominant flow regimes. Since apparent shear thickening occurs in the extensional flow regime, it may also be referred to as extensional viscosity.

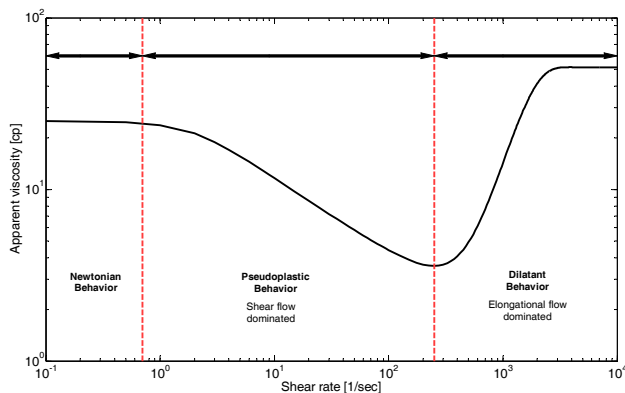


Figure 2. Schematic illustration of apparent viscosity in porous media.

Although its source is poorly understood, extensional viscosity is considered one of the principal aspects of polymer flow in porous media due to its influence on injectivity and oil mobilization. This phenomenon was suggested to be a consequence of elastic properties of polymer solutions (elongational dominated [38] or inertia-dominated flow [39]). As a result, extensional viscosity is often used interchangeably with elongational viscosity, shear thickening behavior, viscosity enhancement, dilatant behavior and viscoelasticity. Two different models are generally used to explain this phenomenon, the transient network model [40–42] and coil stretch model [43]. We adhere to the latter of these models.

Polymer molecules may be envisaged as entangled coils, and when exposed to a flow field, two forces may arise. First, an entropic force that attempts to maintain the existing polymer coil configuration. As coil entanglement increases, higher resistance to deformation is observed. Second the drag force resulting from interactions between solvent fluid and polymer molecules. When shear rate increases beyond a critical rate, molecule configurations change abruptly from coil to stretched states. Therefore,

polymer coils start to deform, resulting in anisotropy and stress differences between elongation and compression. Consequently, normal stresses and elastic properties become more dominant.

Choplin and Sabatie [40] suggested that when polymer molecules are exposed to a simple shear flow at a constant shear rate ($\dot{\gamma}$), molecules rotate at a constant angular velocity (ω) proportional to applied shear rate, and in each rotation polymer molecules are stretched and compressed. The time between each rotation can be calculated by Equation (18).

$$t = \frac{\pi}{2} k \dot{\gamma} \quad (18)$$

where k is a constant of proportionality, related to viscosity. If t is higher than the Zimm relaxation time, no dilatant behavior occurs. Consequently, the critical shear rate at the onset of dilatant behavior may be calculated based on Zimm relaxation time as follows:

$$\lambda_z = \frac{6}{\pi^2} \frac{M_w}{RT} [\mu]_0 \mu_s \quad (19)$$

$$t \leq \lambda_z, \dot{\gamma} \geq \gamma^* \quad We^e \stackrel{We^e}{=} \dot{\gamma} \lambda_z \quad We^* = \lambda_z * \dot{\gamma}^* = \frac{\pi}{2} k \quad (20)$$

Polymer viscosity behavior in extensional flow may be entirely different from its behavior in pure shear flow, i.e., polymer solution may show simultaneous shear thinning and extension thickening behavior. Theoretically, extensional viscosity can be calculated from Equation (21), where N_1 is normal stress difference and $\dot{\epsilon}$ is stretch rate. The relative importance of extensional viscosity and shear viscosity is defined by a dimensionless parameter known as the Trouton ratio (Equation (22)), initially proposed by Trouton [44]. For non-Newtonian fluids (especially viscoelastic fluids), Tr can reach very large values, such as 10^3 to 10^4 (i.e., when polymer solution demonstrates shear thinning and extension thickening simultaneously).

$$\mu_e = \frac{N_1}{\dot{\epsilon}} \quad (21)$$

$$Tr = \frac{\mu_e}{\mu_s} \quad (22)$$

In Figure 2, the in-situ viscosity of viscoelastic polymers is depicted in both shear and extensional flow regime. At the onset of polymer flow, the generated hydrodynamic force from fluid flow (i.e., drag force) is below the threshold value in terms of overcoming entropic forces. Therefore, polymer configuration persists in a coil shape, and viscosity remains constant and equal to the zero-shear rate viscosity (upper Newtonian plateau). As flow rate increases, polymer molecules are exposed to larger drag forces that disentangle polymer coils and aligns them along the flow direction. This coil alignment reduces resistance to flow (i.e., induces viscosity reduction) and is referred to as shear thinning. When the orientation of polymer molecules is completely aligned, they will start to stretch at increasing flow rates. A change in the deformation of polymer molecules may cause normal stress differences. At low stretch rates ($\dot{\epsilon}$), N_1 is very low and by increasing the stretch rate, N_1 dramatically increases. In other words, beyond the critical shear rate ($\dot{\gamma}_c$), instead of intramolecular interaction, intermolecular interactions will develop which generate amorphous structures much larger than average polymer chain dimensions [28,45].

Within the extensional flow regime, the apparent viscosity generally reaches a maximum value, subsequently followed by a decreasing viscosity interval. This phenomenon may be interpreted as high viscoelastic stresses causing polymer rupture and chain halving, and it has been reported as being more severe in low-permeability porous media [46]. As molecular rupture occurs, new molecular weight distributions emerge (larger molecular weight fractions are distorted) and viscosity behavior of the polymer may be governed by a new molecular weight distribution.

The onset of extensional viscosity—the transition point between shear-dominant and extensional dominant flow—depends on polymer, solvent, and porous media properties. The effects of polymer

properties on extensional viscosity can be investigated by using special rheometers that only generate pure extensional flow [47–56]. In the following, the effects of polymer, solvent and porous media properties on the onset of extensional viscosity are explained.

2.2.1. Polymer Concentration

Chauveteau [55] reported that the maximum relaxation time increases with polymer concentration, thus dilatant behavior commences at lower shear rates (Figure 3). He also included the effect of concentration in the expression for Zimm relaxation time, producing Equation (23).

$$\lambda_z = \frac{6}{\pi^2} \mu_s \frac{\mu_{r0} - 1}{C} \frac{M_w}{RT} \quad (23)$$

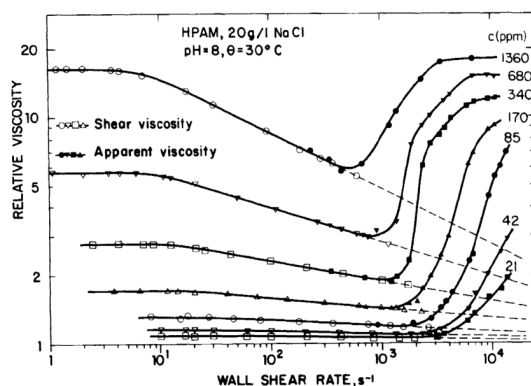


Figure 3. Effect of polymer concentration on the onset of extensional viscosity in a model with 45 successive constrictions. Reproduced with permission from [55].

The effect of concentration on extensional viscosity was also investigated by Lewandowska [56]. In contrast to Chauveteau, he reported that dilatant behavior commences at higher shear rates with increasing polymer concentration. He attributed this observation to the higher degree of entanglement as the concentration increases, thus increasing the extent of the shear thinning region.

Briscoe et al. [57] could not identify a consistent trend between polymer concentration and onset of extensional viscosity. They assumed that only a narrow region of polymer concentrations is able to generate apparent shear thickening behavior. Below a critical concentration limit, defined as the critical overlap concentration (C^*), few polymer chains are able to form transient networks. At concentrations above C^* , the extent of shear thinning may increase and, consequently, the onset of apparent shear thickening may be delayed. This effect was also studied by Dupuis et al. [58], where they observed that the onset of dilatant behavior decreased with polymer concentration. However, rheological behavior above the critical shear rate deviated among different concentration ranges (low: 30–60 ppm; medium: 120–240 ppm; and high: 480–960 ppm). Jiang et al. [59] also confirmed scattered data for the onset of extensional viscosity as function of polymer concentration. Clarke et al. [60] reported that the onset of extensional viscosity is independent of concentration and only depends on molecular weight.

2.2.2. Molecular Weight

The lengths of polymer chains increase with molecular weight, resulting in higher inter- and intramolecular entanglement. Thus, the extent of the shear thinning region increases and, consequently, delay the onset of dilatant behavior [56]. However, this explanation directly contradicts the expression for the Zimm relaxation time (Equation (23)), where the latter increases with molecular weight and causes critical shear rate to occur at a lower shear rate.

Jiang et al. [59] also studied the effects of molecular weight on the onset of extensional viscosity. They concluded that relaxation time increases with molecular weight, thus the onset of extensional viscosity occurs at lower shear rates. In addition, they observed that this trend was not valid above a critical molecular weight.

Clarke et al. [60] proposed the following correlation for the dependency of the onset of extensional viscosity on polymer molecular weight:

$$\lambda_{ext} \propto MW^2 C_p^0 \quad (24)$$

2.2.3. Salinity Effect

The effect of salinity on polymer rheology may be crucial in some reservoir conditions [11,61,62], and depends on polymer type. For typical EOR polymers (e.g., xanthan, HPAM, or generally non-hydrolyzed polymers), increasing salinity generally reduces coil gyration and hydrodynamic radius. Due to the repulsion between ionic groups in HPAM solutions, increasing salinity compresses the electrical double layer on molecular chains and electrostatic repulsion decreases. In the case of HPAM, the reaction mechanism varies for different metal ions i.e., either monovalent (Na^+) or divalent (Ca^{2+}) cations. In the monovalent case, it may suppress the charge effect and reduce the hydrodynamic radius. In the divalent case, reactions between cations (i.e., Ca^{2+}) can play the role of cross-linkers and influence the conformation and rheological properties of HPAM. In both cases, larger shear rates are required to uncoil polymers and the apparent shear thickening commences at larger shear rates [57,58,63].

2.2.4. Degree of Hydrolysis

When HPAM is dissolved in water, electrostatic repulsion forces cause polymer molecules to expand easily and the shear thinning region is shortened. Therefore, as the degree of hydrolysis increases, the onset of apparent shear thickening decreases [56].

2.2.5. Pressure and Temperature Effect

Although polymers are considered incompressible fluids, they do exhibit some degree of compressibility. Thus, pressure may have an impact on viscosity. By increasing pressure, the free volume between polymer molecules decreases and Brownian motion of polymer chains is inhibited, consequently resulting in viscosity increase of polymer solution. Experimental results [64] indicate that the onset of extensional viscosity decrease significantly with pressure.

The effects of temperature on polymer rheology has also been studied extensively [57,59,65,66] and results show that the critical shear rate and onset of dilatant behavior are retarded with increasing temperature. This behavior may have the following two explanations. Firstly, polymer relaxation time and solvent viscosity should both decrease with increasing temperature, based on Equation (23). Secondly, solvent quality decreases with temperature. By decreasing solvent quality, coil size is reduced, and to compensate for this reduction, a larger shear rate is needed to uncoil and elongate the polymer. Therefore, the onset of extensional viscosity occurs at higher shear rates.

2.2.6. Porous Media Properties

In addition to polymer properties, porous media may also significantly influence the generation of extensional flow, as shown by several experimental [25] and numerical studies [67]. Due to variation in cross-sectional area along its propagation path, polymer molecules are forced to accelerate and decelerate. Consequently, they will experience both stretch and shear flow in porous media, and above a critical flow rate, extensional flow will dominate shear flow.

To envisage polymer flow in porous media, the latter may be considered as a simplified contraction-expansion channel. As polymer molecules enter contractions, they will be compressed and stretched. If the flow is below a critical velocity, deformed polymer molecules have sufficient time to

return to their original state. Therefore, when polymer solutions enter subsequent contractions, no stress is stored and no additional resistance to flow is observed. However, if polymer relaxation time is high and polymer molecules are not able to return to their equilibrium state between contractions, stress will be stored and accumulated, thus resulting in steep increases in pressure drop and apparent viscosity. This phenomenon can be interpreted as a memory effect of polymer molecules.

Due to the inherent nature of porous media, polymer molecules are sheared near the wall and elongated at the flow axis. Therefore, molecular momentum is transferred by both tangential and normal stress components in porous media. Seeing that polymer molecules are able to rotate in pore space, molecules are not strained and effective viscosity is only controlled by shear. In contrast, if molecules are exposed to strain for sufficient time, molecule deformation plays a major role and effective viscosity will be defined by strain [25,67–72].

To predict the onset of extensional viscosity in porous media, the dimensionless Deborah number is defined as a ratio between the characteristic relaxation time of a fluid (θ_f) and characteristic time of porous media (θ_p), considered as the average time to travel from one pore body to another (Equation (25)). In other words, the Deborah number may be interpreted as the ratio between elastic and viscous forces. Based on this expression, the Deborah number is zero for Newtonian fluids and infinity for Hookean elastic solids.

$$N_{De} = \frac{\theta_f}{\theta_p} \quad (25)$$

Polymer solutions may have a wide range of molecular weights leading to a large number of relaxation times. Many researchers have used the longest relaxation time as representative of θ_f . However, this may cause the overestimation of Deborah numbers at the onset of extensional viscosity. Relaxation times may also be calculated from normal stress differences [73].

Some experimental observations revealed that the onset of extensional viscosity occurs when N_{De} is larger than 0.5 [74]. However, the Deborah number is not constant in different experiments and a wide range of values has been reported. Marshall and Metzner [73] reported a Deborah number of 0.1 at the onset of extensional viscosity, while Chauveteau [55] reported a relatively high Deborah number of 10. This wide range of reported Deborah numbers at the onset of extensional viscosity is due to difficulties in calculating stretch rates in porous media. To support this idea, Heemskerk et al. [75] reported that by using different polymer types in the same rock sample, critical Deborah numbers (N_{De}) were identical. However, when the same polymer was used in different rock samples, the critical N_{De} varied between 1 and 2. They concluded that measured relaxation times from experimental results can be used to practically define the onset of extensional viscosity, but they acknowledged that equations for calculating stretch rate are not able to capture the exact N_{De} at the onset of extensional viscosity. Zamani et al. [67] proposed that to obtain a more accurate estimation of the critical N_{De} , the stretch rate distribution at the pore scale is required. Metzner et al. [76] concluded that the critical Deborah number might only be used as a first estimation of the onset of extensional viscosity. In Table 3, some suggested equations for the calculation of Deborah number are summarized.

Table 3. Proposed equations for Deborah number calculation.

Model	Equation	Description
Masuda et al. [77]	$N_{De} = \theta_f \dot{\gamma}_{eq}$ $\dot{\gamma}_{eq} = \frac{\dot{\gamma}_c U_w }{\sqrt{k} k_{rw} \phi S_w}$	They used the inverse of the shear rate for θ_f . U_w is the Darcy velocity, k_{rw} is the water relative permeability, S_w is water saturation and $\dot{\gamma}_c$ is a constant equal to $3.97C$, where C is an empirical correlation factor to account for the difference between an equivalent capillary model and real porous media
Hirasaki and Pope [26] Haas and Durst [78] Heemskerk et al. [75]	$\frac{1}{\theta_p} = \dot{\epsilon} = \frac{v}{d} =$ $\frac{U_w}{(1-\phi S_w) \sqrt{150 K_r / (\phi S_w)}}$	

Several experimental results [68,79] show that the Deborah number alone is not sufficient to predict the onset of extensional viscosity. As an explanation, Ranjbar et al. [80] stated that the onset of extensional viscosity highly depends on the elastic properties of polymer solutions and relaxation time alone cannot capture viscoelastic properties. Experimental results reported by Garrouch and Gharbi [79] support this idea. They investigated two different polymer solutions (xanthan and HPAM) in Berea and sand-packs. Calculated Deborah numbers for these two completely and inherently different polymer solutions inside sand-packs were (surprisingly) identical. While xanthan consists of rigid, rod-like molecules that do not show extensional viscosity, HPAM consists of flexible and elastic chain-structured molecules.

Zamani et al. [67] numerically studied the effect of porous media on the onset of extensional viscosity by using real images of porous media obtained from digital rock physics. They confirmed that microscopic features of porous media had significant impact on the onset of extensional viscosity. Furthermore, by increasing the aspect ratio and inaccessible pore volume and decreasing the coordination number, extensional viscosity occurred at lower shear rates, in agreement with several experimental results [55,68,81].

Skauge et al. [37] reported that in radial flow, the onset of extensional viscosity occurred at higher shear rates than at typical core flooding. Since radial flow is more representative of real field conditions, results obtained from radial disks should be more accurate as laboratory data for field implementation.

Briefly summarized, at low shear rates where the amplitude of the elastic component is negligible, flow is controlled by shear forces. In contrast, above a critical shear rate, flow is extensional and governed by elastic forces. Therefore, the response of polymer solutions to imposed stress may be expressed as the sum of shear and elastic components:

$$\Delta P = \Delta P_{shear} + \Delta P_{elastic} \tag{26}$$

$$\mu = \mu_{shear} + \mu_{elastic} \tag{27}$$

The viscosity of polymer solutions under shear flow can be described by empirical equations such as the power-law and Carreau models. To describe viscosity under elongational flow, several models have been suggested, and some of them are summarized in Table 4.

Table 4. Proposed models for calculation of elongational viscosity.

Model	Equation	Description
Hirasaki and Pope [26]	$\mu_{el} = \frac{\mu_{sh}}{[1-N_{De}]}$	
Masuda et al. [77]	$\mu_{elas} = \mu_{sh} C_c (N_{De})^{m_c}$	where C_c and m_c are constant and relate to pore geometry
Delshad et al. [61]	$\mu_{el} = \mu_{max} \left[1 - \exp\left(-(\lambda_2 \tau_r \dot{\gamma})^{n_2-1}\right) \right]$ $\tau_r = \tau_1 + \tau_0 C_p$ $\mu_{max} = \mu_w (AP_{11} + AP_{22} \ln C_p)$	τ_r is the characteristic relaxation time and can be calculated by dynamic frequency sweep test in the laboratory. Some empirical correlations are also proposed for dependency of different parameters on polymer concentration
Stavland et al. [62]	$\mu_{el} = (\lambda_2 \dot{\gamma})^m$ $\lambda_2 = \left\{ N_{De} \left(\frac{1-\phi}{\phi} \right) \left(\frac{6\alpha \sqrt{\pi}}{\lambda_1} \right) \right\}^{-1}$	m is a non-zero tuning parameter which is known as the elongation exponent and depends on the molecular weight and demonstrates linear correlation with $[\mu] C_p$. α in the listed formulation is considered 2.5

2.3. Injectivity

Polymer injectivity is a crucial factor governing the economics of polymer flooding projects and its accurate estimation is a prerequisite in terms of optimizing the upper-limit injection rate [82]. Injection well pressure may increase due to one of the following causes: (1) oil bank formation, (2) in-situ polymer viscosity (especially shear thickening due to viscoelasticity) and (3) different types of retention, which cause permeability reduction.

The highest pressure drops observed during polymer flooding are located in the vicinity of the injection wellbore due to dramatic variations in flow rate. Therefore, it is important to include non-Newtonian effects of polymer solutions to accurately predict polymer injectivity. Although both HPAM and xanthan demonstrate shear thinning behavior at low to moderate shear rates, HPAM exhibits apparent shear thickening above a critical flow rate due to its inherent viscoelastic nature. For field applications, injection rates in the vicinity of the injection well may easily exceed the onset of extensional viscosity, and injectivity will then dramatically decrease. In contrast to HPAM, xanthan shows exclusively shear thinning behavior and will attain its highest value of injectivity in the near-wellbore region.

Injectivity investigations at the lab scale are required before implementing field applications, and effects of polymer solution properties, in-situ rheology, temperature, pH, level of retention and the nature of porous media should be accurately measured [83,84]. Furthermore, if screening criteria for polymer type are disregarded, polymer entrapment in narrow pore throats can have significant effects on its injection rate. The salinity of solutions can also affect polymer solubility, resulting in filter cake formation near injection wells or precipitation of polymer molecules in the reservoir. Inaccurate measurement of in-situ rheology and especially the onset of extensional viscosity may lead to either an underestimation or overestimation of injectivity. In some polymer flooding projects, measured injectivity may differ significantly from the simulation or analytical forecast. These unexpected injectivities may be due to the occurrence of mechanical degradation [82,85,86], induced fractures [87–89], or even inaccurate analytical models for calculating in-situ rheology and predicting extensional viscosity.

3. Radial In-Situ Rheology

Injectivity (I) may be defined as the ratio of volumetric injection rate, Q , to the pressure drop, ΔP , associated with polymer propagation between injection well and producer [1]:

$$I = \frac{Q}{\Delta P} \quad (28)$$

As previously mentioned, formation fracture pressure may constrain the value of volumetric injection rate. Due to its significant effect on project economics, accurate determination of differential pressure, and hence injectivity, at a given injection rate is essential. To achieve this, all factors affecting differential pressure during polymer flooding must be quantified. Darcy's law for radial flow may be expressed in terms of differential pressure as follows:

$$\Delta P = \frac{\mu_{app} Q}{2\pi h k_{e,i}} \ln \frac{r_e}{r_w} \quad (29)$$

where μ_{app} is apparent viscosity, h is disk thickness, $k_{e,i}$ is effective permeability to polymer solution, r_e is disk radius and r_w is injection well radius.

In this paper, the ratio of resistance factor (RF) to residual resistance factor (RRF) is used to represent apparent viscosity of polymer solutions propagating through porous media, thus isolating its viscous behavior, i.e.,

$$\mu_{app} = \frac{RF}{RRF} \quad (30)$$

where the resistance factor (RF) represents the pressure increase of polymer relative to brine and the residual resistance factor (RRF) is defined as the ratio of pressure before and after polymer injection (i.e., pressure caused by irreversible permeability reduction induced by retention mechanisms).

Due to their inherent viscoelastic behavior in porous media, synthetic polymers (e.g., HPAM) will exhibit shear-dependent apparent viscosity. Although the common consensus on apparent shear thickening as a phenomenon is accepted, its viscosifying magnitude is still an ongoing topic of debate in scientific communities.

Accurate polymer rheology estimation is a prerequisite for reasonable injectivity estimates due to the proportionality between apparent viscosity and differential pressure. In linear core floods where steady-state pressure conditions exist, polymer flux will remain constant from inlet to outlet, rendering rheology estimation a straightforward task. However, in radial flow, polymer flux is gradually reduced as it propagates from injection well to producer, therefore attaining a range of viscosities rather than one specific value. Since the degree of mechanical degradation generally increases with injection rate, discrepancies in polymer rheology obtained from different injection rates may transpire. Instead of possessing one definite rheology, polymers propagating through radial disks will exhibit both shear-dependent and history-dependent viscosity behavior, thus increasing the complexity of rheology estimation in radial compared to linear models. To date, no correction factor has been suggested to account for this dual nature phenomenon. Even when mechanical degradation is excluded, i.e., when injected and effluent viscosities are approximately equal, this dual nature phenomenon persists, and is suggested to be attributed to non-equilibrium pressure conditions experienced in radial flow and inherent history-dependent nature of polymer molecules.

In addition, synthetic polymers are susceptible to mechanical degradation at high flux, typically in the near-wellbore region, which will impart an irreversible viscosity reduction due to polymer molecule fragmentation. Mechanical degradation induces a pressure drop that improves injectivity. However, since it disrupts the carefully selected viscous properties of the polymer solutions by a non-reversible viscosity decrease, mechanical degradation is not a sought-after phenomenon in polymer flooding. A remediation measure to reduce mechanical degradation is to pre-shear the polymer before injection. Pre-shearing removes the high molecular weight part of the molecular weight distribution, which is believed to be most susceptible to mechanical degradation [6]. Mechanical degradation may also be minimized by shifting to a lower molecular weight polymer. However, this would require higher amounts of polymer to obtain the same concentration, thus potentially influencing polymer project economics.

As mentioned, in radial geometry, high flux causing mechanical degradation occurs principally in the near-wellbore region, as opposed to linear geometry where this high flux persists throughout the entire propagation distance. Therefore, the time that polymer is exposed to high shear is short in radial transient flow pattern, as opposed to that of a steady-state linear core flood, [34]. Based on this time-differing condition between linear and radial flow, it was suggested by Skauge et al. that polymer is degraded to a lesser extent in radial compared to linear flood when injected at the same volumetric flow rate [33].

In summary, there are two principal factors governing injectivity during polymer flooding in linear geometry: (1) viscoelasticity of polymer that induces large injection pressures mainly due to apparent shear thickening behavior at high flux; and (2) mechanical degradation in the near-wellbore region, which causes an entrance pressure drop [1]. In radial disks, two additional factors should be included: (3) non-equilibrium pressure conditions due to kinetic effects; and (4) memory-effects of polymer molecules in non-constant velocity fields.

4. Materials and Methods

Rock: Bentheimer outcrop rock (porosity of ~23%, permeability of about 2.6 Darcy). Based on XRD measurements, Bentheimer consists predominantly of quartz (90.6%) with some feldspar (4.6%), mica (3.2%) and siderite (1.0%).

Polymer: Flopaam 3630S, 30% hydrolyzed, MW = 18 million Da.

Brine: Relatively low salinity with a low content of divalent ions. Brine composition by ions is given in Table 5.

Table 5. Brine ionic composition.

Ion	Concentration (ppm, <i>w/w</i>)
Na	1741
K	28
Ca	26
Mg	17
SO ₄	160
Cl	2687
TDS	4659
Ionic strength	0.082
Hardness	43

Linear core floods: Core data are summarized in Table 6. All experiments were performed at room temperature and pressure.

Radial core floods: Bentheimer disks were prepared by coating with epoxy resin, vacuuming and saturating with brine. One disk was then drained with an extra heavy oil and aged for 3 weeks at 50 °C to a non-water-wet state. The crude had an initial viscosity of about 7000 cP. The extra heavy oil used for drainage and aging, was then exchanged with a flooding oil of 210 cP. Both experiments were performed at room temperature and pressure. Core data are given in Table 7. The pressure ports were located in the injection and production wells and at radii 0.5, 1.0, 1.5, 2.0, 3.0, 4.0 and 5.0 cm for the disk without oil and at radii 1.1, 2.0, and 5.0 cm for the disk containing oil.

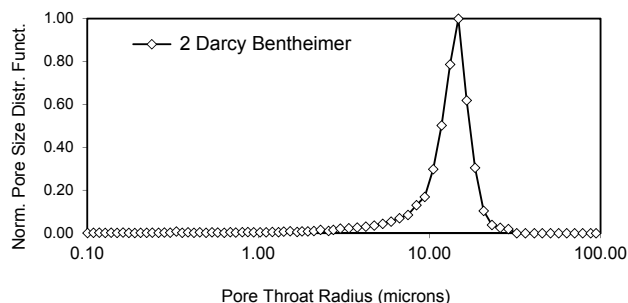
The Bentheimer cores show a pore-throat distribution function similar to other outcrop sandstone material, Figure 4. All porous media have local pore-size variation, involving continuous contraction and expansion of pore-scale transport.

Table 6. Core data for linear core floods.

Experiment	Conc.	L (cm)	D (cm)	ϕ (-)	K_{wi} (Darcy)	K_{wf} (Darcy)	RRF (-)	η_i (cP)	η_e (cP)
No oil	500 ppm	9.54	3.77	0.24	2.48	1.35	1.84	6.81	6.62
No oil	1500 ppm	4.89	3.79	0.24	1.99	0.32	6.29	33.76	32.87
With oil, not aged	500 ppm	10.44	3.78	0.23	1.83	0.36	5.08	6.65	6.77
With oil, aged	500 ppm	9.85	3.78	0.23	2.27	0.27	8.41	6.99	5.90

Table 7. Core data for radial core floods.

Experiment	Diameter (cm)	Thickness (cm)	Well Radius (cm)	ϕ (-)	PV (mL)	Soi (frac)	Sorw (frac)	$K_{w,abs}$ (Darcy)	$K_{w,Sorw}$ (Darcy)	K_{wf} (Darcy)
No oil	30.00	2.20	0.15	0.24	373	n.a.	n.a.	2.600	n.a.	0.056
With oil	29.90	2.21	0.30	0.23	352	0.91	0.22	1.551	0.041	0.039

**Figure 4.** Mercury injection derived pore throat distribution for Bentheimer core material used in the polymer flow experiments.

Simulation: The experimental set-up enabled detailed monitoring of pressure by internal pressure ports located at various distance from the injection well. Differential pressure as function of radial distance was history matched using the STARS simulator, developed by Computer Modeling Group (CMG). The simulation model encompassed a radial grid with 360 sectors, each consisting of 150 grid block cells in radial direction, where the grid block cell size is 1 mm. Porous media permeability (tuning parameter) was obtained by history matching water floods prior to polymer flooding. Local permeability variation improved the history match compared to analytical solution (Darcy's law for radial flow). Permeability data obtained from water floods were used in subsequent polymer floods to isolate the effects of polymer apparent viscosity on differential pressure. In polymer floods, as the permeability obtained from the precursor water flood was held constant, apparent viscosity could be quantitatively investigated as a function of velocity and was used as the tuning parameter to history match differential pressure. The STARS simulation tool can include both shear thinning and thickening behavior of viscoelastic fluids.

Due to the inherent grid averaging calculation method of the simulation tool, the velocity in the first grid block after the injection well was below its analytical value. Because of a rapid velocity decrease with distance in radial models, this phenomenon was addressed by decreasing the injection well radius, thus effectively parallel shifting the position of the first grid block towards the injection well until the correct velocity was attained. This was a necessary step, since the tuning parameter is apparent viscosity as a function of velocity.

5. Polymer In-Situ Rheology in Linear Cores

Four Bentheimer outcrop cores were used to study polymer in-situ rheology in linear systems. Petro-physical properties of core samples as well as properties of polymer solutions are given in Table 6. Two experiments were carried out to examine the effect of polymer concentration on in-situ rheology of the polymer solution. Partially-hydrolyzed Flopaam 3630S at 500 ppm and 1500 ppm was injected into the cores and the in-situ rheology of the polymer solutions was measured. The two concentrations were chosen to give viscosities representative of the upper and lower limit of what would be economically viable for polymer flooding in an oil field. Both concentrations are above the polymer critical overlap concentration, C^* . The results are presented in Table 6 and Figure 5. The bulk viscosity of 1500 ppm 3630S is about 34 cP which is about 5 times that of 500 ppm 3630S. Comparing in-situ rheology of 500 ppm and 1500 ppm 3630S shows that the onset and degree of apparent shear thickening behavior are fairly similar for both concentrations. This is in line with observations by Skauge et al. [8] and Clarke et al. [60] that the onset of extensional viscosity is independent of polymer concentration and only depends on polymer molecular weight. It is noted that this is generally only true for $C^* < C < C_{lim}$, where C_{lim} is the economic limit for polymer concentration, typically between 1500 and 2500 ppm. Table 6 and Figure 5 show that the magnitude of resistance factor (RF) and residual resistance factor (RRF) are about 4 and 3 times higher for 1500 ppm compared to 500 ppm, respectively. This implies that polymer injectivity is a function of polymer concentration, and better injectivity is achieved with lower polymer concentrations.

A series of experiments was also performed to study the effect of the presence of residual oil on polymer in-situ rheology. In these experiments, Bentheimer cores at residual oil saturations of about 22% and different initial wettability states were flooded with polymer and the in-situ rheology behavior was compared to that of single-phase polymer injection in absence of residual oil. Prior to polymer injection, the cores containing oil were water flooded to residual oil saturation. At the end of the water flood, the flow rates were increased to generate pressures higher than that expected for the subsequent polymer flood. This was performed in order to avoid oil mobilization during the polymer flood and, indeed, no oil production was observed during the subsequent polymer flood. The results are presented and compared in Figure 6. As this figure shows, the onset of apparent shear thickening is not affected by the presence of residual oil or the wettability state of the cores. However, the slope of apparent shear thickening and magnitude of resistance factor is significantly affected by oil presence in

the cores. That is, although onset of apparent shear thickening is independent of oil presence in porous media and its wettability condition, the results show that the degree of apparent shear thickening is lower when oil is present in the porous media.

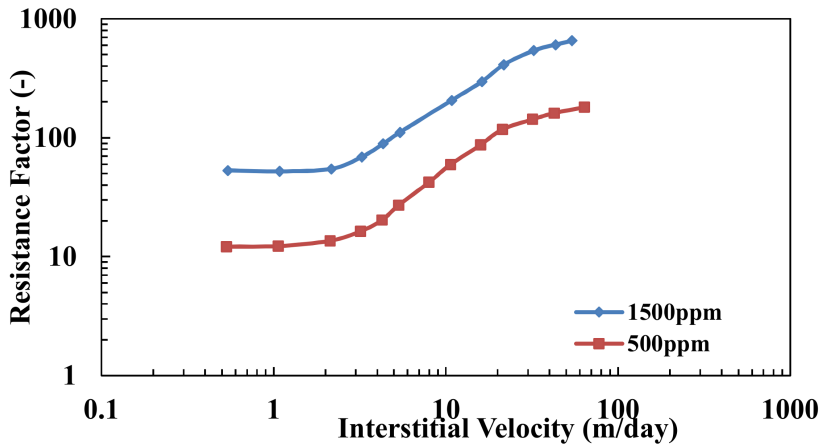


Figure 5. Resistance factor versus interstitial velocity of pre-filtered Flopaam 3630S HPAM polymer dissolved in 1 wt% NaCl brine.

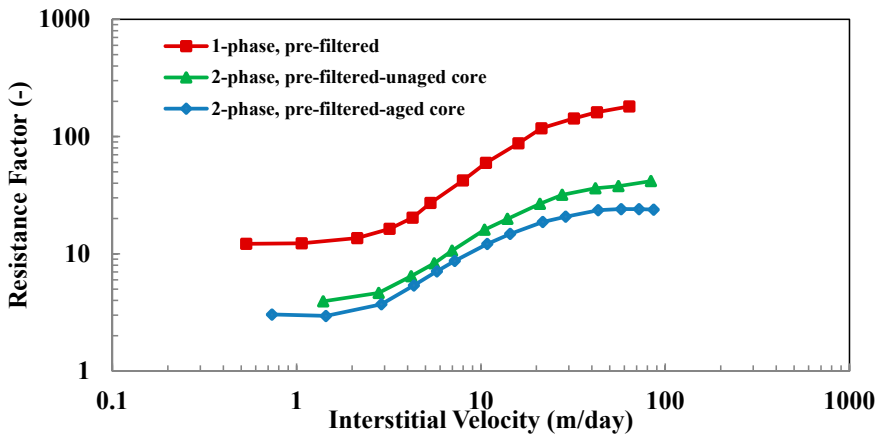


Figure 6. Resistance factor versus interstitial velocity of 500 ppm pre-filtered Flopaam 3630S partially hydrolyzed polyacrylamide (HPAM) polymer dissolved in 1 wt% NaCl brine, single-phase polymer flow and polymer flow at residual oil saturation.

It is important to note that a lower resistance factor in the presence of oil is achieved while porous media is partially occupied by residual oil. Therefore, unlike the single-phase system, in which the pore volume (assuming no inaccessible pore volume) is available for polymer flow, only $PV^*(1-S_{or})$ is available for polymer flow in two-phase system. This influences and reduces permeability and therefore an even higher resistance factor is expected in the presence of oil. However, the results do not show such an effect, and a lower resistance factor and polymer injectivity is observed with the presence of oil in porous media, which supports the significance of the positive effect of oil on polymer injectivity. The effluent polymer viscosity is reduced by 18% compared to the injected polymer solution

for the single-phase, water-wet case, while there is no reduction in effluent viscosity for the two-phase experiments (water-wet and non-water-wet). Shiran and Skauge [90] studied wettability using the same crude oil for aging and found that intermediate wettability was achieved. The end-point water relative permeability confirms that a similar condition was obtained.

Polymer injection in cores with residual oil results in a lower resistance factor which means better polymer injectivity. Furthermore, the resistance factor in the aged core with the non-water-wet state is lower than the resistance factor in the water-wet core. The lower resistance factor in the presence of oil could be attributed to lower adsorption/retention of polymer molecules on rock surface, as reported by Broseta et al. [10]. The rock surface in the presence of an oil film, and especially in less water-wet conditions is partially covered by crude oil polar components during flooding. Therefore, in comparison to single-phase systems, the rock surface has fewer adsorption sites to adsorb polymer molecules. The analysis of reduced apparent viscosity in the presence of oil, assumes that end-point water relative permeability remains constant for polymer as it does for water. The RRF measured with brine after the polymer injection is assumed constant for all rate variation of polymer flow. Under these assumptions a lower resistance factor and better polymer injectivity is expected.

6. Polymer In-Situ Rheology in Radial Flow

Recently, polymer injectivity was analyzed by matching field injectivity tests [5,6,91,92]. In addition to history matching, modification of equations to incorporate fractures and polymer degradation in the near-wellbore zone were reported. The laboratory experiment simplifies the analysis as additional complications like fractures and strong heterogeneity can be avoided.

In earlier studies of radial flow experiments, Skauge et al. [37] used local pressure taps as a function of radial distance from the injection well to derive in-situ rheology. These experiments demonstrated both shear thinning and strong apparent shear thickening behavior.

Two radial flow experiments were performed on circular Bentheimer sandstone disks of 1.6 and 2.6 D permeability with 30 cm diameter and 2.2 cm thickness, see Table 7. The first experiment was performed on a disk that was drained with crude oil and aged to non-water-wet conditions. The second experiment was performed in the absence of oil on a water-wet disk. For the first experiment, the disk was flooded extensively with brine to reach residual oil saturation, $S_{orw} = 0.22$. Bump rates were applied to avoid oil mobilization by viscous forces during the subsequent polymer flood. The polymer flood was performed by first saturating the disk with polymer at a low rate to avoid mechanical degradation due to shearing. Thereafter, rate variations were performed to determine in-situ rheology of the polymer. A brine flush was performed between concentration slugs to remove non-adsorbed polymer.

Concentrations of 800 and 2000 ppm were chosen to represent lower and upper boundaries of the semi-dilute region. The second experiment included the same steps, except for water flooding to S_{orw} . In this case, the water flood was performed to obtain a pressure reference for the subsequent polymer flood. No oil production was detected during polymer floods.

Differential pressure was measured by internal pressure ports located at different radii from the injection well. The 800-ppm HPAM solution was injected in the presence of residual oil at flow rates of 2.2 and 2.8 mL/min, and in the absence of residual oil at 2.0 and 4.0 mL/min. Differential pressure decay as a function of radial distance from injector is shown in Figure 7. The pressure transition zone from semi-steady-state to steady-state is extended compared to the case without oil. Most notable is the difference in pressure in the injection well. While differential pressures measured from internal pressure ports are higher for the two-phase system (as expected), well injection pressure is significantly lower in the presence of residual oil. Taking the pressure ratio of pressure ports at ~1 cm from injection well as a reference, injection pressure should be 5–6 times higher for the disk with oil, compared to the one without. Instead, the injection pressure is 25% lower. There may be several reasons for this observed result. One reason may be that the presence of oil reduces the effective pore volume, thereby leading to higher flow velocities for the polymer in the near-well region. This would

subsequently lead to higher effective shear forces on the polymer, producing mechanical degradation. If mechanical degradation occurs, it has only a minor effect on the shear viscosity. The shear viscosity is 15.1 mPas for the effluent sample taken at 2.0 mL/min, while it was 16.0 mPas for the injected solution (measured at 22 °C, 10 1/s). However, as discussed in Section 2.2, it is the extensional viscosity that is the determining factor for high pressures in near-well region. Changes in extensional viscosity are intrinsically hard to measure and were not performed here. It is still possible that the increase in shear forces for the case with residual oil lead to a reduction in extensional viscosity but not for the case without oil where the effective pore volume was larger. The two other reasons are related to the wetting state of the porous media. If the oil is located in smaller pores, polymer flow is diverted to larger pores where it flows at higher velocities (higher flux). Since the velocity increase takes place in larger pores, only minor degradation would be expected. A third reason may be that porous media is fractionally oil-wet and that there is a difference in the slip conditions for the water-wet and the oil-wet surfaces. This may reduce effective shear for the oil-wet surfaces leading to reduced mechanical degradation. Although there have been speculations on the “lubricating” effect of oil-wet surfaces, no clear evidence of the effect on apparent viscosity or injectivity for core material have been shown to date. It is not possible to differentiate between the three phenomena based on the pressure data alone.

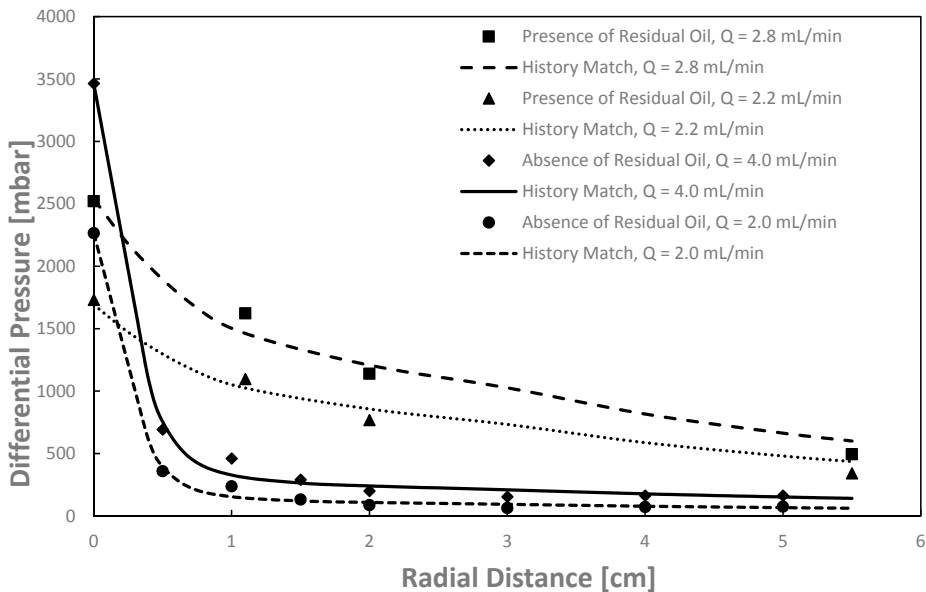


Figure 7. Differential pressure profiles for 800-ppm HPAM floods in the presence and absence of residual oil in radial geometry as a function of distance from injector to producer for four flow rates.

Each of the polymer floods were history matched using STARS (CMG). The measured differential pressures as a function of distance from injection well were used as history match parameters, while polymer apparent viscosity was used as a tuning variable. History matches and polymer rheology from both experiments for 800-ppm HPAM floods are shown in Figures 7 and 8, respectively. It is evident from Figure 8 that the polymer rheology is significantly influenced by the presence of residual oil. In terms of absolute values, the apparent viscosity is between a factor of 5 and 10, and it is higher in the absence, compared to the presence of residual oil. Furthermore, the onset of apparent shear thickening shifts to lower velocities in the presence of residual oil. This occurrence is suggested to result from reduced propagation cross-section caused by the residual oil saturation. When flow

channels in porous media become narrower, the extensional flow regime is reached at a lower flux, and HPAM exhibits viscoelastic behavior at an earlier stage, thus the onset of apparent shear thickening commences at a lower flux. The effect of shifting the onset of apparent shear thickening to a lower flux may be detrimental for injectivity. However, since the apparent shear thickening seems to be much more extensive in the absence of residual oil, the rheology shows that overall injectivity is significantly improved in presence of residual oil.

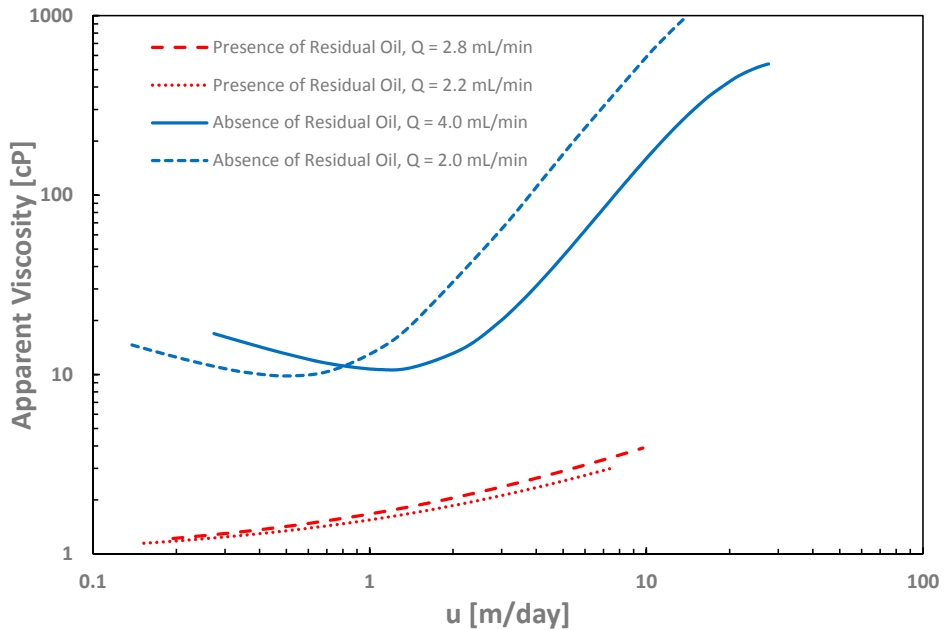


Figure 8. Apparent viscosity from history match of differential pressure for 800 ppm HPAM in presence and absence of residual oil in radial geometry.

History matches and polymer rheology in the presence and absence of residual oil for 2000 ppm floods are shown in Figures 9 and 10, respectively. In order to evaluate the influence of polymer concentration on in-situ rheology, 2000 ppm HPAM was injected in both disks. The differential pressures are shown in Figure 9. In this case, the injection rates were $Q = 2.0$ and 5.0 mL/min for the disk with no oil, and $Q = 1.4$ and 1.6 mL/min for the disk with oil. These data show the same trend as for the 800 ppm injection: strong reduction in injection well pressure in the presence of residual oil and extension of the transition zone.

In accordance with the 800 ppm solution, polymer viscosity was significantly higher in the absence compared to presence of residual oil, and ranged between a factor of 6 and 16 in their joint velocity interval, Figure 10. In addition, the 2000 ppm solution also showed a decrease in the onset of apparent shear thickening in the presence of residual oil, consistent with the lower concentration solution investigated. Similar to the 800 ppm solution, apparent shear thickening is observed to be much more extensive in absence of residual oil, thus improved injectivity in the presence of residual oil is further corroborated.

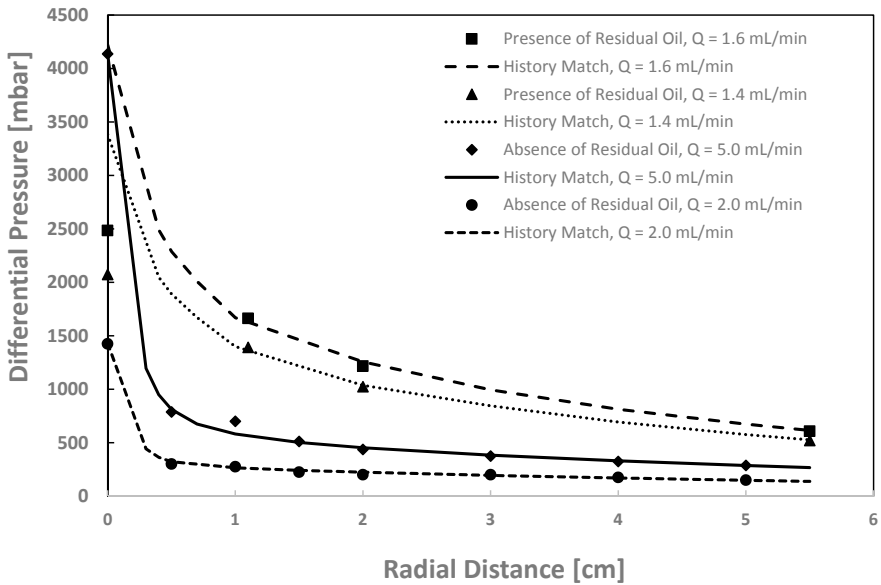


Figure 9. Differential pressure profiles for 2000 ppm 3630S HPAM floods in presence and absence of residual oil in radial geometry as a function of distance from injector to producer for four flow rates.

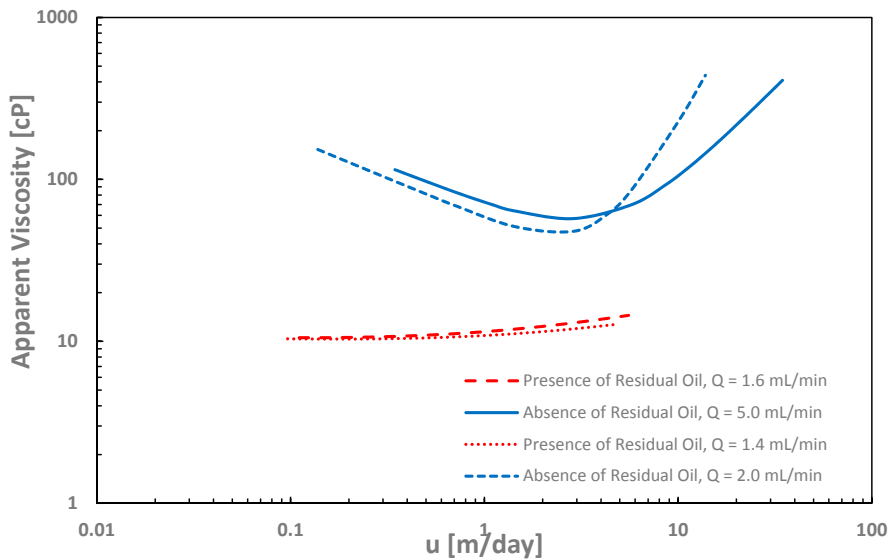


Figure 10. Apparent viscosity from the history match of differential pressure for 2000 ppm 3630S HPAM in the presence and absence of residual oil in radial geometry.

7. Conclusions

A review of polymer flow in a porous medium was presented. The available EOR analytical models we evaluated have limitations in accurately describing flow of polymer at high shear rates, e.g., near injector, and this leads to underestimating or overestimating of polymer injectivity.

The experimental results presented expand our insight into polymer flow in a porous medium. Shear thinning behavior may be present in core floods while bulk rheology is predominant from rheometer measurements. Linear polymer flow experiments are dominated by apparent shear thickening which is not measured in standard rheometers. The extensional viscosity, which is the main cause of the apparent shear thickening behavior, occurs at flow velocities strongly influenced by the porous media.

Linear core floods are commonly used for evaluating polymer in-situ rheology and injectivity, but they suffer from steady-state conditions throughout the core as opposed to the well injection situation where both pressure and shear forces are nonlinear gradients.

In the linear core floods, the onset of apparent shear thickening is independent of polymer concentration, when polymer type, brine composition and porous media are held constant. It is also independent of the presence of oil and wettability for the three cases evaluated here.

Radial flow injections show more complex in-situ rheology. The in-situ rheology shows a much higher degree of apparent shear thickening in the presence of oil. This may be due to restrictions in the pore space available. In the absence of oil, high concentration polymer (2000 ppm) showed shear thinning behavior. The onset of apparent shear thickening was shifted to higher flow velocities. There is a need for further development of numerical models that incorporate memory effects and possible kinetic effects for high polymer flow rates in the near-well region.

Both linear and radial experiments confirm lower apparent viscosity when oil is present in the porous medium. This conclusion is based on the assumption that brine end-point relative permeability is unchanged for polymer injection compared to two-phase flow by water injection. No extra oil was produced during polymer injection and this support the lowering of in-situ polymer viscosity in the presence of oil.

Author Contributions: A.S., B.S.S., and T.S. were responsible for the experimental program and simulation study. N.Z. structured the review contribution, while B.A.-S. and J.G.J. are Ph.D. students working on polymer injectivity, including the experimental study and simulation work. All authors contributed in writing the paper.

Funding: This research received no direct external funding.

Acknowledgments: The authors gratefully acknowledge support from the Norwegian Research Council, Petromaks 2 program. Badar Al-Shakry acknowledge support from, PDO, Petroleum Development Oman. Arne Skauge acknowledge support from Energi Simulations, Canada as the Energi Simulation EOR chair at University of Bergen.

Conflicts of Interest: The authors declare no conflicts of interest.

Nomenclature

A	Cross section area
C	Power-law constant
C_p	Polymer concentration
D_p	Grain size diameter
De	Deborah number
h	Disk thickness
H	Constant, equation 11
k	Constant, equation 18
K_{ei}	Effective permeability to polymer
K	Permeability
L	Length of model
M_w	Polymer molecular weight
N_1	Normal stress difference

n	Ellis, Carreau or power-law constant
P	Pressure
Q	Flow rate
R	Radius
r_e	Disk radius
r_w	Injection well radius
RF	Resistance factor
RRF	Residual resistance factor
R_{eq}	Equivalent radius obtained from Blake-Kozeny model
S_w	Water saturation
T	Temperature
Tr	Trouton ratio
U	Darcy velocity
Wi	Weissenberg number
I	Injectivity
α	Correction factor
β	Constant, equation 10
ω	Angular velocity
$\dot{\epsilon}$	Stretch rate
ΔP	Pressure drop
$\dot{\gamma}$	Shear rate
$\tau_{1/2}$	Ellis model parameter
$\dot{\gamma}_{eff}$	Effective shear rate
$\dot{\gamma}_{app}$	Apparent shear rate
$\dot{\gamma}_c$	Critical shear rate
λ	Polymer relaxation time
λ_z	Zimm relaxation time
μ	Viscosity
μ_{app}	Apparent viscosity
μ_{eff}	Effective viscosity
μ_0	Upper Newtonian plateau
μ_s	Solvent viscosity
μ_{sh}	Shear rate viscosity
μ_e	Elongational viscosity
μ_∞	Lower Newtonian plateau
ϕ	Porosity
ψ	Tortuosity
θ_f	Characteristic relaxation time of fluid
θ_p	Characteristic time of porous media

References

1. Seright, R.S. The Effects of Mechanical Degradation and Viscoelastic Behavior on Injectivity of Polyacrylamide Solutions. *Soc. Pet. Eng. J.* **1983**, *23*, 475–485. [[CrossRef](#)]
2. Shuler, P.J.; Kuehne, D.L.; Uhl, J.T.; Walkup, G.W., Jr. Improving Polymer Injectivity at West Coyote Field, California. *Soc. Pet. Eng. Reserv. Eng.* **1987**, *2*, 271–280. [[CrossRef](#)]
3. Southwick, J.G.; Manke, C.W. Molecular Degradation, Injectivity, and Elastic Properties of Polymer Solutions. *Soc. Pet. Eng. Reserv. Eng.* **1988**, *3*, 1193–1201. [[CrossRef](#)]
4. Yerramilli, S.S.; Zitha, P.L.J.; Yerramilli, R.C. Novel Insight into Polymer Injectivity for Polymer Flooding. Presented at the SPE European Formation Damage Conference and Exhibition, Noordwijk, The Netherlands, 5–7 June 2013. [[CrossRef](#)]
5. Lotfollahi, M.; Farajzadeh, R.; Delshad, M.; Al-Abri, K.; Wassing, B.M.; Mjeni, R.; Awan, K.; Bedrikovetsky, P. Mechanistic Simulation of Polymer Injectivity in Field Tests. Presented at the SPE Enhanced Oil Recovery Conference, Kuala Lumpur, Malaysia, 11–13 August 2015. [[CrossRef](#)]
6. Glasbergen, G.; Wever, D.; Keijzer, E.; Farajzadeh, R. Injectivity Loss in Polymer Floods: Causes, Preventions and Mitigations. Presented at the SPE Kuwait Oil & Gas Show and Conference, Mishref, Kuwait, 11–14 October 2015. [[CrossRef](#)]

7. Al-Shakry, B.; Shiran, B.S.; Skauge, T.; Skauge, A. Enhanced Oil Recovery by Polymer Flooding: Optimizing Polymer Injectivity. Presented at the SPE Kingdom of Saudi Arabia Technical Symposium and Exhibition, Dammam, Saudi Arabia, 23–26 April 2018.
8. Skauge, T.; Kvilhaug, O.A.; Skauge, A. Influence of Polymer Structural Conformation and Phase Behaviour on In-situ Viscosity. Presented at the 18th European Symposium on Improved Oil Recovery, Dresden, Germany, 14–16 April 2015. [[CrossRef](#)]
9. Hughes, D.S.; Teeuw, D.; Cottrell, C.W.; Tollas, J.M. Appraisal of the Use of Polymer Injection To Suppress Aquifer Influx and To Improve Volumetric Sweep in a Viscous Oil Reservoir. *Soc. Pet. Eng.* **1990**, *5*, 33–40. [[CrossRef](#)]
10. Broseta, D.; Medjahed, F.; Lecourtier, J.; Robin, M. Polymer Adsorption/Retention in Porous Media: Effects of Core Wettability on Residual Oil. *Soc. Pet. Eng.* **1995**, *3*, 103–112. [[CrossRef](#)]
11. Sorbie, K.S. *Polymer-Improved Oil Recovery*; Blackie and Son Ltd.: Glasgow, UK, 1991.
12. Lake, L.W. *Enhanced Oil Recovery*; Prentice Hall: Upper Saddle River, NJ, USA, 1989.
13. Savins, J.G. Non-Newtonian Flow through Porous Media. *Ind. Eng. Chem.* **1969**, *61*, 18–47. [[CrossRef](#)]
14. Sadowski, T.J. Non-Newtonian Flow through Porous Media. II. Experimental. *J. Rheol.* **1965**, *9*, 251–271. [[CrossRef](#)]
15. Sochi, T. Non-Newtonian flow in porous media. *Polymer* **2010**, *51*, 5007–5023. [[CrossRef](#)]
16. Sadowski, T.J.; Bird, R.B. Non-Newtonian Flow through Porous Media. I. *J. Rheol.* **1965**, *9*, 243–250. [[CrossRef](#)]
17. Teeuw, D.; Hesselink, F.T. Power-Law Flow And Hydrodynamic Behaviour of Biopolymer Solutions In Porous Media. Presented at the SPE Fifth International Symposium on Oilfield and Geothermal Chemistry, Stanford, CA, USA, 28–30 May 1980. [[CrossRef](#)]
18. Cannella, W.J.; Huh, C.; Seright, R.S. Prediction of Xanthan Rheology in Porous Media. Presented at the 63rd Annual Technical Conference and Exhibition of the Society of Petroleum Engineers, Houston, TX, USA, 2–5 October 1988. [[CrossRef](#)]
19. Fletcher, A.J.P.; Flew, S.R.G.; Lamb, S.P.; Lund, T.; Bjornestad, E.; Stavland, A.; Gjovikli, N.B. Measurements of Polysaccharide Polymer Properties in Porous Media. Prepared for presentation at the SPE International Symposium on Oilfield Chemistry, Anaheim, CA, USA, 20–22 February 1991. [[CrossRef](#)]
20. Sorbie, K.S.; Clifford, P.J.; Jones, E.R.W. The Rheology of Pseudoplastic Fluids in Porous Media Using Network Modeling. *J. Colloid Interface Sci.* **1989**, *130*, 508–534. [[CrossRef](#)]
21. Lopez, X.; Valvatne, P.H.; Blunt, M.J. Predictive network modeling of single-phase non-Newtonian flow in porous media. *J. Colloid Interface Sci.* **2003**, *264*, 256–265. [[CrossRef](#)]
22. Pearson, J.R.A.; Tardy, P.M.J. Models for flow of non-Newtonian and complex fluids through porous media. *J. Non-Newton. Fluid Mech.* **2002**, *102*, 447–473. [[CrossRef](#)]
23. Willhite, G.P.; Uhl, J.T. Correlation of the Flow of Flocon 4800 Biopolymer with Polymer Concentration and Rock Properties in Berea Sandstone. In *Water-Soluble Polymers for Petroleum Recovery*; Springer Publishing: Manhattan, NY, USA, 1988.
24. Bird, R.B.; Stewart, W.E.; Lightfoot, E.N. *Transport Phenomena*; John Wiley and Sons, Inc.: New York, NY, USA, 1960.
25. Christopher, R.H.; Middleman, S. Power-Law Flow through a Packed Tube. *Ind. Eng. Chem. Fundam.* **1965**, *4*, 422–426. [[CrossRef](#)]
26. Hirasaki, G.J.; Pope, G.A. Analysis of Factors Influencing Mobility and Adsorption in the Flow of Polymer Solution Through Porous Media. *Soc. Pet. Eng. J.* **1974**, *14*, 337–346. [[CrossRef](#)]
27. Duda, J.L.; Hong, S.-A.; Klaus, E.E. Flow of Polymer-Solutions in Porous-Media—Inadequacy of the Capillary Model. *Ind. Eng. Chem. Fundam.* **1983**, *22*, 299–305. [[CrossRef](#)]
28. Kishbaugh, A.J.; McHugh, A.J. A rheo-optical study of shear-thickening and structure formation in polymer solutions. Part I: Experimental. *Rheol. Acta* **1993**, *32*, 9–24. [[CrossRef](#)]
29. Pope, D.P.; Keller, A. Alignment of Macromolecules in Solution by Elongational Flow—Study of Effect of Pure Shear in a 4 Roll Mill. *Colloid Polym. Sci.* **1977**, *255*, 633–643. [[CrossRef](#)]
30. Binding, D.M.; Jones, D.M.; Walters, K. The Shear and Extensional Flow Properties of M1. *J. Non-Newton. Fluid Mech.* **1990**, *35*, 121–135. [[CrossRef](#)]
31. Gogarty, W.B. Rheological Properties of Pseudoplastic Fluids in Porous Media. *Soc. Pet. Eng. J.* **1967**, *7*, 149–160. [[CrossRef](#)]

32. Perrin, C.L.; Tardy, P.M.J.; Sorbie, K.S.; Crawshaw, J.C. Experimental and modeling study of Newtonian and non-Newtonian fluid flow in pore network micromodels. *J. Colloid Interface Sci.* **2006**, *295*, 542–550. [[CrossRef](#)] [[PubMed](#)]
33. Sochi, T.; Blunt, M.J. Pore-scale network modeling of Ellis and Herschel–Bulkley fluids. *J. Pet. Sci. Eng.* **2008**, *60*, 105–124. [[CrossRef](#)]
34. Balhoff, M.T.; Thompson, K.E. A macroscopic model for shear-thinning flow in packed beds based on network modeling. *Chem. Eng. Sci.* **2006**, *61*, 698–719. [[CrossRef](#)]
35. Zamani, N.; Bondino, I.; Kaufmann, R.; Skauge, A. Computation of polymer in-situ rheology using direct numerical simulation. *J. Pet. Sci. Eng.* **2017**, *159*, 92–102. [[CrossRef](#)]
36. Hejri, S.; Willhite, G.P.; Green, D.W. Development of Correlations to Predict Biopolymer Mobility in Porous Media. *SPE Reserv. Eng.* **1991**, *6*, 91–98. [[CrossRef](#)]
37. Skauge, T.; Skauge, A.; Salmo, I.C.; Ormehaug, P.A.; Al-Azri, N.; Wassing, L.M.; Glasbergen, G.; Van Wunnik, J.N.; Masalmeh, S.K. Radial and Linear Polymer Flow—Influence on Injectivity. Prepared for presentation at the SPE Improved Oil Recovery Conference, Tulsa, Oklahoma, 11–13 April 2016. [[CrossRef](#)]
38. Faber, T.E. *Fluid Dynamics for Physicists*; Cambridge University Press: Cambridge, UK, 1995.
39. Brown, E.; Jaeger, H.M. The role of dilation and confining stresses in shear thickening of dense suspensions. *J. Rheol.* **2012**, *56*, 875–923. [[CrossRef](#)]
40. Choplin, L.; Sabatie, J. Threshold-Type Shear-Thickening in Polymeric Solutions. *Rheol. Acta* **1986**, *25*, 570–579. [[CrossRef](#)]
41. Indei, T.; Koga, T.; Tanaka, F. Theory of shear-thickening in transient networks of associating polymer. *Macromol. Rapid Commun.* **2005**, *26*, 701–706. [[CrossRef](#)]
42. Odell, J.A.; Müller, A.J.; Keller, A. Non-Newtonian behaviour of hydrolysed polyacrylamide in strong elongational flows: A transient network approach. *Polymer* **1988**, *29*, 1179–1190. [[CrossRef](#)]
43. Degennes, P.G. Coil-Stretch Transition of Dilute Flexible Polymers under Ultrahigh Velocity-Gradients. *J. Chem. Phys.* **1974**, *60*, 5030–5042. [[CrossRef](#)]
44. Trouton, F.T. On the coefficient of viscous traction and its relation to that of viscosity. *R. Soc.* **1906**, *77*, 426–440. [[CrossRef](#)]
45. Edwards, B.J.; Keffer, D.I.; Reneau, C.W. An examination of the shear-thickening behavior of high molecular weight polymers dissolved in low-viscosity newtonian solvents. *J. Appl. Polym. Sci.* **2002**, *85*, 1714–1735. [[CrossRef](#)]
46. Hatzignatiou, D.G.; Moradi, H.; Stavland, A. Experimental Investigation of Polymer Flow through Water- and Oil-Wet Berea Sandstone Core Samples. Presented at the EAGE Annual Conference & Exhibition incorporating SPE Europec, London, UK, 10–13 June 2013. [[CrossRef](#)]
47. McKinley, G.H.; Sridhar, T. Filament-stretching rheometry of complex fluids. *Annu. Rev. Fluid Mech.* **2002**, *34*, 375–415. [[CrossRef](#)]
48. Fuller, G.G.; Cathey, C.A.; Hubbard, B.; Zebrowski, B.E. Extensional Viscosity Measurements for Low-Viscosity Fluids. *J. Rheol.* **1987**, *31*, 235–249. [[CrossRef](#)]
49. Meadows, J.; Williams, P.A.; Kennedy, J.C. Comparison of the Extensional and Shear Viscosity Characteristics of Aqueous Hydroxyethylcellulose Solutions. *Macromolecules* **1995**, *28*, 2683–2692. [[CrossRef](#)]
50. Anna, S.L.; McKinley, G.H.; Nguyen, D.A.; Sridhar, T.; Muller, S.J.; Huang, J.; James, J.F. An interlaboratory comparison of measurements from filament-stretching rheometers using common test fluids. *J. Rheol.* **2001**, *45*, 83–114. [[CrossRef](#)]
51. Shipman, R.W.G.; Denn, M.M.; Keunings, R. Mechanics of the Falling Plate Extensional Rheometer. *J. Non-Newton. Fluid Mech.* **1991**, *40*, 281–288. [[CrossRef](#)]
52. Sridhar, T.; Tirtaatmadja, V.; Nguyen, D.A.; Gupta, R.K. Measurement of Extensional Viscosity of Polymer-Solutions. *J. Non-Newton. Fluid Mech.* **1991**, *40*, 271–280. [[CrossRef](#)]
53. Tirtaatmadja, V.; Sridhar, T. A Filament Stretching Device for Measurement of Extensional Viscosity. *J. Rheol.* **1993**, *37*, 1081–1102. [[CrossRef](#)]
54. James, D.F.; Chandler, G.M.; Armour, S.J. A Converging Channel Rheometer for the Measurement of Extensional Viscosity. *J. Non-Newton. Fluid Mech.* **1990**, *35*, 421–443. [[CrossRef](#)]

55. Chauveteau, G. Molecular interpretation of several different properties of flow of coiled polymer solutions through porous media in oil recovery conditions. Presented at the 56th Annual Fall Technical Conference and Exhibition of the society of Petroleum Engineers of AIME, San Antonio, TX, USA, 5–7 October 1981. [[CrossRef](#)]
56. Lewandowska, K. Comparative studies of rheological properties of polyacrylamide and partially hydrolyzed polyacrylamide solutions. *J. Appl. Polym. Sci.* **2007**, *103*, 2235–2241. [[CrossRef](#)]
57. Briscoe, B.; Luckham, P.; Zhu, S.P. Pressure influences upon shear thickening of poly(acrylamide) solutions. *Rheol. Acta* **1999**, *38*, 224–234. [[CrossRef](#)]
58. Dupuis, D.; Lewandowski, F.Y.; Steiert, P.; Wolff, C. Shear Thickening and Time-Dependent Phenomena—The Case of Polyacrylamide Solutions. *J. Non-Newton. Fluid Mech.* **1994**, *54*, 11–32. [[CrossRef](#)]
59. Jiang, B.; Keffer, D.J.; Edwards, B.J.; Allred, J.N. Modeling shear thickening in dilute polymer solutions: Temperature, concentration, and molecular weight dependencies. *J. Appl. Polym. Sci.* **2003**, *90*, 2997–3011. [[CrossRef](#)]
60. Clarke, A.; Howe, A.M.; Mitchell, J.; Staniland, J.; Hawkes, L.A. How Viscoelastic-Polymer Flooding Enhances Displacement Efficiency. *Soc. Pet. Eng. J.* **2016**, *21*, 675–687. [[CrossRef](#)]
61. Delshad, M.; Kim, D.H.; Magbagbeola, O.A.; Huh, C.; Pope, G.A.; Tarahhom, F. Mechanistic Interpretation and Utilization of Viscoelastic Behavior of Polymer Solutions for Improved Polymer-Flood Efficiency. Prepared for presentation at the 2008 SPE/DOE Improved Oil Recovery Symposium, Tulsa, OK, USA, 19–23 April 2008. [[CrossRef](#)]
62. Stavland, A.; Jonsbråten, H.C.; Lohne, A.; Moen, A.; Giske, N.H. Stavland, A.; Jonsbråten, H.C.; Lohne, A.; Moen, A.; Giske, N.H. Polymer Flooding—Flow Properties in Porous Media Versus Rheological Parameters. Presented at the SPE EUROPEC/EAGE Annual Conference and Exhibition, Barcelona, Spain, 14–17 June 2010. [[CrossRef](#)]
63. Aitkadi, A.; Carreau, P.J.; Chauveteau, G. Rheological Properties of Partially Hydrolyzed Polyacrylamide Solutions. *J. Rheol.* **1987**, *31*, 537–561. [[CrossRef](#)]
64. Lee, K.; Huh, C.; Sharma, M.M. Impact of Fractures Growth on Well Injectivity and Reservoir Sweep during Waterflood and Chemical EOR Processes. Presented at the SPE Annual Technical Conference and Exhibition, Denver, CO, USA, 30 October–2 November 2011. [[CrossRef](#)]
65. Hu, Y.; Wang, S.Q.; Jamieson, A.M. Rheological and Rheoptical Studies of Shear-Thickening Polyacrylamide Solutions. *Macromolecules* **1995**, *28*, 1847–1853. [[CrossRef](#)]
66. Cho, Y.H.; Dan, K.S.; Kim, B.C. Effects of dissolution temperature on the rheological properties of polyvinyl alcohol solutions in dimethyl sulfoxide. *Korea-Aust. Rheol. J.* **2008**, *20*, 73–77.
67. Zamani, N.; Bondino, L.; Kaufmann, R.; Skauge, A. Effect of porous media properties on the onset of polymer extensional viscosity. *J. Pet. Sci. Eng.* **2015**, *133*, 483–495. [[CrossRef](#)]
68. Gupta, R.K.; Sridhar, T. Viscoelastic Effects in Non-Newtonian Flows through Porous-Media. *Rheol. Acta* **1985**, *24*, 148–151. [[CrossRef](#)]
69. Smith, F.W. Behavior of Partially Hydrolyzed Polyacrylamide Solutions in Porous Media. *J. Pet. Technol.* **1970**, *22*, 148–156. [[CrossRef](#)]
70. Kemblowski, Z.; Dziubinski, M. Resistance to Flow of Molten Polymers through Granular Beds. *Rheol. Acta* **1978**, *17*, 176–187. [[CrossRef](#)]
71. Wissler, E.H. Viscoelastic Effects in the Flow of Non-Newtonian Fluids through a Porous Medium. *Ind. Eng. Chem. Fundam.* **1971**, *10*, 411–417. [[CrossRef](#)]
72. Vossoughi, S.; Seyer, F.A. Pressure-Drop for Flow of Polymer-Solution in a Model Porous-Medium. *Can. J. Chem. Eng.* **1974**, *52*, 666–669. [[CrossRef](#)]
73. Marshall, R.J.; Metzner, A.B. Flow of Viscoelastic Fluids through Porous Media. *Ind. Eng. Chem. Fundam.* **1967**, *6*, 393–400. [[CrossRef](#)]
74. Durst, F.; Haas, R.; Interthal, W. Laminar and Turbulent Flows of Dilute Polymer-Solutions—A Physical Model. *Rheol. Acta* **1982**, *21*, 572–577. [[CrossRef](#)]
75. Heemskerk, J.; Rosmalen, R.; Janssen-van, R.; Holtslag, R.J.; Teeuw, D. Quantification of Viscoelastic Effects of Polyacrylamide Solutions. Presented at the SPE/DOE Fourth Symposium on Enhanced Oil Recovery, Tulsa, OK, USA, 15–18 April 1984. [[CrossRef](#)]

76. Metzner, A.B.; White, J.L.; Denn, M.M. Constitutive equations for viscoelastic fluids for short deformation periods and for rapidly changing flows: Significance of the Deborah number. *AIChE J.* **1966**, *12*, 863–866. [[CrossRef](#)]
77. Masuda, Y.; Tang, K.-C.; Miyazawa, M.; Tanaka, S. 1D Simulation of Polymer Flooding Including the Viscoelastic Effect of Polymer Solution. *SPE Reserv. Eng.* **1992**, *7*, 247–252. [[CrossRef](#)]
78. Haas, R.; Durst, F. Viscoelastic Flow of Dilute Polymer-Solutions in Regularly Packed-Beds. *Rheol. Acta* **1982**, *21*, 566–571. [[CrossRef](#)]
79. Garrouch, A.A.; Gharbi, R.C. A Novel Model for Viscoelastic Fluid Flow in Porous Media. Presented at the 2006 SPE Annual Technical Conference and Exhibition, San Antonio, TX, USA, 24–27 September 2006. [[CrossRef](#)]
80. Ranjbar, M.; Rupp, J.; Pusch, G.; Meyn, R. Quantification and Optimization of Viscoelastic Effects of Polymer Solutions for Enhanced Oil Recovery. Presented at the SPE/DOE Eight Symposium on Enhanced Oil Recovery, Tulsa, OK, USA, 22–24 April 1992. [[CrossRef](#)]
81. Kawale, D.; Marques, E.; Zitha, P.L.J.; Kreutzer, M.T.; Rossen, W.R.; Boukany, P.E. Elastic instabilities during the flow of hydrolyzed polyacrylamide solution in porous media: effect of pore-shape and salt. *Soft Matter* **2017**, *13*, 765–775. [[CrossRef](#)] [[PubMed](#)]
82. Seright, R.S.; Seheult, J.M.; Talashek, T. Injectivity Characteristics of EOR Polymers. *SPE Reserv. Eval. Eng.* **2009**, *12*, 783–792. [[CrossRef](#)]
83. Kulawardana, E.U.; Koh, H.; Kim, D.H.; Liyanage, P.J.; Upamali, K.; Huh, C.; Weerasooriya, U.; Pope, G.A. Rheology and Transport of Improved EOR Polymers under Harsh Reservoir Conditions. Presented at the Eighteenth SPE Improved Oil Recovery Symposium, Tulsa, OK, USA, 14–18 April 2012. [[CrossRef](#)]
84. Sharma, A.; Delshad, M.; Huh, C.; Pope, G.A. A Practical Method to Calculate Polymer Viscosity Accurately in Numerical Reservoir Simulators. Presented at the SPE Annual Technical Conference and Exhibition, Denver, CO, USA, 31 October–2 November 2011. [[CrossRef](#)]
85. Manichand, R.N.; Moe Soe Let, K.P.; Gil, L.; Quillien, B.; Seright, R.S. Effective Propagation of HPAM Solutions Through the Tambaredjo Reservoir During a Polymer Flood. *SPE Prod. Oper.* **2013**, *28*, 358–368. [[CrossRef](#)]
86. Zaitoun, A.; Makakou, P.; Blin, N.; Al-Maamari, R.S.; Al-Hashmi, A.-A.R.; Abdel-Goad, M.; Al-Sharji, H.H. Shear Stability of EOR Polymers. *SPE J.* **2011**, *17*, 335–339. [[CrossRef](#)]
87. Suri, A.; Sharma, M.M.; Peters, E. Estimates of Fracture Lengths in an Injection Well by History Matching Bottomhole Pressures and Injection Profile. *SPE Reserv. Eval. Eng.* **2011**, *14*, 405–417. [[CrossRef](#)]
88. Zechner, M.; Clemens, T.; Suri, A.; Sharma, M.M. Simulation of Polymer Injection under Fracturing Conditions—A Field Pilot in the Matzen Field, Austria. *SPE Reserv. Eval. Eng.* **2014**, *18*, 236–249. [[CrossRef](#)]
89. Van den Hoek, P.; Mahani, H.; Sorop, T.; Brooks, D.; Zwaan, M.; Sen, S.; Shuaili, K.; Saadi, F. Application of Injection Fall-Off Analysis in Polymer flooding. Presented at the 74th EAGE Conference & Exhibition incorporating SPE EUROPEC 2012, Copenhagen, Denmark, 4–7 June 2012. [[CrossRef](#)]
90. Shiran, B.S.; Skauge, A. Wettability and Oil Recovery by Polymer and Polymer Particles. Presented at the SPE Asia Pacific Enhanced Oil Recovery Conference, Kuala Lumpur, Malaysia, 11–13 August 2015. [[CrossRef](#)]
91. Al-Abri, K.; Al-Mjeni, R.; Al-Bulushi, N.K.; Awan, K.; Al-Azri, N.; Al-Riyami, O.; Al-Rajhi, S.; Teeuwisse, S.; Ghulam, J.; Abu-Shiekha, I.; et al. Reducing Key Uncertainties Prior to a Polymer Injection Trial in a Heavy Oil Reservoir in Oman. Presented at SPE EOR Conference at OGWA, Muscat, Oman, 31 March–2 April 2014. [[CrossRef](#)]
92. Li, Z.; Delshad, M. Development of an Analytical Injectivity Model for Non-Newtonian Polymer Solutions. Presented at the SPE Reservoir Simulation Symposium, Woodlands, TX, USA, 18–20 February 2014. [[CrossRef](#)]



Paper 2:


Analysis and Simulation of Polymer Injectivity

Paper 3:

Qualification of New Methods for Measuring In Situ Rheology of Non-Newtonian Fluids in Porous Media

Article

Qualification of New Methods for Measuring In Situ Rheology of Non-Newtonian Fluids in Porous Media

Jørgen Gausdal Jacobsen ^{1,2,*}, Behruz Shaker Shiran ², Tormod Skauge ³ ,
Kenneth Stuart Sorbie ^{3,4} and Arne Skauge ^{1,3}

¹ Department of Chemistry, University of Bergen, Allegaten 41, N-5020 Bergen, Norway; arne.skauge@uib.no

² Norce, Norwegian Research Centre AS, Allegaten 41, N-5020 Bergen, Norway; besh@norceresearch.no

³ Energy Research Norway, N-5020 Bergen, Norway; tormod.skauge@energyresearch.no (T.S.);
k.sorbie@hw.ac.uk (K.S.S.)

⁴ Institute of Petroleum Engineering, Heriot Watt University, Edinburgh EH14 4AS, UK

* Correspondence: joja@norceresearch.no; Tel.: +47-9283-2044

Received: 29 November 2019; Accepted: 15 January 2020; Published: 14 February 2020



Abstract: Pressure drop (ΔP) versus volumetric injection rate (Q) data from linear core floods have typically been used to measure in situ rheology of non-Newtonian fluids in porous media. However, linear flow is characterized by steady-state conditions, in contrast to radial flow where both pressure and shear-forces have non-linear gradients. In this paper, we qualify recently developed methods for measuring in situ rheology in radial flow experiments, and then quantitatively investigate the robustness of these methods against pressure measurement error. Application of the new methods to experimental data also enabled accurate investigation of memory and rate effects during polymer flow through porous media. A radial polymer flow experiment using partially hydrolyzed polyacrylamide (HPAM) was performed on a Bentheimer sandstone disc where pressure ports distributed between a central injector and the perimeter production line enabled a detailed analysis of pressure variation with radial distance. It has been suggested that the observed shear-thinning behavior of HPAM solutions at low flux in porous media could be an experimental artifact due to the use of insufficiently accurate pressure transducers. Consequently, a generic simulation study was conducted where the level of pressure measurement error on in situ polymer rheology was quantitatively investigated. Results clearly demonstrate the robustness of the history match methods to pressure measurement error typical for radial flow experiments, where negligible deviations from the reference rheology was observed. It was not until the error level was increased to five-fold of typical conditions that significant deviation from the reference rheology emerged. Based on results from pore network modelling, Chauveteau (1981) demonstrated that polymer flow in porous media may at some rate be influenced by the prior history. In this paper, polymer memory effects could be evaluated at the Darcy scale by history matching the pressure drop between individual pressure ports and the producer as a function of injection rate (conventional method). Since the number of successive contraction events increases with radial distance, the polymer has a different pre-history at the various pressure ports. Rheology curves obtained from history matching the radial flow experiment were overlapping, which shows that there is no influence of geometry on in-situ rheology for the particular HPAM polymer investigated. In addition, the onset of shear-thickening was independent of volumetric injection rate in radial flow.

Keywords: EOR; polymer flooding; in situ rheology; non-Newtonian flow; polymer memory effect

1. Introduction

Polymer flooding is a mature enhanced oil recovery (EOR) technique that has received increased attention during recent years. Water-soluble polymers are added to the injection brine to increase effective viscosity of the injected solution, thus changing the mobility ratio and thereby improving sweep efficiency. The synthetic polymer partially hydrolyzed polyacrylamide (HPAM) is by far the most frequently used polymer for oil recovery purposes [1] and is therefore the focus of this paper. While biopolymers are purely viscous in solution and thus only exhibit Newtonian and shear-thinning behavior, elastic polymers such as HPAM additionally exhibit shear-thickening behavior in flow through porous media.

Accurate measurements of polymer in situ rheology is crucial for obtaining reliable estimates of the mobility ratio between the displacing polymer solution and the displaced oil. Due to the time-consuming nature of in situ measurements, extensive efforts have been made to relate bulk and in situ rheology. Despite numerous attempts, no universally accepted analytical or numerical model exist [2]. Consequently, polymer in situ rheology is estimated from polymer flow experiments in porous media. Generally, these experiments have been performed on linear core plugs [3–7]. However, results from recent years indicate that linear and radial polymer flow are inherently different [2,8]. In addition, it has been observed that presence of residual oil significantly reduces polymer in situ effective viscosity compared to single-phase flow [2]. Based on these results, the radial polymer flow experiment that was history matched in this paper was performed in radial flow geometry in the presence of residual oil since these conditions best mimic the polymer flow out from the injector in oil reservoirs.

Until recently, in situ polymer rheology was mainly calculated from the pressure drop (ΔP) along a linear core as a function of volumetric injection rate (Q). Using this ΔP versus Q data directly, the behavior of the in situ ‘effective viscosity’ could be calculated using Darcy’s law. Consequently, a single effective viscosity value could be obtained for each volumetric injection rate. Unlike the case in linear flow, the velocity is decreasing with distance from the injector in a radial flow system. Thus, internal pressures in radial flow provide a much richer description of the local pressure response from both the shear-thickening regime in the near-wellbore region and the shear-thinning regime further from the injection well. Even though internal pressure ports are also used in linear core floods, they are unable to provide any additional detail from the polymer pressure response due to the constant velocity field in linear flow. Extrapolation of internal pressures may be performed to obtain the polymer entrance pressure drop in linear flow, which is correlated with the degree of mechanical degradation [9]. However, recent results show that the degree of mechanical degradation is significantly reduced in radial compared to linear flow [8]. Therefore, it is the authors’ view that linear flow experiments should not be used as basis for determining the degree of mechanical degradation in radial flow.

A common aspect of all polymer flow experiments, regardless of flow geometry, arises from uncertainties originating from pressure measurement error, which may significantly influence the history match results. Moreover, it has been suggested that the observed shear-thinning behavior of HPAM solutions may be an experimental artifact due to the use of insufficiently accurate pressure transducers [7]. A generic simulation study was therefore performed to establish the sensitivity of both history match methods to pressure measurement error. Initially, a reference (base case) rheology curve was constructed and used as input for radial polymer flow simulations to create a reference dataset. This reference dataset was then randomly ‘contaminated’ with different degrees of pressure measurement error. Rheology curves used to history match datasets with different levels of pressure measurement error were then compared to the reference rheology curve. Consequently, the effect of pressure measurement error on the resulting polymer rheology function could be quantitatively evaluated.

Due to the rapidly changing velocity field in radial flow (radial velocity decreases as $1/r$), different flow regimes may exist within the propagation path between injector and producer for elastic polymers. When the volumetric injection rate and resulting flow velocities are below a certain threshold value, the polymer will have sufficient time to relax completely between each contraction during the entire

propagation distance and the fluid can then be treated as an inelastic fluid for modeling purposes. However, at velocities exceeding this threshold value, the polymer is unable to fully relax between contractions and the elastic nature of the polymer must be considered. Chauveteau (1981) [10] showed that for elastic fluids, a memory effect is observed where the polymer rheology is dependent on the number of prior contraction events that the fluid experiences. These experimental observations have also been reproduced by numerical simulation [11], where it was demonstrated that porous media properties such as; aspect ratio, coordination number, and tortuosity, significantly influence polymer rheology.

The use of internal pressure ports in the radial flow experiment, where the number of contraction events increase with distance from injection well, enabled an investigation at the Darcy scale into the memory effects of the elastic HPAM polymer considered in this paper.

2. Materials and Methods

2.1. Rock Material

The radial flow experiment history matched in this paper was performed on a circular Bentheimer sandstone disc. Based on XRD measurements, Bentheimer consists predominantly of quartz (90.6%) with some feldspar (4.6%), mica (3.2%), and trace amounts of minerals such as siderite, calcite, and pyrite (1.6%). Mercury intrusion tests performed on the Bentheimer outcrop rock showed a uniform and relatively narrow pore size distribution with median pore throat size of approximately 14.7 μm [12]. Dispersion tests were also performed, where the flow behavior of the experimental brine and a tracer brine confirmed homogeneous flow conditions. Table 1 shows the properties of the Bentheimer sandstone disc used in this study.

Table 1. Disc properties

Radius	r	cm	15.0
Injection well radius	r_w	cm	0.325
Thickness	h	cm	2.00
Pore volume	V_p	mL	350.0
Porosity	Φ	-	0.25
Permeability	K	mD	2200

The sample was prepared according to a method previously described in the literature for circular Bentheimer discs with internal pressure ports [2,8,13]. The rock sample preparation was completed by ageing with a heavy crude oil of 7000 cP, followed by flooding with brine to residual oil saturation of 0.34. Pressure ports were located in the injection well and production line and at radii of, $r = 0.8, 1.2, 1.7, 2.4, 3.5, 5, 7,$ and 10 cm (Figure 1). As evident from the illustration, the entire rim of the radial disc constitutes the production line.

Fuji FCX series pressure transducers were used to measure the absolute pressure for individual pressure ports. These pressure sensors have a pressure range of 0–5 bara with a resolution within $\pm 0.2\%$ of the preset maximum pressure value. Differential pressures between individual pressure ports and production line were then calculated from the measured absolute pressures. In radial flow experiments with internal pressure ports, measurement error originate from both pressure measurement noise in pressure transducers and uncertainties from the manual placement of internal pressure ports. Consequently, the effective (or cumulative) pressure measurement error was estimated at approximately $\pm 1\%$ of the preset maximum value for the radial polymer flow experiment conducted in this paper.

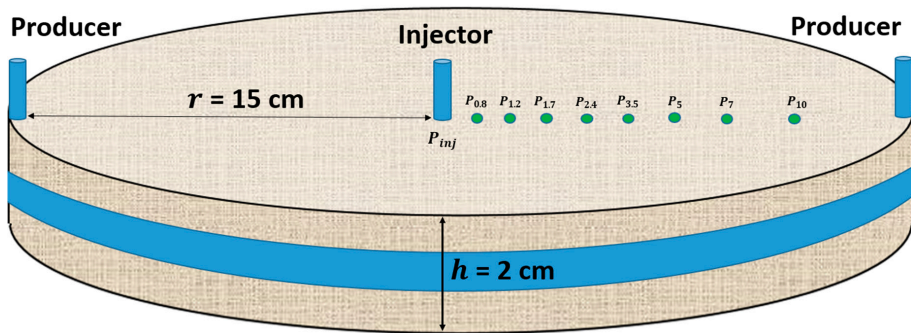


Figure 1. Schematic representation of the circular Bentheimer disc showing the distribution of internal pressure ports mounted between injection well and production line.

2.2. Fluids

The brine used in this study was of relatively low salinity and did not contain any divalent ions. Total dissolved salt content was equal to 7000 ppm, with composition given by 6000 mg/L NaCl and 1000 mg/L NaHCO₃. Brine viscosity was 1.02 cP at the experimental temperature of 22 °C. The 1000-ppm polymer solution reported in this paper was prepared by diluting a 5000 ppm mother solution (Flopaam 3330S, 8 MDa, 30% hydrolysis, from SNF Floerger, Andrèzieux-Bouthèon, France) in brine according to the API method (RP 63, 1900, American Petroleum Institute, Washington, DC, USA). According to the classification of polymer phase categories [14], the polymer solution was within the semi-dilute regime.

The relatively low molecular weight polymer used in this study was chosen to reduce the amount of mechanical degradation and to minimize the residual resistance factor (RRF). In addition, the rather low polydispersity of the HPAM sample was expected to ensure low mechanical degradation compared to a wider distribution [7].

Shear viscosity of the polymer solution (11.5 cP at 10 s⁻¹) was measured at 22 °C using a cone-plate geometry on a Malvern Kinexus Pro rheometer. Shear viscosity was measured for shear rates in the interval 0.1 to 1000 s⁻¹ using a 50 mm titanium spindle with a 2° inclination. The low density of the spindle allowed for accurate measurements at low torque values. The plate was 65 mm in diameter and the gap set to 70 µm at the tip. The solution was viscous dominated. Effluent viscosity measurements showed negligible deviation from injected viscosity, indicating that mechanical degradation did not occur during the radial polymer flow experiment.

2.3. Disc Flooding Procedure

Firstly, brine was injected at ten different flow rates (0.05–2 mL/min) to determine effective permeability to brine in presence of residual oil. Effective permeability to brine ($k_{b,init}$) was obtained from Darcy's law for radial flow

$$k_{b,init} = -\frac{\mu Q}{2\pi h \Delta P} \ln \frac{r}{r_e} \quad (1)$$

where μ is brine viscosity, Q is volumetric injection rate, h is disc thickness, ΔP is the pressure drop between a specified pressure port at radius r and the producer at r_e .

The 1000-ppm polymer solution was then injected at low flow rate (0.1 mL/min) for at least two pore volumes to ensure that polymer retention was completely satisfied and to achieve stable pressure conditions. Then, the polymer solution was injected at 2 mL/min and the injection rate was reduced and measured in a stepwise manner (10 rate steps) until the stabilized pressure had been recorded for the lowest rate of 0.05 mL/min.

Apparent viscosity of polymer solutions flowing in porous media is represented by the resistance factor (RF), defined as

$$RF = \frac{\Delta P_p}{\Delta P_{b,init}} \quad (2)$$

where ΔP_p is the pressure drop during polymer flow and $\Delta P_{b,init}$ is the pressure drop during brine flow before polymer was introduced to the porous media.

Following the 1000-ppm HPAM flood, tapering was performed to minimize residual resistance factor [15], where 700, 400, and 100 ppm polymer solutions were injected sequentially. Lastly, the final brine flood was injected at 10 different flow rates (0.05–2 mL/min) to determine final permeability to brine and to calculate the RRF, defined as

$$RRF = \frac{k_{b,init}}{k_{b,final}} \quad (3)$$

where $k_{b,init}$ is effective permeability to brine before introduction of polymer to the porous media and $k_{b,final}$ is effective permeability to brine after polymer tapering.

2.4. Simulation

The simulation model used for the generic simulation study and for history matching the radial polymer flow experiment was constructed in the STARS simulator (Computer Modeling Group, Calgary, Alberta, Canada). Concentric grid blocks of uniform length delineated the radial grid with radius of 15 cm between injector and producer. After sensitivity analysis, grid block length was optimally chosen to be $\Delta r = 0.1$ cm, resulting in a radial model with 150 concentric rings.

The rheology curves constructed in this paper were generated using an extended version of the Carreau model [16] that incorporates the Newtonian, shear-thinning, and shear-thickening behavior of elastic polymers, as

$$\mu_{app} = \mu_{\infty} + \frac{\mu_0 - \mu_{\infty}}{(1 + (\lambda_1 u)^2)^{\frac{1-n_1}{2}}} + \mu_{max} [1 - \exp(-(\lambda_2 u)^{n_2-1})] \quad (4)$$

where μ_{app} is polymer apparent viscosity, μ_{∞} and μ_0 are limiting Newtonian viscosities at high and low shear limits, respectively, λ and n are empirical polymer constants, u is the superficial velocity of the polymer in porous media and μ_{max} is the shear-thickening plateau viscosity.

2.5. History Match Methods

To model radial polymer flow, Darcy's law may be applied as

$$\Delta P = -\frac{\mu_{app} Q}{2\pi h k_{b,final}} \ln \frac{r}{r_e} \quad (5)$$

where ΔP is the pressure drop between a specified pressure port at radius r and the producer at r_e , μ_{app} is polymer apparent viscosity, Q is volumetric injection rate, h is disc thickness and $k_{b,final}$ is effective permeability to brine after polymer flow.

Permeability obtained from the final brine flood was used as input during history matching of the polymer flood in order to obtain the flow-dependent rheology behavior of the HPAM solution. Thus, we assumed that effective permeability to brine (after polymer flow) and to polymer were equal. This assumption was justified since X-ray imaging showed no additional oil mobilization during polymer flooding beyond the water flood residual oil saturation.

Using Darcy's law for radial flow and assuming constant brine permeability, the differential pressure during polymer flow may be history matched as a function of either volumetric injection rate (conventional method [13], denoted $dP(Q)$) or radial distance (new method [2,8], $dP(r)$):

- $dP(Q)$: Using the conventional method, injection bottom-hole pressure (BHP) is history matched as function of volumetric injection rate, yielding a single polymer in situ rheology curve. Due to the experimental set up using internal pressure ports distributed between injector and producer, differential pressure between each pressure port and producer may also be history matched as a function of injection rate, yielding an individual in situ rheology curve for each pressure port. While the rheology curve obtained from history matching injection BHP spans the entire velocity interval of the polymer rheology from injector to producer, differential pressure between internal pressure ports span decreasing velocity intervals of the complete rheology curve as we move towards the producer.
- $dP(r)$: Using the new method, differential pressure is history matched as a function of radial distance, yielding an individual rheology curve for each volumetric injection rate. Here, rheology curves obtained from each injection rate span different velocity intervals.

Throughout the remainder of this paper, $dP(Q)$ and $dP(r)$ are referred to as the single port match method (SPMM) and the disc match method (DMM), respectively.

2.6. Pretreatment of Polymer Pressure Response: Decoupling Polymer In Situ Rheology

Polymer pressure response from radial flow experiments does not exclusively contain contributions from the in situ rheology. If not accounted for, experimental conditions such as non-uniform residual oil saturation and pseudo-skin effects may distort the true functional relationship of the polymer rheology. However, since these conditions also were present during brine flow, and since X-ray imaging showed no additional displacement of oil by polymer, they can be incorporated into the permeability and effectively be decoupled from the polymer rheology.

Effective permeability to brine across the entire disc (obtained from history matching injection BHP as a function of injection rate during brine flow) was used to history match the polymer flow experiment. However, since the permeability across the entire disc deviated from the local permeabilities between individual pressure ports and producer, correction factors were calculated and internal pressures for the polymer flow were adjusted. Using this pretreatment technique, all experimental factors such as non-uniform residual oil saturation and pseudo-skin effects, which were also present during brine flow, were effectively decoupled from the polymer pressure response. Thus, the contribution of polymer in situ rheology on the radial pressure response could be effectively isolated. The calculated correction factors were between 0.5 – 1.3, and were monotonically decreasing with radial distance.

2.7. Pressure Measurement Error Analysis

To quantify the effect of pressure measurement error on the obtained polymer in situ rheology, the parameter values summarized in Table 2 were used in conjunction with the extended Carraeu model, i.e., Equation (4), to create a reference (base case) rheology curve (Figure 2). This synthetic base case rheology curve is essentially our ‘truth’ case if the data were perfect.

Table 2. Carreau parameters used to create the reference (base case) rheology curve

μ_{∞} (cP)	μ_0 (cP)	μ_{max} (cP)	λ_1 (day/m)	λ_2 (day/m)	n_1	n_2
1	50	75	$5 \cdot 10^7$	$5 \cdot 10^3$	0.7	1.5

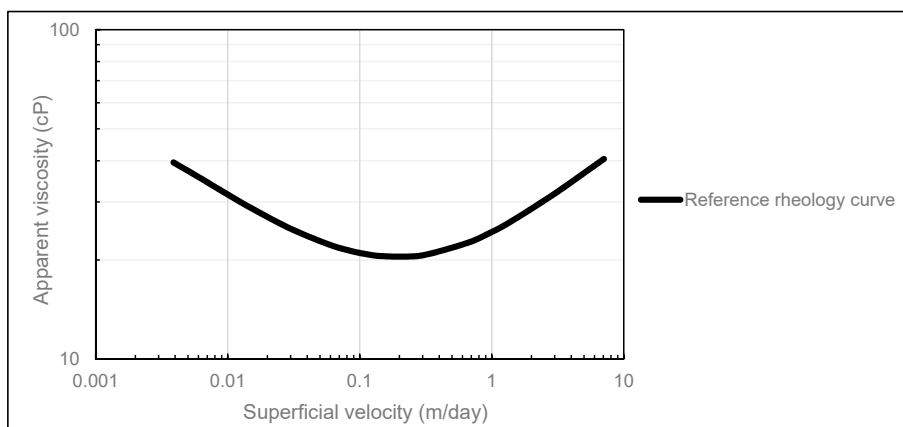


Figure 2. Reference (base case) rheology curve used for pressure measurement error analysis.

The reference rheology curve was then used as input in our radial polymer flow simulations in STARS to generate a reference dataset. In accordance with the radial polymer flow experiment that was history matched in this paper, the reference rheology curve was used in simulation runs with the same 10 injection rates within the rate interval of 0.05–2 mL/min.

2.8. Automatic History Match Tool

To prevent any pre-bias from affecting the results of the error analysis, the automatic history match tool CMOST by Computer Modeling Group (Calgary, Alberta, Canada) was chosen to perform the history match operations. To evaluate the convergence ability of CMOST, the reference dataset was history matched using the particle swarm optimization (PSO) engine. The parameter intervals in Table 3 were selected for all automatic history match operations during the error analysis. These are chosen to give a wide parameter space containing the ‘correct’ value for the base case in situ rheology curve.

Table 3. Carreau parameter intervals used for automatic history match operations in CMOST

μ_{∞} (cP)	μ_0 (cP)	μ_{max} (cP)	λ_1 (day/m)	λ_2 (day/m)	n_1	n_2
1	1–100	1–100	10^4 – 10^8	1 – 10^4	0.3–1	1.3–2

History match results using the PSO engine showed good convergence in most situations. However, in some cases, the engine experienced difficulties converging towards acceptable global minimum values. In these cases, the more robust, although more time consuming engine, Bayesian Markov Chain Monte Carlo (MCMC), was used. During the evaluation of CMOST, where the reference dataset was history matched, average history match error of 1% was set as the convergence criterion. In this work, the average percentage history match error is defined as

$$\frac{1}{n} \sum_1^n \left| \frac{HM - R}{R} \right| \times 100 \quad (6)$$

where n is the number of pressure ports, HM is the differential pressure obtained by CMOST, and R is the corresponding reference differential pressure.

The history match results obtained using both methods (Figures 3 and 4) confirm the convergence ability of CMOST, and we can conclude that it is an appropriate history match tool for the purpose of this analysis.

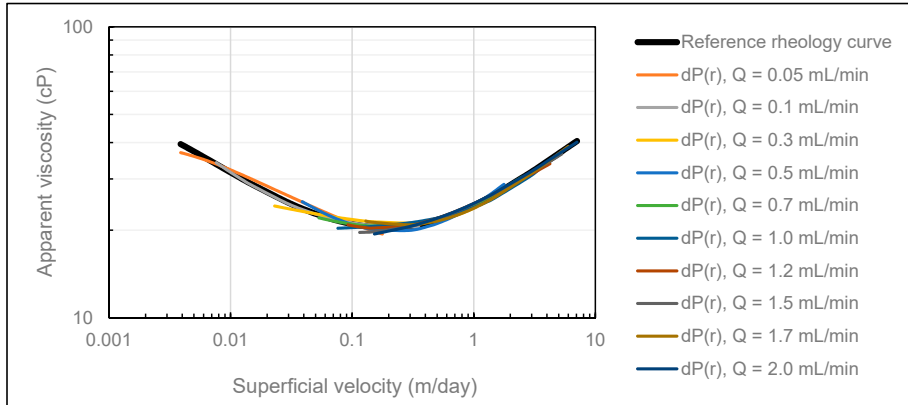


Figure 3. Comparison of the reference rheology curve (black) and rheology curves obtained in CMOST when the reference dataset was history matched using the DMM.

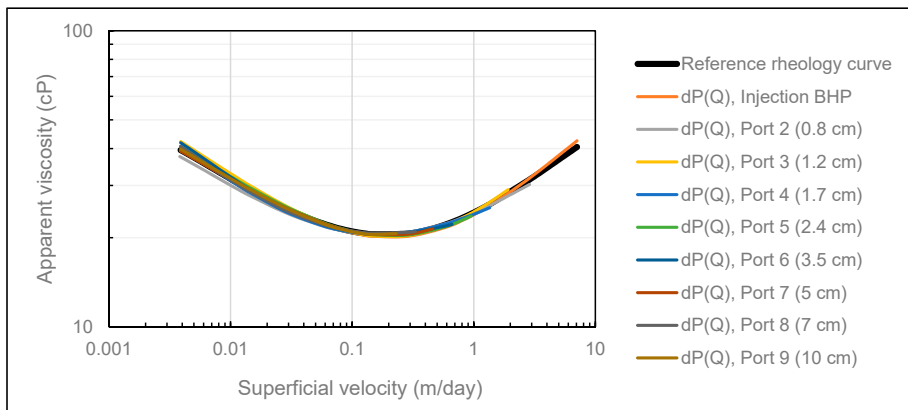


Figure 4. Comparison of the reference rheology curve (black) and rheology curves obtained in CMOST when the reference dataset was history matched using the SPMM.

To investigate the robustness of both history match methods, pressure measurement errors typical for in-house radial flow experiments were randomly added or subtracted from the reference dataset and this contaminated dataset was then history matched. In accordance with the effective pressure measurement error related to the experimental setup in the radial polymer flow experiment, the dataset was randomly contaminated with $\pm 1\%$ of the preset maximum pressure. The maximum pressure was set equal to the reference injection BHP response for each individual injection rate. Thereafter, the error was increased in a stepwise manner until the threshold level was identified above which the in situ rheology pressure contribution was lost in pressure measurement error.

3. Results and Discussion

3.1. Pressure Measurement Error Analysis

In typical experimental error conditions (1% uncertainty of maximum preset pressure), rheology curves using both history match methods showed negligible deviations from the reference rheology curve (Figures 5 and 6).

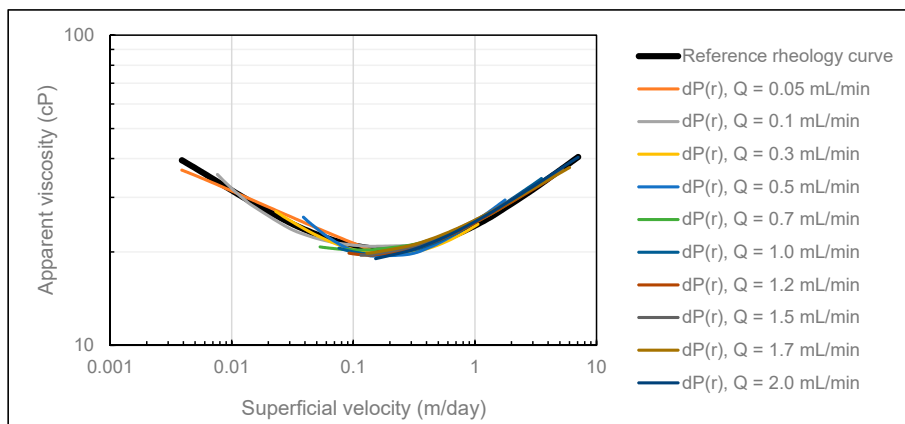


Figure 5. Comparison of the reference rheology curve (black) and rheology curves obtained in CMOST after influence of typical pressure measurement error using the DMM.

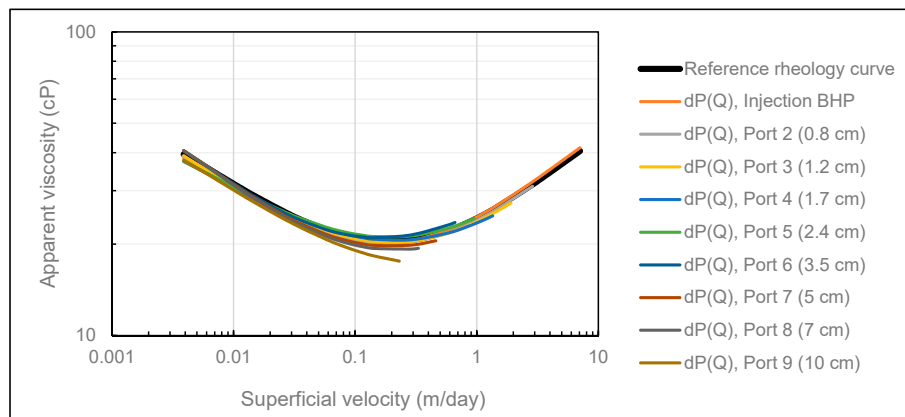


Figure 6. Comparison of the reference rheology curve (black) and rheology curves obtained in CMOST after influence of typical pressure measurement error using the SPMM.

These results clearly demonstrate the robustness of both methods under these experimentally realistic error conditions. As expected, we observe that deviation from the reference rheology increase with radial distance, which is readily evident from Figure 6. Based on these results, pressure measurement error typical for in-house radial flow experiments should not be adequate to distort the obtained rheology curves.

To identify the threshold error level above which the polymer in situ pressure response was lost, the error was increased in a stepwise manner until significant deviation from the reference curve was observed. This error level was determined at 5% of maximum preset pressure, which was five times

the typical error level. Thus, radial polymer flow experiments should be performed in an experimental setup where effective pressure measurement error is well below 5% of the maximum preset pressure.

3.2. History Match of Radial Flow Experiment

The polymer memory effect of HPAM solutions was elegantly demonstrated by Chauveteau (1981) [10] in a series of pore scale experiments in glass models. In said paper, the in situ rheology of HPAM was shown to depend on the number of prior contraction events experienced by the fluid, i.e., on the polymer history. This result was later reproduced by numerical simulation [11], where the polymer memory effect was shown to depend on polymer properties such as molecular weight and porous media properties such as contraction aspect ratio and tortuosity.

To investigate potential polymer memory effects at the Darcy scale of the elastic HPAM polymer used in this study, differential pressure between each pressure port and producer was history matched as a function of volumetric injection rate. Since the number of contraction events increase with radial distance, the polymer had a different pre-history at different locations in the porous medium. The results from applying this approach are shown in Figure 7, where we observe that all polymer rheology curves are overlapping.

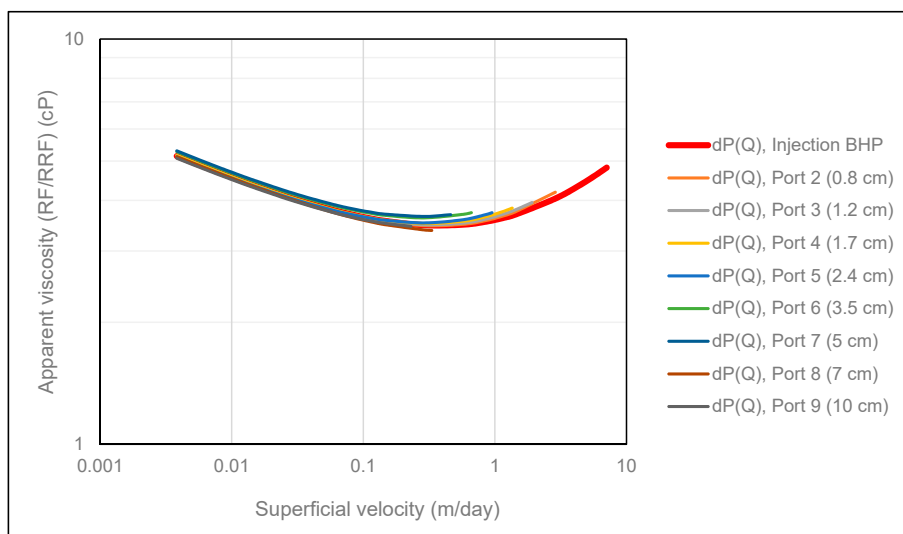


Figure 7. Polymer in situ rheology obtained using the SPMM.

Firstly, this is a strong indication that the pretreatment technique applied to the experimental data was successful in isolating the pressure contribution from the polymer in-situ rheology. However, in circumstances where the polymer is subjected to mechanical degradation, we expect rheology curves obtained from internal pressure ports to deviate from the rheology curve obtained from injection BHP since mechanical degradation mainly occurs in the near wellbore region in radial flow [9]. Thus, injection BHP contains pressure contributions from both degraded and undegraded polymer, in contrast to internal pressures where only pressure response from degraded polymer is recorded. Consequently, we expect the polymer rheology curve obtained from injection BHP to be shifted vertically upwards compared to the rheology curves obtained from internal pressures in circumstances where the polymer is subjected to mechanical degradation in radial flow.

Secondly, since all rheology curves were overlapping, even though they had a different pre-history, no significant memory effects could be observed at the Darcy scale for the polymer solution investigated

in this study. Since Bentheimer sandstone is a relatively homogeneous rock, the micro-scale memory effects are most likely averaged out when viewed from a Darcy scale perspective. In accordance with the results demonstrated by Zamani et al. [11], we suggest that memory effects might be observable at the Darcy scale with increasing molecular weight of the polymer and with increasing heterogeneity of the porous medium.

Figure 8 shows the obtained polymer in situ rheology when history matching differential pressures using the DMM. Results show no rate effects in that all rheology curves are overlapping. Consequently, the onset of shear-thickening is independent of volumetric injection rate in radial flow. However, in cases where the polymer is subjected to mechanical degradation, rate effects are expected because the amount of mechanical degradation generally increases with volumetric injection rate. In these cases, we do not expect the obtained polymer rheology curves to be overlapping.

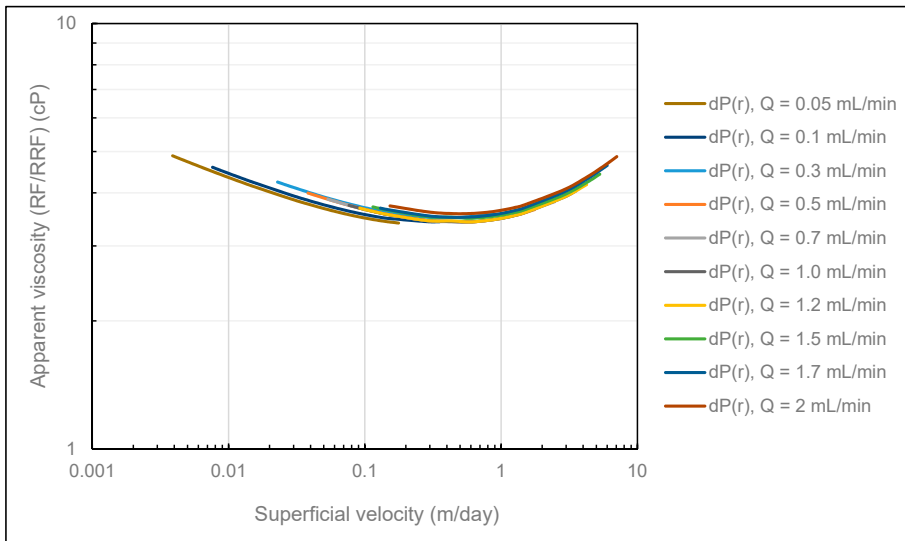


Figure 8. Polymer in situ rheology obtained using the DMM.

To investigate the consistency between the two different history match methods and their accuracy, all rheology curves obtained from both history match methods are collectively shown in Figure 9. Very good consistency is observed between all curves in Figure 9 in that both history match methods provide overlapping in situ rheology curves. Based on the strong consistency observed, we can conclude that both history match methods are very strong tools for determining polymer in situ rheology in radial flow systems.

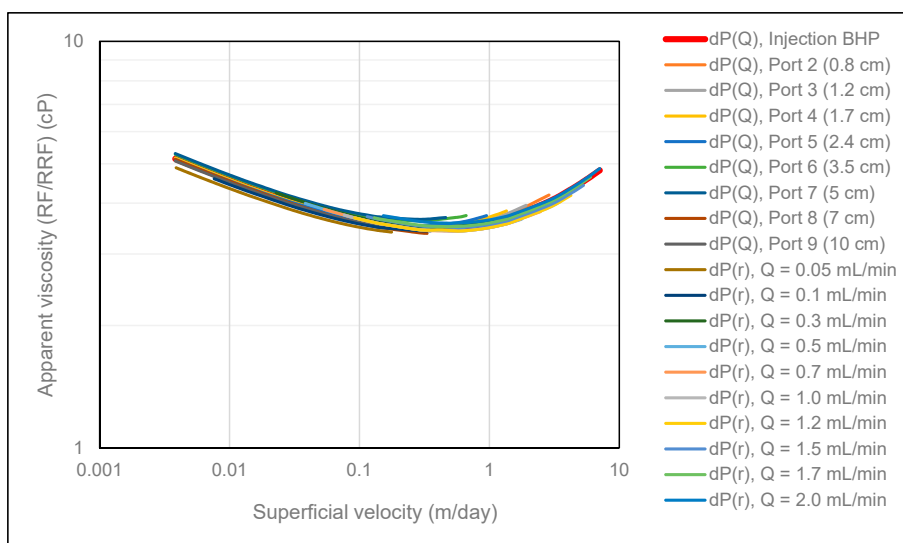


Figure 9. Summary of polymer in situ rheology obtained from both history match methods.

4. Conclusions

In this paper, two novel methods for measuring in situ polymer rheology in radial flow systems were evaluated. Results from the generic simulation study demonstrated the high accuracy and robustness of both history match methods to pressure measurement error. Here, an upper error level of 5% of maximum preset pressure was identified below which accurate estimates of polymer rheology could be made. Thus, the assertion of shear-thinning behavior of HPAM solutions at low flux in porous media being an experimental artifact due to insufficiently accurate pressure transducers is shown to be unlikely.

Memory effects in radial polymer flow were investigated and were not observable at the Darcy scale in Bentheimer sandstone for the HPAM polymer investigated in this study. However, the authors appreciate that memory effects might be observable at the Darcy scale for higher molecular weight polymers and in more heterogeneous porous media.

No rate effects were observed in that the onset of shear-thickening was observed to be independent of rate in radial flow for the mechanically undegraded polymer in this study.

Finally, polymer in situ rheology obtained from each history match method were compared and showed very consistent results. Thus, both methods evaluated in this paper proved to be robust tools for measuring in situ rheology of non-Newtonian fluids.

Author Contributions: J.G.J. was responsible for simulations and for writing the paper. B.S.S. performed the radial polymer flow experiment. A.S., K.S.S., and T.S. contributed in planning of the study, discussion of results, and reviewing the paper. All authors have read and agreed to the published version of the manuscript.

Funding: This research received no external funding.

Acknowledgments: The authors gratefully acknowledge support from the Norwegian Research Council, Petromaks 2 programme. Arne Skauge, acknowledge support from Energi Simulation, Canada as the Energi Simulation EOR Chair at University of Bergen.

Conflicts of Interest: The authors declare no conflict of interest.

References

1. Pope, G.A. Recent Developments and Remaining Challenges of Enhanced Oil Recovery. *J. Pet. Technol.* **2011**, *63*, 65–68. [[CrossRef](#)]
2. Skauge, A.; Zamani, N.; Jacobsen, J.G.; Shiran, B.S.; Al-Shakry, B.; Skauge, T. Polymer Flow in Porous Media: Relevance to Enhanced Oil Recovery. *Colloids Interfaces* **2018**, *2*, 27. [[CrossRef](#)]
3. Pye, D.J. Improved Secondary Recovery by Control of Water Mobility. *J. Pet. Technol.* **1964**, *16*, 911–916. [[CrossRef](#)]
4. Smith, F.W. The Behavior of Partially Hydrolyzed Polyacrylamide Solutions in Porous Media. *J. Pet. Technol.* **1970**, *22*, 148–156. [[CrossRef](#)]
5. Jennings, R.R.; Rogers, J.H.; West, T.J. Factors Influencing Mobility Control by Polymer Solutions. *J. Pet. Technol.* **1971**, *23*, 391–401. [[CrossRef](#)]
6. Heemskerk, J.; Janssen-van, R.; Rosmalen, R.; Teeuw, D. Quantification of Viscoelastic Effects of Polyacrylamide Solutions. In Proceedings of the SPE/DOE 4th Symposium on Enhanced Oil Recovery, Tulsa, OK, USA, 15–18 April 1984.
7. Seright, R.S.; Fan, T.; Wavrik, K.; Balaban, R.C. New Insights into Polymer Rheology in Porous Media. *SPEJ* **2011**, *16*, 35–42. [[CrossRef](#)]
8. Skauge, T.; Skauge, A.; Salmo, I.C.; Ormehaug, P.A.; Al-Azri, N.; Wassing, L.M.; Glasbergen, G.; Van Wunnik, J.N.; Masalmeh, S.K. Radial and Linear Polymer Flow—Influence on Injectivity. In Proceedings of the SPE Improved Oil Recovery Conference, Tulsa, OK, USA, 11–13 April 2016.
9. Seright, R.S. The Effects of Mechanical Degradation and Viscoelastic Behavior on Injectivity of Polyacrylamide Solutions. *Soc. Pet. Eng. J.* **1983**, *23*, 475–485. [[CrossRef](#)]
10. Chauveteau, G. Molecular Interpretation of Several Different Properties of Flow of Coiled Polymer Solutions Through Porous Media in Oil Recovery Conditions. In Proceedings of the 56th Annual Fall Technical Conference and Exhibition of the Society of Petroleum Engineers of AIME, San Antonio, TX, USA, 5–7 October 1981.
11. Zamani, N.; Bondino, I.; Kaufmann, R.; Skauge, A. Effect of porous media properties on the onset of polymer extensional viscosity. *J. Petrol. Sci. Eng.* **2015**, *133*, 483–495. [[CrossRef](#)]
12. Vik, B.; Kedir, A.; Kippe, V.; Sandengen, K.; Skauge, T.; Solbakken, J.; Zhu, D. Viscous Oil Recovery by Polymer Injection; Impact of In Situ Polymer Rheology on Water Front Stabilization. In Proceedings of the SPE Europec featured at the 80th EAGE Conference and Exhibition, Copenhagen, Denmark, 11–14 June 2018.
13. Skauge, T.; Djurhuus, K.; Zimmermann, T.; Bittner, C.; Reichenbach-Klinke, R. Radial Injectivity of an Associative Polymer for EOR. In Proceedings of the 20th European Symposium on Improved Oil Recovery, Pau, France, 8–11 April 2019.
14. Skauge, T.; Kvilhaug, O.A.; Skauge, A. Influence of Polymer Structural Conformation and Phase Behavior on In Situ Viscosity. In Proceedings of the 18th European Symposium on Improved Oil Recovery, Dresden, Germany, 14–16 April 2015.
15. Al-Shakry, B.; Shiran, B.S.; Skauge, T.; Skauge, A. Enhanced Oil Recovery by Polymer Flooding: Optimizing Polymer Injectivity. In Proceedings of the SPE Kingdom of Saudi Arabia Annual Technical Symposium and Exhibition, Dammam, Saudi Arabia, 23–26 April 2018.
16. Delshad, M.; Kim, D.H.; Magbagbeola, O.A.; Huh, C.; Pope, G.A.; Tarahhom, F. Mechanistic Interpretation and Utilization of Viscoelastic Behavior of Polymer Solutions for Improved Polymer-Flood Efficiency. In Proceedings of the SPE Symposium on Improved Oil Recovery, Tulsa, OK, USA, 20–23 April 2008.




Paper 4:

Polymer Injectivity Test Design Using Numerical Simulation

Article

Polymer Injectivity Test Design Using Numerical Simulation

Mohamed Adel Alzaabi ^{1,*}, Jørgen Gausdal Jacobsen ^{1,2}, Shehadeh Masalmeh ³, Ali Al Sumaiti ³, Øystein Pettersen ² and Arne Skauge ^{1,4}

¹ Department of Chemistry, University of Bergen, 5007 Bergen, Norway; joja@norceresearch.no (J.G.J.); arne.skauge@energyresearch.no (A.S.)

² Norwegian Research Center, 5008 Bergen, Norway; oype@norceresearch.no

³ Abu Dhabi National Oil Company, P.O. Box 898 Abu Dhabi, UAE; smasalmeh@adnoc.ae (S.M.); aalsumaiti@adnoc.ae (A.A.S.)

⁴ Energy Research Norway, 5007 Bergen, Norway

* Correspondence: mal075@uib.no

Received: 17 January 2020; Accepted: 20 March 2020; Published: 3 April 2020



Abstract: Polymer flooding is an enhanced oil recovery (EOR) process, which has received increasing interest in the industry. In this process, water-soluble polymers are used to increase injected water viscosity in order to improve mobility ratio and hence improve reservoir sweep. Polymer solutions are non-Newtonian fluids, i.e., their viscosities are shear dependent. Polymers may exhibit an increase in viscosity at high shear rates in porous media, which can cause injectivity loss. In contrast, at low shear rates they may observe viscosity loss and hence enhance the injectivity. Therefore, due to the complex non-Newtonian rheology of polymers, it is necessary to optimize the design of polymer injectivity tests in order to improve our understanding of the rheology behavior and enhance the design of polymer flood projects. This study has been addressing what information that can be gained from polymer injectivity tests, and how to design the test for maximizing information. The main source of information in the field is from the injection bottom-hole pressure (BHP). Simulation studies have analyzed the response of different non-Newtonian rheology on BHP with variations of rate and time. The results have shown that BHP from injectivity tests can be used to detect in-situ polymer rheology.

Keywords: chemical EOR; polymer flooding; in situ rheology; polymer injectivity; polymer modeling

1. Introduction

Polymer flooding is a well-established chemical enhanced oil recovery (CEOR) method that has been widely used for more than half a century. It was initially introduced to alleviate the issues related to unfavorable mobility ratio, induced by reservoir heterogeneity and/or high oil viscosity. These issues were remediated by adding polymers to the injected water to improve overall aerial and volumetric sweep efficiency [1]. The main mechanisms of polymer flooding are sweep improvement that consists of mitigating viscous fingering and improving crossflow between vertical heterogeneous layers [2,3]. In addition, numerous studies indicate that non-Newtonian polymer solutions can improve microscopic displacement efficiency and may reduce water-flood residual oil saturation [3,4].

The most commonly used polymer for CEOR applications is synthetic polymer partially hydrolyzed polyacrylamide (HPAM), with a typical hydrolysis degree range of 15%–33%. In bulk flow, viscosity measurements from rheometers show that HPAM exhibit shear thinning behavior, which can be explained by the disentanglement and realignment of polymer coils as velocity increases in the laminar flow regime. In addition, numerous polymer flow experiments in porous media have shown that HPAM exhibits an apparent shear thickening behavior beyond a critical shear rate [5]. Consequently,

apparent viscosity attains a maximum value in the immediate near-wellbore region. This viscosity increment is often referred to as extensional or elongational viscosity as it is attributed to the extensional flow regime of the polymer. Both the coil-stretch theory and transient network theory has been suggested to account for the extensional flow phenomenon. According to the coil-stretch theory, which is adhered to by the authors of this paper, the flexible coiled molecules of HPAM experience stretching, entanglement and collisions at high shear, which results in a larger flow resistance, i.e., apparent shear thickening behavior. This behavior is a special property of elastic polymers in flow through porous media and is not observed for biopolymers such as xanthan [6].

Injectivity is one of the most important parameters in the design of any reservoir flooding application. Failure in estimating injectivity within acceptable error margins can have a significant impact on the expected recovery increment and thus on the economic feasibility of the project. For polymer flooding applications, accurate estimation of injectivity is more significant due to the polymer high viscosity and its non-Newtonian behavior. This behavior may result in the well operating near (or under) formation fracturing conditions, which can significantly affect in-situ polymer rheology.

Several important observations have been made in recent years that may explain the deviation between field injectivity results compared to initial expectations. Skauge et al. demonstrated that onset of shear thickening occurs at significantly higher velocities in radial compared to linear flow [7]. In addition, the extent of shear thinning was more pronounced in radial flow, while the extent of shear thickening was reduced compared to linear flow. The presence of residual oil is another factor that may have a significant impact on polymer in-situ rheology. Authors of [5] observed a significant reduction of polymer in-situ viscosity in the presence versus absence of residual oil. Furthermore, it was demonstrated through experimental work that the preshearing polymer before injection helps in improving injectivity by reducing elastic properties of the polymer while maintaining viscous properties, i.e., reducing or eliminating the extensional shear thickening behavior at high shear rates near the well-bore [8].

1.1. Modeling and Simulation of Polymer Injectivity

Numerical simulation is an essential tool for the assessment of polymer flooding lab results and fundamental theory. It is also important for designing polymer field projects as well as predicting the performance and outcomes of the project.

One of the early attempts to model polymer flooding was by Zeito (1968) [9]. He created a 3D numerical simulation to predict the performance of polymer flooding in any type of reservoir. His model, however, was missing the component of in-situ non-Newtonian behavior of polymer, which was later found to be fundamental in polymer flooding mechanisms. Bondor et al. (1972) added the polymer in-situ rheology impact through using modified Blake-Kozeny power law for fluids [10]. They also included the impact of other factors such as permeability reduction and non-linear mixing of polymer and water. Seright (1983) developed an analytical model for injectivity in radial coordinates [11]. His model combined a mechanical degradation correlation, linear core flood results of resistance factor and Darcy equation in radial flow, to calculate total injection pressure drop. Recently, Lotfollahi et al. (2016) have proposed an injectivity model to simulate polymer injectivity decline in both laboratory and field tests [12]. Their model coupled the effects of deep-bed filtration and external filter-cake formation caused by polymer adsorption/retention, to the viscoelastic polymer rheology. They also emphasized the advantage of using radial coordinates with a fine gridding scheme to reduce the error of velocity calculation in the near-wellbore area and hence capture polymer rheology more accurately. Some commercial reservoir simulation software have also included modules to model polymer flooding such as STARS of Computer Modeling Group Ltd. (CMG), ECLIPSE 100 of Schlumberger, and REVEAL of Petroleum Experts [13]. The simulator used in this study is STARS of CMG, which includes polymer modules that accounts for polymer rheology dependence on the shear rate or velocity, polymer adsorption, permeability reduction and impact of polymer concentration and salinity on viscosity.

1.2. Paper Objective

This study aims to utilize numerical simulation of polymer flooding on both lab and field scales in order to optimize the design of field polymer injectivity tests. The main objective is to analyze the relationship between the injector bottom-hole pressure (BHP) and polymer in-situ rheology. Beside rheology, the impact of simple heterogeneity is also investigated along with the impact of permeability reduction because of polymer adsorption in low-permeability layers. This is to simplify the process of interpreting field tests data, since the sole source of data in the field is usually BHP variations with time and BHP as a function of different injection rates.

2. Materials and Methods (Lab Scale)

The radial flow experiment history matched in this paper was performed on a circular Bentheimer disc (radius = 15 cm, thickness = 2 cm, injection well radius = 0.325 cm and porosity = 0.25). Before oil was introduced, absolute permeability was measured and was equal to 2200 mD. The sample was prepared according to the method described in the literature for circular Bentheimer discs with internal pressure taps [6,7]; including ageing with heavy crude oil, followed by brine flooding to residual oil saturation of 0.34. Pressure ports were mounted both internally and in an injection well and producer, as depicted in Figure 1.

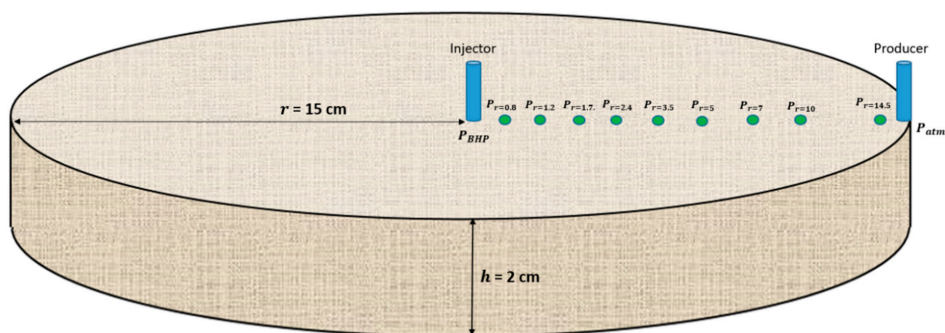


Figure 1. Illustration of the circular Bentheimer disc with pressure ports.

A relatively low salinity brine (7000 ppm TDS) was used in this study, with a viscosity of 1.02 cP at 22 °C. A 1000 ppm HPAM polymer solution was used (Flopaam 3330S, 8 MDa, 30% hydrolysis, SNF Floerger) and prepared according to the API method (RP 63, 1990, American Petroleum Institute). Shear viscosity of the polymer solution was measured to be 11.5 cP at 10 s⁻¹, with zero shear viscosity extrapolated to 13.9 cP. It was concluded that negligible mechanical degradation occurred based on injected versus effluent viscosity measurements.

Initially, the brine solution was injected at ten different flow rates (0.05–2 mL/min) and effective permeability to brine ($k_{b,init}$) was calculated from Darcy's law for radial flow:

$$k_{b,init} = -\frac{\mu Q}{2\pi h \Delta P} \ln \frac{r_i}{r}$$

where μ is brine viscosity, Q is volumetric injection rate, h is disc thickness, ΔP is the pressure drop between a specified port at radius r_i and the producer at r .

Following the initial brine flood, a 1000-ppm HPAM solution was injected at similar injection rates (0.05–2.0 mL/min). Before measurements began, the polymer solution was injected at 0.1 mL/min for at least two pore volumes to ensure that retention was satisfied. Tapering was also performed and the final step of the radial polymer flood experiment consisted of a final brine flood to determine the permeability after the polymer flood and to calculate the residual resistance factor (RRF), which was

equal to 1.2 for this experiment. Since permeability values obtained from initial brine flood was used in simulations, apparent viscosity is equal to resistance factor (RF) in this paper, where RF is defined as:

$$RF = \frac{\Delta P_p}{\Delta P_{b,init}}$$

where ΔP_p is the pressure drop during polymer flow and $\Delta P_{b,init}$ is the pressure drop during brine flow before polymer was introduced to the porous media.

Simulation of Radial Flow Experiments

A radial grid with 360 sectors constituted the simulation model. Each of these sectors consist of 150 grid blocks, where the grid block cell size was 1 mm. Sensitivity analysis showed a negligible accuracy improvement when reducing the grid block size below 1 mm. Residual oil saturation after the brine flood resulted in a non-uniform oil saturation profile between the injector and producer. The history match of the brine differential pressure between internal pressure ports and the producer enabled determination of local permeabilities. Since Bentheimer sandstone is assumed to be homogeneous, the average effective permeability was used together with local permeabilities to calculate correction factors accounting for the non-uniform oil saturation.

3. Results and Discussion (Lab Scale)

Average effective permeability was 33.8 and 28 mD using the differential pressure response from the initial and final brine flood, respectively. Injection BHP build-up was also recorded for each individual injection rate during both brine floods as shown in Figure 2.

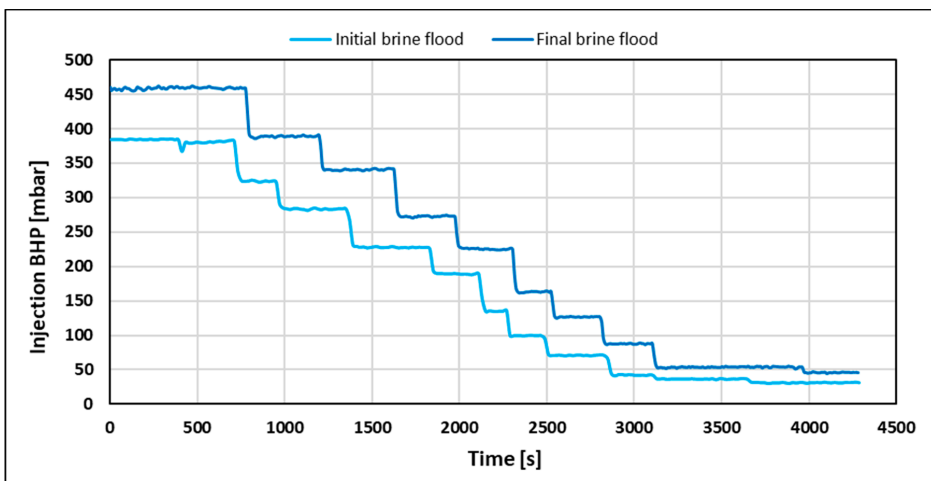


Figure 2. Injection bottom-hole pressure (BHP) versus time for initial (prior to polymer flood) and final brine flood (after polymer tapering).

Injection BHP stabilization time was independent of volumetric injection rate and equal to 40 s for both brine floods. However, pressure stabilization was expected to occur instantaneously when injecting a Newtonian fluid. Thus, it was concluded that the system had a delay of 40 s. The delay was attributed to incomplete pressure communication due to low values of counter pressure from the production line (2–4 mbar). To investigate if stabilization time is dependent on polymer rheology, the injection BHP build-up for the polymer (Figure 3) was also recorded.

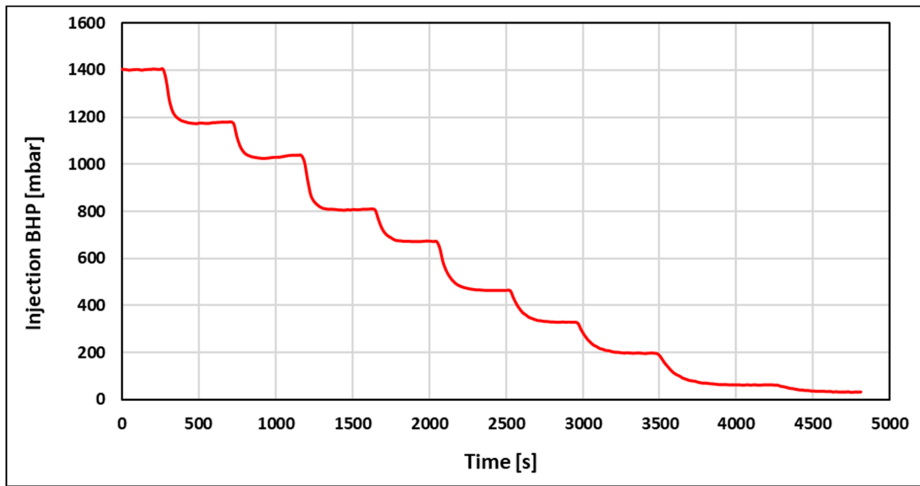


Figure 3. Pressure build up for the 1000-ppm polymer flood.

Injection BHP build-up from the polymer flood was clearly distinguishable from the Newtonian pressure response obtained from brine floods. Firstly, pressure stabilization time during the polymer flood was significantly higher (3–9 times) than for brine floods. In addition, stabilization time increased monotonically with decreasing volumetric injection rate (from 140 at 2 mL/min to 360 s at 0.05 mL/min). This suggests that the polymer rheology behavior is different at low compared to high injection rates.

To quantitatively analyze the polymer rheology of the 1000-ppm HPAM solution in the presence of residual oil, stabilized polymer pressure response was history matched as a function of both the volumetric injection rate, $dP(Q)$, and radial distance, $dP(r)$:

- $dP(Q)$: Analogue to conventional polymer rheology estimation from field data, pressure drop across the entire disc (injection BHP) is history matched as a function of the volumetric injection rate, yielding a single rheology curve. Since injection BHP is influenced by near-well effects such as skin and mechanical degradation, the robustness and accuracy of this method may be debatable.
- $dP(r)$: Using only internal pressure ports, the pressure drop between individual ports and the producer is history matched as a function of the radial distance, yielding an individual rheology curve for each volumetric injection rate. This method excludes the near-well effects mentioned above and will provide local rheology curves for each injection rate, spanning different velocity intervals of the complete rheology curve.

History match of injection BHP as a function of the volumetric injection rate (Figure 4) shows excellent agreement with the polymer pressure response. The history match error, defined in accordance with Gogarty, W.B. 1967, was 2.38% [14]. The history match of internal pressures as a function of radial distance (Figures 5 and 6) also showed very good agreement with the polymer pressure response. Here, the average of history match errors was equal to 2.94%.

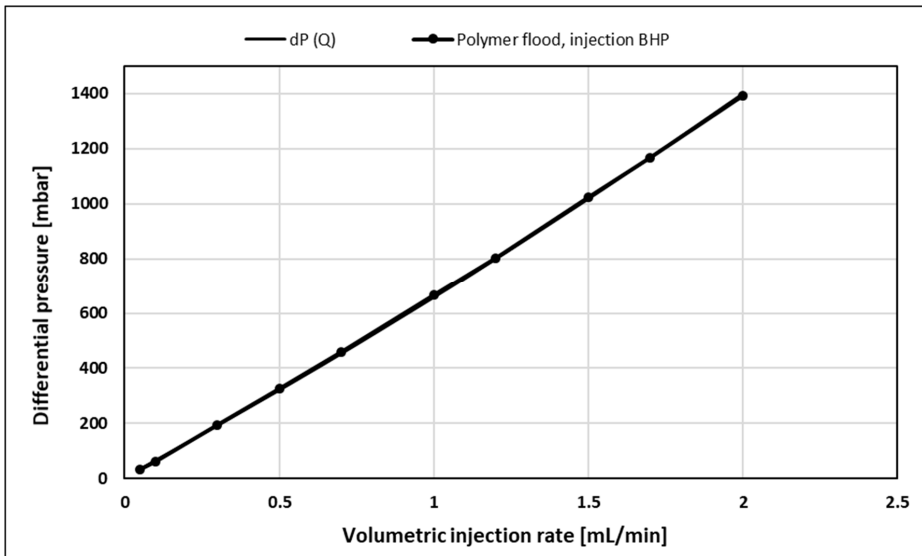


Figure 4. History match of injection BHP as a function of volumetric injection rate, $dP(Q)$, for polymer flood.

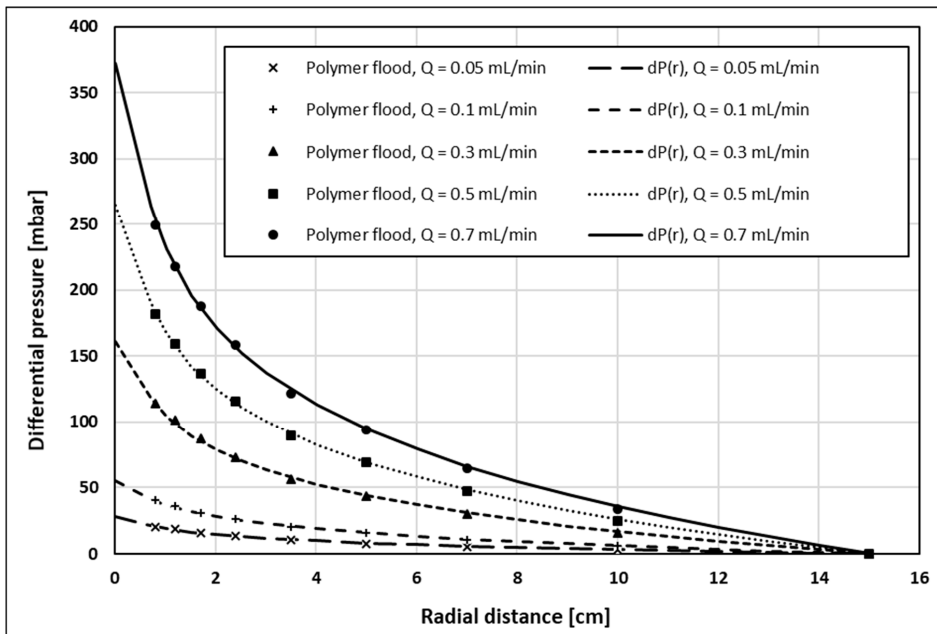


Figure 5. History match of internal pressures as a function of radial distance, $dP(r)$, for volumetric injection rates of 0.05–0.7 mL/min.

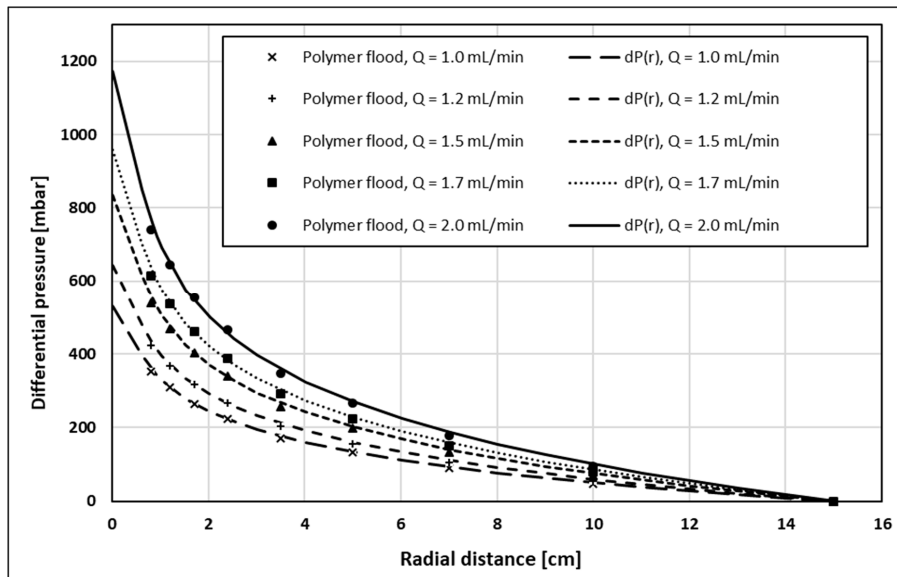


Figure 6. History match of internal pressures as function of radial distance, $dP(r)$, for volumetric injection rates of 1.0–2.0 mL/min.

Polymer rheology curves obtained from both history match methods are shown in Figure 7. Since permeability obtained from the initial brine flood (before polymer flood) was used, apparent viscosity is represented by RF. Here, polymer rheology curves obtained by history matching differential pressure as a function of radial distance from the injection well are denoted $dP(r)$. Using this history match method, individual rheology curves are obtained for each volumetric injection rate. However, since each curve was obtained at different injection rates, their maximum velocities at the injection point and their minimum velocity at the production rim were different. Rheology curves obtained at the lowest injection rates spanned the lower velocity interval, and were representing the shear-thinning rheology regime. In contrast, the highest injection rates spanned the higher velocity interval where the polymer behavior was increasingly shear-thickening. Even though they represent different injection rates and resulting velocity ranges of the polymer rheology, overlapping rheology curves were obtained, thus excluding the occurrence of rate effects. In addition, differential pressure was history matched as a function of the volumetric injection rate using injection BHP. This curve is denoted $dP(Q)$ and shows the same shape as the remaining rheology curves.

Therefore, all polymer rheology curves show approximately the same functional relationship (shape) and two distinct flow regimes: Shear dominant flow is occurring at low to intermediate rates while extensional dominant flow is predominant in the high velocity regime. This rheology behavior is in accordance with the injection BHP build-up response where stabilization time was decreasing with injection rate, thus representing the transition from shear thinning behavior at a low rate to shear thickening behavior at higher injection rates.

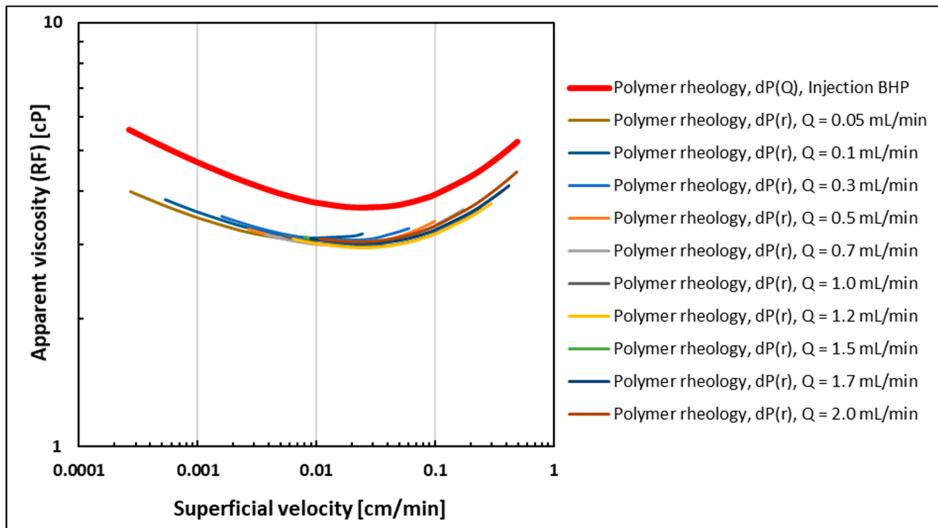


Figure 7. Polymer rheology curves obtained from history matching injection BHP as a function of the volumetric injection rate (red) and internal differential pressures as a function of radial distance (remainder of curves).

The parallel shift between rheology curves obtained from injection BHP versus curves obtained from internal pressures is a consequence of performing history matches using the initial permeability (before the polymer is introduced). Since pressure measurements were conducted after retention was satisfied, permeability would be reduced both internally mainly due to adsorption, but also at a greater extent in the near wellbore region due to mechanical entrapment of polymer molecules. The greater local permeability reduction in the wellbore region versus the internal reduction would induce a higher pressure response for injection BHP and thus effectively shift the apparent viscosity to higher values due to retention effects. However, the consistency between the functional relationship obtained from injection BHP and internal pressures shows that injection BHP is a robust tool for estimating in-situ polymer rheology.

4. Field Scale Simulation Approach

A radial model was built using CMG STARS to simulate the field-scale polymer injection test at several injection rates for different in-situ rheology cases. The objective was to confirm the findings from the lab scale experimental and simulation studies in order to assess the design of polymer injectivity tests and define in-situ rheology signatures on BHP responses.

The model was used to test three different in-situ rheology behaviors: Shear thinning only, shear thickening only and shear thickening followed by shear thinning (combined). These three cases represent nearly all possible in-situ rheology behaviors expected in the near wellbore area of a polymer injector. The shear thinning case is representative for xanthan biopolymer, as well as types of synthetic polymers (such as HPAM) at certain low molecular weight and/or low concentrations, where shear flow dominates the in-situ behavior of polymer even at high shear [7]. In contrast, at certain high molecular weights or high concentrations, synthetic polymers might observe only shear thickening behavior in the near-wellbore region if they were dominated by extensional flow for the whole spectrum of encountered shear rates, shadowing the thinning behavior even at low shear rates. The third case (combined) represents the in-situ behavior observed in the lab for synthetic polymers where apparent shear thickening occurs at high shear rates followed by shear thinning away from the injection point.

Generic in-situ rheology curves were constructed using a modified version of the extended Carreau model introduced by Delshad et al. 2008 that relates apparent viscosity to Darcy velocity and includes both shear and extensional components [15]:

$$\mu_{app} = \left[\mu_{\infty} + \left[(\mu_0 - \mu_{\infty}) * \left[1 + (\lambda_1 u)^2 \right]^{\frac{n_1-1}{2}} \right] \right] + \left[\mu_{max} * \left(1 - e^{-[\lambda_2 u]^{n_2-1}} \right) \right]$$

where μ_{app} is polymer apparent viscosity, μ_{∞} and μ_0 are limiting Newtonian viscosities at high and low shear limits, respectively, λ and n are empirical polymer constants, u is the superficial velocity of the polymer in porous media and μ_{max} is the shear-thickening plateau viscosity.

Using this equation, apparent viscosity was calculated for the range of expected velocities in the near-wellbore region for all injection rates (Figure 8). The first part of the equation (shear flow component) was used for the shear thinning only case while the second part (extensional flow component) was used for the shear thickening only case. The sum of both parts was used for the combined rheology case. In order to ensure coverage of the entire expected velocity spectrum encountered in the reservoir, the model was first tested with the highest and lowest injection rates, then the velocity profiles were used as references for the rheology calculation. “ μ_{∞} ” was set at 1 cp since it represents pure solvent viscosity (water in our case). Other viscosity terms in the equation (μ_{max} and μ_0) represent the endpoints of the rheology curve and can be obtained from lab measurements with reasonable accuracy. Both were assumed at 10 cp in our study. λ and n parameters were tuned so that the curves are smooth and consistent for all rheology cases without compromising model stability. The sensitivity of shear thinning and shear thickening curves to λ and n parameters is illustrated in Figures A1–A4. Table 1 below shows a summary of the extended Carreau model parameters used for rheology curves.

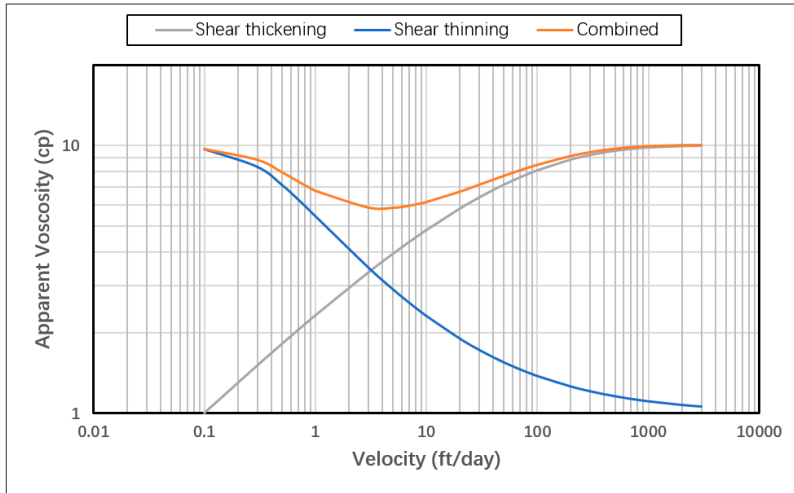


Figure 8. In-situ rheology curves obtained using extended Carreau model

Table 1. Extended Carreau model parameters used for rheology cases.

μ_{∞}	μ_0	λ_1	n_1	λ_2	n_2	μ_{max}
1	10	1.0×10^6	0.46	1.0×10^4	1.4	10

4.1. Model Description

The radial coordinates system was selected to minimize the error in the velocity calculation induced by the smear of the velocity front in the Cartesian gridding scheme. A grid system of exponentially increasing grid size was applied for the near-wellbore area around the injector up to a 100 ft. radius (Figure 9). This gridding scheme was selected in order to accurately capture the expected exponentially decreasing velocity profile, and to improve simulation efficiency by avoiding unnecessary fine gridding further away from wellbore. The size of the innermost grid (injector grid) was set at 0.41 ft. while the size of the outermost grid was 5.58 ft. with a total of 60 grids in the radial direction.

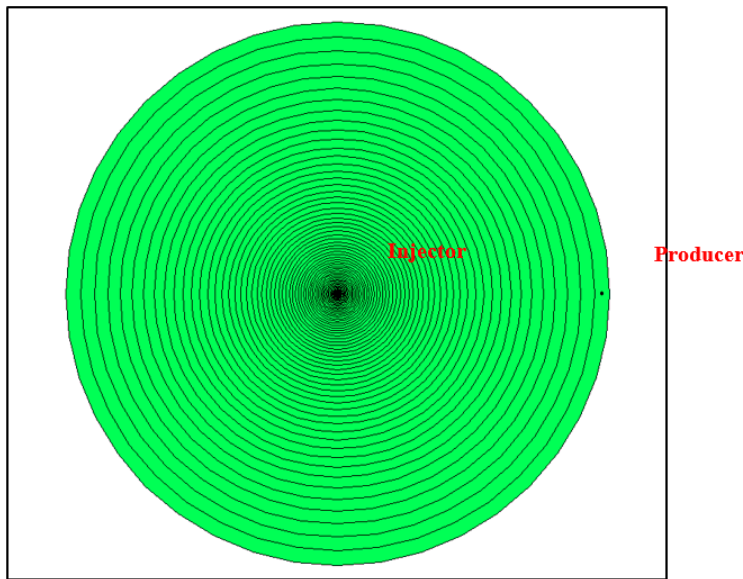


Figure 9. 2D aerial map showing the radial gridding scheme of the model.

This gridding system was generated automatically through the CMG Builder tool by defining a specific outer radius, the number of grids along the radius, and the size of the inner-most grid size (well grid). The arbitrarily selected grid sizing was based on the criterion of achieving sufficiently fine grids around the well-bore while maintaining model stability over all encountered viscosities at all injection rates. This is based on the fact that the finest-grid case represents the closest approximation to the realistic Darcy velocity at the wellbore sand-face and near-wellbore region, which is the only parameter that influences the predefined non-Newtonian viscosity functions that are inputted in the model as viscosity–velocity tables. Hence, grid sensitivity was not an issue of concern in this study.

Likewise, the model radius selection was subjective since it may not represent actual near-well bore area in many reservoirs as it varies widely based on reservoir properties. However, the radius was assumed at 100-ft to cover a wider spectrum of Darcy velocities/shear rates since the main objective is to inspect theoretical in-situ rheology impact on injection pressure rather than representing actual field cases. Therefore, the model was also assumed to be homogenous with no fractures or faults and saturated with water only.

Other factors that might impact BHP such as polymer adsorption and compressibility were not included as well. Polymer was injected at 800 ppm concentration represented by a 1.8×10^{-6} mole fraction input. Polymer adsorption was neglected and linear mixing rule was assumed between

polymer and water viscosities. The range of tested rates is between 1000 and 10,000 bbl/day, which covers typical injection rates in field applications. The parameters of the model are summarized in Table 2 below.

Table 2. Basic parameters and assumptions of the field scale model.

Parameter	Value
Well type	Vertical
Thickness	50 ft
Injector grid size	0.41 ft
Porosity	15%
Permeability	100 mD
Initial water saturation	100%
Reservoir pressure	2000 psi

4.2. Producers Pattern Sensitivity

A simple sensitivity study was performed to assess the impact of the number of producers on the simulation output in order to optimize the model's pattern selection. The aim was to isolate the effect of polymer's non-Newtonian viscosity by increasing the number of producers placed at the model's outermost grids and thus eliminating a no-flow boundary impact on the injection pressure response. However, this may come at the price of increasing computation time by increasing the total number of grids in the model and hence lowering the simulation efficiency. The examined producer patterns were one producer only, two producers, four producers (five-spot), eight producers (nine-spot) and 12 producers. Figure A5 shows 2D maps of producer pattern sensitivity cases. Figure 10 shows the BHP response for each pattern under the conditions of an injecting polymer at 6000 bbl/day with a shear thickening in-situ rheology. The case with one producer shows a significant boundary effect after injecting 1 PV while the nine-spot and 12-producers patterns shows almost a no boundary effect. It takes 20 s to run the case with one producer compared to 120 s for the 12-producers case. It was decided that a nine-spot pattern was the most suitable for the purpose of this study, since the results were very close to the 12-producers case while simulation efficiency was not compromised significantly.

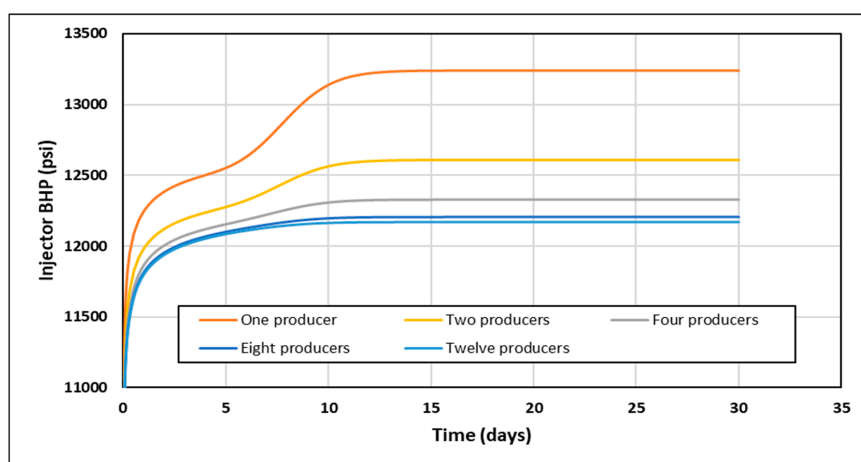


Figure 10. BHP response for each producer pattern at 6000 bbl/day with a shear thickening in-situ rheology.

4.3. Viscosity Mixing in the Reservoir

One of the concerns when modeling polymer flooding is the mixing of polymer viscosity with other reservoir fluids viscosities, especially at the front of polymer slug. As the front is progressing, polymer viscosity behind it is following the predefined viscosity–velocity functions of the model. However, the viscosity ahead of the front will follow a viscosity mixing rule that creates a transition between polymer viscosity and reservoir fluid viscosity (Figure 11), and hence it would have an impact on the injector’s BHP that does not follow input viscosity functions. To isolate the non-Newtonian behavior effect on injector’s BHP, a minimum of 1 PV of polymer is required to be injected in order to achieve the intended viscosity profile within the near-wellbore region (Figure 12). In this study, STARS default linear mixing rule was applied between polymer and water viscosities.

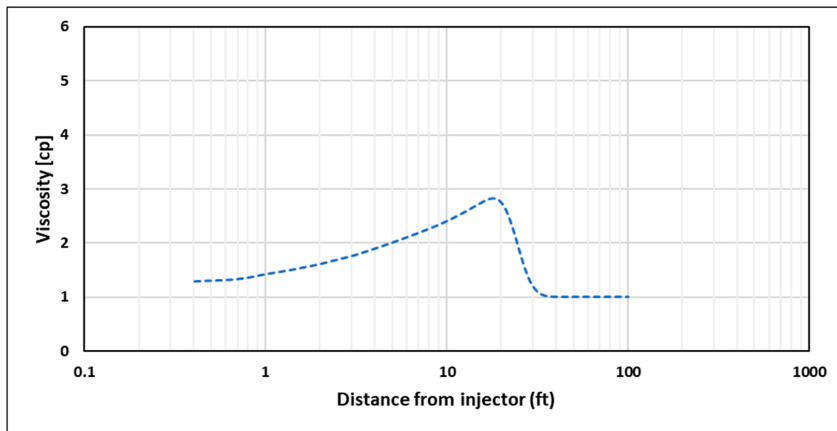


Figure 11. Viscosity profile after injecting 0.06 PV at 5000 bbl/day for shear thinning rheology.



Figure 12. Viscosity profile after injecting 1 PV at 5000 bbl/day for shear thinning rheology.

4.4. Impact of High-Permeability Layers and Residual Resistance Factor

Heterogeneity of reservoirs adds more complexity to the challenges in determining in-situ rheology of a polymer from the injectivity test data. The presence of thief zones such as high permeability layers, open fractures, vuggy channels, etc., exposes the polymer to several different shear fields in the reservoir and creates the possibility of having several in-situ rheology behaviors occurring at the same

time in different locations. Besides, the skin effect induced by polymer adsorption and/or mechanical entrapment in low permeable zones is another factor to be considered when tackling heterogeneity. The skin effect is usually addressed through the residual resistance factor (RRF), which is a parameter measured in lab core-floods and defined as the ratio between differential pressure after and before polymer injection.

To test the impact of different polymer in-situ rheology on layered reservoirs, the base model was modified to have alternating high and low permeability layers. High permeable zones were assigned a permeability value of 1000 mD, while low permeability zones were at 100 mD (Figure 13). The same rheology curves used for homogenous cases were used to ensure consistency of comparison. To test the impact of polymer adsorption and retention on low permeability zones, an extra case was investigated where an RRF value of two was set to the 100-mD layers while maintaining no adsorption (RRF = 1) in the high permeability layers.

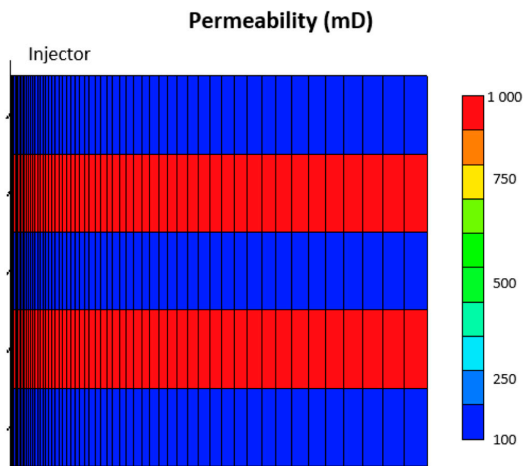


Figure 13. Cross section view showing the permeability distribution in the layered reservoir case.

5. Results and Discussion (Field Scale)

Results of simulations were used to plot stabilized BHP versus injection rate and time for homogeneous and layered cases at different in-situ rheology conditions.

5.1. Homogeneous Case

Figure 14 shows BHP versus injection rate for the homogeneous cases. The BHP was fitted to a second order polynomial. The coefficient of second order term is positive or negative dependent on the type of rheology. It was found that stabilized BHP trend has an increasing slope for shear thickening only and a decreasing slope for the shear thinning only cases. The combined rheology showed a combination of increasing and decreasing slopes along the trend. This is attributed to the effect of shear thickening behavior for high shear rate near-wellbore, and shear thinning behavior for lower shear rates further away.

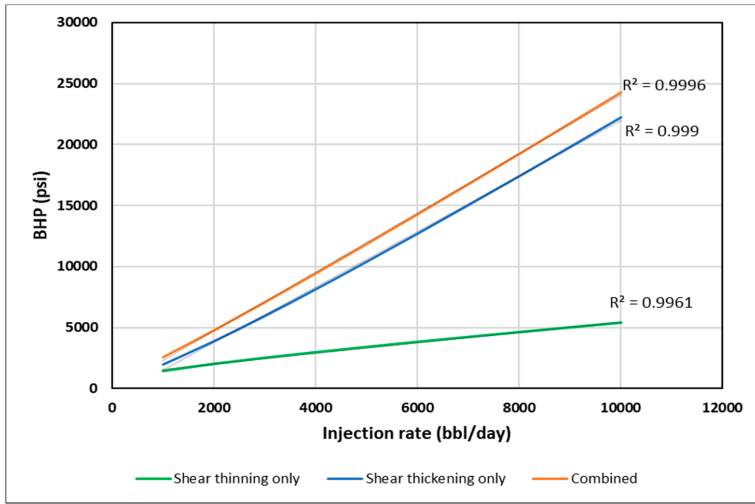


Figure 14. Stabilized BHP versus injection rate for different in-situ rheology in the homogeneous case.

As discussed earlier, stabilized pressure is not reached until at least 1 PV of the polymer is injected, as viscosity mixing at the front is eliminated and the steady-state condition is reached. This interval, however, is too long for polymer injectivity tests where rate steps are usually much shorter. Hence, BHP was plotted at 0.001 PV, 0.01 PV and 0.1 PV for each rate, to confirm if the same signal could be obtained at early times with transient condition and the presence of viscosity mixing. The slopes of BHP trends become less distinct with shorter injection times (Figures 15–17). The slope change, however, is detectable by using the coefficient of second order polynomial trendline function (Table 3).

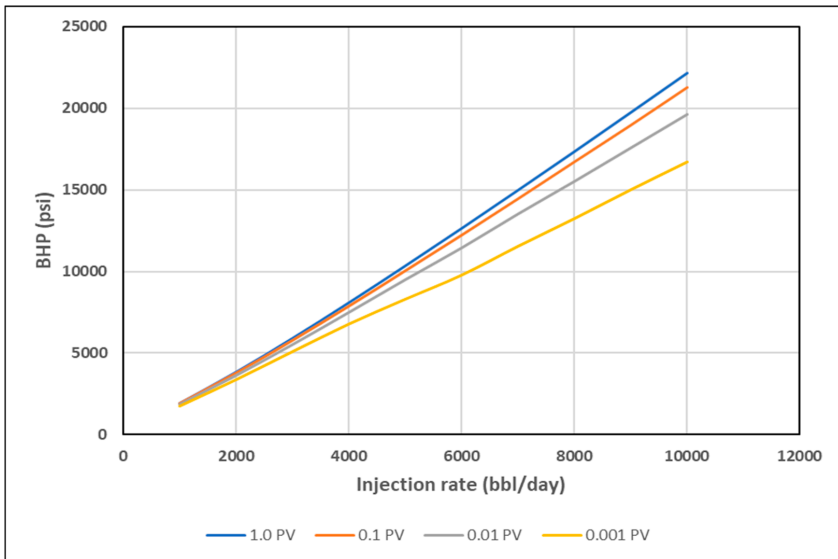


Figure 15. BHP vs. Q for shear thickening homogeneous case at different PVs.

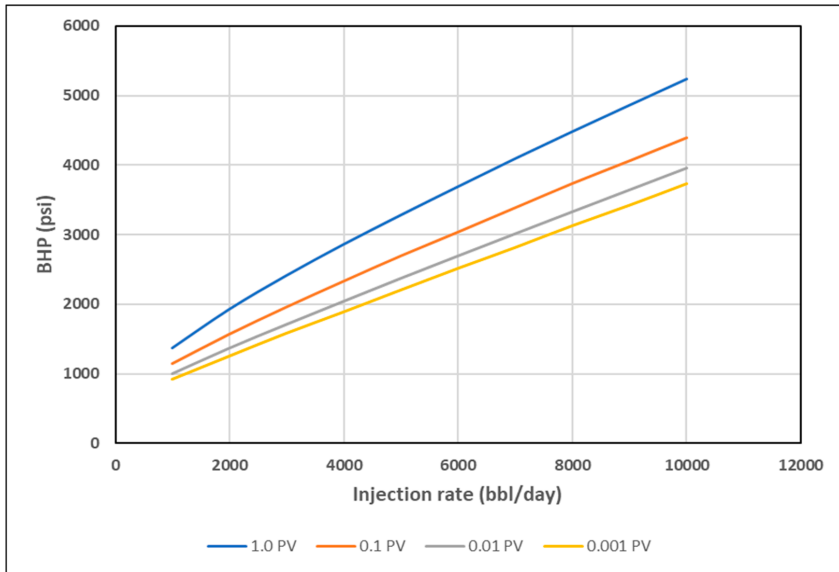


Figure 16. BHP vs. Q for shear thinning homogeneous case at different PVs.

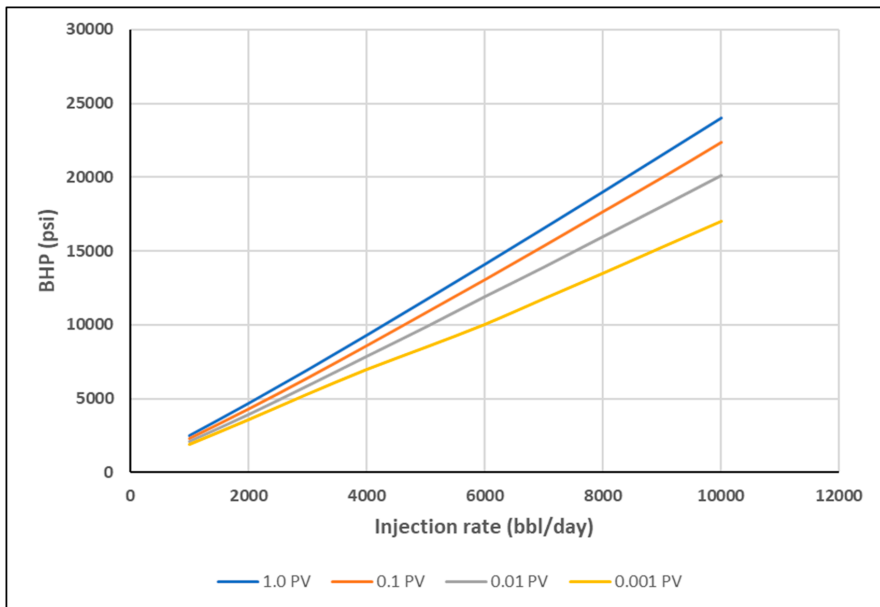


Figure 17. BHP vs. Q for combined rheology homogeneous case at different PVs.

Table 3. Coefficients of 2nd order polynomial trendline functions of BHP vs. injection rate at different injected PV's for different rheology cases.

Rheology	Coefficient of 2nd Order Polynomial Trendline Function ($\times 10^{-5}$)											
	0.001 PV			0.01 PV			0.1 PV			1.0 PV		
	High	Med	Low	High	Med	Low	High	Med	Low	High	Med	Low
Shear thinning	0.8	-0.4	-0.2	-0.03	-0.3	-1.0	0.3	-0.4	-2.0	-0.2	-0.5	-4.0
Shear thickening	-3.0	6.0	5.0	-2.0	2.0	6.0	3.0	2.0	7.0	6.0	2.0	8.0
Combined rheology	-1.0	6.0	3.0	0.9	0.5	6.0	4.0	1.0	5.0	-0.05	1.0	4.0

Negative values indicate shear thinning while positive values indicate shear thickening. For more detailed analysis of the coefficients, injection rates were divided into three ranges: low range from 1000 to 3000 bbl/day, medium range from 4000 to 7000 bbl/day and high range from 8000 to 10,000 bbl/day. From the obtained coefficients one can see that shear thinning and shear thickening behaviors can be detected by negative and positive values, respectively, even if shorter injection rate steps were implied. However, the behavior is more detectable as the injection time increases. The combined rheology is generally showing shear thickening behavior (positive values) due to the fact that apparent viscosity gain is the first encountered behavior in the near well bore area. The outliers that show positive for shear thinning and negative for shear thickening are attributed to the viscosity mixing phenomena.

Although the signal is not significantly pronounced in the BHP vs. Q plots, the slope change verifies the significance of rate-stepping in polymer injectivity tests. A minimum of three rate steps is thought to be sufficient in order to be able to detect in-situ rheology near-wellbore since it would yield two slope points that can indicate an increase or decrease in viscosity. The rates selected have to be selected so that they cover high, medium and low ranges of expected in-situ velocity.

The second part of the analysis is focused on the BHP versus time plots. It was noticed that each in-situ rheology yields a distinctive signal during early times. Figure 18 shows, the BHP profile versus log time for each rheology at the injection rate of 5000 bbl/day. The shear thickening rheology reflects a sharp increase in BHP shortly after starting injection up to less than 0.005 PV. In contrast, shear thinning rheology is characterized by a gradual increase in BHP all the way to 1 PV. The combined rheology reflects a combination of the two behaviors of thickening and thinning. These signals are attributed to the viscosity that the injector "sees" first into the reservoir and then further away from it. These findings suggest that a minimum of 0.0001 PV of the near-well bore region may be sufficient to decide whether we encounter shear thickening or shear thinning rheology at the near wellbore area, however, the combined rheology would require longer periods of at least 1 PV to be detected through BHP versus time measurements. It is worth to note here that these findings are based on ideal case simulation results without considering other near well bore effects such as skin, fractures, filtrate cake, etc. Nevertheless, the suggested PV can be used as a base to analyze the BHP response near wellbore and to preassess in-situ rheology from early data obtained in the field.

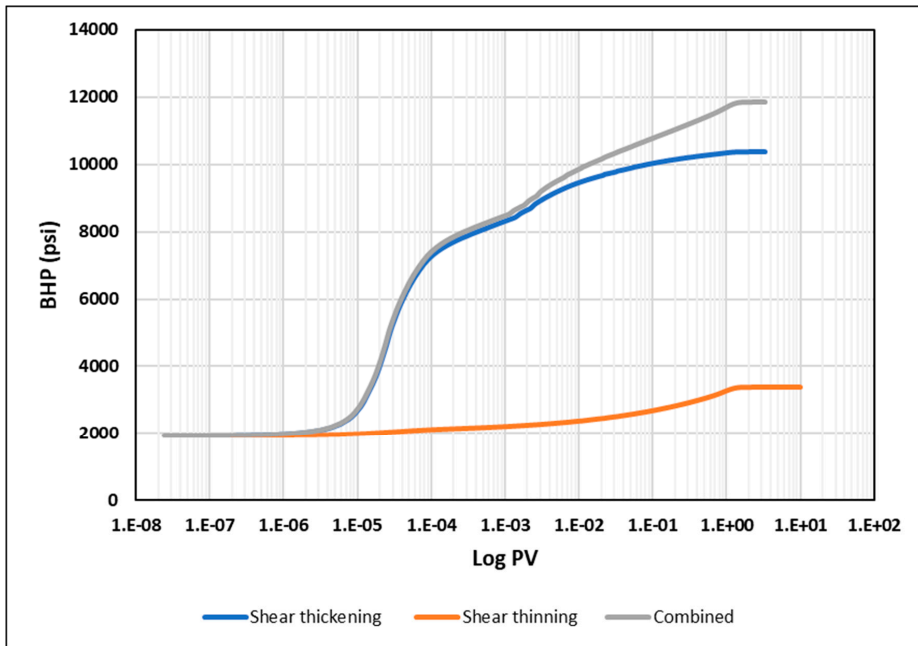


Figure 18. BHP versus log PV for different in-situ rheology at 5000 bbl/day in a homogeneous reservoir.

5.2. Layered Case

A basic heterogeneity case was investigated to observe the impact of high permeability streaks on the injection BHP compared to the homogeneous results. It is anticipated that high permeability layers can significantly enhance injectivity by lowering injection BHP. Nonetheless, we aim to find if heterogeneity can affect the distinctive signals of different in-situ rheology. The modified case is a layered reservoir with alternating high permeability (1000 mD) streaks (Figure 13). Figure 19 illustrates the BHP versus injection rate for the layered case. The trends of BHP responses are similar to the ones in homogeneous cases. This suggests that a similar method could be used for both homogeneous and heterogeneous reservoirs. Besides, the signature on the BHP vs. log time is affected, and each rheology can be distinguished with the same characteristics observed in the homogeneous case (Figure 20).

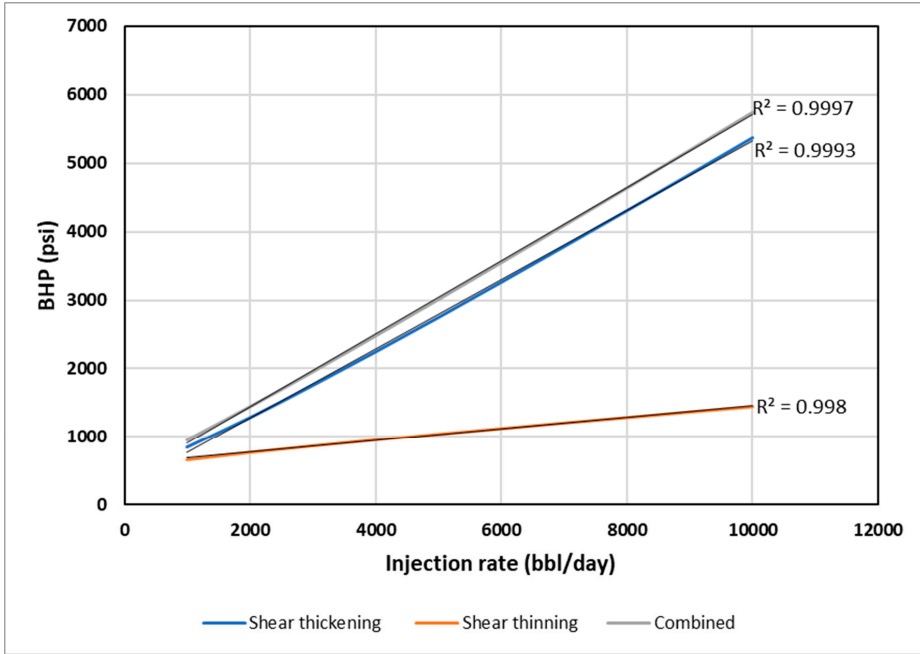


Figure 19. BHP versus injection rate for different in-situ rheology in the layered reservoir.

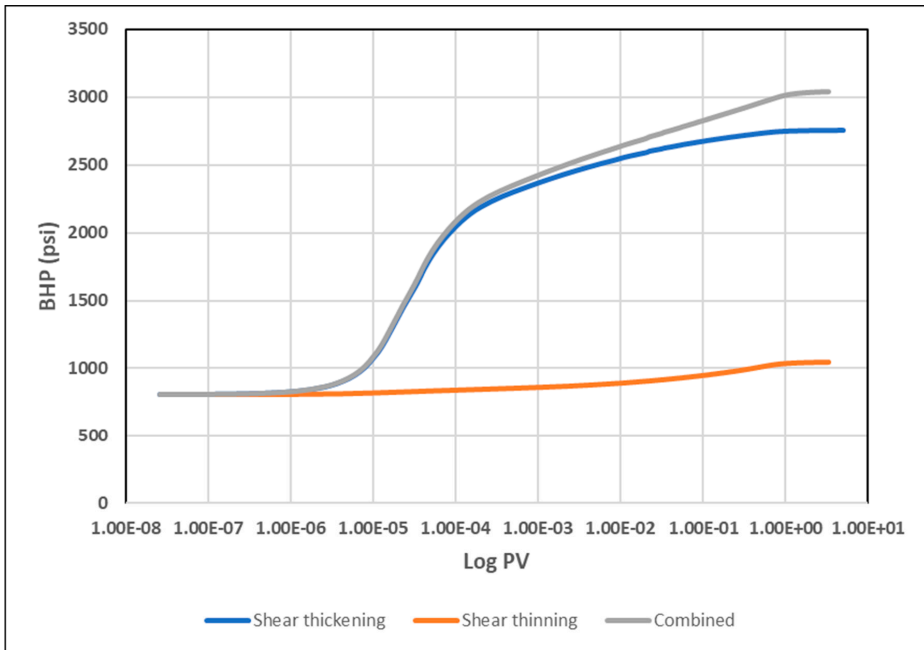


Figure 20. BHP versus log PV for different in-situ rheologies at 5000 bbl/day in the layered reservoir.

6. Conclusions

The findings presented in this study contribute to optimizing the design of polymer injectivity tests for enhanced oil recovery (EOR) polymer flooding projects. The main issue addressed was the impact of polymer in-situ rheology in porous media on the injector's BHP response, since BHP is the main—and sometimes the only—source of data available in field tests. We suggest from this study that adapting a rate-stepped scheme in polymer injectivity tests is of a significant benefit in optimizing our understanding of polymer in-situ rheology at reservoir conditions and hence optimizing the design of polymer injectivity tests based on each individual reservoir characteristics.

The main conclusions are based on two simulation approaches: (1) history matching the results of a radial water and polymer flood lab experiments, (2) using generic up-scaled field-size model to test the impact of different in-situ rheology on BHP.

The experiment results showed that it is possible to distinguish between water and polymer floods based on BHP pressure build-up time. Moreover, the experiment confirmed the ability to differentiate between different rheological regimes based on BHP pressure-build up time, where shear-thickening behavior stabilizes pressure quicker than shear thinning. Lab-scale simulation findings confirmed the injection BHP as a robust tool for estimating in-situ polymer rheology in radial flow in porous media.

The field-scale simulation approach confirmed that BHP could be used to obtain information about in-situ rheology if rate variation is included in the procedure of field polymer injectivity tests. The rate-variation should include a minimum of three rate steps covering the whole range of velocities from low to high. Respective BHP readings then are used to determine the polymer rheology behavior as it propagates into the reservoir.

Besides the rate variation, it is important to assess the time the pressure needs to stabilize so it can be representative of the rheology signal. The findings suggest that the time for pressure stabilization at a given injection rate, is slower for shear-thinning fluids, compared to Newtonian and shear-thickening fluids. In addition, combined rheology exhibits a combination of shear thickening and shear-thinning behaviors that can be detected from BHP vs. time. Although pressure stabilization is affected by viscosity mixing at the front and hence it is not achievable before at least 1 PV is injected, the results confirmed that a minimum of 0.0001 PV could still be used to detect rheology signal. That being said, one can obtain information from a stepped-rate injectivity test only when comparing equal injected PVs for each rate. This finding is highly subjective to the specific assumptions of the model, but it can be used as a rough estimate to decide minimum injection duration at each rate step.

Furthermore, for heterogenous-layered reservoirs, it was found that the method is still applicable, despite the fact the rheological signal is noticeably reduced.

For future studies, we recommend investigating the impact of other near well bore effects such as skin, fractures, filtrate cake, etc. In addition, the impact of viscosity mixing needs to be quantified and further assessed in order to have better understanding of its impact on BHP response.

Author Contributions: M.A.A. and J.G.J.: Simulation work, results analysis, and manuscript writing. A.S.: Results analysis and discussion. S.M., A.A.S. and Ø.P.: Reviewing the paper and following up. All authors have read and agreed to the published version of the manuscript.

Funding: This research received no external funding.

Acknowledgments: Mohamed Alzaabi acknowledges financial support from ADNOC for his PhD studies at the University of Bergen, Norway. Arne Skauge recognizes support from Energi Simulation as the Energi Simulation Industrial Research Chair in EOR. The research project appreciates support from PETROMAKS 2 program at the Norwegian Research Council through the Project Upscaling EOR.

Conflicts of Interest: The authors declare no conflict of interest.

Appendix A

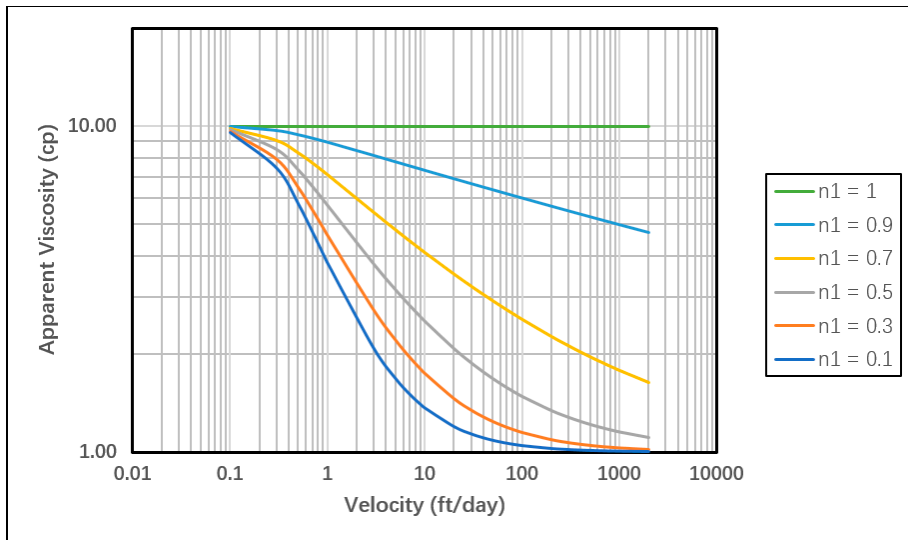


Figure A1. Sensitivity of shear thinning curve to different n_1 values.

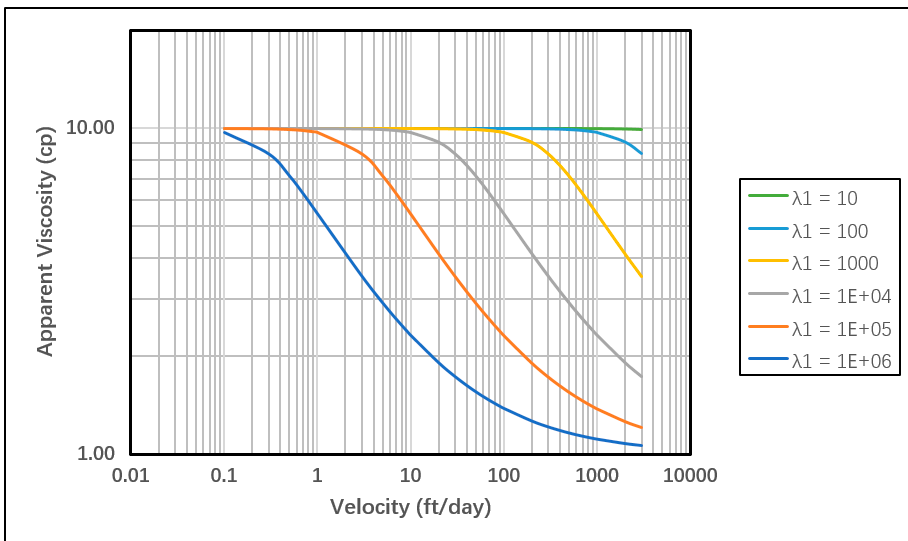


Figure A2. Sensitivity of shear thinning curve to different λ_1 values.

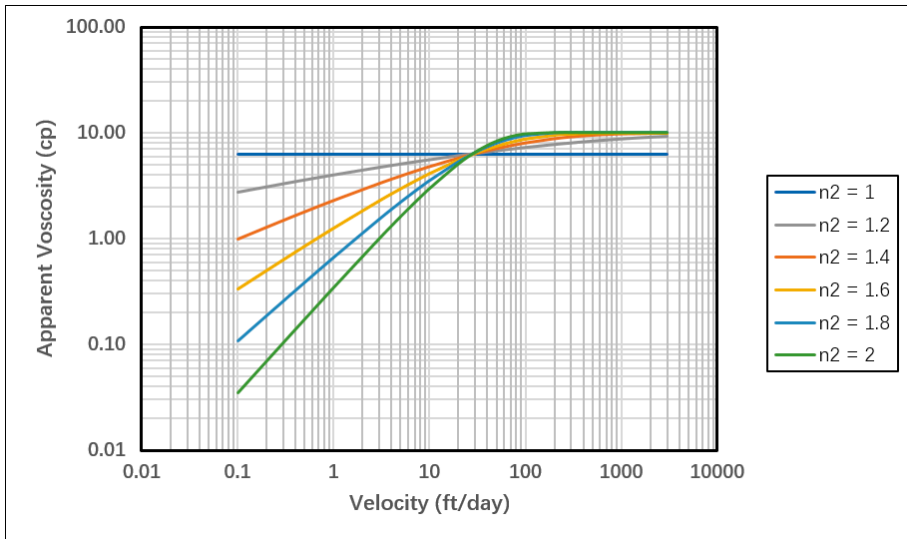


Figure A3. Sensitivity of shear thickening curve to different n_2 values.

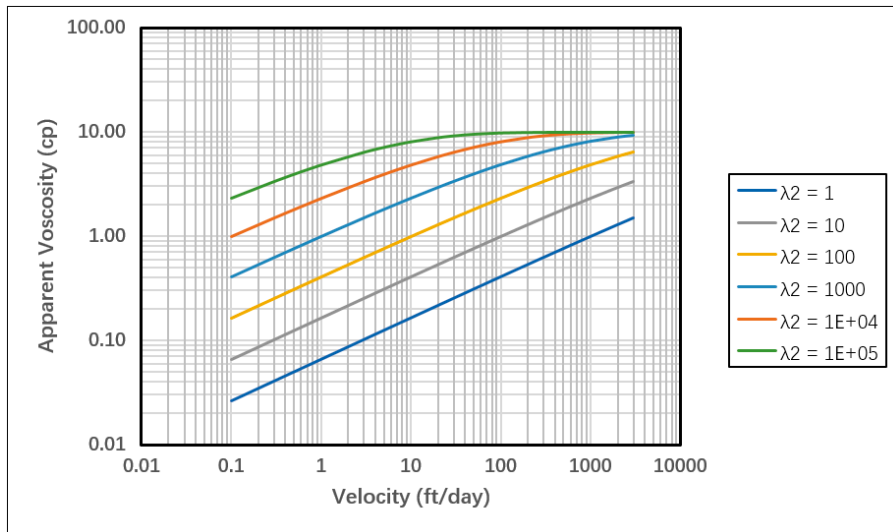


Figure A4. Sensitivity of shear thickening curve to different λ_2 values.

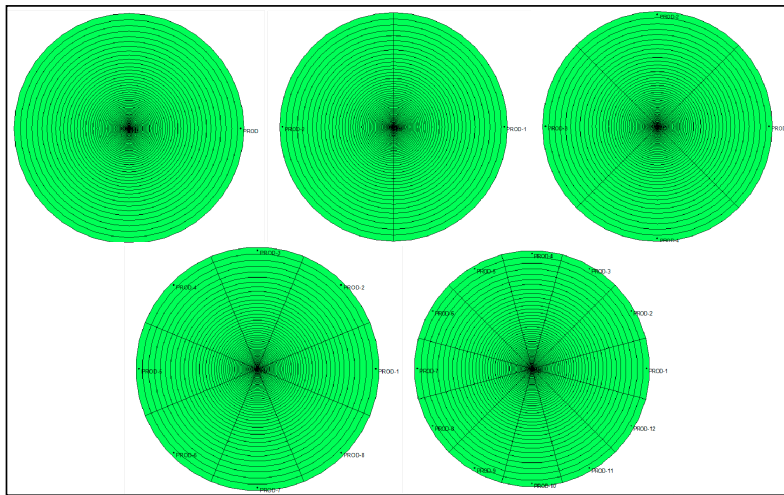


Figure A5. 2D maps of producer pattern sensitivity cases.

References

1. Pope, G.A. The Application of Fractional Flow Theory to Enhanced Oil Recovery. *Soc. Pet. Eng. J.* **1980**, *20*. [\[CrossRef\]](#)
2. Masalmeh, S.; Hillgartner, H.; Al Mjeni, R.; Jing, X.D. Simultaneous Injection of Miscible Gas and Polymer (SIMGAP) to Improve Oil Recovery and Sweep Efficiency from Layered Carbonate Reservoirs. In Proceedings of the SPE EOR Conference at Oil & Gas West Asia, Muscat, Oman, 11–13 April 2010. [\[CrossRef\]](#)
3. Sheng, J.J.; Leonhardt, B.; Azri, N. Status of Polymer-Flooding Technology. *J. Can. Pet. Technol.* **2015**, *54*. [\[CrossRef\]](#)
4. Huh, C.; Pope, G.A. Residual Oil Saturation from Polymer Floods: Laboratory Measurements and Theoretical Interpretation. In Proceedings of the SPE Symposium on Improved Oil Recovery, Tulsa, OK, USA, 20–23 April 2008. [\[CrossRef\]](#)
5. Skauge, A.; Zamani, N.; Gausdal Jacobsen, J.; Shaker Shiran, B.; Al-Shakry, B.; Skauge, T. Polymer Flow in Porous Media—Relevance to Enhanced Oil Recovery. *Colloids Interfaces* **2018**, *2*, 271. [\[CrossRef\]](#)
6. Sorbie, K.S. *Polymer-Improved Oil Recovery*; Blackie and Son Ltd.: Glasgow, UK, 1991.
7. Skauge, T.; Skauge, A.; Salmo, I.C.; Ormehaug, P.A.; Al-Azri, N.; Wassing, L.M.; Glasbergen, G.; Van Wunnik, J.N.; Masalmeh, S.K. Radial and Linear Polymer Flow—Influence on Injectivity. In Proceedings of the SPE Improved Oil Recovery Conference, Tulsa, OK, USA, 11–13 April 2016. [\[CrossRef\]](#)
8. Al-Shakry, B.; Skauge, T.; Shaker Shiran, B.; Skauge, A. Polymer Injectivity: Investigation of Mechanical Degradation of Enhanced Oil Recovery Polymers Using In-Situ Rheology. *Energies* **2019**, *12*, 49. [\[CrossRef\]](#)
9. Zeito, G.A. Three Dimensional Numerical Simulation of Polymer Flooding in Homogeneous and Heterogeneous Systems. In Proceedings of the Fall Meeting of the Society of Petroleum Engineers of AIME, Houston, TX, USA, 29 September–2 October 1968. [\[CrossRef\]](#)
10. Bondor, P.L.; Hirasaki, G.J.; Tham, M.J. Mathematical Simulation of Polymer Flooding in Complex Reservoirs. *SPE J.* **1972**, *12*, 369–382. [\[CrossRef\]](#)
11. Seright, R.S. The Effectsof Mechanical Degradation and Viscoelastic Behavior on Injectivity of Polyacrylamide Solutions. *SPE J.* **1983**, *23*, 475–485. [\[CrossRef\]](#)
12. Lotfollahi, M.; Farajzadeh, R.; Delshad, M.; Al-Abri, A.-K.; Wassing, B.M.; Al-Mjeni, R.; Awan, K.; Bedrikovetsky, P. Mechanistic Simulation of Polymer Injectivity in Field Tests. *Soc. Pet. Eng. J.* **2016**, *21*. [\[CrossRef\]](#)

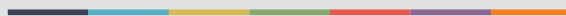
13. Goudarzi, A.; Delshad, M.; Sepehrnoori, K. A Critical Assessment of Several Reservoir Simulators for Modeling Chemical Enhanced Oil Recovery Processes. In Proceedings of the SPE Reservoir Simulation Symposium, The Woodlands, TX, USA, 18–20 February 2013. [[CrossRef](#)]
14. Gogarty, W.B. Mobility Control With Polymer Solutions. *Soc. Pet. Eng.* **1967**. [[CrossRef](#)]
15. Delshad, M.; Kim, D.H.; Magbagbeola, O.A.; Huh, C.; Pope, G.A.; Tarahhom, F. Mechanistic Interpretation and Utilization of Viscoelastic Behavior of Polymer Solutions for Improved Polymer-Flood Efficiency. In Proceedings of the SPE Symposium on Improved Oil Recovery, Tulsa, OK, USA, 20–23 April 2008. [[CrossRef](#)]



© 2020 by the authors. Licensee MDPI, Basel, Switzerland. This article is an open access article distributed under the terms and conditions of the Creative Commons Attribution (CC BY) license (<http://creativecommons.org/licenses/by/4.0/>).



Graphic design: Communication Division, UIB / Print: Skjipes Kommunikasjon AS



uib.no

ISBN: 9788230861585 (print)
9788230840252 (PDF)